

## Durham E-Theses

---

### *The petrology and mineralogy of the South Qroq centre, Igaliko complex, south Greenland*

Davd Stephenson

#### How to cite:

---

Stephenson, Davd (1973) The petrology and mineralogy of the South Qroq centre, Igaliko complex, south Greenland. Doctoral thesis, Durham University.

#### Use policy

---

The full-text may be used and/or reproduced, and given to third parties in any format or medium, without prior permission or charge, for personal research or study, educational, or not-for-profit purposes provided that:

- a full bibliographic reference is made to the original source
- a <https://etheses.durham.ac.uk/id/eprint/8733/> is made to the metadata record in Durham E-Theses
- the full-text is not changed in any way

The full-text must not be sold in any format or medium without the formal permission of the copyright holders.

Please consult the [full Durham E-Theses policy](#) for further details.

THE PETROLOGY AND MINERALOGY OF THE  
SOUTH QOROQ CENTRE, IGALIKO COMPLEX, SOUTH GREENLAND

David Stephenson, B.Sc. (Dunelm)  
Grey College

A thesis submitted for the Degree of Doctor of Philosophy  
in the University of Durham.

February, 1973



### Frontispiece

The southern part of the Narssarssuaq - Qôroq peninsula, viewed across Tunugdliarfik Fjord from near Qagssiarsuk. The principal outcrops of the South Qôroq Centre are to be found on the plateau, the cliffs on the coast section being of SS2. The high mountains in the background are beyond Qôroq Fjord and are composed of Igdlérfigssalik Centre syenites with Eriksfjord Formation sandstones and lavas to the right.



## ABSTRACT

The South Qôroq Centre is one of four high-level, major intrusive centres comprising the Igaliko Nepheline Syenite Complex. Three elliptical stocks of foyaite were emplaced in fairly rapid succession by ring fracture and block subsidence, followed by a partial ring/dyke of augite syenite. Petrographic and mineralogical data shows that the intrusions become successively less differentiated with time. Inward-dipping microsyenite sheets appear to be associated with the ring dyke and four earlier, satellitic stocks occur around the periphery of SS2.

Feldspar, nepheline, iron-titanium oxide, olivine, clinopyroxene and amphibole have been investigated in each of the principal rock units by electron-microprobe. Most minerals show a considerable range in composition, often with chemical zoning, forming continuous series from the augite syenites through the foyaites. Variations within the three individual foyaites are usually slight, but the alkali clinopyroxenes have distinct compositional ranges in each intrusion. Estimates of liquidus temperatures are made from the nepheline and alkali feldspar compositions. Alkali feldspars provide estimates of  $P_{H_2O}$  and mafic minerals give an indication of  $f_{O_2}$  conditions.

Major and trace element analyses of the rocks were made by X-Ray fluorescence. Variation diagram trends are interpreted mainly in terms of fractionation of feldspar and the mafic phases. Trace element distributions are highly characteristic of fractional crystallisation series, but may not be compatible with progressive partial melting. The analyses are compared with phase equilibria in the experimental systems Q - Ne - Ks and  $Na_2O - Fe_2O_3 - Al_2O_3 - SiO_2$ .

It is suggested that the centre evolved from an underlying, differentiated magma chamber, formed by crystal accumulation, possibly with associated liquid fractionation. Successively lower portions of the chamber were tapped, producing batches of fractionated magma. Post-emplacement differentiation was restricted mainly to slight outward diffusion of alkalis and volatiles under a thermal diffusion gradient.

Physico-chemical conditions during recrystallisation near to the Igdlerfigssalik Centre are interpreted from textural, geochemical and mineralogical changes.

## ACKNOWLEDGEMENTS

The work has been made possible through the award of an N.E.R.C. Research Studentship. Support during the field work was provided by Grønlands Geologiske Undersøgelse (G.G.U.) and I would like to express my gratitude to the Director, Mr. K. Ellitsgaard Rasmussen for this and for subsequent assistance in many ways. Mr. A. Vidstein and the crew of the G.G.U. vessel "K.J.V. Steenstrup" provided hospitality during part of the stay in Greenland and gave valuable assistance in coastal sampling. Professors G. M. Brown and M. H. P. Bott made available the research facilities of the University of Durham.

I am greatly indebted to Dr. C. H. Emeleus who supervised the study, provided many of the samples and gave much helpful guidance and constructive criticism. He and Dr. B. G. J. Upton also provided an invaluable introduction to the field relationships of the Gardar Province during the 1969 field season.

I have benefitted greatly from discussion with the staff and fellow research students in the University of Durham and from other workers on the Gardar Province. In particular I would like to thank Professor G. M. Brown, Mr. A. D. Chambers, Mr. E. B. Curran, Dr. R. C. O. Gill, Mr. J. L. Knight, Mr. R. Phillips and Mr. G. Rowbotham for their help. Mr. J. Engell, Mr. P. Greenwood and Mrs. Lotte Melchior kindly provided access to unpublished data and gave useful discussion.

Advice on the use of the electron-microprobe, X-Ray fluorescence techniques and computer programs were provided by Mr. E. B. Curran, Dr. J. G. Fitton, Mr. F. B. Frost, Dr. G. H. Gale, Dr. R. C. O. Gill, Dr. A. Peckett and Dr. M. Reeves.

Thin sections and probe slides were prepared by Mr. L. MacGregor and Mr. G. Randall. Mr. G. Dresser made photo-reductions of the text figures.

Finally, I would like to thank Miss Susan Langford, whose patience and endurance during the typing of the manuscript was greatly appreciated.

## CONTENTS

ABSTRACT	iii
ACKNOWLEDGEMENTS	v
CONTENTS	vi
TEXT FIGURES	ix
TABLES IN THE TEXT	xi
PLATES	xii
<hr/>	
<u>1</u> INTRODUCTION	
(a) Nature and Scope of Work.	1
(b) The Gardar Province.	2
(c) The Igaliko Nepheline Syenite Complex.	8
(d) Previous Work.	9
(e) Sampling.	11
<u>2</u> FIELD RELATIONSHIPS OF THE SOUTH QÔROQ CENTRE	
(a) The South Qôroq Centre Syenites.	
i Syenite SS2.	14
ii Syenite SS3.	15
iii Syenite SS5.	17
iv The SS4 Syenites.	18
v Satellitic Syenites and Other Intrusions.	23
(b) Internal Contacts within the Centre	
i SS2/SS3.	24
ii SS3/SS4.	25
iii SS4/SS5.	26
iv SS3/SS5.	27
(c) Contacts with Country Rock	
i Contacts with Julianehåb Granite.	30
ii Contacts with Supracrustal Rocks.	31
iii Contacts with Earlier Syenites.	35
(d) Effects of the later Igdlérfigssalik Centre	36
(e) Faulting	37

CONTENTS (continued)

3 PETROGRAPHY OF THE SYENITES

- (a) Foyaites SS2, SS3 and SS5. 45
- (b) Augite Syenites and Related Rocks in SS4. 56
- (c) Other Intrusions Associated with the Centre. 59

4 MINERALOGY

- (a) Introduction. 68
- (b) Pyroxenes. 68
- (c) Amphiboles. 79
- (d) Olivines. 86
- (e) Iron-Titanium Oxides. 94
- (f) Nephelines. 100
- (g) Alkali Feldspars. 104
- (h) Other Minerals. 113

5 ROCK GEOCHEMISTRY

- (a) Introduction. 119
- (b) Major Element Variation. 119
- (c) Trace Element Variation. 132
- (d) Normative Mineralogy and Comparisons with Experimental Systems. 136

6 CONCLUSIONS

- (a) Intrusive Mechanisms. 145
- (b) Source and Primary Evolution of the South Qôroq Centre Magmas. 146
- (c) Conditions of Crystallisation and Late-Stage Evolution of the South Qôroq Centre. 155
- (d) Effects of Recrystallisation Around the Igdlerfigssalik Centre. 158

CONTENTS (continued)

APPENDIX I. ELECTRON MICROPROBE ANALYSIS	160
(techniques and analytical conditions).	
APPENDIX II. X-RAY FLUORESCENCE - WHOLE ROCK ANALYSIS	
(a) Sample Preparation.	163
(b) Major Element Analysis.	164
(c) Trace Element Analysis.	165
APPENDIX III. ELECTRON MICROPROBE MINERAL ANALYSES	172
Pyroxene Analyses.	173
Pyroxene Partial Analyses.	190
Amphibole Partial Analyses.	202
Olivine Analyses.	210
Magnetite Analyses.	218
Ilmenite Analyses.	224
Nepheline Analyses.	227
Feldspar Analyses.	239
APPENDIX IV. WHOLE ROCK ANALYSES AND C.I.P.W. NORMS	
Table IV.1 List of Samples.	255
" IV.2 Major and Trace Element Analyses.	256
" IV.3 C.I.P.W. Norms.	274
<hr/>	
REFERENCES	296

## TEXT FIGURES

<u>1.1</u>	General geological map of the Gardar Province.	3
<hr/>		
<u>2.1</u>	The South Qôroq Centre showing major units within the Centre, satellitic intrusions and principal faults.	13
<u>2.2</u>	Sketch section of the west side of Qôroq Fjord opposite the entrance to Flink's Dal, showing contact relationships between syenites and internal structures.	22
<u>2.3</u>	Cross section of the South Qôroq Centre across the Narssarssuaq - Qôroq plateau, from Tunugdliarfik Fjord to Qôroq Fjord.	22
<u>2.4</u>	Faulting and crush zones in the area between Narssarssuaq and Augpalugtut.	41
<u>2.5</u>	Sketch map showing detail of branching in the southern transcurrent fault of the South Qôroq Centre, around the 1969 camp site.	41
<u>2.6</u>	Attempted correlations of faults on the west and east sides of Tunugdliarfik Fjord.	42
<hr/>		
<u>4.1</u>	Analyses of pyroxenes from the South Qôroq Centre and ranges of compositions within individual intrusions.	71
<u>4.2</u>	Variations of major and minor elements in the pyroxenes relative to the fractionation index (Na minus Mg).	72, 73
<u>4.3</u>	Zoning within representative pyroxene grains from each intrusion.	76
<u>4.4</u>	Comparison between the South Qôroq pyroxene trends and other published data.	77
<u>4.5</u>	Variation of alkalis, Fe and Mg in South Qôroq amphiboles and fractionation trends for the various syenites.	81

TEXT FIGURES (continued)

- 4.6 Variations of K, Na and Si with Ca in the South Qôroq amphiboles 82  
suggesting possible cation substitutions in the A, X and Z sites.
- 4.7 Olivine major element variation in terms of Forsterite-Fayalite - 88  
Tephroite.
- 4.8 Variation in Ca content of the olivines relative to the fractiona- 89  
tion index (Mn - Mg) atoms per 4 oxygens.
- 4.9 Zoning in individual olivine grains from the various units of the 90  
centre.
- 4.10 Variation of oxygen fugacity with temperature in natural rock suites 91  
with reference to the synthetic buffer curves haematite - magnetite  
(HM) and fayalite - magnetite - quartz (FMQ).
- 4.11 Compositions of iron-titanium oxides (magnetite and ilmenite) 97  
plotted in terms of Mol.% RO, RO<sub>2</sub> and R<sub>2</sub>O<sub>3</sub>.
- 4.12 Variation of the principal minor elements (Mn and Al) in the 98  
iron-titanium oxides.
- 4.13 South Qôroq Centre nepheline compositions plotted in terms of 102  
molecular weight percent nepheline, kalsilite and excess SiO<sub>2</sub>.
- 4.14 Compositions of the South Qôroq Centre feldspar bulk analyses in 106  
the system Albite - Orthoclase - Anorthite.
- 4.15 Average 2V values for unmixed feldspars as a function of the mean 107  
bulk feldspar composition in each electron-probe slide.
- 
- 5.1 Variation of major elements and major element ratios with the 121, 122, 123  
"Fractionation Index" of Macdonald (1969).
- 5.2 A - F - M diagram for the South Qôroq Centre major intrusive 126  
units.
- 5.3 Variations in selected element concentrations horizontally, 127  
across the outcrops of SS2 and SS4.

TEXT FIGURES (continued)

<u>5.4</u>	Trace element variation of the South Qôroq Centre rocks.	129, 130
<u>5.5</u>	Potassium versus Rubidium diagram for the South Qôroq Centre rocks.	131
<u>5.6</u>	Analyses from the main units of the South Qôroq Centre plotted in the Q - Ne - Ks "Residua System". Phase equilibria relationships at 1 Atm., 1 kb P <sub>H<sub>2</sub>O</sub> , and 5 kb P <sub>H<sub>2</sub>O</sub> .	135
<u>5.7</u>	Analyses from individual units of the South Qôroq Centre together with coexisting average feldspar and nepheline analyses where available, plotted in the "Residua System" Q - Ne - Ks.	138, 139
<u>5.8</u>	South Qôroq Centre and Ilímaussaqa Intrusion analyses plotted in the Na <sub>2</sub> O - Fe <sub>2</sub> O <sub>3</sub> - Al <sub>2</sub> O <sub>3</sub> plane of the "Peralkaline Residua System" after Bailey and Schairer (1966) and Engell (in press).	142

---

TABLES IN THE TEXT

<u>1</u>	Analyses of alkali amphiboles from the South Qôroq Centre Pegmatites.	85
<u>2</u>	South Qôroq Centre Sodalite analyses.	114
<u>3</u>	Electron microprobe analysis of perovskite from a magnetite-rich metasomatic vein.	115
<u>4</u>	Correlation coefficients between trace elements in the South Qôroq Centre Syenites.	128

## PLATES

<u>Frontispiece</u>	The Southern part of the Narssarssuaq - Qôroq peninsula, viewed across Tunugdliarfik Fjord from near Qagssiarssuk.	ii
<u>1</u>	(inside back cover) Geological map of the Igaliko Nepheline Syenite Complex. Scale 1:50,000. (From Emeleus and Harry, 1970, with modifications based on the present work.)	
<u>1A</u>	(inside back cover) Specimen locality map for the South Qôroq Centre. Scale 1:50,000.	
<u>2</u>	Panoramic view south-east from the 970m summit of the Narssarssuaq - Qôroq plateau towards Giesecke's Dal.	12
<u>3</u>	Pegmatite vein cutting through syenite SS2 on the Tunugdliarfik coast section.	16
<u>4</u>	Surface of typical, coarse grained SS3 showing blades of alkali feldspar, dark mafic areas and interstitial areas of red-weathering, altered nepheline. Narssarssuaq - Qôroq peninsula.	16
<u>5</u>	Vertical mafic banding in syenite SS4b - west coast of Qôroq Fjord.	19
<u>6</u>	Igneous lamination in syenite SS5 - west coast of Qôroq Fjord.	19
<u>7</u>	Slumped mafic schlieren in syenite SS5 - west coast of Qôroq Fjord.	20
<u>8</u>	SS2/SS3 contact on the west side of the Narssarssuaq - Qôroq peninsula.	28
<u>9</u>	Marginal pegmatitic facies of SS5 near to the contact with SS3 - east coast of Qôroq Fjord.	29
<u>10</u>	Coarse grained lens containing biotite, calcite, pyroxene, magnetite and accessories in a metasomatised, magnetite-rich sill cutting Julianehåb Granite - Tunugdliarfik coast section.	29

PLATES (continued)

- |           |  |    |
|-----------|--|----|
| <u>11</u> | Sharp contact between marginal SS2 syenite and an angular, xenolithic block of basalt very near to the main contact - 1 km east of Narssarssuaq Harbour. | 32 |
| <u>12</u> | Brecciated SS2/basalt contact exposed near the coast south of Narssarssuaq Harbour.  | 32 |
| <u>13</u> | "Knobbly" surface of hornfelsed basalt due to the weathering out of ophitic mafic patches - east of Narssarssuaq.  | 33 |
| <u>14</u> | Basalt with calc-silicate bands presumably derived from calcareous tuffs - 1.5 km east of Narssarssuaq Harbour.  | 33 |
| <u>15</u> | Syenite SS5 cut by Igdlarfigssalik syenite SI2 on the south side of Giesecke's Dal Bay, Qôroq Fjord.   | 34 |
| <u>16</u> | The southern, sinistral transcurrent fault cutting the South Qôroq Centre on the west side of Qôroq Fjord.   | 40 |
| <u>17</u> | Branches of the southern sinistral fault cutting the South Qôroq Centre on the east side of Tunugdliarfik Fjord.   | 40 |

---

Photomicrographs:-

- |           |  |    |
|-----------|--|----|
| <u>18</u> | Marginal SS2 showing a pronounced lamination of tabular, perthitic feldspar and rounded nepheline. | 51 |
| <u>19</u> | Simultaneous crystallisation of alkali feldspar and nepheline in SS3.                              | 51 |
| <u>20</u> | Typical texture of the felsic minerals from one of the microsyenite sheets cutting SS3.            | 51 |
| <u>21</u> | Typical large, tabular, twinned crystal of perthitic alkali feldspar in SS5.                       | 52 |
| <u>22</u> | Large tabular alkali feldspars showing multiple twinning in SS5.                                   | 52 |
| <u>23</u> | "Blebs" of nepheline within irregular grains of microperthitic alkali feldspar in SS4b.            | 52 |
| <u>24</u> | Euhedral grains of nepheline enclosed by interstitial, isotropic sodalite in SS2.                  | 53 |

PLATES (continued)

<u>25</u>	Interstitial nepheline between grains of microperthitic feldspar in SS4b.	53
<u>26</u>	Reaction between nepheline and interstitial calcite giving an intervening, radiating fringe of cancrinite in SS5.	53
<u>27</u>	Typical "mossy" mafic aggregate in SS2.	54
<u>28</u>	Mafic cluster in SS3.	54
<u>29</u>	Typical cluster of mafic minerals in a mafic band from SS4b.	54
<u>30</u>	Biotite-rich aggregate in recrystallised SS5 near to the contact with the Igdlarfigssalik Centre.	55
<u>31</u>	Radiating growths of carbonate replacing the central part of a pegmatite vein.	55
<u>32</u>	Large blade of alkali pyroxene growing inwards from the walls of the same pegmatite vein as Plate 31.	55
<u>33</u>	Zoned aegirine augite with subhedral inclusions of magnetite and a well developed rim of arfvedsonite in SS2.	63
<u>34</u>	Aegirine augite with a sharply defined rim of arfvedsonite in SS5.	63
<u>35</u>	Typical, irregular aegirine augite in SS5, with zoning not very pronounced optically.	63
<u>36</u>	Typical grain of lilac coloured titanaugite with inclusions of apatite and subhedral magnetite in SS4b.	64
<u>37</u>	Intergrowth of needles of aegirine augite with feldspar on the edge of an aegirine augite grain in SS2.	64
<u>38</u>	Secondary pale greenish acmite formed by reaction between magnetite and residual liquid in SS3.	64
<u>39</u>	Fayalite with heavy rims of iron ore enclosed by aegirine augite and arfvedsonite in SS5.	65
<u>40</u>	Rounded fayalite enclosed by aegirine augite and biotite in SS5.	65

PLATES (continued)

<u>41</u>	Olivine rimmed by interstitial titanite in SS4b.	65
<u>42</u>	Olivine with a thin rim of turquoise amphibole from a mafic band in SS4b.	66
<u>43</u>	Rounded grains of magnetite with well developed, coarse exsolution lamellae of pleochroic ilmenite parallel to the 111 cleavage.	66
<u>44</u>	Subhedral, rounded grains of euclite in an SS3 marginal pegmatite.	66
<u>45</u>	Zoned, euhedral euclite - mesodialyte in an SS3 marginal pegmatite.	67
<u>46</u>	Typical euhedral euclite from an SS3 marginal pegmatite.	67
<u>47</u>	Poikilitic, zoned euclite - mesodialyte from an SS3 marginal pegmatite as Plates 44 - 46.	67

---

## 1. INTRODUCTION

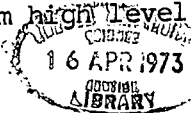
### (1a) Nature and Scope of Work

The South Q̄roq Centre is one of the four major intrusive centres comprising the Igaliko Nepheline Syenite Complex in the Late Precambrian Gardar Igneous Province of South Greenland. The Complex was mapped by C. H. Emeleus and the late W. T. Harry between 1961 and 1966. Their map and general description (Emeleus and Harry, 1970) forms the basis for the present work, which is part of a more detailed investigation of the various units of the complex, at present in progress at the University of Durham.

A visit to the area was made in the summer of 1969 whilst in the employment of Grønlands Geologiske Undersøgelse (G.G.U.). Two weeks were spent on the South Q̄roq Centre and, in addition to collecting further samples to supplement those of Emeleus and Harry, field relationships were investigated, resulting in several slight revisions to the published map.

The laboratory investigations which form the bulk of this work were carried out in the Department of Geology, University of Durham, between October 1969 and September 1972. Whole rock analyses for major and trace elements were obtained by X-Ray Fluorescence techniques for most of the samples, and a detailed mineralogical study was made of selected representative samples using an electron microprobe. From the analyses it has been possible to draw conclusions on the origin of the centre and its subsequent magmatic evolution. The mineralogical data has been particularly useful in determining magmatic conditions both prior to and after emplacement to the present level, and is also useful in interpreting the effects of later recrystallisation.

It is hoped that the results and conclusions will make a significant contribution to the understanding of the evolution of the Gardar Province as a whole, and to problems of alkali rock genesis. Certain aspects may also have a bearing on the general evolution of magma chambers at depth which are subsequently tapped to form high level intrusions or surface volcanoes.



(1b) The Gardar Province

The Gardar Igneous Province is situated between latitudes  $60^{\circ}30'$  and  $61^{\circ}30'N$ , extending approximately 80 km. from north to south and 180 km. from east to west (Fig. 1.1). General summaries of the geology are given by Berthelsen and Noe-Nygaard (1965) and Upton (in press).

**Pre-Gardar Geology:-**

The pre-Gardar geology can be divided into the pre-Ketilidian and the Ketilidian, which have been correlated with the Kenoran and Hudsonian of Labrador (Allaart et al., 1969). The pre-Ketilidian rocks give ages between 2,500 and 2,700 My. and occur northwards from the Ivigtut area where they form the country rock of the northern Gardar intrusions. They consist mainly of high grade gneisses, but also include anorthosite bodies, amphibolites and mica schists; a belt of locally migmatized supracrustal rocks; and later basic dykes. These rocks are overlain unconformably by Ketilidian metasediments and metavolcanics. When traced south towards the centre of the Ketilidian mobile belt, these show progressive deformation and increased plutonism so that the centre of the belt consists largely of orogenic granite (the Julianehab<sup>o</sup> granite). This main Ketilidian plutonic episode is dated at 1,800 My. and has north-east trending structures which exerted considerable control on later Gardar features. The orogeny culminated in the Sanerutian plutonic episode, dated at 1,500 to 1,640 My., with reactivation of older granites and the emplacement of post tectonic norites, diorites and granites, of similar age to those of the Elsonian "orogeny" in Labrador. The Gardar period occurred during the succeeding cratogenic interval, with alkaline magmatism between 1,000 and 1,300 My. (Allaart et al., 1969). The province is unaffected by later orogenic activity (i.e. the Grenvillian) and hence the rocks are preserved with no regional deformation.

Fig. 1.1

General geological map of the Gardar Province showing major plutonic intrusions; locations of the three Mid-Gardar dyke swarms; the extent of the Early-Gardar Eriksfjord Formation; and major faults. (From Emeleus and Harry, 1970)



### Gardar Igneous Activity:-

Resting unconformably on the Ketilidian Julianehåb granite in the area around Tunugdliarfik fjord is a thick sequence of continental sediments and lavas, known as the Eriksfjord Formation (Poulsen, 1964; Stewart, 1964). A total of about 3 km. of deposits is preserved in an east north east trending, downfaulted trough, which is believed to have been subsiding during the intermittent eruption of fissure volcanoes with aeolian, lacustrine and alluvial sedimentation. The proportion of lavas increases in the upper part of the succession and the flows, which are 1 to 15 m. thick with pahoehoe or aa characteristics, are predominantly of alkali olivine basalt. Volcanic breccias are found at the base of the formation and some of the higher flows are trachybasalt or trachyte. In the more northern outcrops bedded ashes and tuffs are quite widespread. These would appear to have been derived by explosive activity related to carbonate-rich magmas, as many small, alkaline ultramafic diatremes, and vents filled with carbonate rich rock fragments are found (Stewart, 1970). Outside of the downfaulted trough, the basalt/sandstone succession is assumed to have been much thinner, but its widespread presence is inferred from included blocks in later central complexes and boulders in recent moraines margining the ice cap.

Large volumes of basic magma are also represented by the numerous Gardar dykes which are found over a wide area, largely between Julianehåb in the south and Ivigtut in the north. Between three and five generations can usually be recognised, spread in time over most of the Gardar period, and these are used to define an Early, Mid and Late Gardar (Upton, 1962). The great majority trend between north-east and east-north-east, parallel to the dominant structural trend of the Ketilidian basement. Particularly dense swarms occur in three east-north-east trending zones through Ivigtut, Nunarssuit and Ilímaussaq. The majority of the dykes are dolerite or olivine dolerite, but an early swarm may have tholeiitic affinities, and other early swarms include some lamprophyres (Upton, 1970). Later dykes

in the Ivigtut and Ilímaussaq zones are felsic in nature and include great numbers of orthotrachytes and phonolites. The Nunarssuit and Ilímaussaq zones include very persistent "giant dykes" up to 800 m. wide, many of which show synformal igneous layering and associated structures (Upton, 1962; Pulvertaft, 1965). Such dykes are usually composite with a margin of gabbro or syenogabbro and a core of syenogabbro, syenite, nepheline syenite or granite, and an intervening hybrid zone. Considerable remelting of the country rock occurs around some basic dykes, and since at least the lower members of the Eriksfjord Formation are cut by dykes having a petrographic similarity to the lavas, it is reasonable to suppose that they acted as feeders for fissure volcanoes at the surface.

Xenoliths of anorthosite and gabbro-anorthosite are abundant in many of the early dykes ranging from doleritic to trachytic in composition, and often comprise up to 80% of the dyke. The texture and composition of the xenoliths suggest that they are derived from basic, layered igneous cumulates such as those found in intrusions of a similar age in eastern Labrador (Bridgwater, 1967). These "big feldspar dykes" are found throughout the Gardar province and hence suggest that wide areas are underlain by a substantial layer of anorthositic rock (Bridgwater and Harry, 1968).

The Gardar is best known for its alkaline intrusions, many of which probably represent the roots of central complexes connecting with surface volcanoes (Upton, in press). They vary in size from 2 to 30 km. in diameter and their relative ages are spread throughout most of Gardar time. Some complexes such as Grønnedal-Íka are early (about 1,200 My., Larsen, 1969) and have been cut by most of the Gardar dykes and faults of the area, but others, such as the Ilímaussaq complex, are very late (about 1,020 My., Bridgwater, 1965) being cut by few dykes and being relatively unaffected by faulting. The Igaliko complex is comprised of several intrusive centres and was active over a considerable period of time, since early intrusions are cut by both dykes and faults which become less prominent in the latest intrusions.

The complexes are invariably salic in character with augite syenite, quartz syenite, foyaitic nepheline syenite and alkali granite being the predominant rock types. Small amounts of alkali gabbro are occasionally present, but are very subordinate and usually occur as late ring dyke structures. Carbonatite magma was intruded at a late stage into the Grønnedal-Íka complex and several late sheets and dykes of carbonate rock are found at Igaliko and elsewhere. Igneous layering, with associated feldspar lamination and cumulus textures, is found in nearly all of the centres, with rhythmic, gravity stratified, inward dipping layers being the most common. These are well seen in certain units of the Ilímaussaq complex (Ferguson, 1964, 1970; Sørensen, 1969). In other intrusions (e.g. Kûgnât) cryptic layering has been recorded (Upton, 1960). Most of the better known layered complexes are reviewed by Wager and Brown (1968). Field evidence suggests that the intrusions were permissive, having been emplaced by cauldron subsidence and stoping, and once established, the earlier intrusions usually acted as foci for later pulses of magma so that many of them are composite.

Differentiation sequences due to fractional crystallisation, either at depth or during emplacement, are known from many of the complexes, and it is found that there are two categories: (a) the oversaturated, proceeding from augite syenite through quartz syenite to alkali granite with increased fractionation; and (b) the undersaturated, passing from nepheline bearing augite syenite to foyaites and other highly undersaturated, derivatives. In each case, petrographic and field evidence suggests an immediate parental magma of augite syenite composition, which plots close to the high temperature thermal barrier in the "residua system". Hence, small variations in the composition of this magma would result, during subsequent fractionation, in a trend towards either the oversaturated granitic minimum or the undersaturated minimum close to the composition of nepheline syenites. Deviations from these ideal trends do occur, notably in the Ilímaussaq complex, (Sørensen, 1966; Upton, in press).

The existence of layered basic igneous bodies at depth is indicated by the presence of gabbroic and anorthositic xenoliths in the "big feldspar dykes", so it is reasonable to suppose that the Gardar rocks were developed by fractionation of an alkali olivine basalt magma in deep crustal or upper mantle reservoirs. These were tapped to produce the regional dyke swarms and lava sequences, with early crystallisation, forming horizons of gabbro and anorthosite, depleting the magma in Ca, Al and Mg. Thus the upper parts of the reservoir were enriched in alkalis and silica to form a syenitic magma as an immediate parent for the major intrusions.

The province is cut by many faults which play an integral part in the siting of major intrusive centres, and in the development of the province as a whole (Berthelsen and Noe-Nygaard, 1965). A conjugate set of transcurrent faults consisting of large east or east-south-east, sinistral dislocations and a subordinate dextral set trending between  $N30^{\circ}E$  and  $N30^{\circ}W$  determine the principal structural blocks of the province (Fig. 1.1). Other shear zones and minor faults occur, trending east-north-east, to north-east parallel to the grain of the pre-Gardar basement. This is also the dominant direction of dyke emplacement, and determines the course of the larger fjords in the area.

The major east-south-east sinistral faults often have displacements of several kilometres with an aggregate of between 15 and 20 km. over the whole area. In some cases the faults were active prior to Gardar times (Henriksen, 1960), but the majority were probably a Gardar development being intermittently active throughout the period. Most of the major intrusions are located at the intersections of east-south-east transcurrent faults with one of the three main zones of north-east trending dykes, suggesting that the faults exerted a considerable structural control on the magmatism. The dykes presumably indicate the positions of elongate magma chambers, above which the major intrusives were emplaced during periods of stress release.

Vertical movements on the Gardar faults are generally more difficult to prove. Faults along several of the north-east trending shear zones, must have a considerable vertical movement, and those responsible for the outcrop of the Eriksfjord Formation have a maximum throw of 2 to 3 km. which gradually lessens north-eastwards. A throw of up to 2 km. during the pre-Gardar development of one of the east-south-east sinistral faults has been postulated (Henriksen, 1960) although in general these faults show little more than a few hundred metres of vertical movement.

(1c) The Igaliko Nepheline Syenite Complex

The Igaliko Complex is situated at about 61°N and 45°W covering an area of about 450 square kilometres of mountainous country between Tunugdliarfik and Igaliko Fjords and the inland ice (Fig. 1.1). Plate 1 is the map of the complex prepared by Emeleus and Harry (1970) on which slight modifications made in the light of the present work are shown.

Four major intrusive centres were emplaced in the apparent sequence Motzfeldt, North Qôroq, South Qôroq and Igdlerfigssalik, with the centre of activity precessing in an anticlockwise direction with time. Smaller satellitic stocks, partial ring dykes and inclined sheets are also present, and most units of the complex are cut by dykes associated with the regional Mid-Gardar swarms. Igneous activity began in the Mid-Gardar since the Eriksfjord sediments and lavas, and an early dolerite dyke are cut by the earlier centres. However, it would appear that at least four later intrusions in the Igdlerfigssalik Centre belong to the Late-Gardar since they post-date most of the dykes, although Emeleus and Harry (1970) consider them to be slightly earlier than later members of the Ilímaussaḡ Intrusion and Tugtutôḡ Central Complex. (Since dykes cutting the late Igdlerfigssalik syenites are displaced by east-south-east sinistral faults related to those cut by the Ilímaussaḡ Intrusions).

Each centre is made up of several intrusions having arcuate, steep sided outcrops with discordant intrusive relationships towards earlier members. They are all high level intrusions since they cut the Early-Gardar basalt/sandstone cover. Their mode of intrusion was principally by ring fracture and block subsidence, and some of the intrusions appear to be ring-dykes and partial ring-dykes. Concentric, inward dipping internal structures defined by igneous layering and mineral lamination are common within several individual intrusions. These are often sharply truncated by later intrusions within the same centre, suggesting a reasonable time lapse. However, in other cases contacts are rather diffuse, marked only by a zone of marginal pegmatites, suggesting rapid, successive pulses of magma from the same source.

All members of the Igaliko Complex are silica - undersaturated, nepheline bearing rocks, except where contamination with country rock has occurred. By far the most common rock type is "foyaite" consisting principally of perthitic alkali feldspar, nepheline and alkali clinopyroxene with alkali amphibole, biotite, iron-titanium oxides, sodalite and apatite. Slightly less fractionated syenites are termed "augite syenites" and are similar mineralogically and texturally to the Oslo larvikites (Barth, 1944). Alkali gabbro ("essexite") is present in small amounts as discontinuous wide dykes and partial ring dykes. Within the syenites, pegmatitic areas are common (particularly towards the margins) and veins of pegmatite up to 1 m. wide, often rich in carbonate, cut some of the units.

#### (1d) Previous Work

A detailed history of investigation of the Igaliko Complex as a whole is given by Emeleus and Harry (1970, pp. 14 - 16), including the surrounding country rocks, the famous pegmatite locality at Narssârssuk and the Gardar dyke swarm. The following is a summary of previous work relevant to the South Qôroq Centre.

The Igaliko area was visited during the early years of the 19th century by Giesecke who made notes on the rocks of the area, including a "granite" at Qôroq (Giesecke, 1910 pp. 36-37, 216-218). However, the presence of a large area of nepheline syenite was not known until the start of detailed geological and mineralogical investigations in South Greenland (Steenstrup and Kornerup, 1881; Flink, 1898). The first detailed mapping in the area was done by N. V. Ussing and O. Bøggild, mainly on the coast sections between Narssarssuaq and Qôroq and around Flinks Dal (Ussing, 1894; 1912). They were the first to distinguish between a marginal group of "Augite Syenites" (probably mainly in the Igdlerfigssalik Centre) and the remainder, most of which were termed foyaites of the "Korok Type". The latter were extensively developed around Qôroq Fjord and are probably equivalent to syenite SS5 of the South Qôroq Centre. Ussing also recognised many dykes of syenite porphyry and tinguaité cutting these syenites, west of Qôroq Fjord and in Flink's Dal.

After Ussing's work the investigations were extended to the south-east by Ødum (1927) into the area which includes the Østfjordsdal satellitic syenite, but the next major contribution was made by Wegmann (1938) during a broad reconnaissance survey of the area south of Frederikshåb. In the Igaliko area this work was concentrated mainly around the valley at Narssarssuaq and on the Narssarssuaq - Qôroq coast section. Wegmann (op.cit., p.81) came to the conclusion that the nepheline syenites originated by migmatitic transformation of pre-existing rocks (a similar origin was also proposed for the Ilímaussaq Complex), and claimed to have found relic earlier dykes within what is now termed the North Qôroq Centre. This hypothesis was followed by Bondam (1955) in an investigation of some trachyte dykes, but is not now generally accepted.

Emeleus and Harry (1970) give a detailed map of the whole Igaliko Complex, and a general description of the petrography and field relationships. The mapping was carried out jointly in 1961, 1962 and 1963 with further visits by C. H. Emeleus in 1966 and 1969 after the death of W. T. Harry. Their

original field diaries and G.G.U. internal field reports were available for consultation throughout the present work. Most of the mapping of the South Qôroq Centre (particularly on the Narssarssuaq - Qôroq peninsula) was carried out by C. H. Emeleus, but W. T. Harry mapped the lower Flinks Dal area, and certain coast sections were investigated jointly.

(1e) Sampling

Over most of the South Qôroq Centre exposure is good and in general there are no great problems in sampling. The rocks are usually fresh, but very coarse grained and hence large samples are necessary in order to obtain a representative analysis. Samples were available from most parts of the centre from the collecting of Emeleus and Harry, and further sampling was carried out by the author in 1969. However, the south eastern part of the centre is difficult to gain access to and hence has neither been mapped or sampled in great detail. Thus this work is based mainly on samples from the Narssarssuaq - Qôroq peninsula, lower Flinks Dal and lower Gieseckes Dal. It is also difficult to obtain samples from the steep sides of the fjords and hence the vertical extent of sample cover is mainly restricted to sea level and over 500 m. O.D.

The sequences of G.G.U. sample numbers used in this investigation are listed in Appendix IV together with their respective collectors and year to facilitate reference to original field diaries. The specimen localities are shown on Plate 1A.

Plate 2

Panoramic view south-east from the 970 m. summit of the Narssarssuaq - Q̄roq plateau towards Giesecke's Dal. The outer contact of the South Q̄roq Centre with Julianehåb Granite can clearly be seen on the left, on the slopes of Q̄rqp qaqai. Much of the area around Giesecke's Dal consists of the south-eastern part of the South Q̄roq Centre, but the mountains on the right are in the Igdlerfigssalik Centre. The rubbly surface of the plateau in the foreground is composed mainly of syenites SS3, SS4 and SS5.

Аӧрқуп қақай

Giesecke's Dal

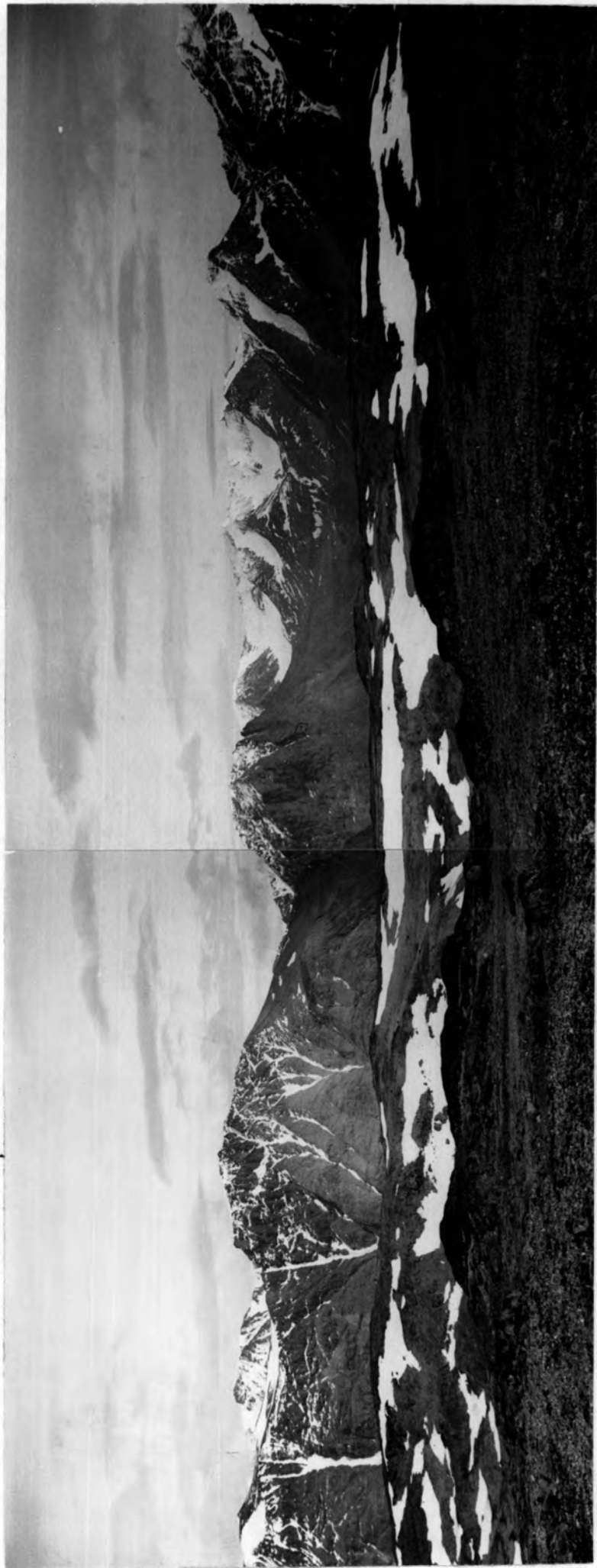
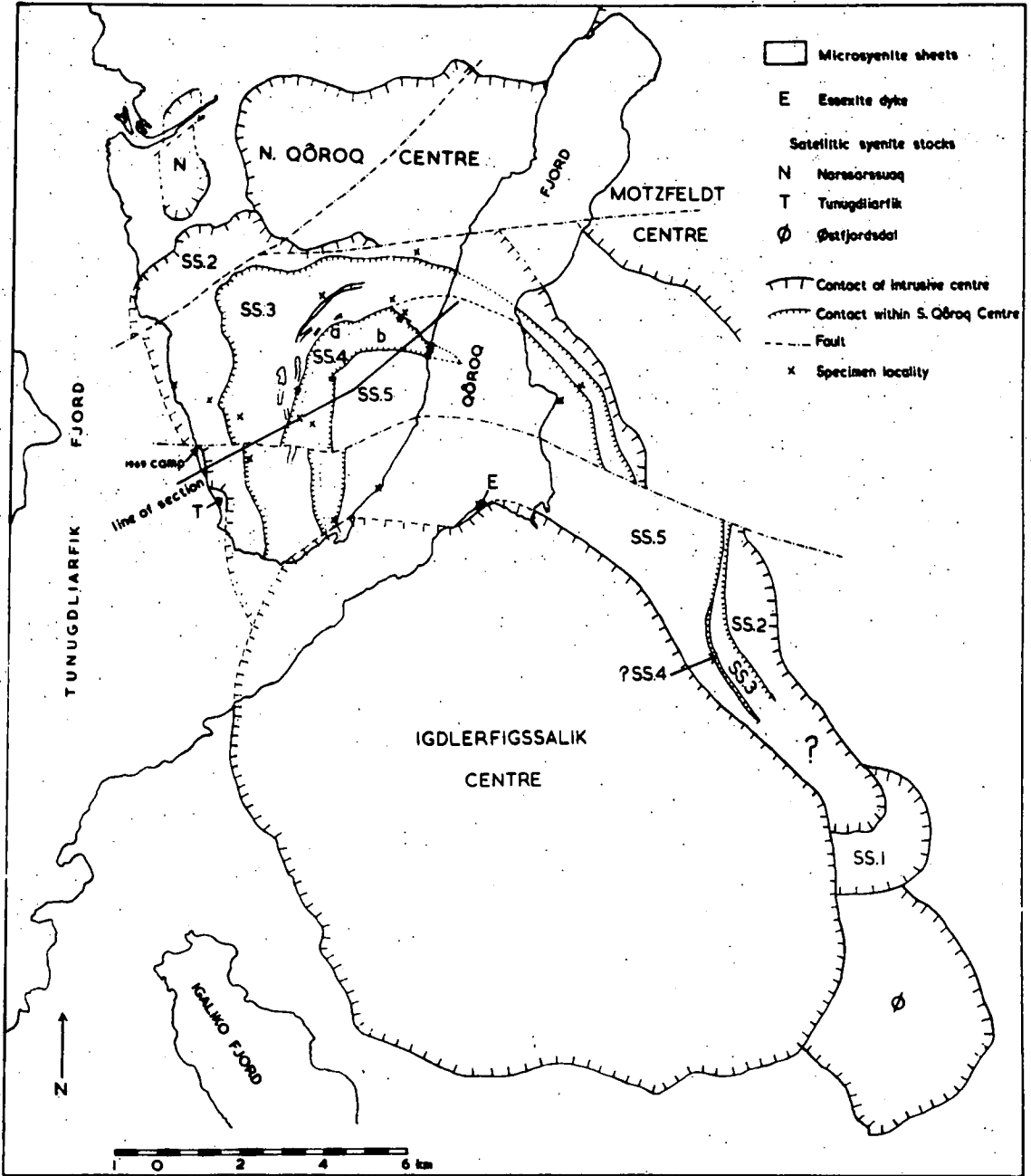


Fig. 2.1

The South Qôroq Centre showing major units within the centre, satellitic intrusions and principal faults. The locations of samples used for electron microprobe analysis are shown by crosses. (Modified after Emeleus and Harry, 1970).



## 2. FIELD RELATIONSHIPS OF THE SOUTH QÔROQ CENTRE

The South Qôroq Centre consists of four concentric syenite intrusions (SS2, SS3, SS4 and SS5) (Plate 1; Fig. 2.1). Four smaller earlier stocks occur around the periphery of SS2, and SS3 is cut by several inclined sheets of microsyenite which appear to focus on SS4. Pegmatites are fairly common throughout the centre. The only basic rock is a short, 100 m. wide essexite dyke cutting SS5. From the recent field studies and laboratory investigations SS4 is now considered to be a partial ring dyke, consisting of two or possibly more pulses and the order of intrusion (as given by Emeleus and Harry, 1970) has been modified to SS2 - SS3 - SS5 - SS4a - SS4b.

The centre is cut by many trachytic dykes of the Mid-Gardar regional swarm. Outside the centre and elsewhere in the Igaliko Complex these have a fairly constant trend of about  $060^{\circ}$ , but in the Narssarssuaq - Qôroq peninsula they undergo an unusual 'S' shaped deflection, so that their trend becomes between  $000^{\circ}$  and  $015^{\circ}$ . This would appear to be related to the regional faulting (see section 2e).

### (2a) The South Qôroq Centre Syenites

#### (i) Syenite SS2:-

This is the earliest syenite in the centre with an extensive distribution, and has an outcrop 0.25 - 1.5 Km. wide around most of the centre. It outcrops extensively east and south of Narssarssuaq, particularly on the Tunugdliarfik coast section; and high up on the north east side of Giesecke's Dal.

The rock is a medium to coarse grained, non porphyritic, grey nepheline syenite, which is very distinctive in the field on account of characteristic "mossy", poikilitic aggregates of mafic minerals. It is very homogeneous, apart from becoming finer grained towards its outer contact, as is well seen on the Tunugdliarfik coast section. Within 100 m. of outer contacts, the fine grained facies of SS2 develops a weak, vertical flow lamination of tabular feldspars, which becomes more pronounced nearer the contact.

In the normal rock the feldspars occur as thin tablets, often showing twinning and measuring 10 x 1 mm. although in the marginal facies they are only 3 mm. long. Nepheline occurs as grey interstitial areas when fresh, but is more conspicuous on weathered surfaces, where it has a milky white appearance. The "mossy" aggregates of mafics are generally about 10 mm. across and constitute up to 20% of the rock.

Pegmatites are not common in SS2, but a few isolated veins occur, near the contact on Akuliaruseq, and in the Tunugdliarfik coast section. The latter are up to 1 m. thick and contain large crystals of feldspar, long prismatic blades of pyroxene perpendicular to the contact, and nepheline (Plate 3). Some horizontal veins are composite, and appear to be differentiated with dark green pyroxene in the lower part becoming lighter green upwards (see 4b) towards a carbonate-rich core. Occasional pegmatitic patches contain prismatic feldspar and pyroxene with a white, lustrous mica (? polyolithionite). The syenite is normally free from inclusions, but on the Tunugdliarfik coast numerous small, rounded or oval, dark inclusions occur, and near the contact with the Tunugdliarfik Syenite (Fig. 2.1) there are inclusions of dark, mafic syenite.

(ii) Syenite SS3:-

This syenite has an arcuate outcrop inside that of SS2. It outcrops extensively on the Narssarssuaq - Qôroq peninsula over a zone 1 km. wide, and also on the north-east side of Giesecke's Dal as a narrow .25 km strip, south-west of SS2. The rock is a coarse grained nepheline syenite, grey or pinkish in colour, and characterised by very large blade-like or tabular crystals of perthitic alkali feldspar up to 30 x 7 mm. which commonly show simple twinning in hand specimen. Nepheline tends to be intergrown with the feldspar and occurs as small pinkish or milky white grains. The remainder of the rock consists of irregular, interstitial areas of mafic minerals up to 10 mm. wide (Plate 4).

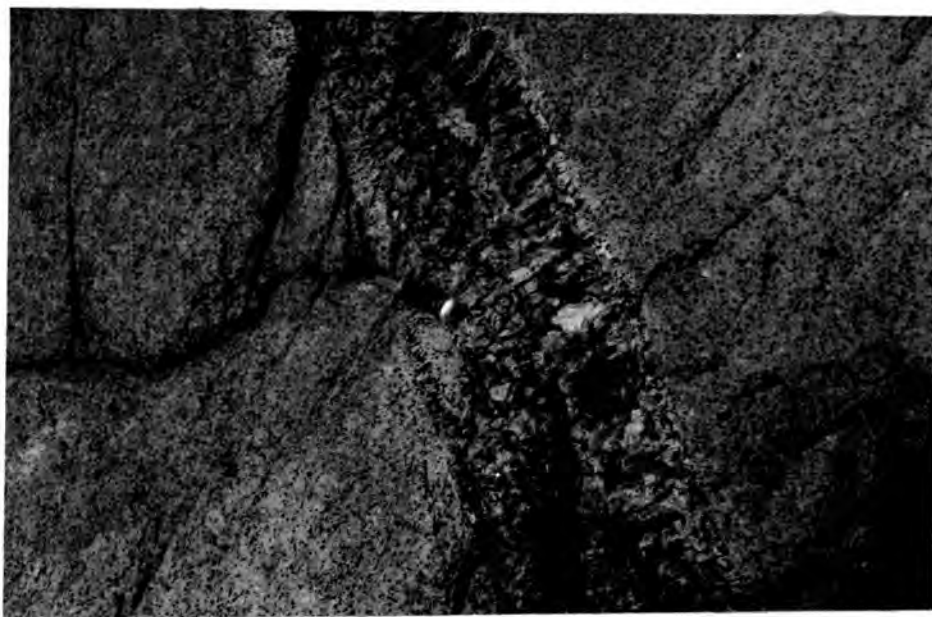


Plate 3

Pegmatite vein cutting through syenite SS2 on the Tunugdliarfik coast section. Large crystals of aegirine (see analyses of 127071 in section 4b) can be seen growing perpendicular to the walls. Note the "mossy" aggregates of mafics visible in the SS2. (Knife is 22cm long.) Photo: B.G.J. Upton.

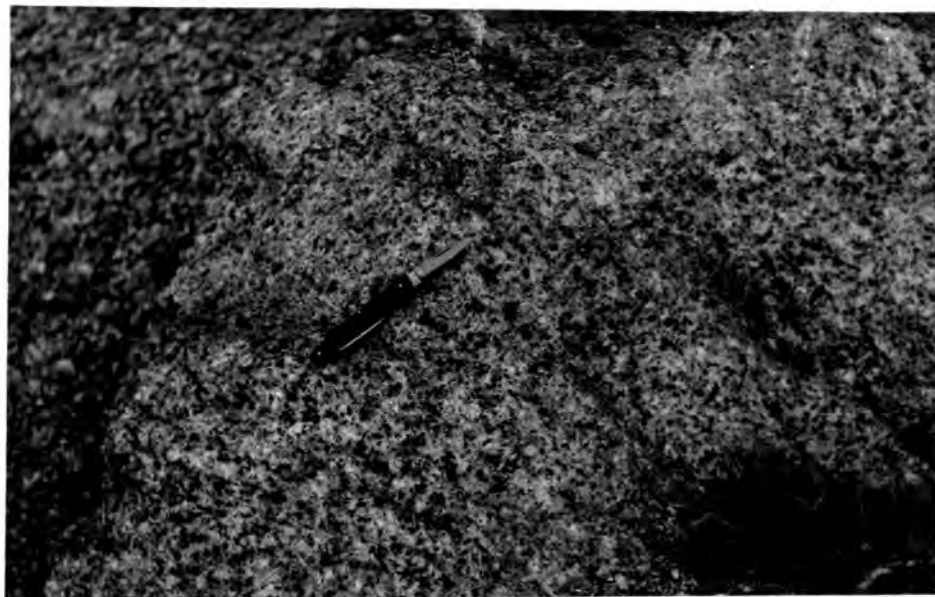


Plate 4

Surface of typical, coarse grained SS3 showing blades of alkali feldspar, dark mafic areas and interstitial areas of red-weathering altered nepheline. Narssarssuaq - Qôroq peninsula. (Penknife is 13 cm long.)  
Photo: C.H. Emeleus.

Slight variations in texture occur over the outcrop, mainly due to the degree of development of tabular feldspars. However, there is a marked decrease in grain size towards the contact with SS2 and in some places SS3 looks almost like a coarse variety of SS2 with large "mossy" aggregates of mafics. The rock is usually massive with no mafic banding and only occasional feldspar lamination. Where present the laminations dip inwards at low to moderate angles.

Pegmatites are quite common in SS3 and are usually quite leucocratic, although some have a high proportion of pyroxene prisms. In several localities marginal pegmatites contain large, euhedral crystals of red eudialyte (e.g. west of Flink's Dal). An unusual pegmatite just south of the 970 m. summit contains blue sodalite, sulphides and carbonates.

(iii) Syenite SS5:-

SS5 is the innermost of the South Qôroq syenites and outcrops extensively on the Narssarssuaq - Qôroq peninsula, around lower Flink's Dal, in Geisecke's Dal, and on Agdlerulik Mountain. An area north of the SS4 outcrop on the west side of Qôroq Fjord, previously assigned to SS3 by Emeleus and Harry (1970) is now known from petrographic and mineralogical data to be SS5 (see amendment on Plate 1). The pyroxene compositions lie within the range found in SS5 (see 4b) and features of mafic banding etc. match those found in SS5 on the opposite side of Qôroq Fjord, rather than SS3. There is also a small outcrop on the south side of Geisecke's Dal Bay, where SS5 is cut by the wide essexite dyke, both being cut out by the Igdlérfigssalik syenites to the south.

The rock is a coarse grained foyaitite with tabular alkali feldspars up to 30 x 3 x 2 mm. in size. In some outcrops it resembles SS3, but generally it is coarser and is characterised by a well developed feldspar lamination. The feldspar is usually twinned and is accompanied by greyish or white nepheline up to 1 cm. wide, which commonly becomes red on alteration.

Mafic minerals occur as interstitial aggregates in which biotite and olivine are conspicuous in hand specimen, the latter as rusty brown grains. Areas of irregular pegmatite are common throughout the syenite and are well seen on the Qôroq coast sections.

The feldspar lamination is usually very regular, strikes parallel to the contacts, and dips inwards towards the centre of the intrusion (Plate 6). Near the margin the dips are about  $70^{\circ}$ , but they become shallower towards the centre ( $20^{\circ}$ ). Occasionally mafic mineral layering is present, conformable with the lamination, and south of Flink's Dal, Harry (field diary, 1961) records a zone several metres wide of dark grey microsyenite inclusions 10 - 20 cm. long, orientated parallel to the lamination. On the west side of Qôroq Fjord 2 km. north-north-east of Niaqornarsuk, Emeleus and Harry (1970, p.49, Fig.17) record some brecciated mafic layering in loose blocks, in which laminated structures wrap around the mafic layers. Further along Qôroq Fjord west-north-west of the end of Flink's Dal, lenticular inclusions of mafic material containing normal syenite in their centre are aligned parallel to a faint lamination which dips southwards at  $50^{\circ}$  (Plate 7). The lamination is distorted slightly around the inclusions, which are up to .5 m. long and are discoidal or spindle shaped in three dimensions. When spindle shaped, their longest axis lies in the strike of the lamination. As well as the mafic margins there are also other mafic concentrations on the inside forming semiconcentric loops and spiral structures. They do not appear to be corroded xenoliths and seem more likely to be mafic schlieren or poorly formed mafic bands disturbed and "rolled up" during slumping of a partly consolidated crystal mush.

(iv) The SS4 Syenites:-

The syenite SS4 has an arcuate outcrop of maximum width 1 km. on the Narssarssuaq - Qôroq plateau between syenites SS3 and SS5. The outcrop narrows considerably to about .25 km. on the coast of Qôroq Fjord, opposite Flink's Dal, and SS4 does not appear to outcrop to the east of the fjord except possibly for a narrow strip between SS3 and SS5 on the south side of Agdlerulik Mountain. Emeleus and Harry (1970) consider that SS4 has been

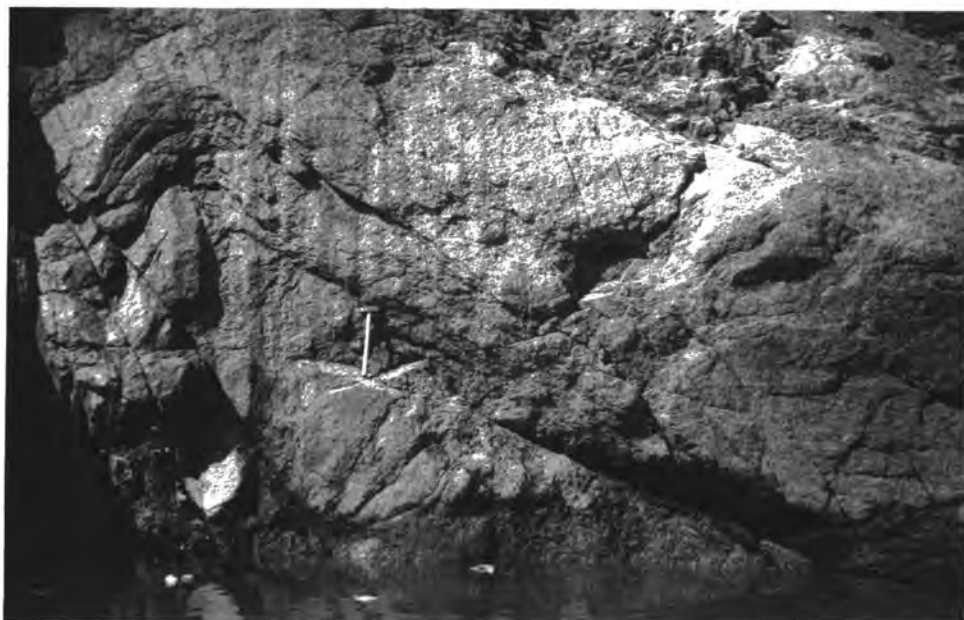


Plate 5

Vertical mafic banding in syenite SS4b - west coast of Qôroq Fjord.

(Hammer shaft is 35 cm long.)



Plate 6

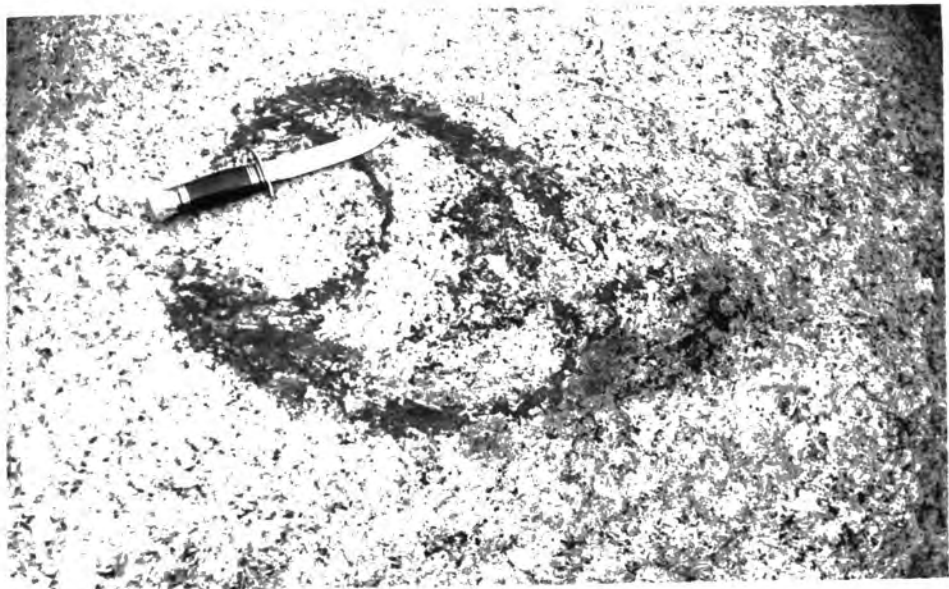
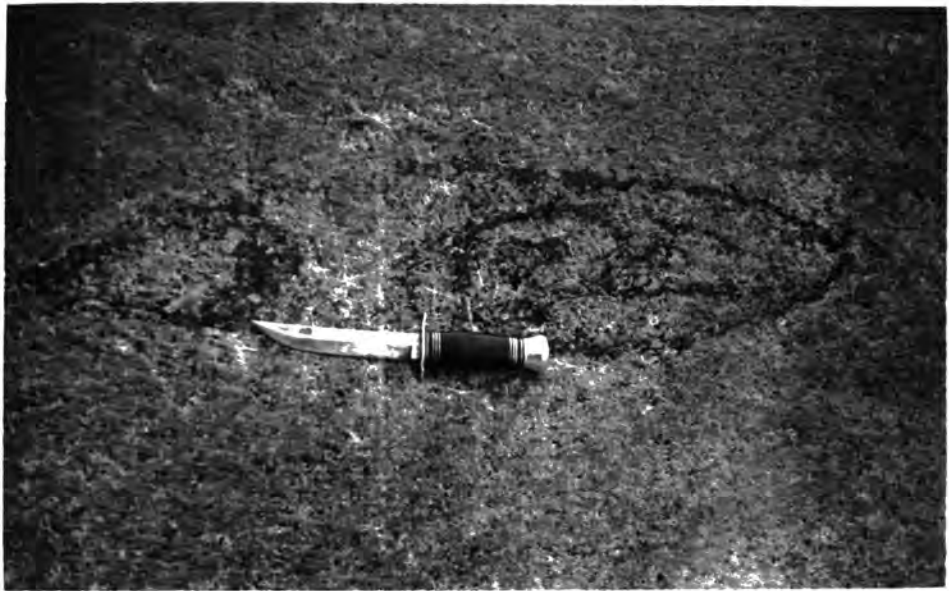
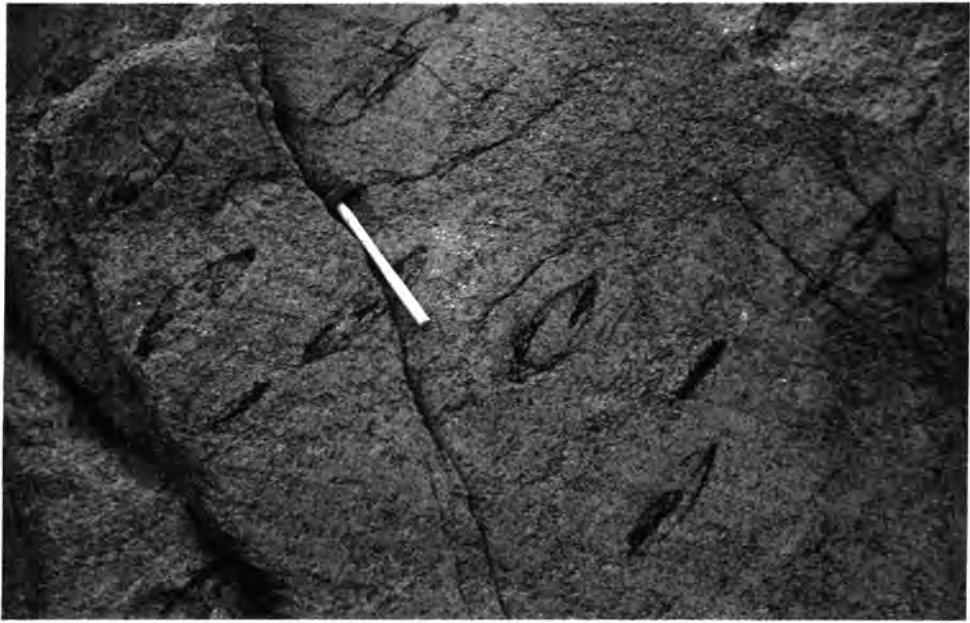
Igneous lamination in syenite SS5 dipping inwards, towards the centre of the intrusion at  $25 - 30^{\circ}$  - west coast of Qôroq Fjord. (Hammer shaft is 35 cm long.)

Plate 7

Slumped mafic schlieren in syenite SS5 - west coast of Q8roq Fjord.

- (a) General view of the outcrop with schlieren aligned parallel to a faint lamination of platy feldspars.
- (b) Section perpendicular to the lamination.
- (c) Section parallel to the lamination.

(Knife is 22 cm. long. Hammer shaft is 35 cm. long.)



partially cut out by a later SS5, but there is now strong evidence from field and laboratory data suggesting that SS4 is a later partial ring dyke intruded along the SS3/SS5 contact (see 2b).

The rock is in general an equigranular, medium to coarse grained nepheline syenite, having stumpy crystals of feldspar measuring up to 10 x 5 mm. In fresh outcrops the feldspars are often schillerised, giving the rock a dark, bluish-grey colour and a characteristic "larvikitic" appearance. Mafic minerals occur interstitially or in shiny, black aggregates in which olivine is quite prominent. Nepheline is not very conspicuous in hand specimen, and in general the rock is less fractionated than the other South Qôroq syenites, which have a foyaitic nature. The texture of the rock is quite variable from outcrop to outcrop and there may be two or more separate syenites (see below).

Feldspar lamination is only occasionally found in SS4, but mineral layering is present and is particularly well exposed on the west side of Qôroq Fjord, where finer grained mafic bands, rich in olivine and pyroxene, alternate with coarser, more leucocratic syenite in bands 10 - 20 cm. thick. The layering is steep to vertical and appears to parallel contacts (Plate 5).

In the Qôroq Fjord section a marginal facies is developed within the SS4 syenite. This consists of irregular pegmatitic patches with intervening fine grained syenite and is typical of marginal nepheline syenites in the Igaliko Complex. There thus appears to be a contact between two larvikitic-looking syenites, the northern one being characterised by more platy feldspars. The southern syenite contains the marginal facies and hence appears to be the younger, and also contains mafic banding younging to the south (Fig. 2.2). For the purpose of further work SS4 has been divided into two units, SS4a and SS4b, the latter being younger than the former and occupying the inner part of the arcuate SS4 outcrop shown in Plate 1.

From petrographic and mineralogical work there is evidence to suggest

Fig. 2.2

Sketch section of the west side of Qôroq Fjord opposite the entrance to Flink's Dal, showing contact relationships between syenites and internal structures. 'P' = areas of marginal facies pegmatites.

Fig. 2.3

Cross section of the South Qôroq Centre across the Narssarssuaq - Qôroq plateau, from Tunugdliarfik Fjord to Qôroq Fjord. (cf. Emeleus and Harry, 1970, Fig. 18). Contacts with good evidence of age relationships are shown with shading on the younger side. See Fig. 2.1 for line of section.

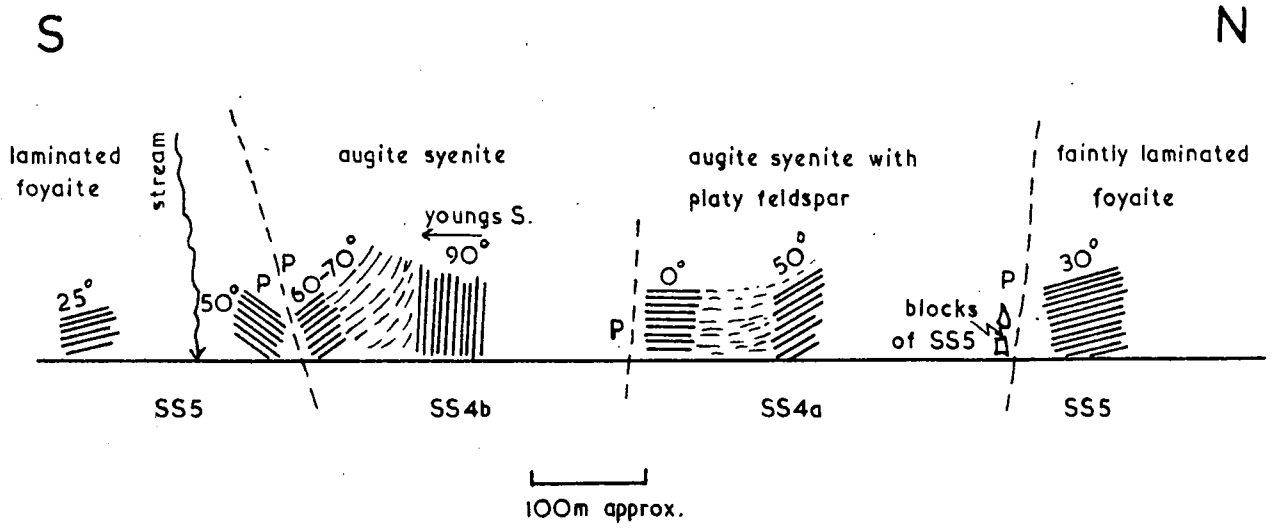


Fig. 2·2

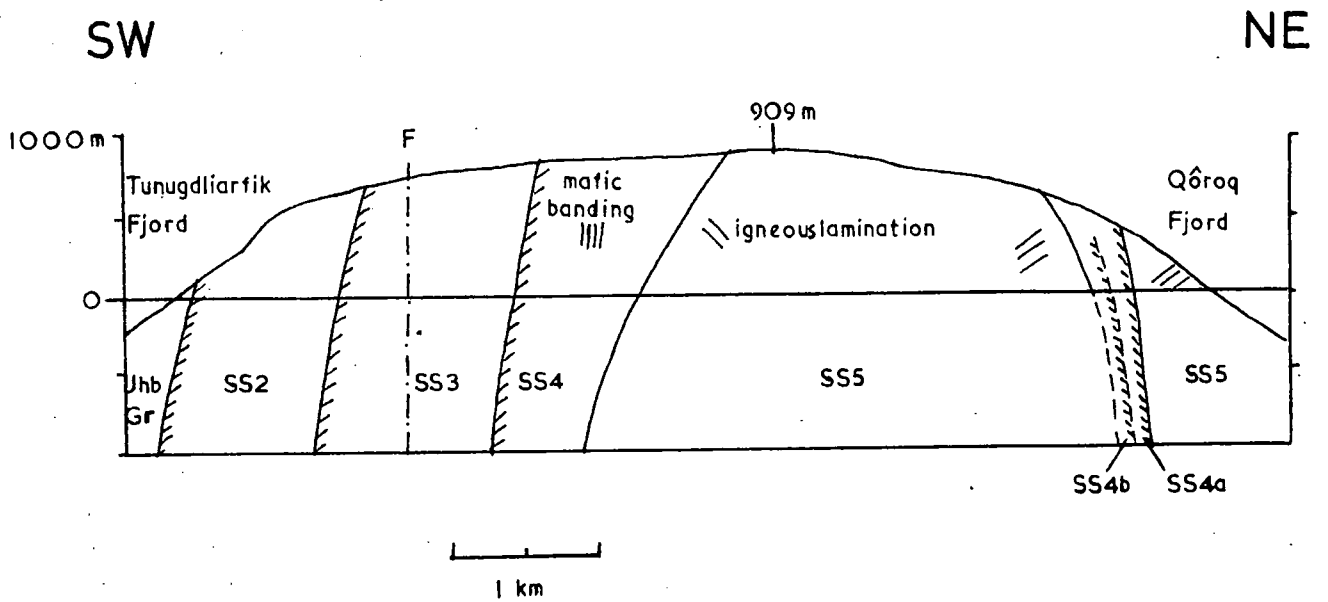


Fig. 2·3

that there are possibly several pulses of magma comprising SS4, which varies considerably across its width. The basic ring dyke at Kûngnât also has a variable petrography and Upton (1960) records internal contacts in certain areas.

(v) Satellitic Syenites and Other Intrusions:-

Around the margins of the South Qôroq Centre are four satellitic intrusions of nepheline syenite, if one regards SS1 as a satellite. The Tunugdliarfik Syenite, the Østfjordsdal Syenite and SS1 are all cut by the main centre, but the age relationships of the Narssarssuaq stock are uncertain.

SS1 occupies a small, fairly inaccessible area on the south-east margin of the centre. The trend of the outer contact with country rock is similar to the trend of the SS2 contact, and for this reason Emeleus and Harry (1970) include it as the earliest member of the South Qôroq Centre proper. Occasional weak feldspar laminations dip inwards towards the centre, but the rock is generally massive. It does not appear anywhere else and hence is included as another satellitic intrusion.

The Tunugdliarfik Syenite appears to be a marginal facies over much of its outcrop, with patchy pegmatitic areas, although further to the south it becomes a more regular leucocratic syenite. The bulk of the rock, as seen on the hillside above the coast, is a coarse, larvitic looking syenite with tabular feldspar measuring 2 x 3 cm., poikilitically enclosed by 3 - 4 cm. mafic areas. Nepheline is present mainly as euhedral inclusions in the mafics.

The Østfjordsdal Syenite has a slightly elliptical outcrop at the south-east end of the centre. It is cut by SS1, but is younger than a distinctive early group of nepheline porphyry dykes. The rock is fairly coarse grained with tabular alkali feldspar (30 x 10 mm.), grey-green nepheline and interstitial aggregates of mafics. There are several variations to the syenite including a fine grained marginal facies, and a medium grained variety occurring around numerous inclusions of quartzite and basic rock (? derived from the Eriksfjord Formation). Feldspar lamination is developed parallel to the outer contact

and in the centre of the intrusion there is a suggestion of mineral layering.

The Narssarssuaq Syenite occurs in a small, steep sided intrusion cutting the Eriksfjord Formation near Narssarssuaq. Its age relationships to the South Qôroq Centre are not established, but it is cut by the regional dyke swarm. The rock type is medium grained, equigranular nepheline syenite which is commonly weathered to a dull brown colour, fresh specimens being rare. Sporadic xenoliths of porphyritic syenite are found.

The South Qôroq Centre syenites are cut by several inclined sheets of microsyenite. Most of these occur in SS3 on the Narssarssuaq - Qôroq plateau, dipping steeply inwards and apparently focussing on SS4. They vary in width from 50 - 100 m. and are usually laminated, although considerable variations in texture and colour can be found. Some varieties are porphyritic, the lamination being due to alignment of platy feldspars separated by mafics and brick-red weathering nepheline. SS4 is not cut by such sheets and it would appear as though they are off-shoots related to this later syenite, as they centre upon it and fresh samples often bear a resemblance to the SS4 rock types. Microsyenite sheets also occasionally cut the country rocks particularly near the SS2/basalt contact around Narssarssuaq.

On the south side of Giesecke's Dal Bay, SS5 is cut by a 100 m. wide alkali gabbro ("Essexite") dyke, which trends north - south for 200 m. before being cut out by SI2. Near vertical mafic banding is present in some places and there is a pronounced chill against SS5, although the contact is complex in detail due to reaction with the syenite. In the centre of the dyke large blocks of SS5 are included and these tend to be pegmatitic. The dyke is entirely within the zone of alteration due to the later Igdlerfigssalik Centre (see below, 2d).

## (2b) Internal Contacts within the Centre

### (i) SS2/SS3:-

Syenite SS3 has a central position within SS2, becomes finer grained towards the contact, and develops irregular pegmatitic areas. These marginal

facies pegmatites are common throughout the Igaliko Complex and consist of coarse, irregular patches of feldspathic pegmatite, separated by interstitial areas of fine grained nepheline syenite (Plate 9). Hamilton (1964) records similar marginal pegmatites from the Ilímaussaḡ Augite Syenite and the Narssaḡ gabbro. He suggests three possible modes of origin:-

- (a) local accumulation of trapped water and volatiles,
- (b) the first stage in a build up of water and volatiles moving outwards under a thermal diffusion gradient,
- (c) an alkali rich liquid derived from selectively remobilised country rock.

In the South Qôroḡ Centre, in view of the marginal nature of the pegmatites, and the lack of evidence for remobilisation of surrounding syenites (except possibly for SS5 around SS4), (b) would seem to be the most likely explanation. (The pegmatites may thus be compared with the drusy marginal facies of other high level intrusions.) Whole rock geochemistry supports this interpretation in that it provides further evidence for thermal gradients (see Chapter 5).

Eneleus and Harry (1970) record a transitional passage from SS2 to SS3 over about 50 - 100 m., and in some localities this is clearly the case. However, in two separate outcrops, a sharp contact was found between the two syenites dipping outwards at 70 - 80°, demonstrating a true intrusive relationship. SS3 is not chilled and there is no alteration of SS2, but it is clear that SS3 is the later syenite, being intruded only a short while after SS2, before the latter had completely cooled (Plate 8). Hence in some areas a gradation between the two is produced, and as the two magma types are very similar they may represent two pulses from the same magma source (Harry and Richey, 1963).

(ii) SS3/SS4:-

This contact often appears to be gradational with SS4 becoming finer grained towards SS3 and developing a marginal pegmatite facies. However, in many places on the Narssarssuaḡ - Qôroḡ plateau the contact is ill defined due to bad exposure or alteration. Also, the relationships may be further

confused by the superimposition of two contact zones close together, due to several pulses within SS4 (see above) giving an unusually wide marginal zone. Above Niaqornarsuk the contact appears to be gradational over about 150 m. but SS4 becomes finer grained, and Emeleus (field diary, 1962) has found blocks of SS3 enclosed in SS4.

Thus SS4 is younger than SS3 and occupies a central position within the latter. The contact is xenolithic in places but varies from quite sharp to diffuse and somewhat gradational.

(iii) SS4/SS5:-

The relationship between SS4 and SS5 is problematic in that it is not absolutely certain from actual contact relationships which is the younger:-

SS5 is usually seen to become irregular in grain size, with pegmatitic patches near to SS4. Emeleus (field diary, 1962) records contact zones 10 cm. wide of mixed rocks and marginal type pegmatites, but no evidence anywhere of age relationships. He also records minor shearing in many places associated with the contact. Above Niaqornarsuk there is a slight decrease in grain size of SS4 towards SS5, although it is not as pronounced as in SS4 towards SS3.

On the north-west coast of Qôroq Fjord coarse, laminated SS5 is in contact with coarse, larvikitic looking SS4b to the north. The syenites on both sides of the contact are irregular with a marginal pegmatitic facies, and the contact is gradational over 0.5 m. The structure is obscured by much crushing and from the contact there is no evidence of age, but the general impression gained is that SS5 could be younger as the contact truncates mafic layers and schlieren in SS4b (Fig. 2.2). To the north SS4a is in contact with a syenite also now considered to be SS5 (see 2a, iv). The contact is sharper and, although relationships are still rather obscure, blocks of SS5 are found in SS4a, the latter having fine grained mafic banding, which increases in grain size away from the contact.

In general the SS4/SS5 contact is vertical or dipping steeply outwards,

but in the north it dips out at a moderate angle, and hence the outcrop width of SS4 is much reduced at fjord level (Fig. 2.3) and is eventually cut out on the east side of Qôroq Fjord. Although the detailed contact relationships give conflicting evidence of age in some cases, broader considerations tend to indicate that SS4 is a ring-dyke, younger than SS5. The crushing and vertical banding associated with its contacts, and the possible reduction in grain size towards both of its margins, with development of a marginal facies are consistent with this hypothesis. Furthermore, the identification of SS5 both north and south of SS4 on the west side of Qôroq Fjord makes it difficult to envisage any other mechanism. Ring-dykes of nepheline syenite are described by Emeleus and Harry (1970) in the Igdlérfigssalik and Motzfeldt Centres, but not from South Qôroq.

The petrography of the syenites would also seem to be consistent with SS4 being the latest syenite since, being larvikitic, it continues a trend towards more basic syenites with time. SS2, SS3 and SS5 are reasonably similar in mineralogy and hence could be three separate pulses from the same magma source. SS4 could then be a later tapping of a more basic magma from possibly lower down in the magma chamber. (c.f. later trend to more basic syenites and finally an alkali gabbro ring-dyke at Kûngnât - Upton, 1960). This hypothesis will be further developed in subsequent chapters. If there are two or more syenites in SS4 as suggested above, then these could represent several pulses of ring-dyke magma, possibly very close together. The apparent marginal facies seen in SS5 at some contacts could be due to alteration or remobilisation by the ring-dyke, or be a marginal facies developed prior to the intrusion of SS4.

(iv) SS3/SS5:-

As outlined above, SS4 does not outcrop on the east side of Qôroq Fjord and hence SS5 is in direct contact with SS3. This contact is seen on the coast section about 1 km. north of Flink's Dal entrance, but it can be traced inland at several localities, although locating the actual line is difficult as the two syenites are quite similar apart from the strong lamination usually

Plate 8

SS2/SS3 contact on the west side of the Narssarssuaq - Øbroq peninsula.

(a) General view of the contact showing outward inclination. (SS3 on the right)

(b) Close up showing the pegmatite developed along the edge of SS3, and the normal texture preserved in SS2.

(Pencil is 12 cm. long)

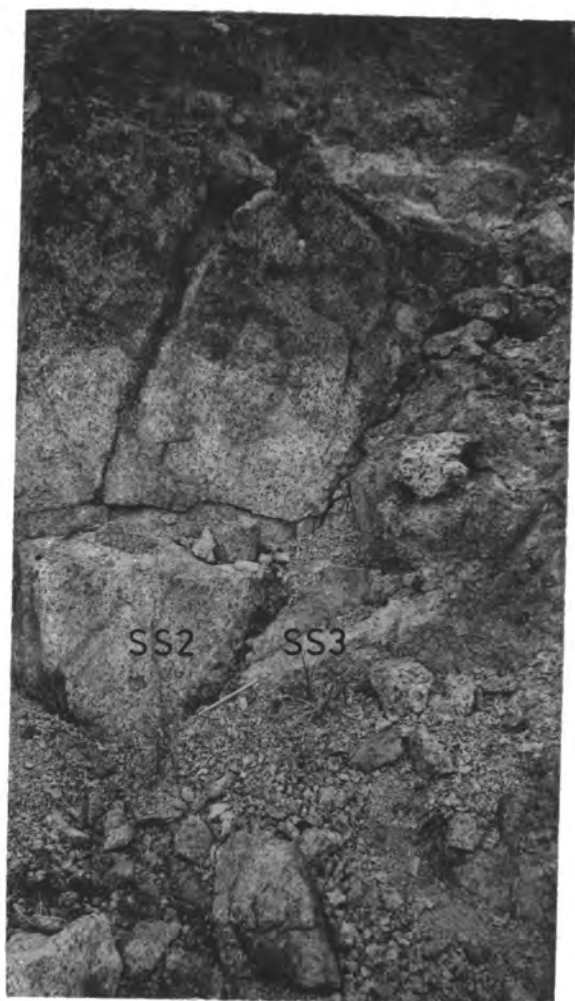




Plate 9

Marginal pegmatitic facies of SS5 near to the contact with SS3 - east coast of Qôroq Fjord. Note the irregular coarse areas separated by interstitial areas of fine grained syenite. (Hammer shaft is 35 cm long.)



Plate 10

Coarse grained lens containing biotite, calcite, pyroxene, magnetite and accessories in a metasomatised, magnetite-rich sill cutting Julianehåb Granite - Tunugdliarfik coast section. (Knife is 22 cm long.)

Photo: C.H. Emeleus.

developed in SS5. However, in the coast section a marginal facies is very prominent in SS5 (Plate 9) which is well laminated up to 50 m. from the contact.

(2c) Contacts with Country Rock

(i) Contacts with Julianehåb Granite:-

Julianehåb Granite forms the metamorphic basement into which the Igaliko Complex is intruded and consists of coarse granite and granite gneiss with veins and dykes of amphibolite. Where exposure is good, the line of contact can easily be seen from a distance and on air photographs, as the gravelly weathering, light grey syenites contrast strongly with dark, granitic outcrops. This is particularly well seen high in the cliffs above Giesecke's Dal, where the contact is seen to dip steeply outwards (Plate 2).

On the Tunugdliarfik coast and north of Flink's Dal, SS2 becomes finer grained towards the Julianehåb Granite, but still retains its small, mossy mafic aggregates, and is quite normal in appearance up to 50 m. from the contact. The outer 50 m. consists of a marginal pegmatitic facies with interstitial, fine grained syenite, veins of which penetrate into the granite. The actual contact, where seen, is quite sharp but is often obscured by gulley features.

Within a few metres of the contact the granite shows signs of alkali metasomatism, with thin veins and patches of a bluish-green amphibole, and in some cases the amount of quartz has been considerably reduced due to fenitisation. On the Tunugdliarfik coast section there are many irregular veins, about 2 m. thick, containing dark, magnetite-rich material, which are generally quite flat lying. Similar rock types are to be found in sill-like bodies and thicker veins, which look as though they may originally have been amphibolites. These are essentially dense, zoned magnetite - aegirine augite - biotite - hornblende rocks, 2 - 3 m. thick, with lenses of coarser material. The latter contain large "books" of biotite with calcite, pyroxene and interstitial fluorite, magnetite, perovskite, corundum, apatite and chlorite (Plate 10).

From the mineralogy and textural relationships of the above it is suggested that they are due to metasomatism around the syenites with a considerable introduction of alkali elements. The more regular dykes and sills were probably amphibolites in the basement, and it would appear that dykes, joints and fracture zones acted as channels for the metasomatic emanations, hence becoming much more altered than the surrounding granite which, except for a few metres around the contact shows very little thermal or metasomatic effect.

Near to the contacts, both SS2 and the Julianehåb Granite are cut by a few sheets of carbonatite. These are up to 0.5 m. thick and are sometimes zoned with an outer zone 5 - 10 cm. thick, rich in opaques, and an inner zone rich in mica. In section the carbonatite is seen to contain phlogopite, magnetite and haematite. In the zoned sheets, magnetite and haematite occur in equal amounts in the margins, but the centres have only magnetite with occasional haematite.

(ii) Contacts with Supracrustal Rocks:-

The supracrustal rocks which rest on top of the Julianehåb Granite are members of the Early-Gardar Eriksfjord Formation consisting mainly of basaltic lavas and tuffs with interbedded sandstones. Syenite SS2 is seen in contact with these in the area south-east of Narssarssuaq, where the bedding dips south or south-east towards the centre at about  $15^{\circ}$ , steepening to  $25^{\circ}$  near the contact. This effect is also observed around the Igdlerfigssalik Centre and suggests some form of collapse associated with the emplacement of the early syenites in each centre.

At the contact SS2 forms a persistent, sinuous cliff feature. The contact is irregular in detail, presumably following joint surfaces in the basalts and occasionally xenoliths of basalt up to 2 m. long occur, suggesting localised stoping during emplacement (Plate 11). It is usually sharp, with a 3 - 4 cm. wide chill, outside of which platy feldspars and occasionally mossy mafic aggregates are aligned parallel to the contact. In some places marginal pegmatites are developed, although they do not appear to be as extensive as



Plate 11

Sharp contact between marginal SS2 syenite and an angular, xenolithic block of basalt very near to the main contact - 1 km east of Narssarssuaq Harbour. (Hammer shaft is 35 cm long.)



Plate 12

Brecciated SS2/basalt contact exposed near the coast south of Narssarssuaq Harbour. (Hammer shaft is 28 cm long.)



Plate 13

"Knobbly" surface of hornfelsed basalt due to the weathering out of ophitic mafic patches - east of Narssarssuaq. (Hammer shaft is 35 cm long.)

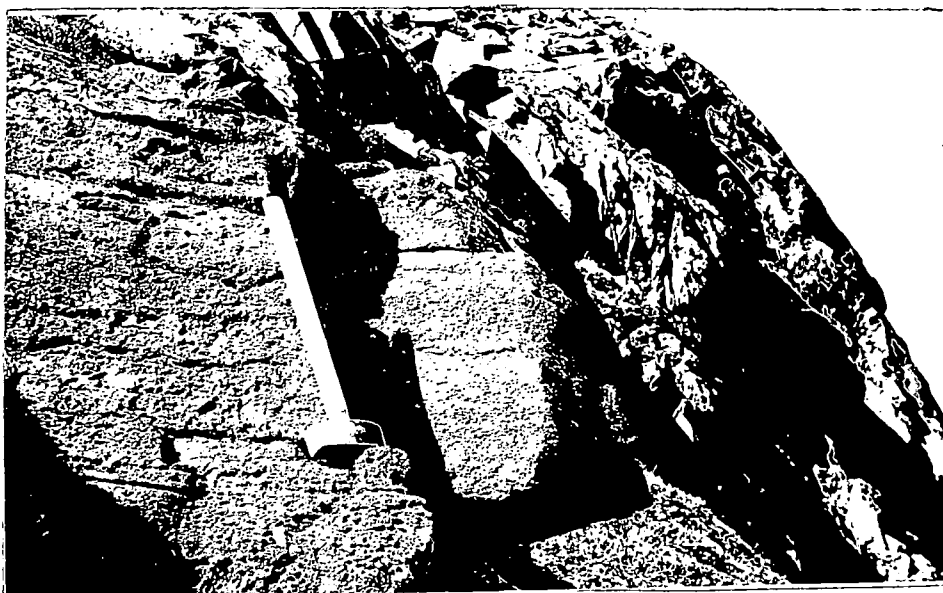


Plate 14

Basalt with calc-silicate bands presumably derived from calcareous tuffs. The massive outcrop in the background is of syenite SS2 - 1.5 km east of Narssarssuaq Harbour. (Hammer shaft is 35 cm long.)



Plate 15

Syenite SS5 cut by Igdlarfigssalik syenite SI2 on the south side of Giesecke's Dal Bay, Qôroq Fjord. (Hammer shaft is 35 cm long.)

at the contact with Julianehåb Granite, and do not form a wide zone.

Immediately south of Narssarssuaq Harbour the contact relationships are complicated by dykes and faults in the basalts. The actual contact has a breccia-like structure with blocks of syenite separated by stringers of basic material in a zone about 10 m. wide (Plate 12). The general impression is that the basic material has flowed around the syenite, although back veining of intermediate by more basic material seems unlikely. It would appear that either (a) at this particular locality there is an intrusion breccia developed, although it is not seen anywhere else; or (b) the structure is due to later faulting and shearing; or (c) there could be a combination of both mechanisms.

The supracrustal rocks exhibit quite widespread contact effects and the basalts tend to be hard and splintery with a "knobbly" hornfelsed appearance (Plate 13) due to dark, ophitic patches weathering out. Very near to the contact the basalt has a thin porcelainous layer of very fine-grained black hornfels with 1 cm. long white blobs aligned parallel to the contact, in a zone 10 cm. wide, before giving way to a fresh aphyric basalt with small needles of plagioclase. Interbedded with the basalts are whitish bands of carbonate rich rock, which are probably calc-silicate bands derived from calcareous tuffs (Plate 14). These have a rough weathering surface due to differential weathering of the calcareous bands. The basalts are cut by syenite veinlets and in places seem to have been metasomatised, as at Narssarssuaq Harbour, dense bands rich in magnetite and biotite have a similar mineralogy and texture to the metasomatised basic material within the Julianehåb Granite. The sandstones have been affected by metasomatism and are sometimes rich in alkali pyroxene and alkali feldspar.

(iii) Contacts with Earlier Syenites:-

East of Narssarssuaq SS2 is in contact with the earlier North Qôroq Centre and its relationship to the syenite SN1 can be seen in several places. The contact is very sharp and small-scale flow banding of feldspar can be seen parallel to the contact, with larger platy feldspar phenocrysts showing prominent alignment. The lamination persists for a few tens of metres away

from the contact, but there is no development of pegmatite anywhere in the area. SN1 at the contact is coarse grained and not visibly altered, although it is cut by small veins of chilled SS2.

About 6 km. south of Narssarssuaq Harbour marginal SS2 is chilled against coarse grained Tunugdliarfik Syenite, which itself appears to have a marginal facies developed. Thus the original Tunugdliarfik Syenite/Julianehab Granite contact was probably nearby and is now obliterated by SS2. Coarse veins of nepheline syenite cut across both syenites, and SS2 has patchy pegmatites rich in pyroxene. Further south SS2 has a few xenoliths of earlier syenite.

#### (2d) Effects of the later Igdlerfigssalik Centre

Much of the southern part of the South Qoroq Centre is cut out by the later Igdlerfigssalik Centre and the relationship between these two centres can be seen around the lower part of Qoroq Fjord. On the south side of Giesecke's Dal Bay, syenite SS5 occurs as a narrow strip along the coast up to 200 m. wide, and is cut by the Igdlerfigssalik syenite SI2. This becomes fine-grained towards the contact in a 50 m. wide marginal zone and is chilled against SS5. The line of contact is irregular (Plate 15) with occasional lobes of SS5 surrounded by the later syenite, although SS5 does not appear to have suffered much recrystallisation. Near to the contact, SI2 has a few dark, fine grained mafic horizons and xenoliths of SS5, but it becomes more regular inwards and is coarser grained in the lower parts of Giesecke's Dal.

On the west side of Qoroq Fjord, at Niaqornarsuk there are three strips of syenite parallel to the coast, considered to be Igdlerfigssalik syenites SI6, SI3 and SI1 (Emeleus and Harry, 1970, p.57, Fig. 19). Beyond these syenites, on the hillside, South Qoroq Centre syenites and trachytic dykes show signs of recrystallisation. SS5 has recrystallised mafics in the form of rounded blobs 1 - 2 cm. wide and well formed crystals seem to be absent. The dykes have similar dark, mafic spots, commonly with lighter coloured rims, and the feldspar phenocrysts show signs of reaction.

Throughout most of the area around Niaqornarssuk the South Qôroq syenites are cut by sheets of microsyenite and pegmatite, often associated with zones of whitish alteration and thin veins of magnetite-rich material. The contact between SI1 and SS3 is exposed near the southern tip of the Narssarssuaq - Qôroq peninsula (Emeleus and Harry, 1970), where fine grained SI1 cuts SS3 causing considerable remobilisation and back veining. A zone of recrystallisation about 1 km. wide can be recognised around the Igdlerfigssalik Centre from petrographic and mineralogical work. The approximate limit is shown on Plate 1 based principally on the instability of olivine within the zone (see Chapters 3 and 4).

From the above relationships it is evident that there was a significant time lapse between the emplacement of the later South Qôroq syenites and the earlier Igdlerfigssalik syenites, during which time a period of dyke emplacement occurred. Thus the Igdlerfigssalik Centre was intruded into a solidified fairly cool country rock, causing considerable contact metamorphism and veining with some remobilisation of the host, around Niaqornarssuk. However, on the south side of Giesecke's Dal, recrystallisation is not so intense, which may reflect differences between the various Igdlerfigssalik syenites (i.e. augite syenites SI1 and possibly SI4 at Niaqornarssuk, but foyaitic SI2 in Giesecke's Dal) (C.H. Emeleus, personal communication, 1972).

(2e) Faulting

The Igaliko Complex is situated on the line of one of the major east-south-east fault zones, which cut the Gardar Province (Fig. 1.1). The Grønnedal-Íka, Nunarssuit and Ilímaussaq Complexes occur along similar, parallel fault zones where the three Mid-Gardar dyke swarms intersect the fault systems, and hence, as stated in Chapter 1, there would appear to be a correlation between the faulting, the dyke swarms and the major intrusive centres. The orientation of the two complementary sets of tear faults (sinistral ESE-WNW and dextral N-S) in the province suggests a stress system consisting of a maximum north-east - south-west stress and a minimum north-west - south-east stress. This is further

indicated by north-east - south-west trending tensional features such as the dyke swarms and the Eriksfjord "graben" structure. Many of the major intrusive centres, including South Qôroq, are elongated along a north-west - south-east axis, also suggesting a maximum north-east - south-west stress.

Pre-syenite faults have been mapped in the Igaliko Fjord area, where they cut the Eriksfjord formation, but do not appear to continue into the Igdlerfigssalik and Østfjordsdal syenites. However, no such faults were found around the South Qôroq Centre.

Several minor faults with a trend between north - south and north-east - south-west cut the centre. These do not have any considerable movement above a few hundred metres but, in addition, there are many broad zones of reddening and crushing with a similar trend, which can give rise to topographic features. This is well seen between Augpalugtut and Narssarssuaq, (Fig. 2.4).

On the Narssarssuaq - Qôroq plateau a north-east trending fault occurs which appears to have a vertical movement with a downthrow to the south-east. Evidence for this comes from the displacement of the SS4/SS5 contact, which is known to dip outwards, and which is displaced in opposite directions in different parts of the fault, (i.e. sinistral in the south-west and dextral in the north-east). The fault cuts several trachytic dykes and can be followed for about 4 km. to the coast of Qôroq Fjord, where it can be seen in the cliffs as a prominent red line, truncating the dykes.

The centre is cut by several faults and shear zones parallel to the major, regional east or east-south-east trending faults, but most of the movement in the centre is along two large fault zones, which are marked by prominent topographic features and wide zones of crushing and discolouration. The northern fault occurs as a prominent valley feature across the Motzfeldt Centre (upper Flink's Dal) and continues slightly south of west across the South Qôroq Centre as a 200 m. wide crush zone until, 3 km. east of Narssarssuaq Harbour, where there is a sharp deflection to a trend of  $050^{\circ}$ . The fault then continues to the Tunugdliarfik coast in the broad valley of Augpalugtut.

On either side of this valley there is a very wide zone of crushing for up to 400 m. and it may be that two faults are superimposed along the valley (Fig. 2.4). One reason for the deflection may be that the fault runs into one of the north-east trending crush zones, which can be followed through the North Qôroq Centre for over 10 km. as a long, straight valley feature. A much attenuated extension of the original fault may continue westwards through Akuliaruseq, since a reddened zone can be seen passing down the hillside and most of the coast section between the harbour and Augpalugtut is very discoloured (Fig. 2.4). As in most of the Gardar east - west faults, the displacement is predominantly horizontal and sinistral, remaining quite constant at 2 km. (from the displacement of distinctive dykes) between Augpalugtut and Motzfeldt Sô.

The southern fault can be seen on the north side of Giesecke's Dal as a reddened line on the slopes of Qôrqup qaqai, truncating several dykes. The drag on these dykes indicates displacement in a sinistral sense and there is a zone of crushing up to 100 m. wide. West of Qôroq Fjord, the fault continues across the Narssarssuaq - Qôroq plateau with only minor variations in trend (Plate 16). In Giesecke's Dal, the displacement of the SS2/Julianehåb Granite contact indicates a sinistral movement of about 1 km., but on the plateau the syenite contacts and dykes are never displaced by more than 400 m. This is due to a splitting of the fault into at least three branches, each of which has subsidiary, parallel, sinistral faults associated with it. This subsidiary faulting has been mapped in detail in the area shown in Fig. 2.5. The major branches can be seen from Tunugdliarfik Fjord as lines on the hillside, occasionally truncating dykes (Plate 17.)

The two main faults do not intersect and no direct evidence is found of relative ages. Both of the faults truncate the regional dykes, although a few of the later trachytes are not affected by the southern fault. Thus the southern fault is probably the earlier and faulting continued more or less contemporaneously with the later dyke emplacement.



Plate 16

The southern, sinistral transcurrent fault cutting the South Qôroq Centre on the west side of Qôroq Fjord. The reddened line of the fault is seen as a dark, diagonal line truncating dykes which are approximately parallel to the coast at this locality.



Plate 17

Branches of the southern sinistral fault cutting the South Qôroq Centre on the east side of Tunugdliarfik Fjord.

Fig. 2.4

Faulting and crush zones in the area between Narssarssuaq and Augpalugtut. (Tr = trachytic dyke; Dol = dolerite dyke)

Fig. 2.5

Sketch map showing detail of branching in the southern transcurrent fault of the South Qôroq Centre, around the 1969 camp site, 6 km. south of Narssarssuaq Harbour. The locality is marked on Fig. 2.1.

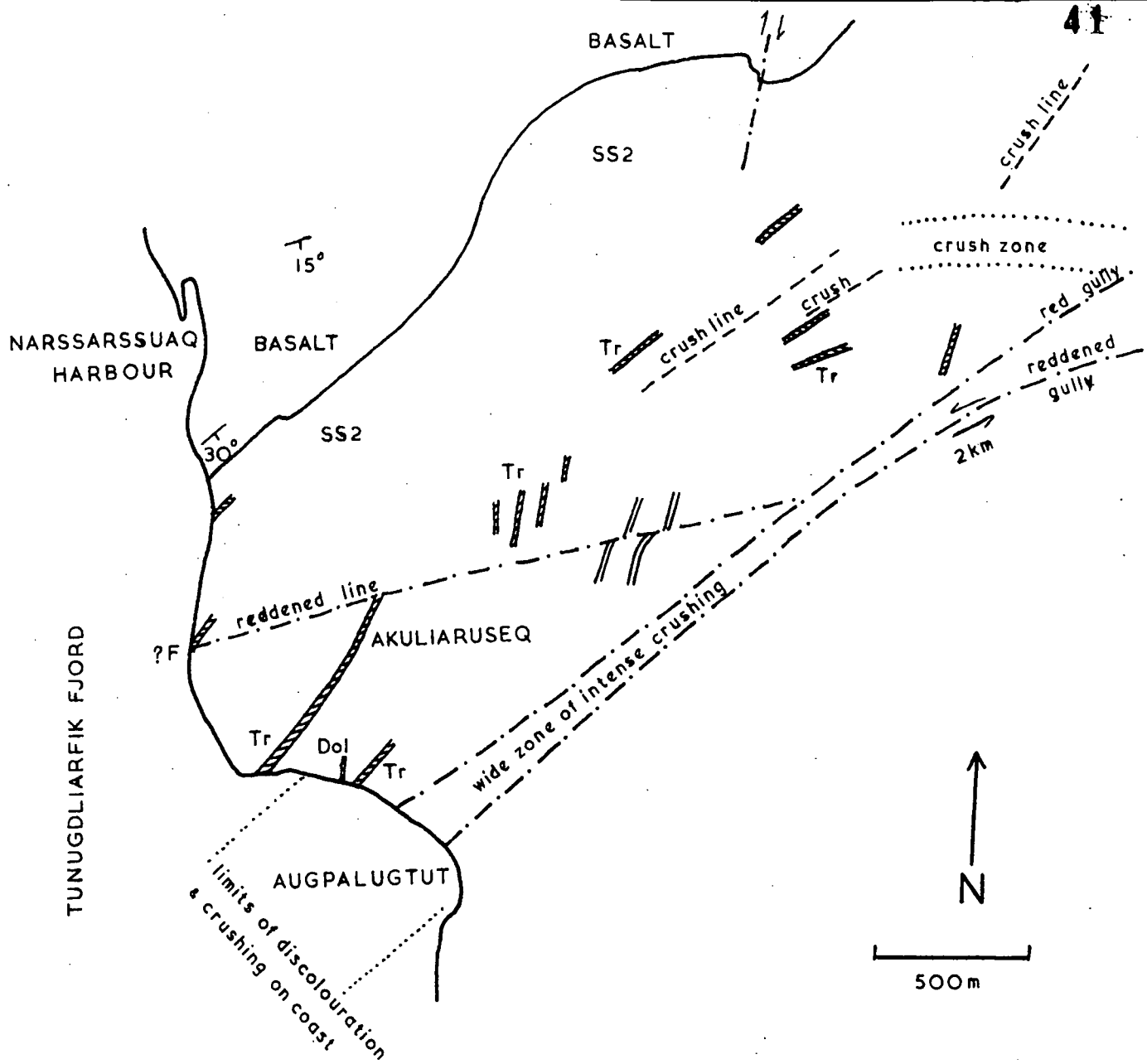


Fig. 2.4

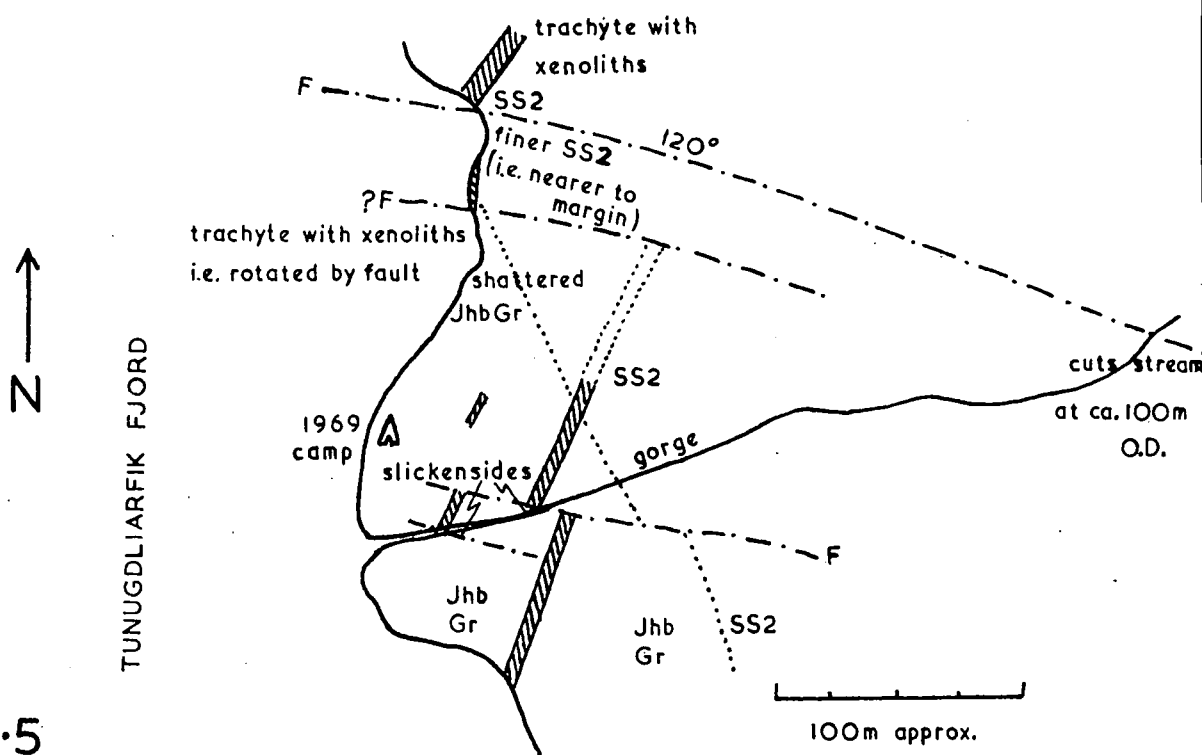
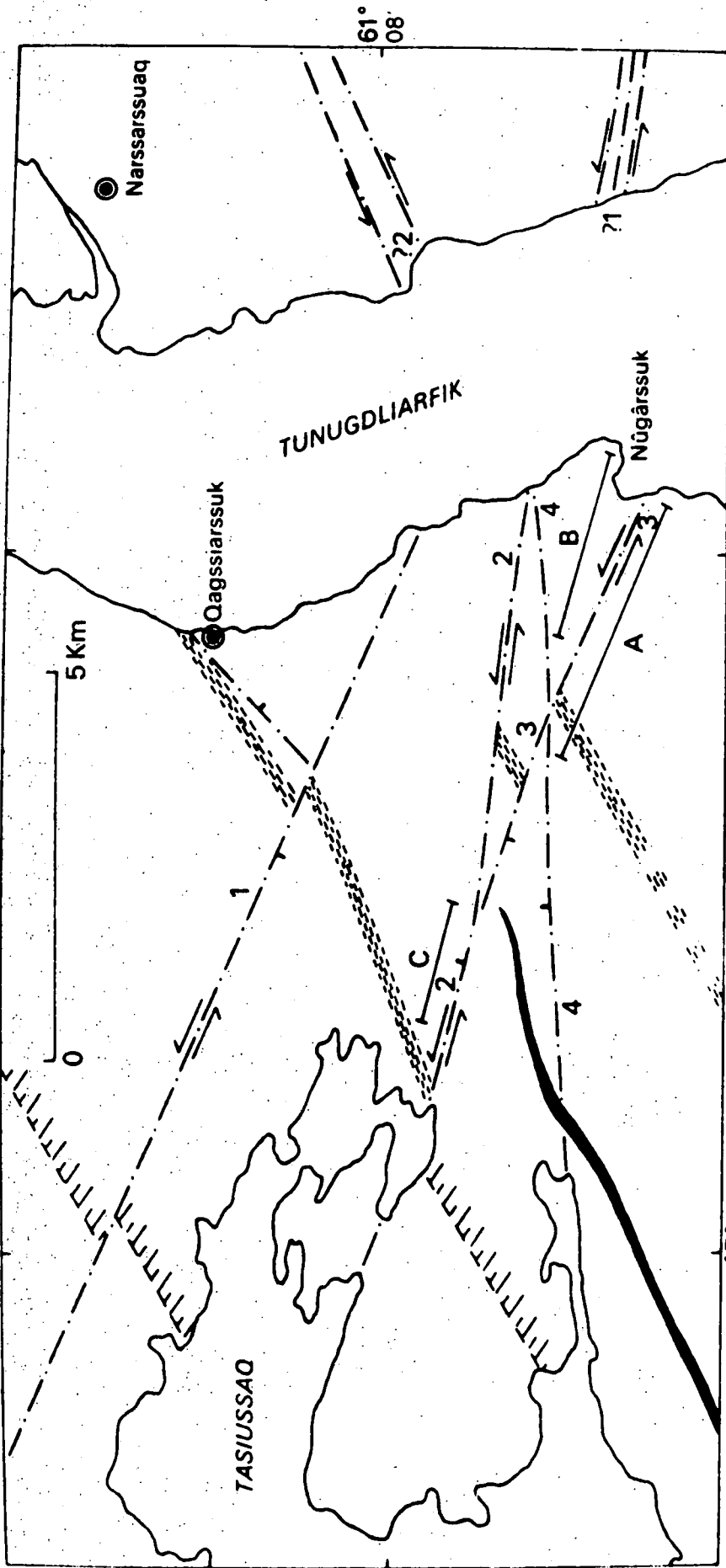


Fig. 2.5

Fig. 2.6

Attempted correlations of faults on the west and east sides of  
Tunugdliarfik Fjord. (From Emeleus and Stephenson, 1970).



- Fault, direction of horizontal displacement and downthrown side indicated
- Zone of distinctive dykes
- Gabbro dyke
- Approximate NW margin of Gardar dyke swarm
- Measured section across dyke swarm

During the 1969 season, some time was spent in the Qagssiarsuk area, examining the westward continuation of the fault zone, and tentative correlations were made across Tunugdliarfik Fjord (Emeleus and Stephenson, 1970), (Fig. 2.6). Four faults were studied in detail, one normal fault and three sinistral tear faults. Movement along each sinistral fault is from 400 m. to 5 km. and there is a total movement along the three faults of 6 - 6.5 km. When compared with the faults east of Tunugdliarfik Fjord it is clear that no simple correlation may be made, even though there is clearly a continuation of the fault zone. A total sinistral fault movement of 2.5 - 3 km. has been measured in the South Qoroq Centre, 2 km. of which is along the northern fault. However, a total offset of between 6 and 7 km. may be obtained in this centre by taking into account the sinuous deflection of the Gardar dykes, which is in a sinistral sense and amounts to 4 - 5 km. when resolved in an east-west direction (Plate 1). This is then consistent with the amount of movement west of Tunugdliarfik Fjord.

Emeleus and Harry (1970) propose two explanations for the deflection of the dykes. As there is no deflection of the dyke swarm elsewhere in the region, it is possible that the development of the Igdlerfigssalik Centre could have modified the regional stress pattern. However, the dyke distribution does not correspond to that found in other igneous centres where this is known to occur (Odé, 1957), and also some of the affected dykes are probably later than the Igdlerfigssalik Centre. From the evidence of the fault displacements and from the fact that the faulting appears to be contemporaneous with the dyke emplacement, it would seem more likely that stresses associated with the transcurrent faulting were superimposed on the regional stresses at the time of emplacement, causing a deflection from the normal trend. This acted as a form of stress release, reducing the amount of movement along the faults.

Evidence for a vertical component in the faults was found in the Qagssiarsuk area from the elevation of the Eriksfjord Formation base, but except for one fault with a downthrow of about 100 m. to the south, the amount of throw could not be estimated. Emeleus and Harry (1970) propose a downthrow of at least 400 m. to the south for the southern fault cutting the South Qoroq

Centre, based on the height of the Eriksfjord Formation base south-east of Flink's Dal and at the head of Igaliko Fjord.

It is possible that there is a fault along the line of Qôroq Fjord earlier than the two east-west sinistral faults (Emeleus and Harry, 1970, p.102). However, owing to the recent amendments, the map now shows no apparent displacement of syenite boundaries, and although the possibility of a fault still exists, the remaining evidence (i.e. the presence of shear zones and mineralisation) is rather circumstantial.

### 3. PETROGRAPHY OF THE SYENITES

The principal syenites within the South Qôroq Centre may be classified as either foyaites (SS2, SS3, SS5) or augite syenites (SS4b) with possibly intermediate compositions in SS4a. The general petrographic and textural features of the intrusions are described below, with further details on individual mineral phases in Chapter 4.

#### (3a) Foyaites - SS2, SS3 and SS5

The three foyaitic syenites have in general a similar petrography, although significant differences in the compositions of certain mineral phases will be described in Chapter 4. They are considered to have been emplaced in fairly rapid succession, possibly as pulses from the same underlying magma (see 2b).

#### Syenite SS2:-

The typical SS2 rock type, as found on the Narssarssuaq - Qôroq peninsula and around lower Flink's Dal consists of approximately 80% perthitic alkali feldspar and nepheline in approximately equal proportions, sodalite, and aggregates of mafic minerals. The alkali feldspar and nepheline are usually subhedral to euhedral and may be cumulus. Often, particularly nearer the margins, large tabular phenocrysts of Carlsbad or Manebach twinned alkali feldspar are set in a slightly finer-grained groundmass of alkali feldspar laths and subhedral nepheline (Plate 18). Nepheline appears to have been crystallising from quite an early stage, since small grains are frequently included in the phenocryst feldspars, but most of the feldspar and nepheline appears to have crystallised simultaneously. From the shape of the feldspar crystals it would appear that they originally crystallised as sanidine before exsolving under sub-solidus conditions into orthoclase perthites (see 4g). Occasionally narrow rims of albite occur around the perthite crystals.

The mafic aggregates, which give the rock its spotted, "mossy" appearance in hand specimen, contain combinations of aegirine augite, arfvedsonitic amphibole, biotite, iron-titanium oxides, aenigmatite and apatite (Plate 27).

The minerals are also found separately in interstitial areas. A discontinuous reaction series is developed from aenigmatite (which is present in certain samples only as cores), to zoned aegirine augite, to arfvedsonite which is often found rimming the pyroxene (Yagi, 1953) (Plate 33). However, in many instances the mafic minerals just form intergrown aggregates, and aenigmatite is often absent. Biotite is sometimes present as an additional hydrous phase, although it is not as widespread as in the other foyaites. Fayalite is scarce in SS2 and, apart from the problematic south-eastern area (see below), is only found in one area, above the Tunugdliarfik coast (e.g. samples 59730, 127020, 127021). Here it appears to be early formed and is present as small, rounded grains, rimmed by iron ore and frequently enclosed by other mafic minerals, particularly pyroxene and amphibole. Magnetite is usually present as small, rounded grains and invariably has quite coarse, exsolved lamellae of ilmenite. It sometimes appears to have crystallised early, being almost euhedral, but in some samples it occupies interstitial areas between feldspar and nepheline grains. Around the edges of the mafic patches there is frequently an intergrowth of pyroxene needles and alkali feldspar. The needles grow outwards from larger pyroxene grains with which they are in optical continuity (Plate 37; see 4b).

In most of the samples there is a considerable amount of interstitial, isotropic sodalite, which clearly forms later than all the other primary minerals (Plate 24). In hand specimen it is greenish grey and fluoresces bright orange under ultra-violet light. It is thus seen to be confined to patches up to 1 cm. wide scattered irregularly throughout the rock. Cancrinite is also frequently present interstitially, usually around nepheline grains. This suggests that it probably formed by reaction between nepheline and a  $\text{CO}_2$ -rich residual liquid as part of the nepheline - cancrinite - calcite discontinuous reaction series (Saether, 1957).

Apatite is the most common accessory mineral and usually occurs as prismatic

grains included in the mafic aggregates. Small, subhedral grains of sphene and zircon are visible in some samples and a pale yellow, interstitial mineral is frequently present. This mineral is slightly pleochroic, has fairly high relief, a high 2V (-ve) and a fairly high birefringence. A qualitative electron probe scan shows it to be a calcium silicate with moderate amounts of sodium and titanium suggesting that it may be lavenite.

Towards the margins of the syenite, the rock begins to develop a lamination and becomes finer-grained. Alkali feldspar phenocrysts are then prominent in a finer groundmass of feldspar and nepheline. Mafic minerals tend to occur interstitially rather than in aggregates, and amphibole rims around pyroxenes become better developed. Within a few centimetres of the contact, nepheline frequently disappears due to contamination by country rock, and there is a tendency for amphibole to develop in excess of pyroxene. Sections from the contact east of Narssarssuaq sometimes show a fine brecciation adjacent to the basalt.

Where the syenite has been recrystallised near to the Igdlerfigssalik Centre, the feldspars and nephelines are larger, more irregular in shape and develop interlocking margins. Feldspars are more coarsely perthitic and mafic aggregates develop much more magnetite and biotite. Around the major fault in Giesecke's Dal, the zone of recrystallisation extends further than normal, nepheline is highly altered and the mafic aggregates are completely chloritised.

At the south-eastern end of the intrusion, (around the ridge between Østfjordsdal and Giesecke's Dal) the rock type is completely atypical of SS2. Large perthitic laths of alkali feldspar and irregular shaped nephelines are closely interlocked, often with lobate margins. Mafic aggregates occur, but the pyroxene is titanite rather than aegirine augite, and subhedral magnetite has radiating rims of biotite. Fayalite is common and the mafics are characteristically "larvikitic", resembling those of the augite syenites of SS4b rather than SS2. In view of this contrast in petrography it is

suggested that there is another satellitic intrusion in this area between SS1 and SS2 (see Plate 1).

Syenite SS3:-

In many ways SS3 is similar to SS2 and much of the above description may be applied to either syenite. SS3 is generally coarser grained with large, tabular orthoclase perthites up to 30 x 7 mm. showing multiple Carlsbad or Manebach twins. Nepheline grains are often large, irregular and have interlocking or lobate margins with feldspar. As in SS2 some small, euhedral nephelines are enclosed by larger feldspars, but in general there appears to be simultaneous crystallisation of the two phases (Plate 19).

Aggregates of mafic minerals commonly occur, but are not as ubiquitous as in SS2 (Plate 28), and more frequently the mafics occur in separate interstitial areas. Iron-titanium oxides occur as in SS2, but generally there is a higher proportion of the hydrous phases arfvedsonite and biotite. Arfvedsonite rims are often well developed around small relic cores of aegirine augite, but in some samples biotite is the only hydrous phase. Fayalite and aenigmatite are completely absent from SS3. In many samples there are indications that magnetite has reacted with the residual liquid to form acmite (Plate 38; see 4b). Aegirine augite/alkali feldspar intergrowths occur as in SS2.

Sodalite and cancrinite occur as in SS2 and apatite is always an abundant accessory. Sphene is fairly common associated with the iron-titanium oxides, and the pale yellow, interstitial accessory (? lävenite) is present in a few samples. A colourless interstitial mineral, which as yet has not been identified, is sometimes present in SS3 and certain other rocks associated with small amounts of fluorite.

The syenite does not alter much towards its margin with SS2 (see 2b) apart from the more frequent development of pegmatitic areas, having coarse

crystallisation and more coarsely exsolved feldspar than the normal rock. Some pegmatites have large, euhedral nepheline with interstitial feldspar and calcite. Aegirine is frequently present, both as large twinned crystals and as overgrowths on arfvedsonite. Zoned, poikilitic eudialyte is developed in several pegmatites, together with occasional euhedral zircon. However, near the margin on the east side of Qôroq Fjord, early euhedral grains of zoned eucolite - mesodialyte up to 2 cm. wide constitute up to 50% of the pegmatite (Plates 44, 45, 46). Poikilitic eucolite (Plate 47) also occurs in the same pegmatite which has a groundmass of alkali feldspar laths and euhedral nepheline enclosed by larger, irregular nepheline. Mafic minerals are mainly iron-titanium oxide and an unusual bright red biotite, together with some arfvedsonite and aegirine augite/aegirine. An unusual pegmatite nearer the centre of the intrusion contains blue sodalite which fluoresces pale purple under ultra-violet light. However, this is surrounded by rims of more normal orange-fluorescing, grey sodalite.

Near the southern tip of the Narssarssuaq - Qôroq peninsula, SS3 is intensely recrystallised by the Igdlerfigssalik Centre. Feldspars become irregular and coarsely perthitic, with interlocking or lobate margins against nepheline. The mafic minerals are completely altered with development of "knots" of iron ore and decussate biotite flakes. At this locality there is much spene associated with the ore which could be due to the recrystallisation causing separation into magnetite, ilmenite and spene (see 4e).

Electron microprobe studies on the minerals of SS3 clearly show that it is the most fractionated of the South Qôroq Centre syenites (see Chapter 4). The mineral variations are not in general obvious from optical examination, but certain petrographic facts tend to indicate a more fractionated state, i.e. the increased abundance of hydrous mafic phases compared to the other foyaites; the development of aegirine and eucolite - eudialyte in marginal pegmatites, suggesting a higher peralkalinity; the common occurrence of the reaction magnetite + liquid = acmite; the instability of olivine; and the

sporadic appearance of fluorite.

Syenite SS5:-

Texturally SS5 is similar to SS3 except that it often possesses a strong lamination of tabular alkali feldspars. The feldspars are orthoclase perthites with simple and multiple twinning (Plates 21, 22) and have relationships with nepheline as outlined for the other foyaites. Mafic minerals are usually interstitial or in aggregates and vary considerably in their relative proportions. Aegirine augite and iron-titanium oxides are usually present with varying amounts of arfvedsonite and/or biotite. The aegirine augite is often a deep apple-green colour, and zoning is less apparent optically than in the other foyaites. In some samples magnetite has reacted with the liquid to give secondary acmite, but this is not as common as in SS3. Arfvedsonite rims are often well developed on aegirine augite (Plates 34, 35), and iron-titanium oxides sometimes have radiating rims of biotite. Fayalite is quite abundant in certain samples (e.g. 46243, 58230) and is heavily rimmed by iron ore, pyroxene or amphibole (Plates 39, 40). Sodalite and cancrinite are common, and occasionally the full series nepheline - cancrinite - calcite is observed (Plate 26). Common accessories are apatite and sphene, but zircon also occurs sporadically and one sample (46271) contains a colourless interstitial mineral associated with small areas of fluorite.

Mafic bands are common in SS5 (see 2a), consisting largely of subhedral aegirine augite, fayalite, iron-titanium oxide (with rims of biotite), and apatite. Towards the edges of the bands these minerals are packed tightly into interstices between cumulus feldspar and nepheline. In some bands the pyroxenes are euhedral to subhedral titanaugites, considerably less fractionated than in the normal SS5.

Much of the SS5 on the west side of Qôroq Fjord has been recrystallised by the Igdlérfigssalik Centre, and progressive alteration can be traced southwards along the coast section. Fayalite, the first mineral to react, is pseudomorphed by chlorite and iron ore and finally disappears. Aegirine augite and biotite

Plate 18

Marginal SS2 showing a pronounced lamination of tabular, perthitic feldspar, and rounded nepheline. A small perthite phenocryst is seen on the left. (Sp. No. 46276, crossed polars, X 20)

Plate 19

Simultaneous crystallisation of alkali feldspar (with perthitic texture) and nepheline (smaller, rounded to subhedral grains) in SS3. (Sp. No. 46269, crossed polars, X 20)

Plate 20

Typical texture of felsic minerals from one of the microsyenite sheets cutting SS3. Twinned, tabular perthite (bottom), rounded nephelines (top), surrounded by interstitial cancrinite; isotropic, interstitial sodalite (top right). (Sp. No. 58233, crossed polars, X 20)

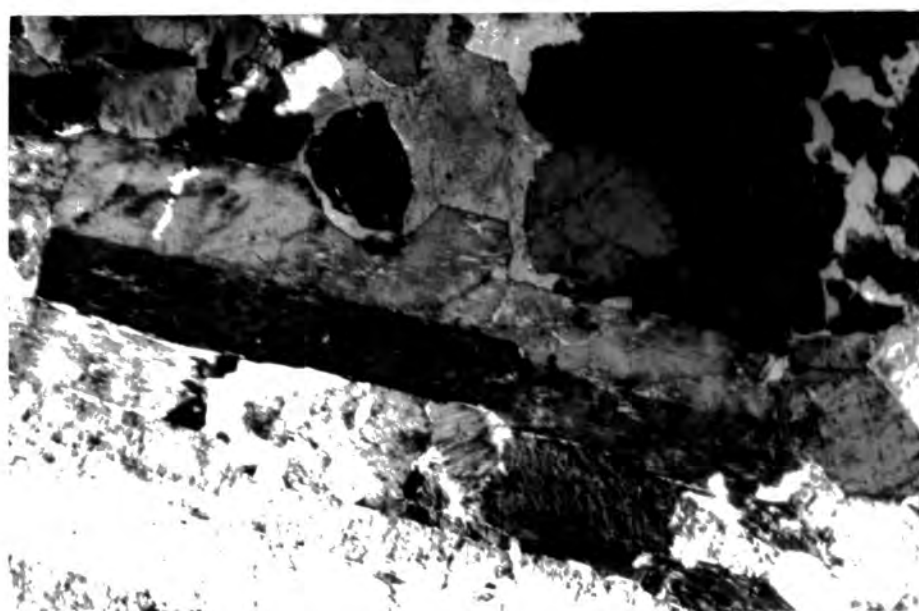
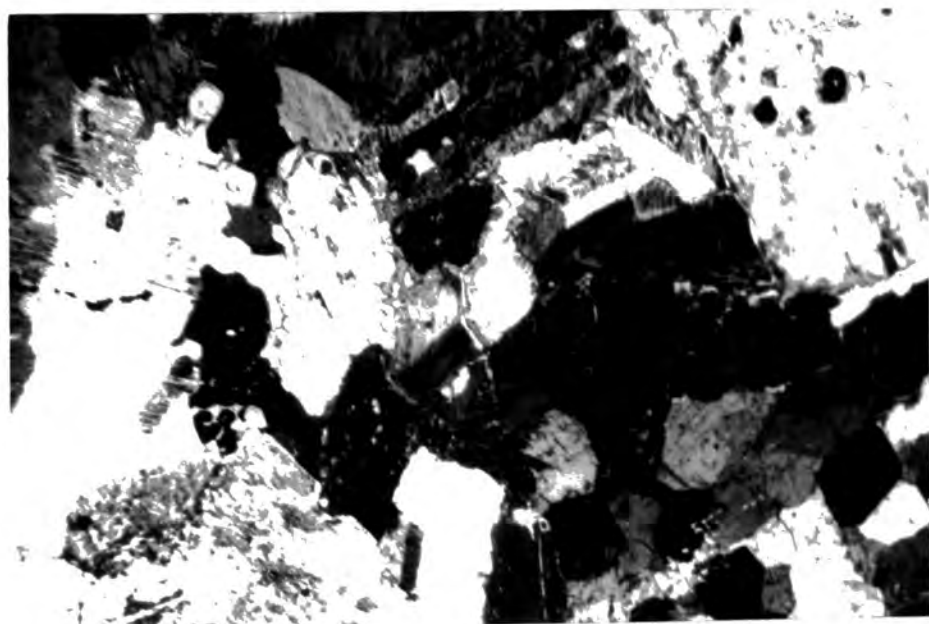
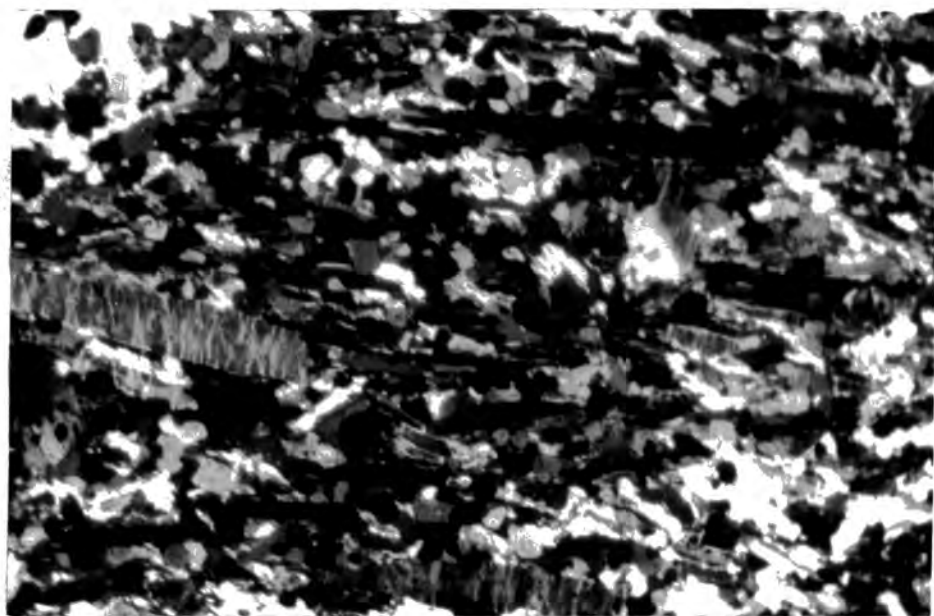


Plate 21

Typical, large, tabular, twinned crystal of perthitic alkali feldspar in SS5. (Sp. No. 46244, crossed polars, X 20)

Plate 22

Large tabular alkali feldspars showing multiple twinning in SS5. (Sp. No. 46241, crossed polars, X 20)

Plate 23

"Blebs" of nepheline within irregular grains of microperthitic alkali feldspar in SS4b. The "blebs" are in optical continuity within individual grains and have the appearance of an exsolution texture. (Sp. No. 58259, crossed polars, X 20)

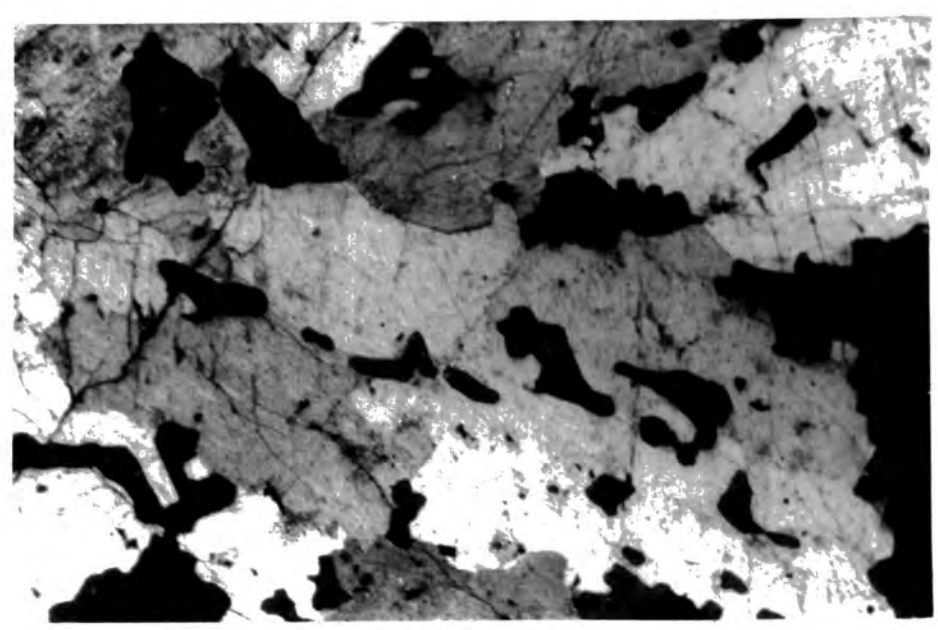


Plate 24

Euhedral grains of nepheline enclosed by interstitial, isotropic sodalite in SS2. (Sp. No. 46255, crossed polars, X 75)

Plate 25

Interstitial nepheline (grey) between grains of microperthitic feldspar (white) in SS4b. (Sp. No. 58221, crossed polars, X 20)

Plate 26

Reaction between nepheline (top) and interstitial calcite (rhombohedral cleavage-centre) giving an intervening, radiating fringe of cancrinite in SS5. (Sp. No. 59644, crossed polars, X 75)

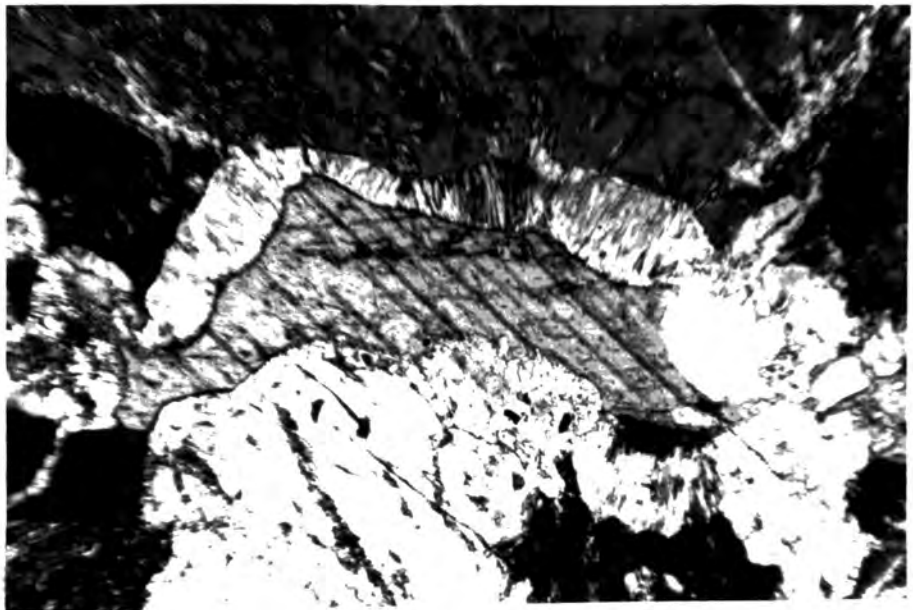
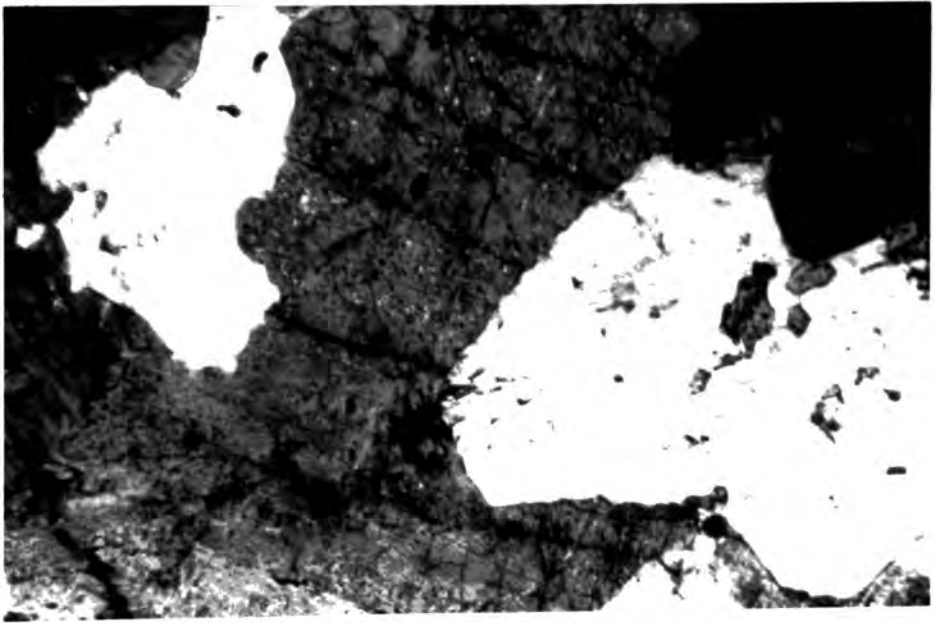
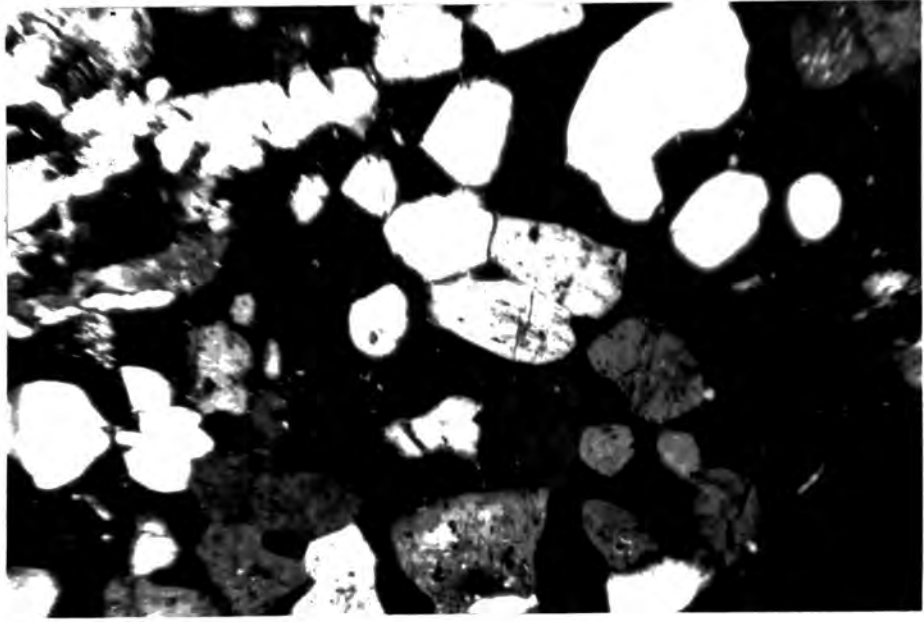


Plate 27

Typical "mossy" mafic aggregate in SS2. (P = pyroxene, A = amph, Ap = apatite.) Alkali amphibole is forming a discontinuous rim around the aegirine augite. (Sp. No. 58231, pyroxene and amphibole analyses 58231.1, ordinary light, X 40)

Plate 28

Mafic cluster in SS3. In this particular sample, the mafics are exclusively aegirine augite (P) and biotite (B), with fairly abundant prisms of apatite (Ap). (Sp. No. 46269, ordinary light, X 20)

Plate 29

Typical cluster of mafic minerals in a mafic band from SS4b. Subhedral olivine (O) and titanite (P) with prisms of apatite (Ap). (Sp. No. 59672, pyroxene and olivine analyses 59672.3, ordinary light, X 40)

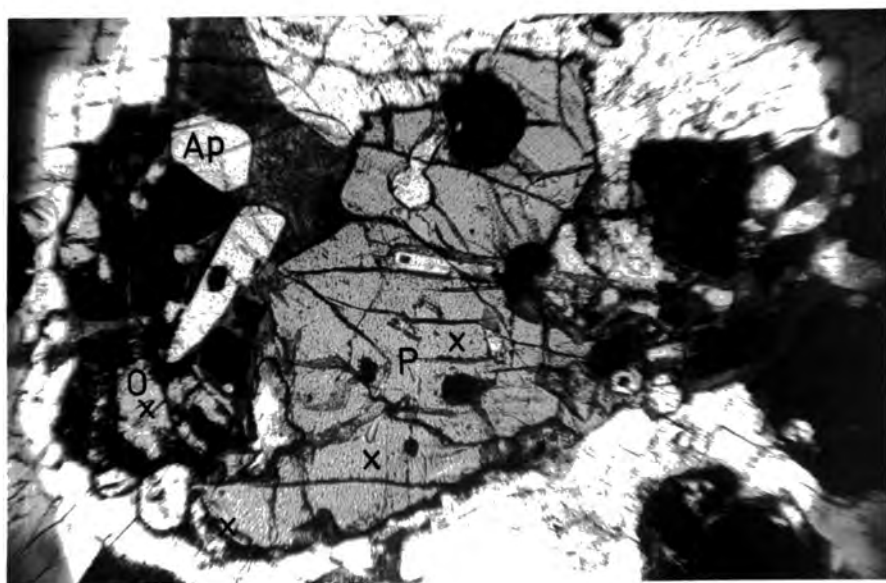
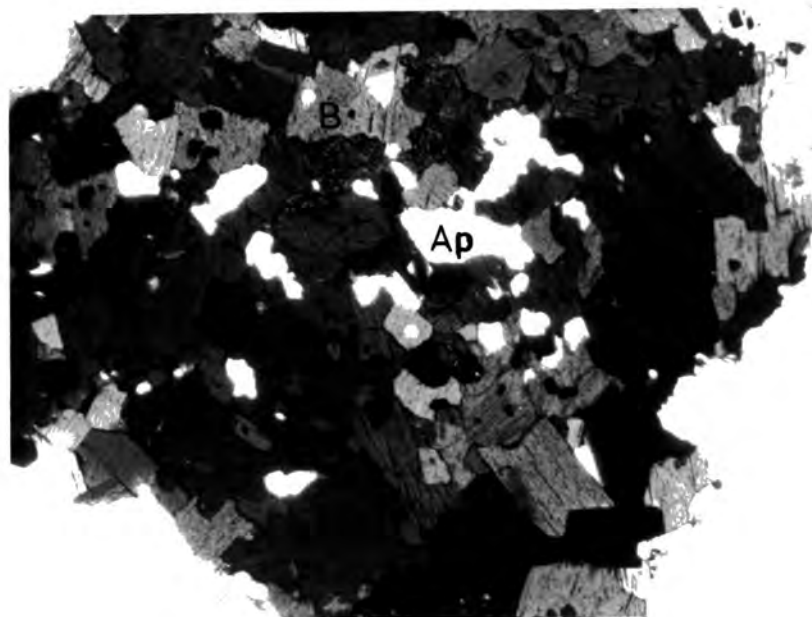
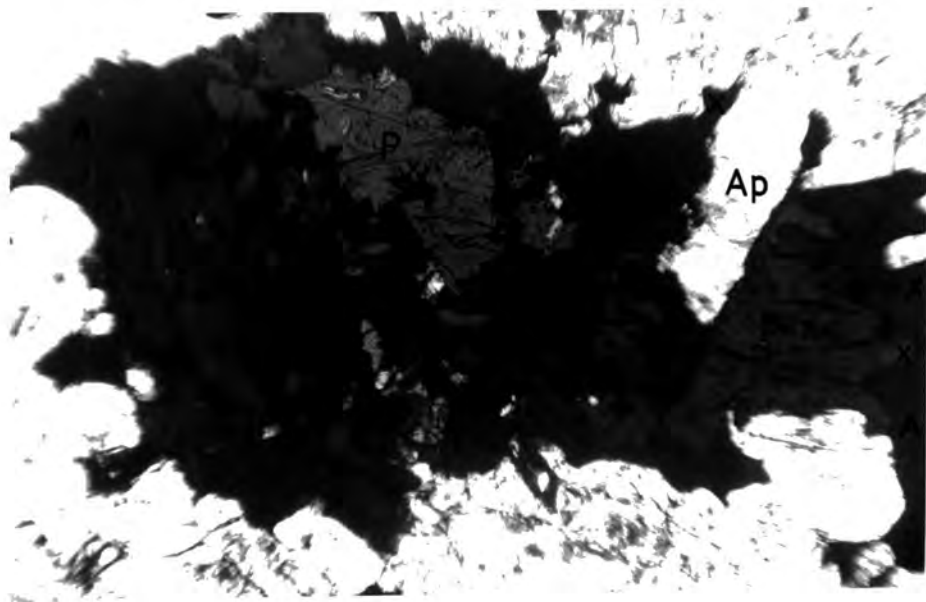


Plate 30

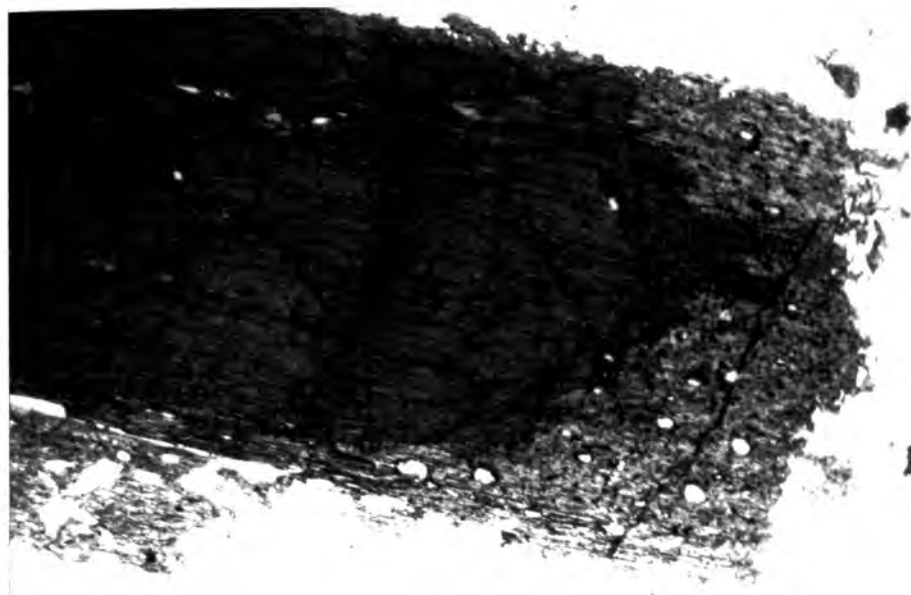
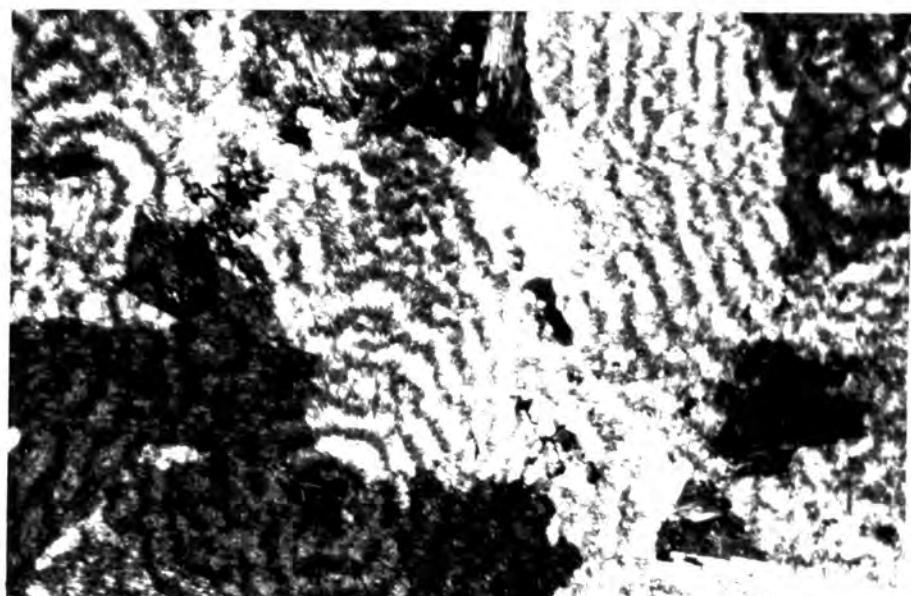
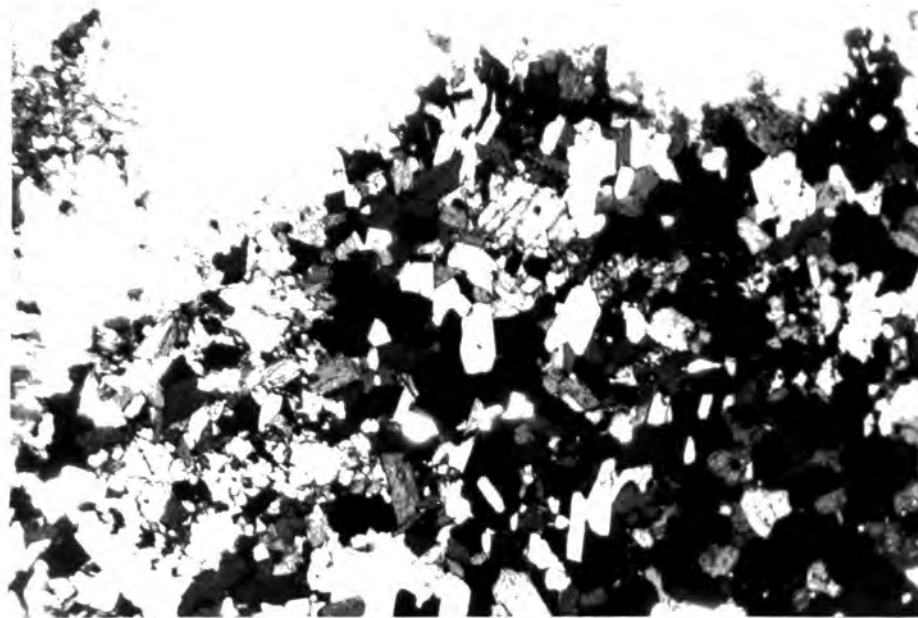
Biotite-rich aggregate in recrystallised SS5 near to the contact with the Igdlarfígssalik Centre. All the mafic minerals in this aggregate are either biotite or opaque oxides. (Sp. No. 58160, ordinary light, X 20)

Plate 31

Radiating growths of carbonate replacing the central part of a pegmatite vein. "Ghost" prisms of aegirine can be seen in the bottom left. (Sp. No. 127072, crossed polars, X 20)

Plate 32

Large blade of alkali pyroxene growing inwards from the walls of the same pegmatite vein as Plate 31. The dark, inner zone is deep apple-green, strongly pleochroic aegirine, and the rim is colourless to pale yellowish-brown acmite. The compositional difference between the two zones is very slight. (Sp. No. 127071, pyroxene analyses 127071.1, ordinary light, X 20)



begin to show a clearly recrystallised, poikilitic texture, and very near to the contact the mafics are almost completely made over to "knots" of iron ore (with associated sphene) and decussate biotite (Plate 30). Feldspars are irregular shaped and coarsely perthitic, nepheline is highly altered and there is much development of interstitial cancrinite and calcite. Recrystallisation is not so intense on the south side of Giesecke's Dal Bay but is well developed near the Igdlarfigssalik Centre further up Giesecke's Dal (where the augite syenite SI4 is closer - see 2d).

As with SS3 there is little variation towards the edge of the intrusion apart from the development of marginal pegmatitic areas. The pegmatites are similar to the ones in SS3 but contain zircon instead of eudialyte. Interstitial areas between the pegmatite patches are filled with a microsyenite having small laths of alkali feldspar with nepheline, iron ore and interstitial or poikilitic aegirine augite, arfvedsonite and biotite. Sometimes this microsyenite has an irregular flow structure.

### (3b) Augite Syenites and Related Rocks within SS4

The syenites of SS4 are continuously exposed on the west coast of Qôroq Fjord opposite to Flink's Dal. Samples from other areas may be related to this type section, where the division into SS4a and SS4b was first recognised (see 2a.iv).

#### Syenite SS4b:-

SS4b is a true augite syenite, very similar in texture and mineralogy to the Oslo larvikites (Barth, 1944). In typical samples, the feldspar occurs as irregularly shaped grains of microperthite, which are schillerised in hand specimen giving the rock a bluish tint. Within the microperthite, more coarsely exsolved areas frequently occur, and in some samples all the feldspar is coarsely exsolved. The grains have interlocking, lobate margins with each other and, in marked contrast to the foyaites, nepheline occurs in interstitial areas which are frequently altered (Plate 25). Near the inner margin of the

intrusion, nepheline constitutes only 10% of the rock, but there is a tendency for it to become more abundant outwards, reaching about 30% near the boundary with SS4a. A feature common to almost all the SS4 syenites, but absent from the foyaites, is the presence of irregular, rounded "blebs" of nepheline within the alkali feldspar (Plate 23). Within a particular feldspar grain all the "blebs" are in optical continuity and thus may be an exsolution feature. Identical textures are found in alkali feldspars from augite syenites of the Igdlarfigssalik Centre (C. H. Emeleus, personal communication 1972), and similar textures in the Oslo larvikites are considered to be due to sub-solidus exsolution by Widenfalk (1972).

Sequences of crystallisation are often difficult to establish with any certainty, but many of the mafic minerals appear to be formed earlier than the nepheline, and probably earlier or at about the same time as the feldspar. This is in strong contrast to the foyaites where most of the mafics are interstitial. Olivine, iron-titanium oxide and apatite are always early; pyroxene is usually irregular or subhedral, but often shows early euhedral tendencies with later overgrowths; and amphibole and biotite are always interstitial or poikilitic. The iron-titanium oxides occur as rounded, subhedral grains of magnetite with coarsely exsolved ilmenite (Plate 43), and usually have radiating fringes of biotite (Plate 42). Olivine is present in almost all the samples and is frequently enclosed by other mafic minerals (Plates 41, 42). It often has thick rims of iron ore, but is also frequently rimmed by a turquoise blue amphibole. Apatite is abundant, associated with the mafics, and occurs as quite large, euhedral prisms (Plate 29). The pyroxene is lilac coloured titanaugite and only occasionally shows a slight green colouration on the edges (Plate 36). Well developed rims of muddy brown/green arfvedsonitic amphibole are common (sometimes enclosing euhedral pyroxene) and in some samples amphibole also occurs as separate poikilitic areas. Biotite also occurs occasionally as separate interstitial grains in addition to rimming the oxides. Accessory minerals are rare, but occasional specks of yellow

sulphides (probably pyrite) are detected in reflected light. Sodalite is present only in very small amounts, probably as thin rims around nepheline.

Mafic bands are common in SS4b, and most samples show a cumulus development of mafic minerals to a greater or lesser extent (Plate 41). Apatite, iron-titanium oxide, olivine and titanite are the cumulus phases, often constituting up to 60% of the rock. Of these, apatite appears to be the earliest, being included by all other minerals, and titanite is fairly late as it is sometimes interstitial. Amphibole and biotite occur as rims and interstitially as in the normal rock, but the amphibole is often a deep red colour and is probably barkevikite (see 4c). The intercumulus material consists of small, irregular grains of microperthite and a little interstitial nepheline.

Marginal pegmatites within SS4b are similar to the normal rock in their content of mafic minerals, but are more coarsely crystalline and have large, irregular grains of very perthitic feldspar. Nepheline also occurs as irregular, interstitial grains, often with rims of cancrinite. The earlier formed mafics tend to be altered but interstitial amphibole is fresh.

Syenite SS4a:-

SS4a has many features in common with SS4b such as the "blebs" of nepheline in microperthitic alkali feldspar; rounded iron-titanium oxides with fringes of biotite; and early olivine and apatite. However, it would appear to be transitional towards the foyaites, since the pyroxene is pale green, zoned aegirine augite, usually with well developed rims of arfvedsonite, and nepheline is generally more abundant. In some samples, the alkali feldspar occurs as large, irregular, interlocking grains with interstitial nepheline as in SS4b, but in others stumpy, rectangular perthite and square or hexagonal to subhedral nepheline are clearly cumulus. In the latter feldspar and nepheline are in approximately equal proportions as in the foyaites, with interstitial areas filled by smaller alkali feldspar and nepheline grains.

Sodalite is frequently present, and some samples have cancrinite. Apart from the composition of the pyroxene, the mafics are similar to those of SS4b except that olivine, although present in most samples is less abundant. Marginal pegmatitic areas are developed but mafic bands are rare.

Both SS4a and SS4b are recrystallised by the Igdlarfigssalik Centre in the area above Niaqornarsuk. Feldspar becomes very coarsely perthitic and nepheline is usually altered with the development of much cancrinite. Some samples also have additional fresh nepheline which may be developed during recrystallisation. The pyroxene becomes more sodic, green aegirine augite (see 4b) but some retain cores of titanite. As in the recrystallised foyaites, olivine is unstable and amphibole, where present, is often a blue-green variety. Aggregates of decussate biotite flakes develop in the extremely recrystallised rocks, and magnetite and ilmenite recrystallise as separate phases.

The thin strip of SS4 in Giesecke's Dal is similar to SS4b rather than SS4a, particularly in the character of the felsic minerals, and in the presence of titanite. However one sample has abundant, poikilitic red amphibole, which is probably barkevikitic, with lesser amounts of titanite, ore and apatite, and no olivine or biotite. (The lack of olivine is probably due to proximity to the Igdlarfigssalik Centre.) There is considerable variation in the character of both mafic and felsic minerals in the outcrops of SS4a and SS4b and occasional areas similar to one syenite are found within the other. Although the sample cover is not extensive enough to investigate this in detail, it may be that SS4 consists of several distinct areas, representing several pulses of ring dyke magma (see Chapter 2).

### (3c) Other Intrusions Associated with the Centre

#### Syenite SS1:-

The SS1 syenite has quite a variable petrography, but generally consists of large, interlocking, coarsely perthitic grains of alkali feldspar and nepheline, with irregular, interstitial mafic aggregates. In some areas the feldspar is more tabular and the nepheline is interstitial. "Exsolved blebs"

of nepheline occur in the feldspar, as in SS4, and interstitial sodalite is widespread. The mafics are subhedral ore, fayalite and apatite with interstitial aegirine augite and arfvedsonite. Biotite is present in only minor amounts and some samples have no olivine. A marginal sample contains numerous irregular grains of olivine and ore with poikilitic amphibole, in a fine grained groundmass consisting of rounded grains of alkali feldspar and nepheline. However, this would appear to be a mafic band.

#### The Tunugdliarfik Syenite:-

This syenite contains large, subhedral to euhedral nepheline grains and tabular, multiple-twinned, perthitic alkali feldspar. Both minerals show a tendency to enclose the other in places, suggesting simultaneous crystallisation. Interstitial sodalite and cancrinite are common. Mafic aggregates contain aegirine augite, arfvedsonite, iron-titanium oxides with biotite fringes, and apatite but no olivine.

#### The Østfjordsdal Syenite:-

In general, this syenite contains large, tabular crystals of perthitic alkali feldspar (some with "exsolved blebs" of nepheline) and areas of smaller, subhedral nepheline grains. There is usually interstitial sodalite, sometimes with cancrinite and calcite. Olivine is not present, except in one marginal sample, but subhedral, rounded iron-titanium oxide is common. Interstitial aggregates contain apatite, aegirine augite and arfvedsonite with variable amounts of biotite. Some samples have accessory zircon and ? lavenite. A pegmatite near to the south-west margin contains irregular perthite, calcite, aegirine, apatite, zircon and fluorite.

#### The Narssarssuaq Syenite:-

The Narssarssuaq Syenite is texturally quite variable and most features are obscured by intense alteration throughout the whole outcrop. The groundmass consists of small laths of Carlsbad-twinned perthite and rounded

or interstitial, altered nepheline. Occasionally the rock is porphyritic with larger, tabular perthites, and in one sample the groundmass nepheline shows a pronounced lamination. Sodalite is not present, except in areas of secondary veining, and the mafics are usually completely altered, so that only relics of iron ore and ? aegirine augite can be detected. Near to the margin the rock becomes very fine grained and is affected by much shearing.

#### The Microsyenite Sheets:-

Most of the sheets cutting SS3 are porphyritic microsyenites, often with a pronounced lamination. The phenocrysts are usually tabular, Carlsbad or Manebach-twinned alkali feldspar, in a groundmass of more "stumpy", rectangular perthites and subhedral to euhedral nepheline (Plate 20). Nepheline and feldspar are present in approximately equal amounts, and appear to have crystallised simultaneously. Some feldspars have "exsolved blebs" of nepheline. Interstitial sodalite and cancrinite are present in some samples but not in others. Rounded iron-titanium oxide and aegirine augite are often included in the feldspar, but usually occur interstitially or in aggregates. Arfvedsonite rims are usually well developed, and biotite occurs sporadically, but fayalite was found in only one sheet. Apatite and sphene are common accessories.

#### Essexite:-

The 100 m. wide essexite dyke contains large, irregular crystals of plagioclase feldspar, strongly zoned towards rims of microperthite and albite. Individual laths of albite are also present with nepheline and analcime occurring interstitially. There are abundant, well-formed grains of apatite, olivine and iron-titanium oxide with large, poikilitic crystals of titanite and deep red biotite. In one sample olivine constitutes up to 30% of the rock, and is clearly a cumulus phase, along with apatite and iron-titanium oxide.

### Veins Cutting the Syenites:-

Apart from the marginal pegmatitic patches, already described under each individual intrusion, the syenites are also cut by several veins of pegmatite and carbonatite. The pegmatite veins usually have long blades of pyroxene, consisting of dark green aegirine cores and a pale green to brownish acmite rim (see 4b; Plate 32), growing perpendicular to the vein margin. Some veins show several sharp, internal boundaries upon which renewed pyroxene growth has taken place. Between the pyroxene blades, small laths of albite occur with larger, but less abundant, nepheline, occasional poikilitic antiperthite and interstitial cancrinite. There are also small amounts of ore, biotite and zircon. The central parts of these veins are similar to the marginal groundmass but with the development of much calcite. Certain areas appear to be in the process of being replaced by radiating growths of carbonate (Plate 31).

Occasional, irregular 5 - 10 cm. veins of carbonate-rich, feldspathic material cut the syenites on the west coast of Q̄roq Fjord, and around the margins of the centre, more regular, 1 m. thick carbonatite sheets occur. These consist of interlocking grains of calcite, with poikilitic ? diopside and small grains of magnetite. Towards the rim, magnetite and haematite become more abundant, and occasional bands contain finely disseminated fluorite.

Plate 33

Zoned aegirine augite with subhedral inclusions of magnetite and a well developed rim of arfvedsonite in SS2. (Sp. No. 58231, pyroxene and amphibole analyses 58231.2, ordinary light, X 75)

Plate 34

Aegirine augite with a sharply defined rim of arfvedsonite in SS5. (Sp. No. 46243, pyroxene and amphibole analyses 46243.2, ordinary light, X 40)

Plate 35

Typical, irregular aegirine augite in SS5, with zoning not very pronounced optically. Rim of arfvedsonite mostly at extinction. (Sp. No. 46243, pyroxene and amphibole analyses 46243.3, ordinary light, X 40)

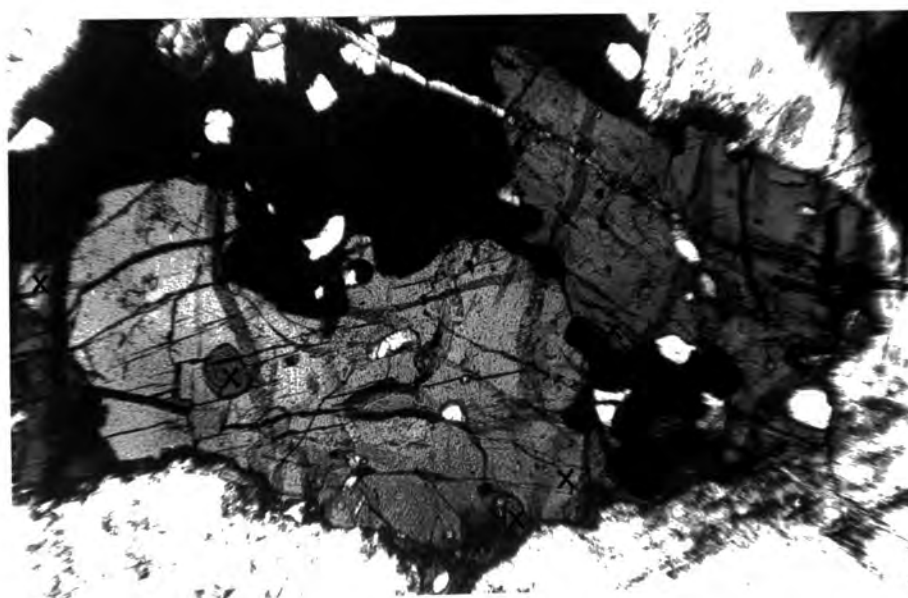
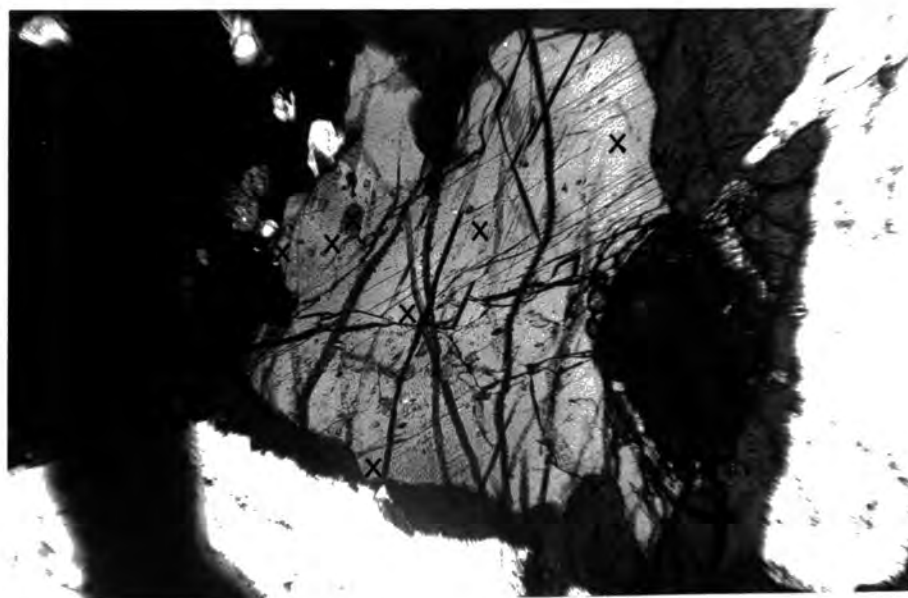


Plate 36

Typical grain of lilac-coloured titanaugite with inclusions of apatite and subhedral magnetite in SS4b. (Sp. No. 59672, pyroxene analyses 59672.4, ordinary light, X 75)

Plate 37

Intergrowth of needles of aegirine augite with feldspar on the edge of an aegirine augite grain in SS2. (Sp. No. 127021, ordinary light, X 75)

Plate 38

Secondary pale greenish acmite (centre) formed by reaction between magnetite and residual liquid in SS3. Small grains of opaque magnetite can still be seen, and biotite is visible at the top of the photograph. (Sp. No. 127038, acmite analyses 127038.2, ordinary light, X 75)

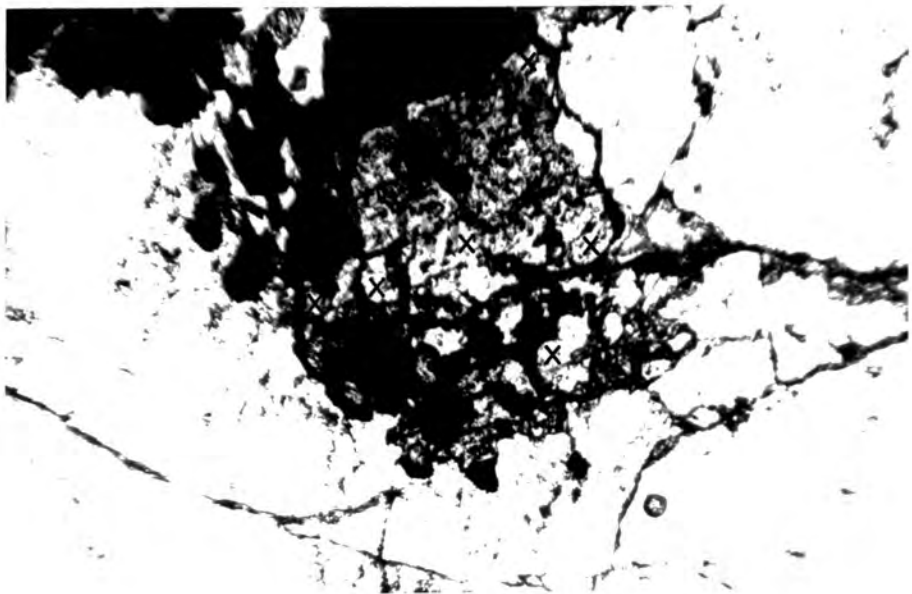


Plate 39

Fayalite (centre) with heavy rims of iron ore enclosed by aegirine augite (top right) and arfvedsonite (bottom left) in SS5. (Sp. No. 46243, olivine analyses 46243.1, ordinary light, X 75)

Plate 40

Rounded fayalite enclosed by aegirine augite (left) and biotite (bottom) in SS5. (Sp. No. 58230, olivine analyses 58230.2, ordinary light, X 40)

Plate 41

Olivine rimmed by interstitial titanaugite in SS4b. Also seen are prismatic apatite and irregular, opaque magnetite. (Sp. No. 59673, ordinary light, X 20)

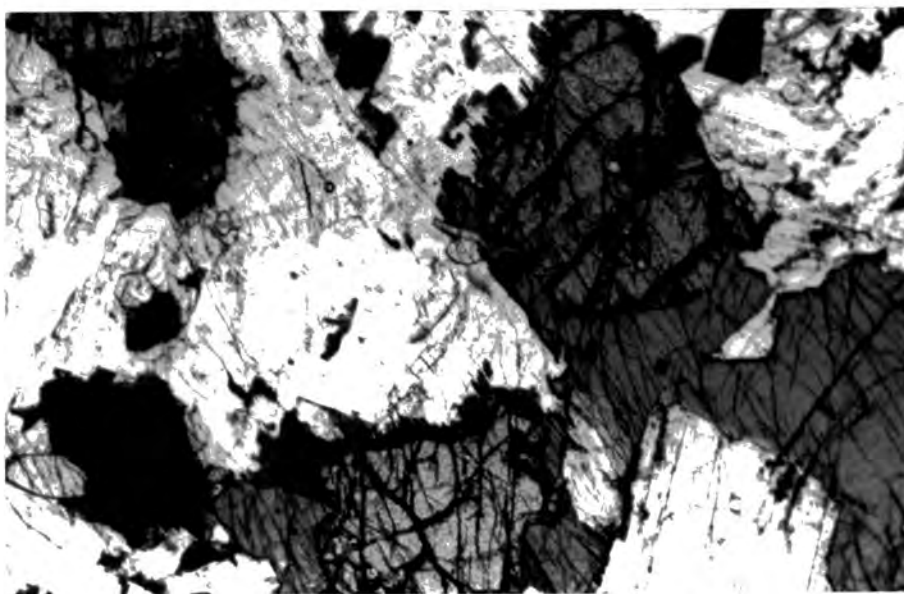
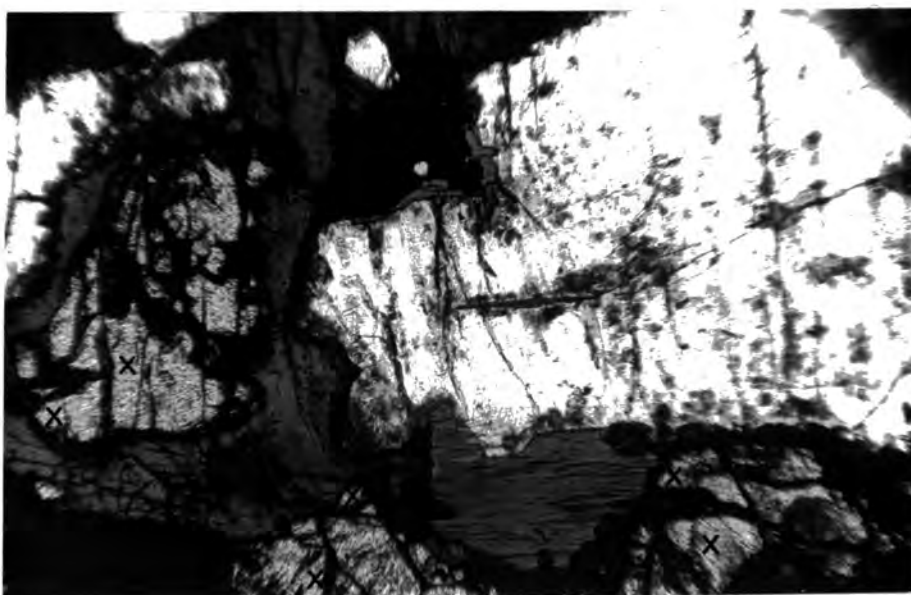


Plate 42

Olivine (hortonolite) with a thin rim of turquoise amphibole from a mafic band in SS4b. Also seen is a rounded grain of magnetite with radiating fringes of biotite (bottom right). (Sp. No. 59672, olivine analyses 59672.5, ordinary light, X 40)

Plate 43

Rounded grains of magnetite (light grey) with well developed, coarse exsolution lamellae of pleochroic ilmenite (black and white) parallel to the 111 cleavage. (Sp. No. 46243, reflected light, crossed polars, X 750)

Plate 44

Subhedral, rounded grains of euclite in an SS3 marginal pegmatite. (Sp. No. 59661, ordinary light, X 20)

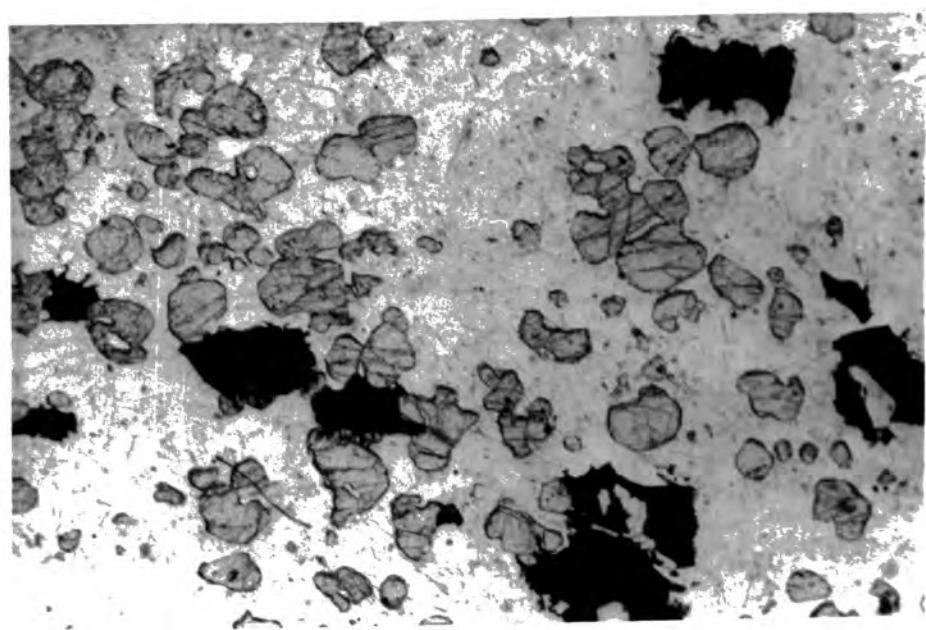
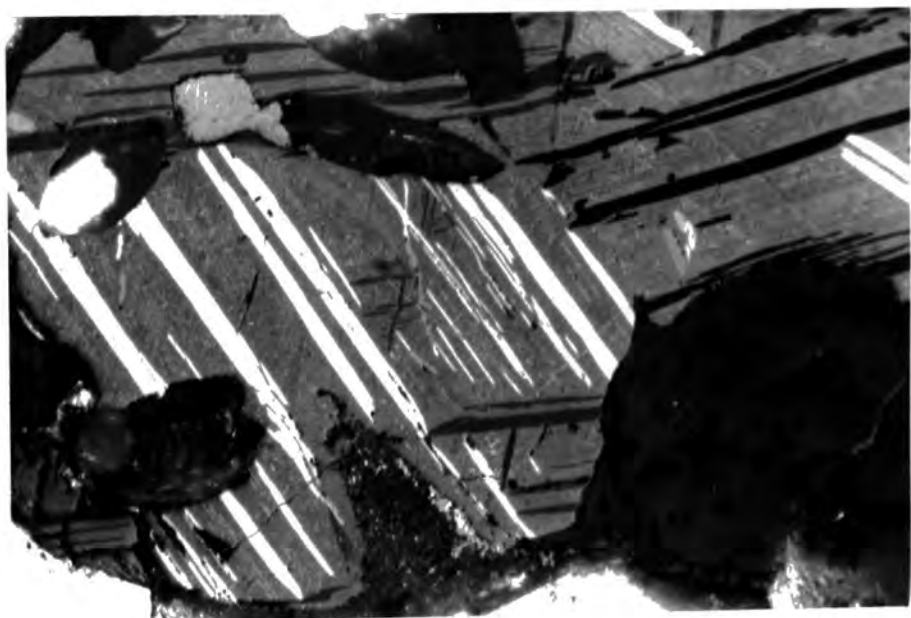
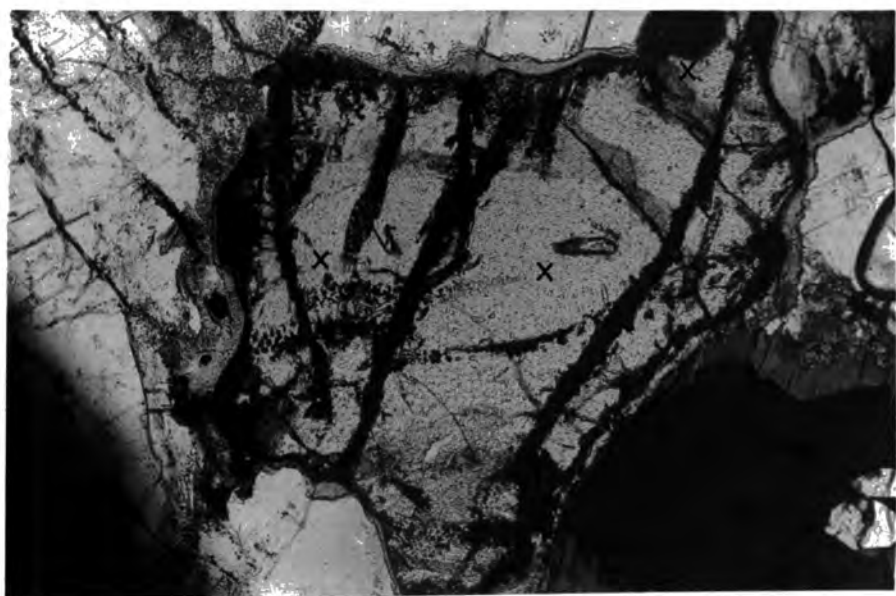


Plate 45

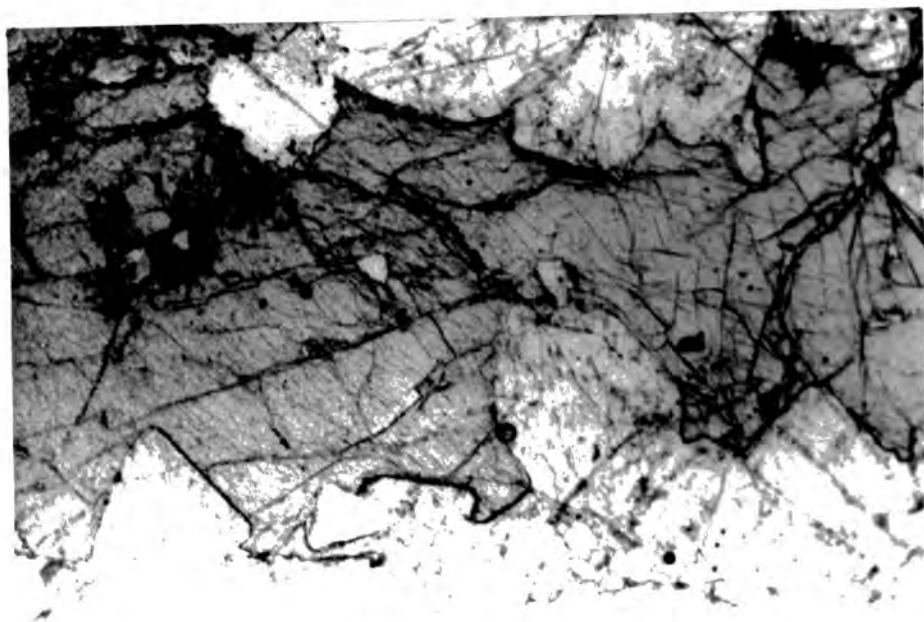
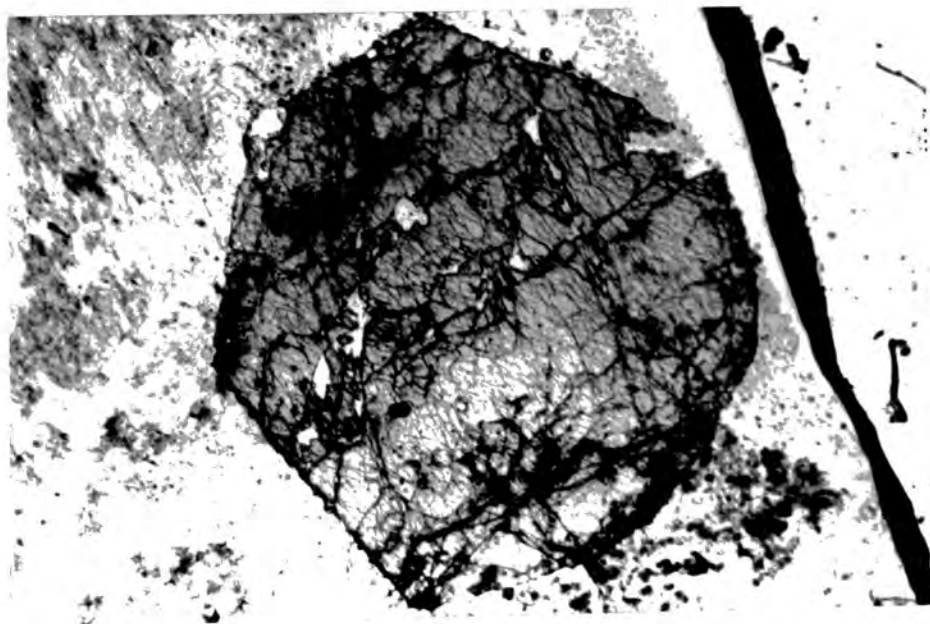
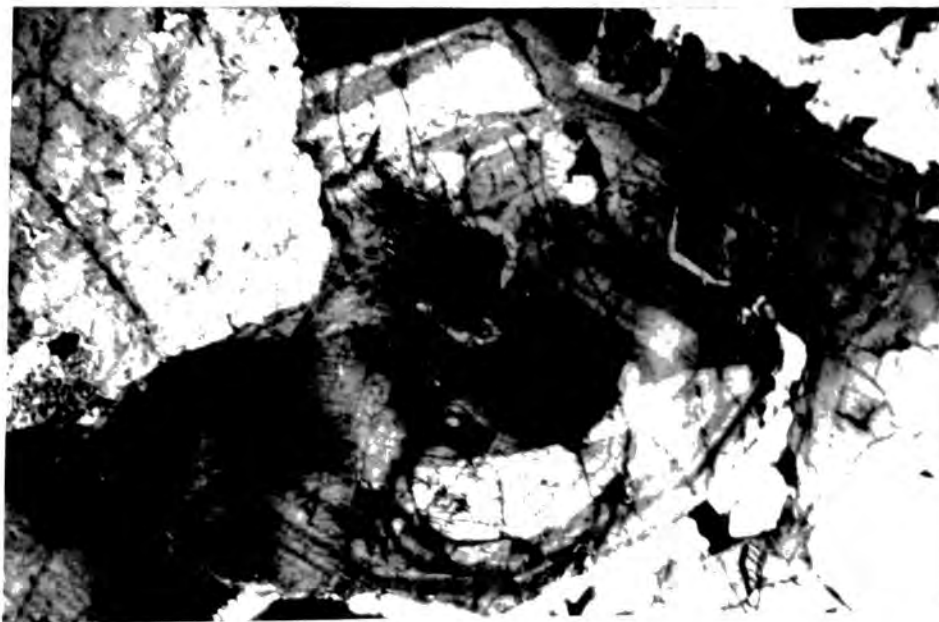
Zoned, euhedral eucolite-mesodialyte in an SS3 marginal pegmatite.  
(Sp. No. 59662, crossed polars, X 20)

Plate 46

Typical euhedral eucolite from an SS3 marginal pegmatite as Plates  
44 and 45. (Sp. No. 59663, ordinary light, X 20)

Plate 47

Poikilitic, zoned eucolite-mesodialyte from an SS3 marginal pegmatite  
as Plates 44 - 46. (Sp. No. 59665, ordinary light, X 20)



#### 4. MINERALOGY

##### (4a) Introduction

All analyses were made using a Geoscan electron microprobe, and were corrected for counter dead time, atomic number effect, mass absorption, fluorescence and electron back scatter (Sweatman & Long, 1969) using the computer program (ABFAN) of Boyd et al. (1969). The standards used were pure metals, stable oxides or analysed stoichiometric minerals. Details of sample preparation, standards, running conditions for each element and computer programs used are given in Appendix I.

Three to five samples were chosen from various localities in each of the major units (SS2, SS3, SS4a, SS4b, and SS5); one from a microsyenite sheet; one from the Essexite dyke; one each from SS2 and SS3 pegmatites and one recrystallised sample from each of SS4b and SS5. The locations of probe samples are shown in Fig. 2.1, and complete listings of analyses are given in Appendix III.

##### (4b) Pyroxenes

The pyroxenes have proved to be the most informative mineral group in the present investigation. It is therefore convenient to discuss them first so that the other mineral data may be interpreted in conjunction with them. Most of this section has already been published (Stephenson, 1972), but several modifications have been made in the light of more recent work.

In general, the pyroxenes of the foyaites are strongly zoned aegirine augites with pale green, or sometimes neutral cores and darker green rims, although in some cases zoning is not apparent and the grains are a uniform dark green. The zoning is usually continuous, but occasionally there is a sharp break between core and rim, probably representing a period of arrested growth. They are all strongly pleochroic, particularly the darker varieties with  $\alpha$  apple green,  $\beta$  yellow green,  $\gamma$  yellow brown. Grains are usually anhedral and vary in size up to 8 mm. They can occur

individually, but commonly form clusters with other mafic minerals and occasionally form small, interstitial areas between felsic minerals. Iron-titanium oxides and apatite, and occasionally olivine, nepheline and alkali feldspar occur as inclusions.

Amphibole is intimately associated with the pyroxene in most samples and frequently forms rims or partial rims in a manner which suggests a discontinuous reaction series. Biotite also occasionally forms rims on a smaller scale, this being most apparent when amphibole is absent or subordinate. Replacement along cleavage planes often erroneously suggests amphibole or biotite as inclusions. Frequently, the pyroxene grain boundaries have overgrowths of small pyroxene laths in optical continuity, intergrown with nepheline or alkali feldspar.

In several samples of SS3, and possibly other foyaites, grains of secondary, pale greenish-brown acmite occur, which appear to be forming as a result of reaction between magnetite and residual liquid (Bowen et al., 1930; Bailey, 1969). Acmitic compositions are also found in pyroxenes from coarse pegmatitic areas in the syenites. In pegmatite veins, large prismatic crystals of pyroxene up to 30 cm. long grow inwards from the walls. They frequently have cores of deep green, pleochroic aegirine, and rims of pale brown to colourless acmite.

The pyroxenes of the augite syenite have many features in common with those of the foyaites (grain size and form; inclusions; thin rims of amphibole), but are less sodic in composition, being predominantly lilac coloured titanaugites, with pale green, pleochroic rims marking the start of alkali enrichment. In the mafic bands, where pyroxenes are a major constituent, zoning is not apparent, but in samples which have been recrystallised by the Igdlarfigssalik centre, regular zoning becomes quite pronounced. Overgrowths upon grain boundaries are not as common as in the foyaites, except in the recrystallised rocks.

The essexite pyroxenes are similar to the titanaugites of SS4b and occur as large, poikilitic crystals, frequently showing orientated, exsolved rods of iron oxide. However, these may be modified by thermal effects. SS4a, and to a lesser extent the microsyenites, have many petrographic similarities to SS4b, but contain strongly zoned, green pyroxenes often with well developed rims of amphibole.

Several grains were selected from each probe sample, and each grain was analysed at several representative points. In this way the whole pyroxene series was represented; variations from syenite to syenite were determined; and variations in the zoning of individual grains within the same sample could be seen. A total of 167 complete analyses and 117 partial analyses (Ca, Na, Fe, and Mg only) were made.

Since the oxidation state of iron cannot be determined satisfactorily by electron probe analysis, it was necessary to allocate a  $Fe^{3+}/Fe^{2+}$  ratio according to the amount of alkalis present. In fully analysed alkali pyroxenes (Na + K) is always matched by almost exactly equal amounts of  $Fe^{3+}$  (Carmichael, 1962). Hence an atomic percent of Fe, equal to that of Na (K was not detected) was allocated to  $Fe^{3+}$ , the remainder being taken as  $Fe^{2+}$ .

As the majority of the pyroxenes are sodic, the major element variation can be shown on a molecular proportion plot of diopside - hedenbergite - acmite (Fig. 4.1). The corresponding minor element trends are shown in Fig. 4.2. The parameter (Na-Mg), based upon atomic proportions on the basis of 6 oxygens, has been chosen as a fractionation index, since initial depletion in Mg (with insignificant amounts of Na), is followed by a build up in Na (with insignificant amounts of Mg) during the evolution of the pyroxenes. Thus all parts of the trend can be represented by the same simple index (Na-Mg).

From Fig. 4.1 it can be seen that a continuous solid solution series exists between compositions of  $Di_{69}Hd_{25}Ac_6$  and  $Di_6Hd_{17}Ac_{77}$ . The trend is further extended by aegirines (green) and acmites (brown to colourless)

Fig. 4.1

Analyses of pyroxenes from the South Qorroq Centre. The average trend for the normal syenites and modified trends from the recrystallised syenites SS4b and SS5 are shown. The lower diagram shows the range of compositions within individual intrusions. (Molecular percent based on recalculation to 6 oxygens)

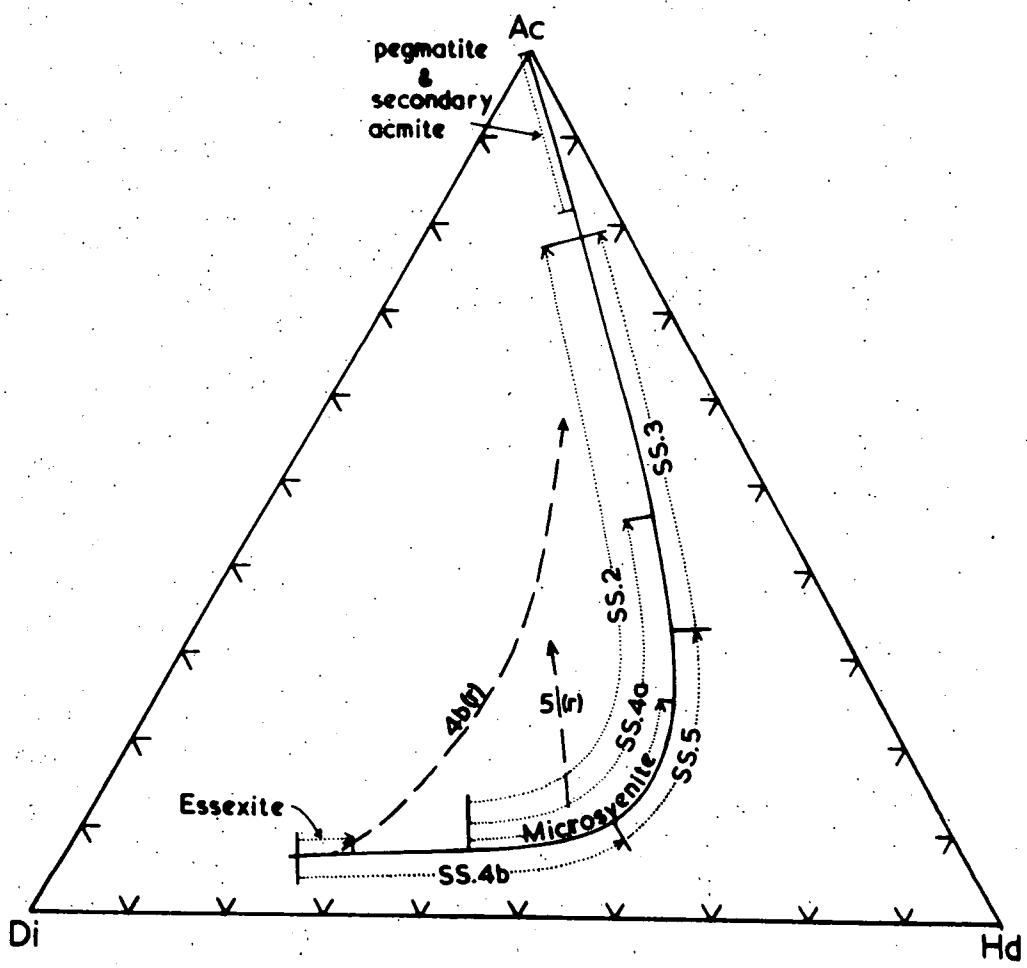
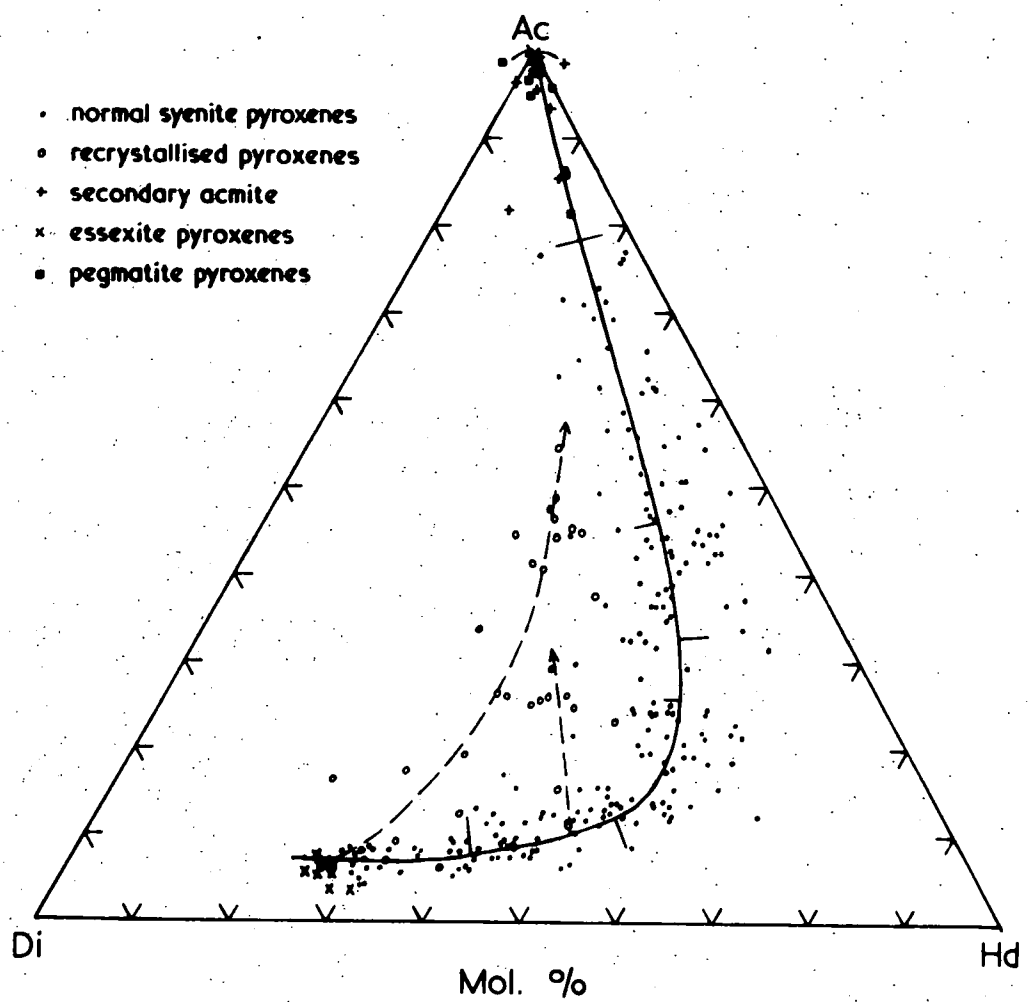


Fig. 4.2 (Two pages)

Variations of major and minor elements in the pyroxenes relative to the fractionation index (Na minus Mg). Bars at the base of the diagram show the range within each intrusion. Symbols as for Fig. 4.1. N.B.  $\text{Fe}^{3+}/\text{Fe}^{2+}$  is calculated from the alkali content, therefore in effect  $\text{Fe}^{2+} = \sum \text{Fe-Na}$ . (Atomic proportions on the basis of 6 oxygens)

Fig. 4.2a

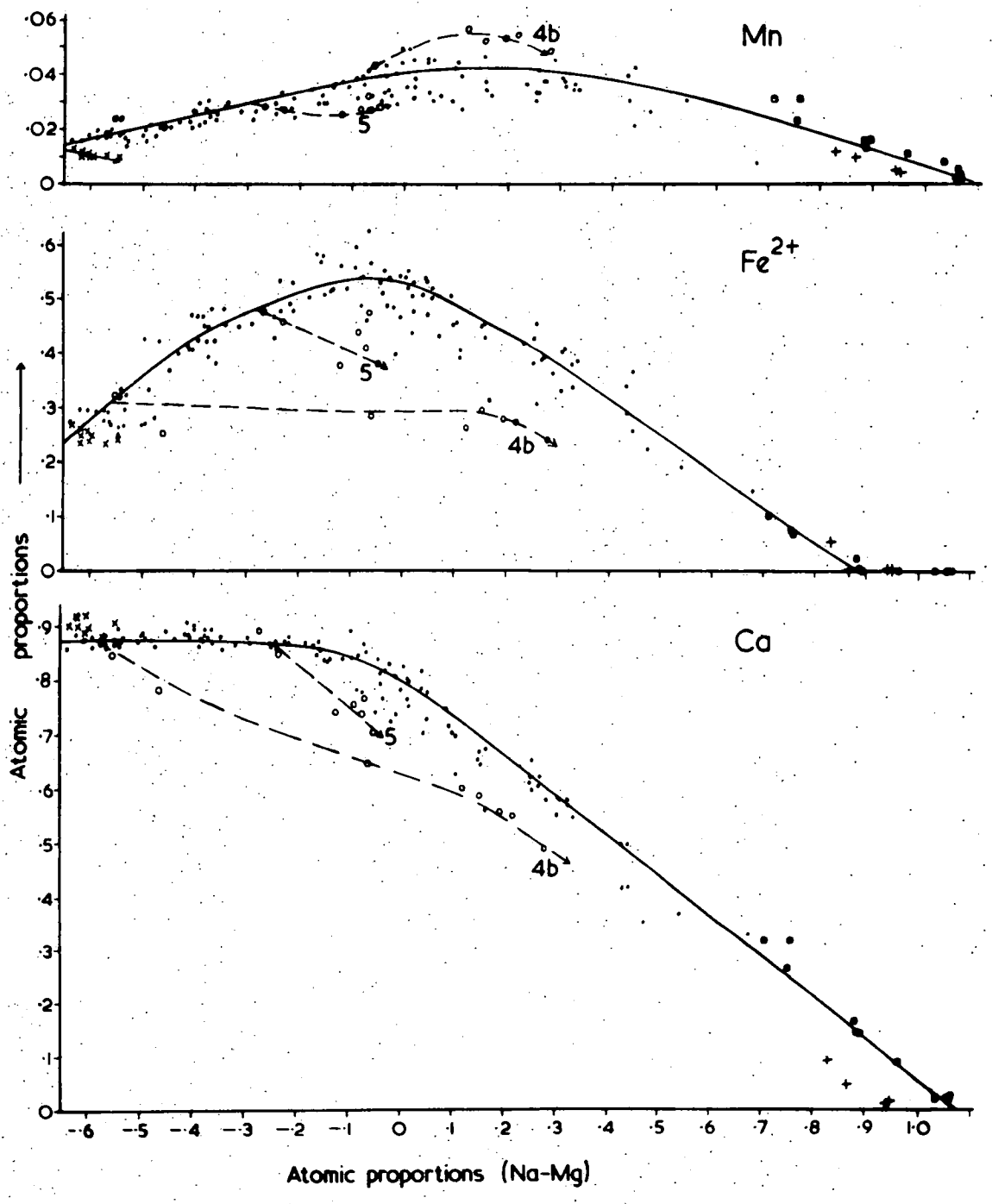
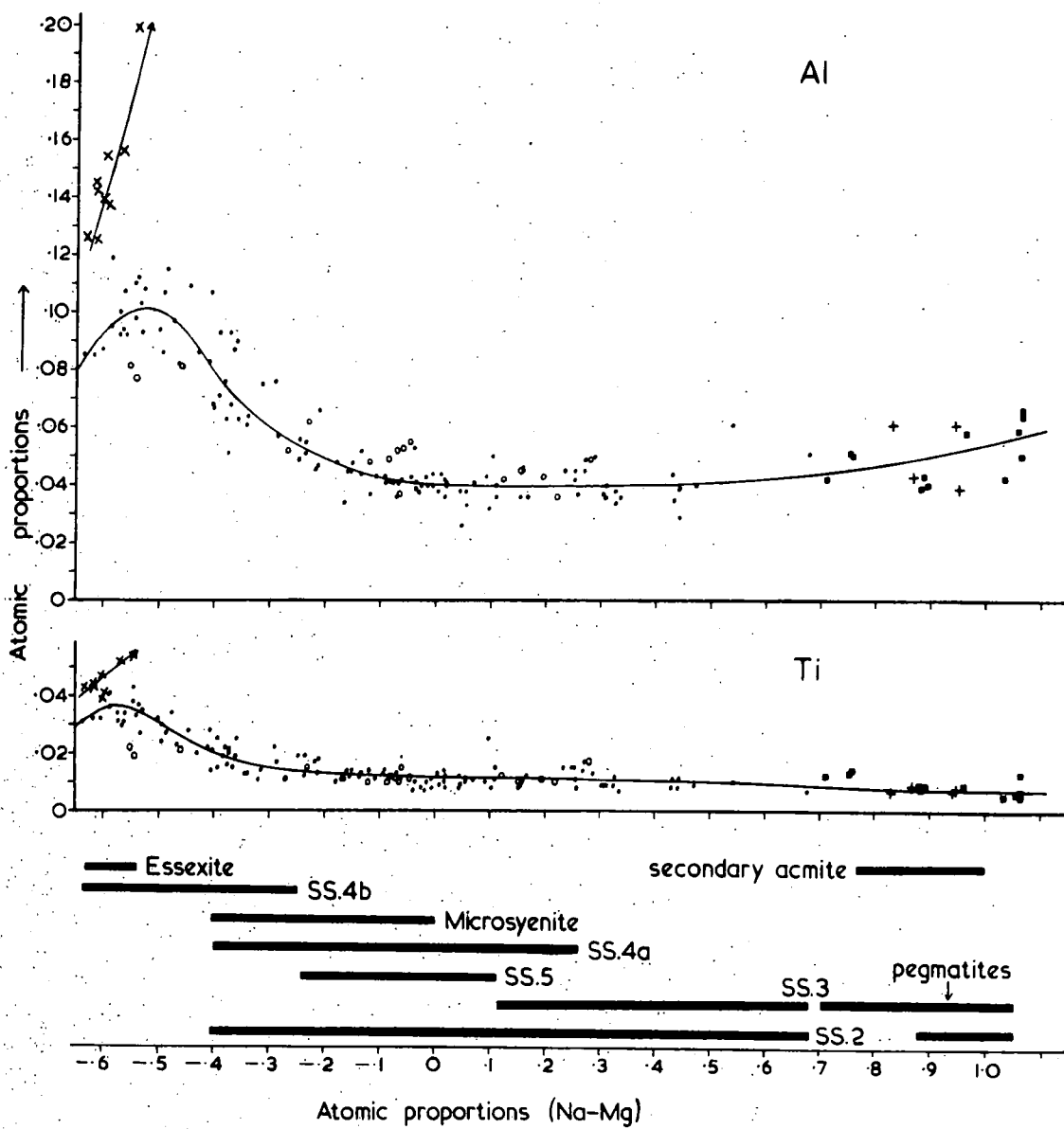


Fig. 4.2b



from the pegmatites and by secondary acmites from SS3, which show ranges from  $\text{Di}_4\text{Hd}_{10}\text{Ac}_{86}$  to  $\text{Ac}_{100}$ . Each syenite is seen to contain a distinct part of the pyroxene series, the lack of overlap between the fields of SS4b and SS5, and SS5 and SS3, being very noticeable. The earliest syenite (SS2) has a very extensive trend, but this ends at the same composition as for SS3 ( $\text{Di}_6\text{Hd}_{17}\text{Ac}_{77}$ ). The recrystallised syenites from SS4b and SS5 have trends which start at the same composition as their respective unaltered equivalents, but which become enriched in  $\text{NaFe}^{3+}$  at a much earlier stage relative to  $\text{CaFe}^{2+}$ .

Fig. 4.2 illustrates the behaviour of major and minor elements relative to the fractionation index (Na-Mg). Values of Si tend to be rather erratic, due to analytical error, and hence have not been included. Clearly the main substitution is  $\text{CaFe}^{2+}$  for  $\text{CaMg}$  during the first part of the trend, followed by  $\text{NaFe}^{3+}$  for  $\text{CaMgFe}^{2+}$ . The point at which  $\text{NaFe}^{3+}$  enrichment becomes dominant (about Na-Mg = -0.1) is clearly seen on the Ca plot as the point where Ca starts to decrease with increasing Na in an approximately 1:1 ratio. Similarly  $\text{Fe}^{2+}$ , after increasing steadily in the early stages, also shows a decrease from this point, with a sympathetic variation in Mn content. Al and Ti show a sympathetic variation and increase sharply during the very early stages of fractionation, when Na has little effect, as found by Kushiro (1960) and Le Bas (1962). Most of the Al is probably in tetrahedral co-ordination, and  $\text{Ti}^{4+}$  is used to balance the positive charge deficiency. However, this trend is followed by a rapid fall and levelling off such that later parts of the series have fairly low, uniform Al and Ti.

Pyroxenes from recrystallised rocks are seen to deviate from the normal trend in some elements, and of particular interest is the constant concentration of  $\text{Fe}^{2+}$  in the recrystallised SS4b pyroxenes. This would tend to suggest a fairly constant buffering of oxygen fugacity ( $f_{\text{O}_2}$ ) during recrystallisation. A slight increase in  $\text{Fe}^{3+}/\text{Fe}^{2+}$  is detectable

in the bulk geochemistry of these rocks (see Chapter 5), and magnetite and ilmenite occur as discrete grains instead of in the normal oxidation-exsolution relationship. Fayalite appears to become unstable during recrystallisation and is not found within the recrystallised zone, indicating that the  $f_{O_2}$  was at least higher than the fayalite - magnetite - quartz buffer curve (see considerations of oxygen fugacity in section 4d).

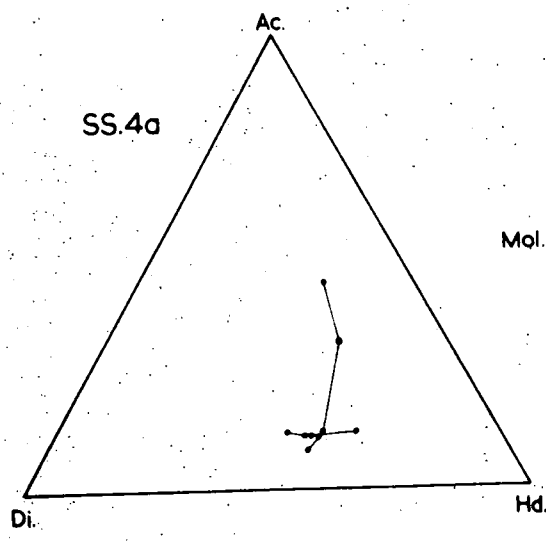
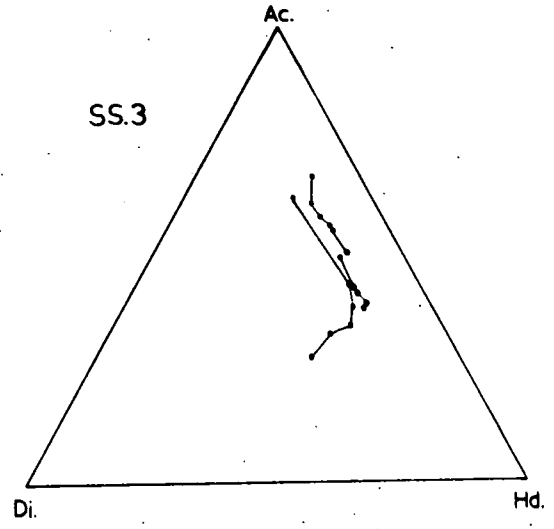
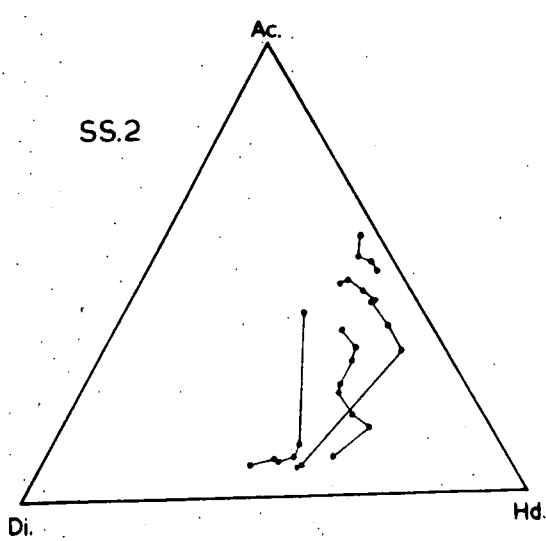
The more basic nature of the essexite is illustrated by deviations from the main pyroxene trends, and particularly in the higher concentrations of Ti and Al. However, the pyroxenes are poikilitic and clearly crystallised in situ, thus precluding a deeper level origin.

The extent of zoning in individual grains from each syenite is shown in Fig. 4.3. This stresses the fact that the line drawn through the points in Fig. 4.1 is, at the most, only an average trend for the whole pyroxene series. Individual grains, even within the same rock section, can show very different trends, particularly in that part of the series occupied by pyroxenes of SS5 and similar compositions. This is the critical area in which  $NaFe^{3+}$  enrichment becomes dominant, and the great variation can probably be attributed to crystals growing in their own chemical micro-environment, particularly with regard to  $f_{O_2}$  and availability of Na in the liquid. Pyroxenes from mafic bands are usually unzoned with compositions corresponding to the cores in unbanded equivalents, due to removal from the liquid at an early stage.

Very few published analyses are available of pyroxenes from the Gardar Province and there are no continuous series analysed. However, trends from several other alkaline provinces are plotted on Fig. 4.4. together with the few published Gardar analyses. The South Qôroq trend, in common with those from other undersaturated plutonic suites (Yagi, 1953; Tyler and King, 1967; Gomes et al., 1970) shows an enrichment in  $NaFe^{3+}$  at a fairly early stage relative to the  $CaMg-CaFe^{2+}$  substitution.

Fig. 4.3

Zoning within representative pyroxene grains from each intrusion. Closed circles, normal grains. Open circles, grains from recrystallised syenites.



Mol. %

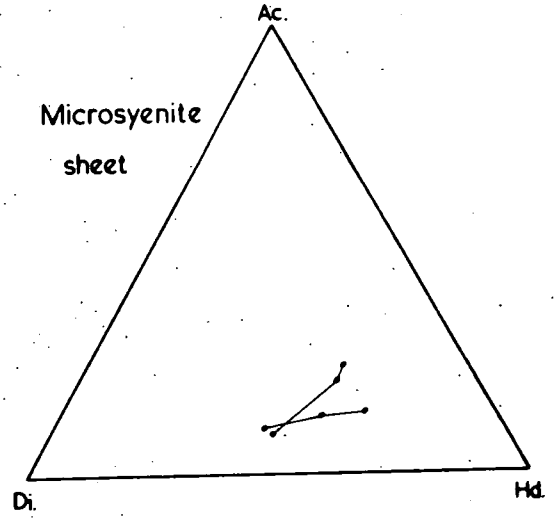
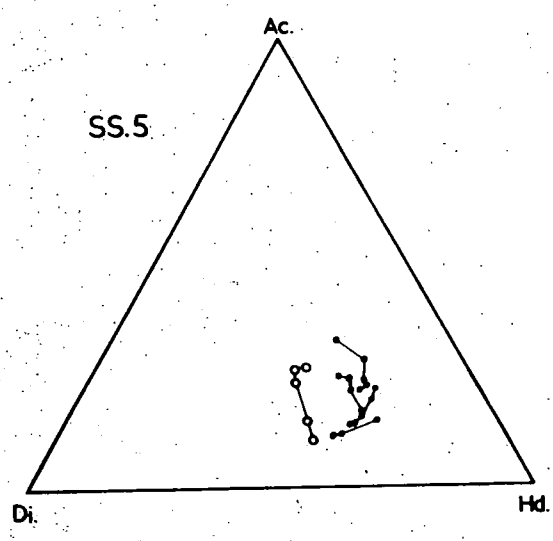
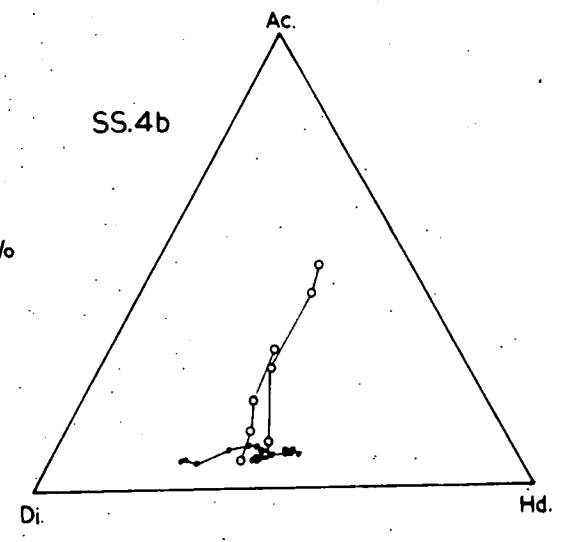


Fig. 4.4

Comparison between the South Qôroq pyroxene trends and other published data.

Analyses from the Gardar Province, South Greenland:

(S), Sørensen, 1962, p.192.(U), Upton, 1964, pp.28 & 64.

(W), Washington & Merwin, 1927, P.249.

Pyroxene trends from other provinces:

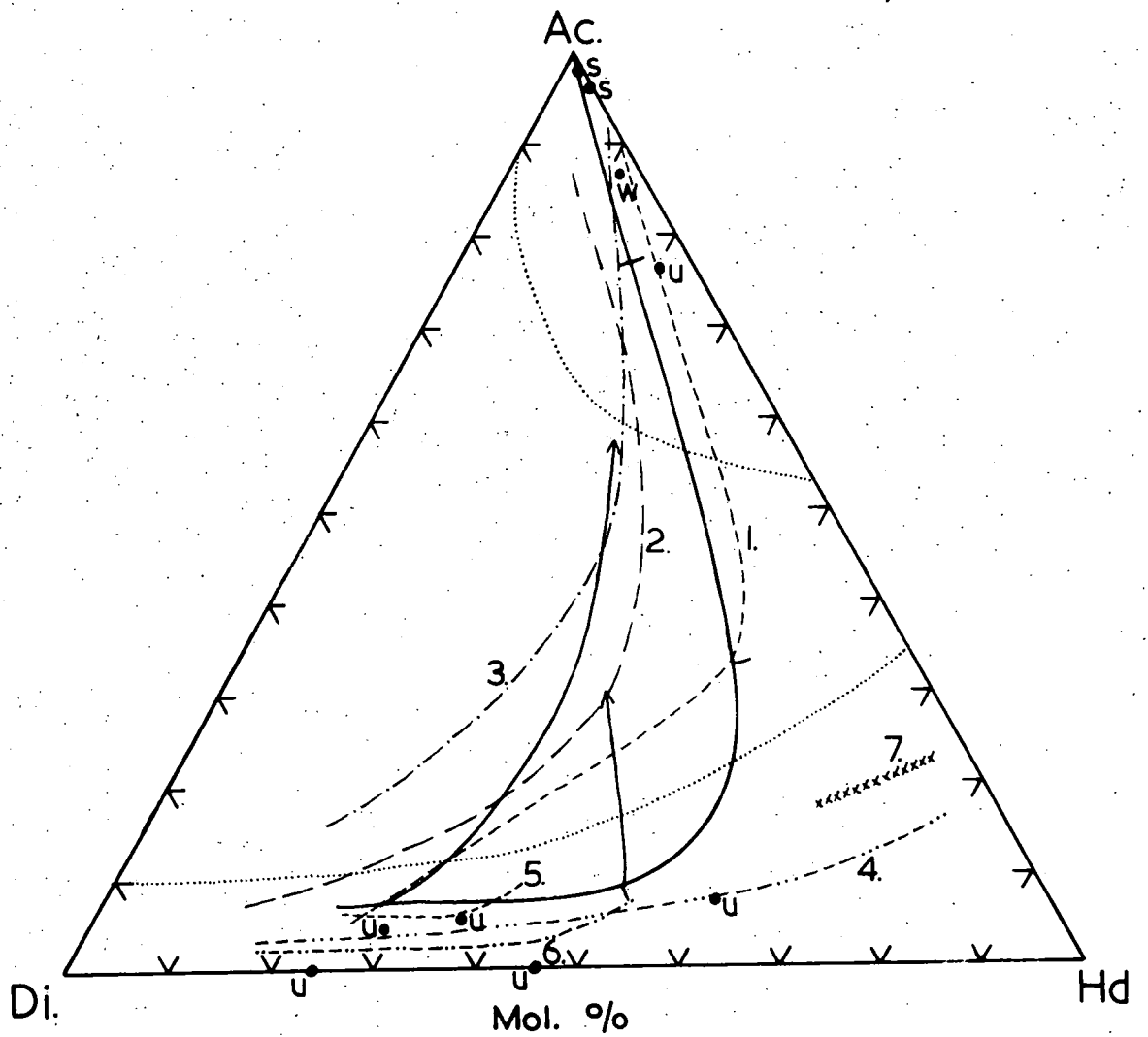
(1), Morutu, Sakhalin (Yagi, 1953). (2) Uganda (Tyler & King, 1967). (3) Itapirapuã, Brazil (Gomes et al., 1970).

(4) 'Alkali basalt - trachyte series' (Aoki, 1964).

(5) Black Jack sill, New South Wales (Wilkinson, 1957).

(6) Garbh Eilean sill, Shiant Isles (Murray, 1954).

(7) Pantellerite trend (Carmichael, 1962).



- South Qoroq Centre trends.
- 1-7 Trends from other alkaline igneous provinces.
- Published Gardar pyroxene analyses.
- ..... Fields of Ca & Na rich alkali pyroxenes, after Aoki (1964).

However, the alkali basalt-saturated trachyte trend of Aoki (1964) and the pantellerite trend of Carmichael (1962) proceed much further towards a hedenbergite composition. A similar situation occurs in the Gardar Province in the oversaturated, plutonic alkaline complex at Nunarssuit, where the pyroxenes trend towards hedenbergite before becoming enriched in  $\text{NaFe}^{3+}$  (P. Greenwood, personal communication, 1971). There is no evidence from South Qôroq to suggest a trend such as that found in the Shonkin Sag laccolith (Nash & Wilkinson, 1970 p.265-266), in which for each successive rock type the mildly sodic pyroxene cores progress from salite to sodic hedenbergite, but subsequently fractionate along different trends.

From comparison with these other alkali pyroxene trends, it would seem that in general undersaturated igneous suites produce pyroxene trends which show  $\text{NaFe}^{3+}$  enrichment at an early stage compared with oversaturated suites. An exception to this is the Gardar, undersaturated Ilímaussaq Complex. Apart from titanaugites from the marginal Augite Syenite all the pyroxenes from this complex fall along the hedenbergite - acmite join (L. Melchior, personal communication, 1972). However, it is perhaps significant that the complex is agpaitic with very little Mg available in the magma for inclusion in pyroxenes. Considering the effect of recrystallisation upon SS4b pyroxenes (in which the trend is moved away from the hedenbergite composition, whilst  $\text{Fe}^{2+}$  is kept fairly constant) it would seem that  $f_{\text{O}_2}$  may exert some control upon the relative position of contrasted trends. However, since little quantitative data is available at present on  $f_{\text{O}_2}$  in alkaline rock suites, very little can be deduced about the nature of this control (see section 4d).

Clearly the pyroxenes are important as they provide diagnostic criteria for recognising each syenite where petrography and whole rock geochemistry fail due to overall homogeneity, and are subtle indicators of recrystallisation, often where it is not apparent from rock textures.

They also support the order of intrusion deduced from field relationships, since the earlier rocks contain the most fractionated pyroxenes, and compositions become progressively less fractionated with time. This recession of starting composition for successive syenite pyroxene trends has considerable implications on the origin and subsequent magmatic evolution of the South Qorroq Centre, and will be discussed at greater length in Chapter 6 in conjunction with other evidence.

#### (4c) Amphiboles

Amphibole is present as a primary mafic phase in all major units of the centre, although it is occasionally absent from small localised areas particularly in SS3. The grains are anhedral and commonly occur in clusters with other mafics or in interstitial areas. Frequently they are found as rims to pyroxene in a discontinuous reaction series, but in some samples the two minerals are intergrown and may have grown together at least during part of their crystallisation history. Amphibole is not present in the essexite and is less abundant in recrystallised rocks, which are correspondingly enriched in biotite.

The amphiboles of the foyaites, SS4a and microsyenite sheets are alkaline and are probably members of the Katophorite - arfvedsonite series (see below). Their intense absorption, dispersion and variable pleochroism makes accurate determination of optical properties difficult. However, they are usually pleochroic from yellowish brown ( $? \gamma$ ) through "muddy" brown ( $? \beta$ ) and dark "muddy" green ( $? \alpha$ ) with occasionally a bluish green. They are always biaxial -ve, have a low extinction angle, and usually have a fairly low 2V which varies between approximately  $10^\circ$  and  $40^\circ$ . Zoning is sometimes detectable optically, but is seldom well developed. In the augite syenites amphibole is generally less alkaline with clearer (as opposed to "muddy") brown colours. The pleochroism is from yellowish brown ( $? \gamma$ ) to dark brown ( $? \alpha$ ). In some mafic bands (e.g. 59672) the amphibole is a reddish brown to pale yellowish and resembles barkevikite

in optical properties.

It is difficult to obtain complete analyses of amphiboles by electron probe due to the presence of volatiles and the lack of any simple relationship from which to calculate the  $\text{Fe}^{3+}/\text{Fe}^{2+}$  ratio (Rucklidge et al., 1971). Hence this work is confined principally to an investigation of the continuation of the pyroxene - amphibole discontinuous reaction series mentioned in 4b. Amphiboles from selected slides of the major units were analysed partially for Si, Fe, Mg, Ca, Na and K. Of the elements not determined only Al is considered to be present in significant amounts. In addition, two large amphibole crystals from pegmatites were analysed completely for major and trace elements and these will be considered separately.

In Fig. 4.5 the analyses are plotted on a  $(\text{Na}+\text{K}) - \Sigma\text{Fe} - \text{Mg}$  diagram to facilitate comparison with the pyroxenes in Fig. 4.1. It should be noted that in Fig. 4.5 (amphiboles) 'Fe' is  $\Sigma\text{Fe}$ , whereas in Fig. 4.1 (pyroxenes) 'Fe' is  $\text{Fe}^{2+}$ , and also that the amphiboles contain appreciable K which is not present in the pyroxenes. Zoning is less well pronounced in the amphiboles, and there is considerable overlap of individual trends, but in general it can be seen that the start of each amphibole trend regresses in the order SS2-SS3-SS4a-SS5-microsyenite-SS4b, which is identical to the order of regression of the ends of the respective pyroxene trends. Thus, in agreement with the textural relationships, it would appear that the end of the pyroxene trend for any particular syenite is governed by the appearance of amphibole. The barkevikitic amphiboles from the mafic band 59672 follow a different trend to the foyaite amphiboles, and probably reflect a more "basic" late stage liquid in such bands.

Several workers have commented on the discontinuous reaction series aegirine augite - arfvedsonite - aegirine (Yagi, 1953; Sørensen, 1962). Yagi observed that aegirine augite becomes unstable as water becomes concentrated in the residual magma during crystallisation, and alkali

Fig. 4.5

Variation of alkalis, Fe and Mg in South Qôroq amphiboles. The fractionation trends for various syenites are marked with solid lines and it can be seen that the general order of regression of the starting points of the trends is identical to the order of regression of the ends of respective pyroxene trends in Fig. 4.1. Thus it would appear that the end of each pyroxene trend is determined by the appearance of amphibole. The analysis connected by a dotted line to the SS4a trend is an earlier grain enclosed in a pyroxene.

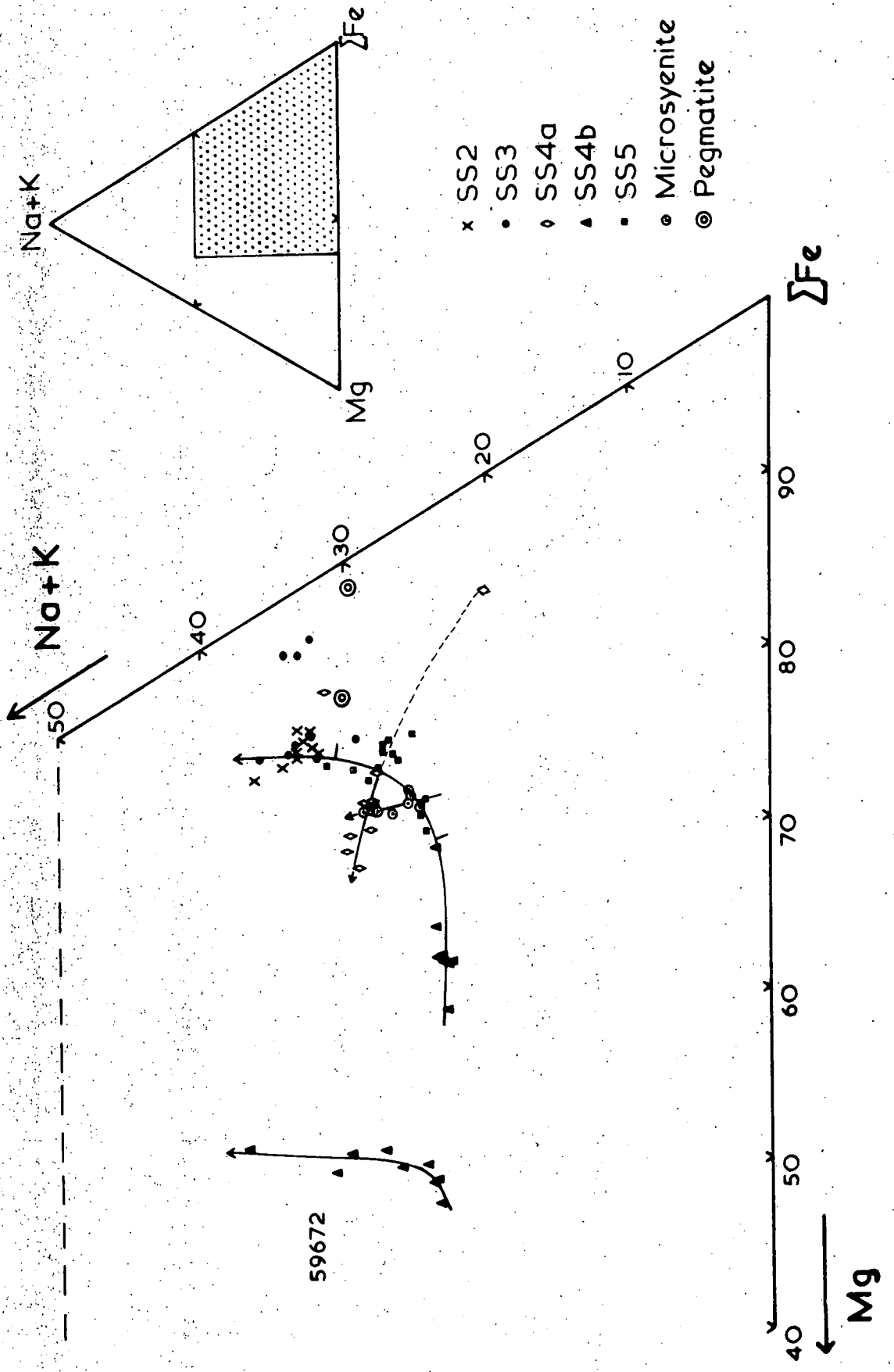
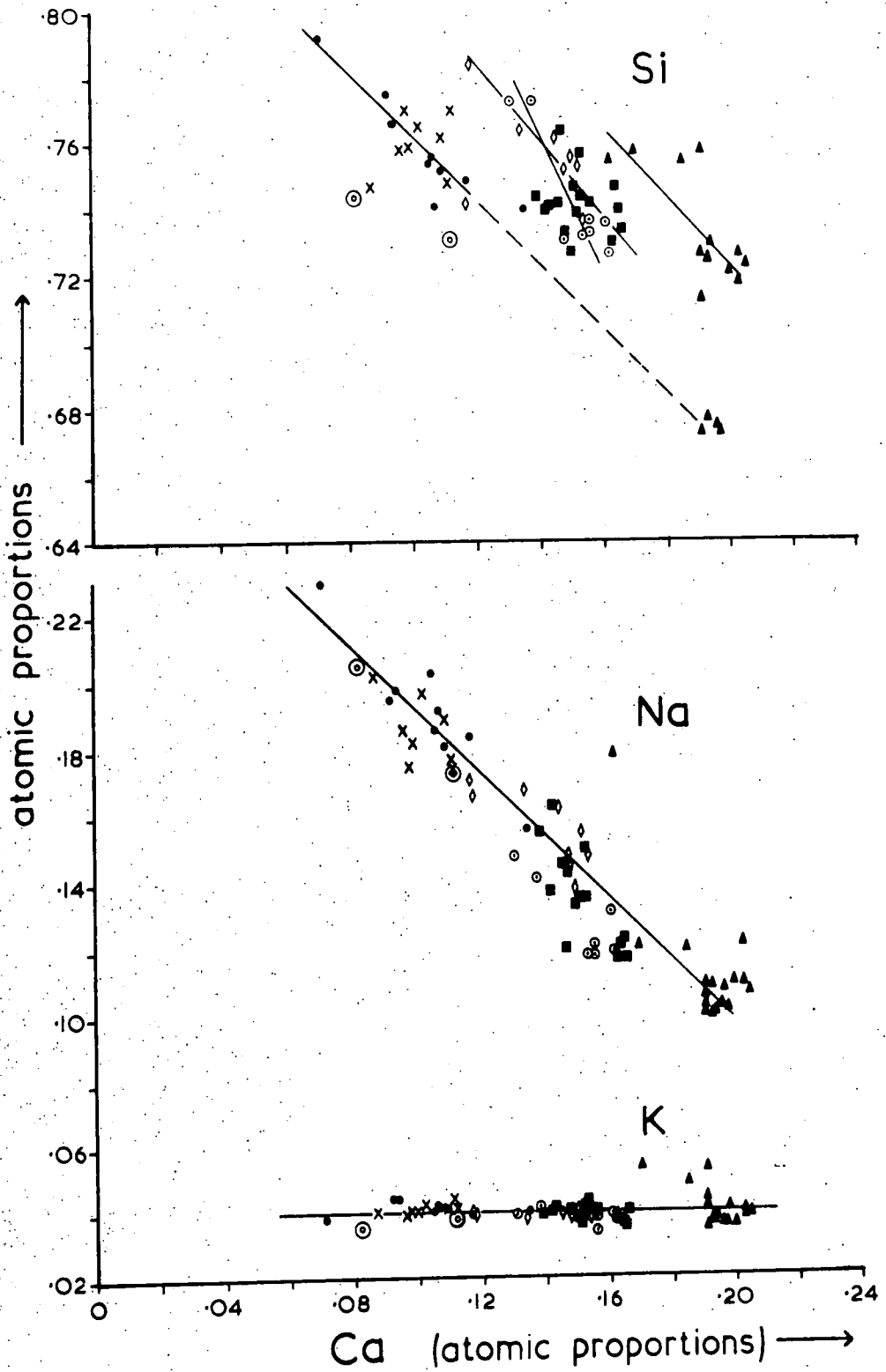


Fig. 4.6

Variations of K, Na and Si with Ca in the South Qôroq amphiboles, suggesting possible cation substitutions in the A, X and Z sites (see text). The offsets of Si v Ca lines could just be due to analytical error in Si. Symbols as in Fig. 4.5.



amphibole follows in a reaction relationship. Ernst (1962) has shown experimentally that arfvedsonite is only stable at fairly low temperatures (<700°C) and moderately low oxygen fugacity (between the wustite - magnetite and fayalite - magnetite - quartz buffer curves) under fairly high  $P_{H_2O}$  conditions. Such conditions are to be expected in the South Qôroq syenites during the later stages of crystallisation (see section 4d for considerations of oxygen fugacity), and hence the position of the pyroxene - amphibole reaction is probably determined largely by the rate of build up of  $P_{H_2O}$  in each intrusion.

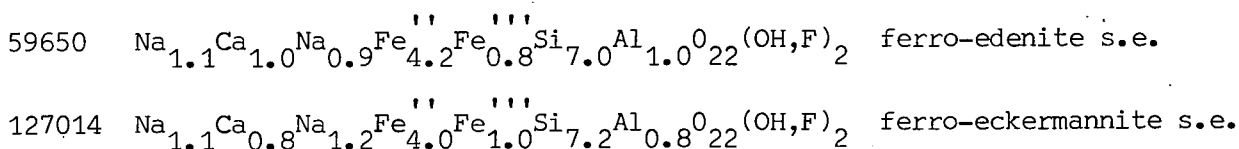
Bailey (1969), investigating the stability of acmite in the presence of water, found that at low temperatures arfvedsonite becomes unstable and gives way to acmite even at quite high  $P_{H_2O}$  if there is an increase in oxygen fugacity, particularly if this is accompanied by a build up in Na in the residual liquid. The build up of  $P_{H_2O}$  could be sufficient to raise the oxygen fugacity slightly in the later stages of crystallisation, or the appearance of another mafic mineral such as biotite could similarly provide a new, internal  $f_{O_2}$  buffer (see section 4d). Thus the full discontinuous reaction series becomes aegirine augite - arfvedsonite - aegirine. This complete series is observed within single samples from certain units of the Igdlérfigssalik Centre (C. H. Emeleus, personal communication, 1971), but not in South Qôroq. However, the large, acmitic pyroxenes present in late pegmatite veins complete the series within this centre as a whole.

Further element variations in the amphibole series are shown in Fig. 4.6 in which K, Na and Si are plotted against Ca (atomic proportions). It is seen that with fractionation there is a 1:1 replacement of Ca by Na, but K remains remarkably constant throughout the series at about 1.5 Wt.%. Similarly, within individual samples Si increases 1:1 with Ca, suggesting that it is involved in a coupled substitution (see below).

The displacement of the Si v Ca lines for certain individual samples could just be due to slight systematic errors in the Si determination.

Two complete analyses were made of large amphibole crystals from pegmatites (59650 & 127014) which appear similar to the other partial analyses. 59650 is from a 1 m. wide vein cutting SS5, but 127014 is from scree, although it probably originated in SS2 or SS3. Most of the elements (including F & Cl) were determined by electron probe, FeO and H<sub>2</sub>O were determined wet chemically, and trace elements were determined by X-Ray fluorescence. The analyses are listed in Table 1 and have been recalculated to give cation allocations using the method of Phillips (1963).

The structural formulae (neglecting minor constituents) and names obtained from the Phillips recalculation are as follows:-



They are thus very close to the theoretical katophorite composition of  $Na_1Ca_1Na_1Fe_4Fe_1Si_7Al_1O_{22}(OH,F)_2$  in which all the Al occurs substituting for Si in the Z site, and which has a substantially higher Ca content than arfvedsonite. The trace element data shows particularly strong concentrations of Zr and Nb, but this could be due to contamination by small inclusions of zircon. The moderate values for Zn, Pb, La and Y are probably in the amphibole itself, although magnetite and aegirine are also present as inclusions.

From the relationships seen in Fig. 4.6 and considerations of the two complete analyses, it would seem that the principal substitutions operating in the amphibole series are Na for Ca in the X site and Al for Si in the Z site. These are balanced by an increase in Na in the A site and a substitution of Fe<sup>3+</sup> for Fe<sup>2+</sup> in the Y site. There is also probably a substitution of F for OH as has been found in Ilímaussaq and Tugtutôq amphiboles (G. Rowbotham, personal communication, 1972).

	<u>59650</u>	<u>127014</u>	<u>ppm</u>	<u>59650</u>	<u>127014</u>
SiO <sub>2</sub>	43.91	44.61	La	64	280
TiO <sub>2</sub>	0.98	1.05	Ba	27	36
Al <sub>2</sub> O <sub>3</sub>	5.74	4.84	+ Nb	1246	1134
Fe <sub>2</sub> O <sub>3</sub>	7.21	9.77	+ Zr	6840	6470
FeO	23.31	24.21	Y	39	127
MnO	1.39	0.91	Sr	26	45
MgO	2.17	0.44	Rb	23	29
CaO	6.24	4.61	Pb	100	58
Na <sub>2</sub> O	5.36	6.31	Zn	842	612
K <sub>2</sub> O	1.75	1.63	Cu	15	14
H <sub>2</sub> O+	1.22	1.33	Ni	7	4
F	0.66	0.70	V	5	3
Cl	-	-	U	0	4
	<u>99.94</u>	<u>100.40</u>	Th	0	9
O ≡ F	0.28	0.30			
TOTAL	<u>99.66</u>	<u>100.10</u>			

Formulae on the basis of 24 oxygen atoms :-

	<u>59650</u>	<u>127014</u>
Z { Si 7.044 } { Al 0.956 }	8.000	7.152 } 0.848 } 8.000
Y { Ti 0.118 } { Al 0.126 } { Fe <sup>3+</sup> 0.870 } { Fe <sup>2+</sup> 3.128 } { Mn 0.189 } { Mg 0.519 }	4.950	0.127 } 0.067 } 1.179 } 3.246 } 0.124 } 0.105 } 4.848
X { Ca 1.073 } { Na 0.927 }	2.000	0.792 } 1.208 } 2.000
A { Na 0.740 } { K 0.358 }	1.098	0.754 } 0.333 } 1.087
OH 1.306 } F 0.335 }	1.641	1.422 } 0.355 } 1.777

+ Probably contamination of the sample by zircon inclusions.

TABLE 1. Analyses of Alkali Amphiboles from South Qorroq Centre Pegmatites

The partial analyses of the augite syenite and foyaite amphiboles resemble the two katophorites in the concentrations of elements which have been analysed, and their low Si concentrations suggest a similar degree of Al - Si substitution. However, it is not known how much of the series katophorite - arfvedsonite is represented and some of the more sodic compositions may be arfvedsonitic. Miyashiro (1957) demonstrates that katophorites crystallise at somewhat higher temperatures than arfvedsonites, being more characteristic of basic alkaline rocks and volcanics. The series represented in the South Qôroq Centre is continuous with the arfvedsonite series of Ilímaussaq, but reflects the generally higher crystallisation temperatures of the former intrusion. However, it is difficult to reconcile the presence of katophorite in the South Qôroq pegmatites with the findings of Miyashiro and it appears that its stability range may be greater than was originally thought.

#### (4d) Olivines

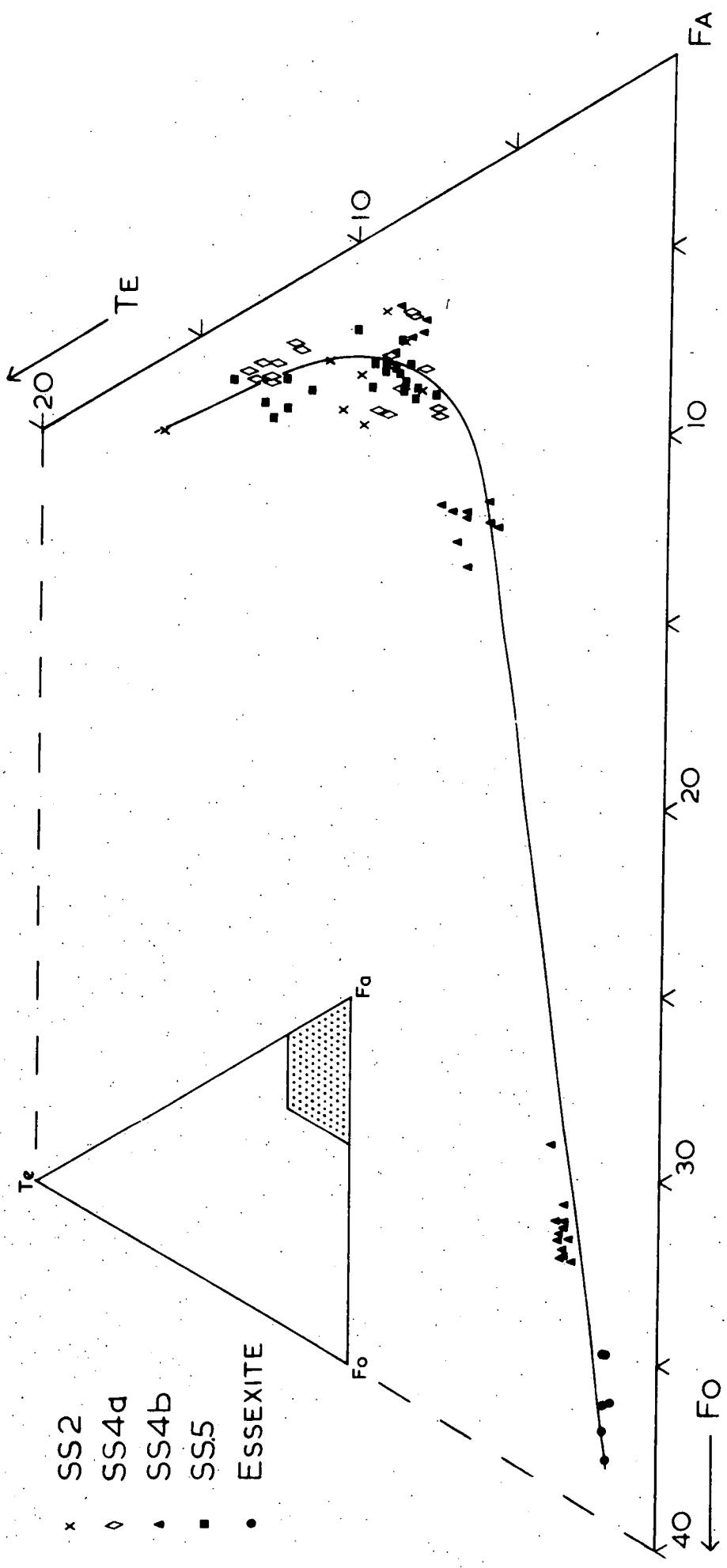
Olivine is present in varying proportions in most units of the centre. However, it is absent from syenite SS3, from pegmatite patches and veins, and from the zone of alteration surrounding the Igdlérfigssalik Centre. Its distribution in the foyaites and microsyenite sheets is sporadic, some samples having no olivine or only accessory amounts, whereas in parts of SS4a and SS5 it can form up to 2-3% of the rock. It usually occurs as early formed, slightly yellowish, rounded grains varying in size from 0.2 - 5 mm. These show signs of oxidation in the form of thick rims and exsolved lamellae, both of iron ore (usually magnetite). The grains often occur in clusters with other mafic minerals and frequently act as nuclei for pyroxene and amphibole crystallisation, possibly forming a discontinuous reaction series. In the augite syenites of SS4b olivine is more abundant and in general shows less late-stage oxidation. However, in mafic bands it is cumulus, very fresh and can form up to about 8% of the rock. The essexite contains about 15% olivine which is similar in appearance to those of the mafic bands.

All the olivines analysed are iron-rich, and in the foyaites they are also manganiferous. The major element variation and fractionation trend can thus be shown in part of the system forsterite - fayalite - tephroite (Fig. 4.7) which shows a range from  $\text{Fo}_{36}\text{Fa}_{62}\text{Te}_2$  to  $\text{Fo}_2\text{Fa}_{82}\text{Te}_{16}$ . The most magnesium rich olivines are found in the essexite dyke, but even these have only 36% Fo. The syenites of SS4a and SS4b show a considerable range of olivine compositions, the most magnesian of which are found as fresh grains in mafic bands. With increase in  $\text{Fe}^{2+}$ , Mn also increases steadily until, in olivines of SS4a and the foyaites, Mn becomes the principal fractionating element. Clearly the foyaite olivines are compositionally distinct from those of the augite syenite and essexite, but there is no distinction between those of individual foyaites as is the case with the pyroxenes. Simkin and Smith (1970) report a general high Mn content of up to 1.5 Wt.% Mn in olivines from undersaturated plutonic rocks. However, in the South Qoroq foyaites the average Mn content is around 5 Wt.%, and values of up to 8.6% occur.

Of the minor elements only Ca occurs in any significant amount, ranging from 0.2 to 0.6 Wt.% Ca (Fig. 4.8). This is considerably higher than the normal limit for plutonic olivines of 0.1 Wt.% proposed by Simkin and Smith (1970), although they do report that the higher values tend to be found in undersaturated rocks. C. H. Emeleus and A. D. Chambers (personal communications - 1972) have found similar high values of Mn and Ca in olivines from the Igdlarfigssalik and North Qoroq Centres, suggesting that Simkin and Smith may have used only a small range of alkali rocks. Simkin and Smith suggest that the Ca content may be pressure controlled, in which case the high level nature of the Igaliko centres could account for the high Ca. Alternatively they suggest that slow cooling in plutonic rocks allows diffusion of larger Ca ions out of olivines in late stages of crystallisation. This could have been prevented in the Igaliko olivines by the thick oxidised rim around the grains. Ti is usually present in very

Fig. 4.7

Olivine major element variation in terms of Forsterite (Mg) -  
Fayalite ( $\text{Fe}^{2+}$ ) - Tephroite (Mn). (Molecular % based on  
recalculation to 4 oxygen atoms.)



- x SS2
- ◊ SS4d
- ▲ SS4b
- SS5
- ESSEXITE

Fig. 4.8

Variation in Ca content of the olivines relative to the fractionation index (Mn - Mg) atoms per 4 oxygens. The index has been chosen so as to represent the full range in composition as seen in Fig. 4.7 (cf. pyroxene fractionation index Na - Mg, see section 4b). Symbols as for Fig. 4.7.

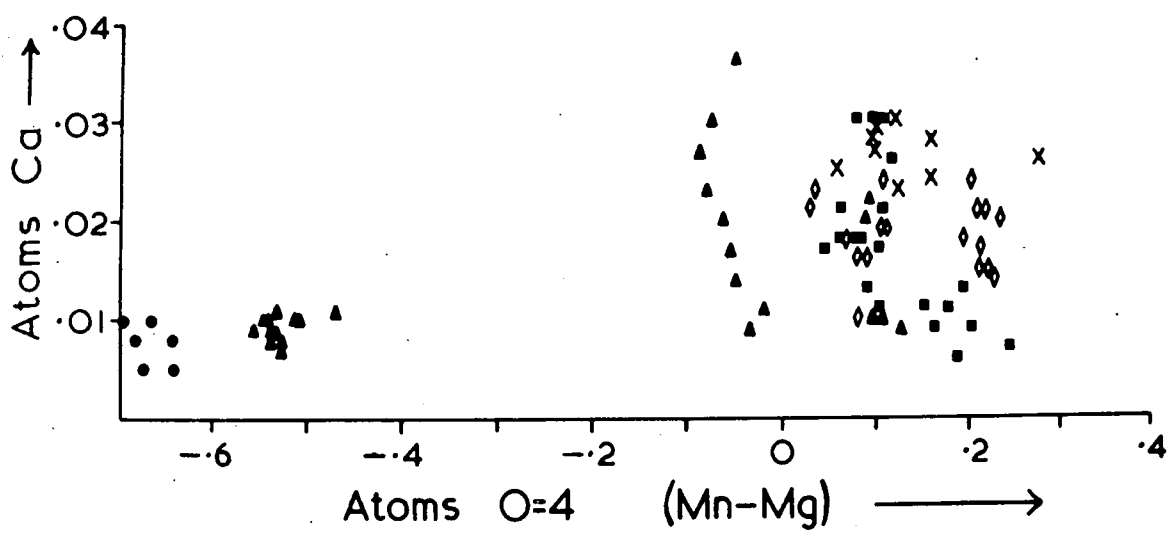


Fig. 4.9

Zoning in individual olivine grains from the various units of the Centre. Symbols as for Fig. 4.7.

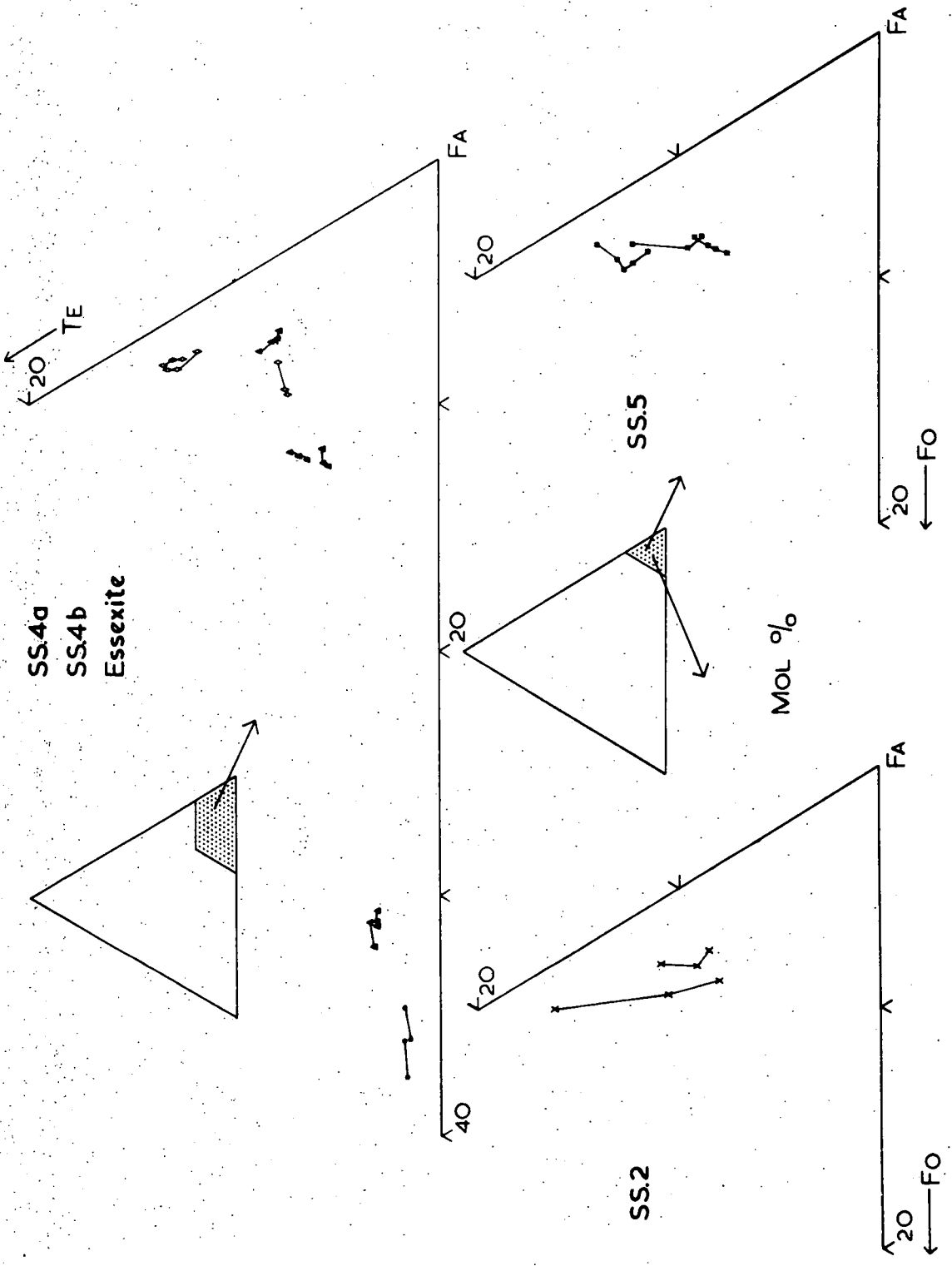
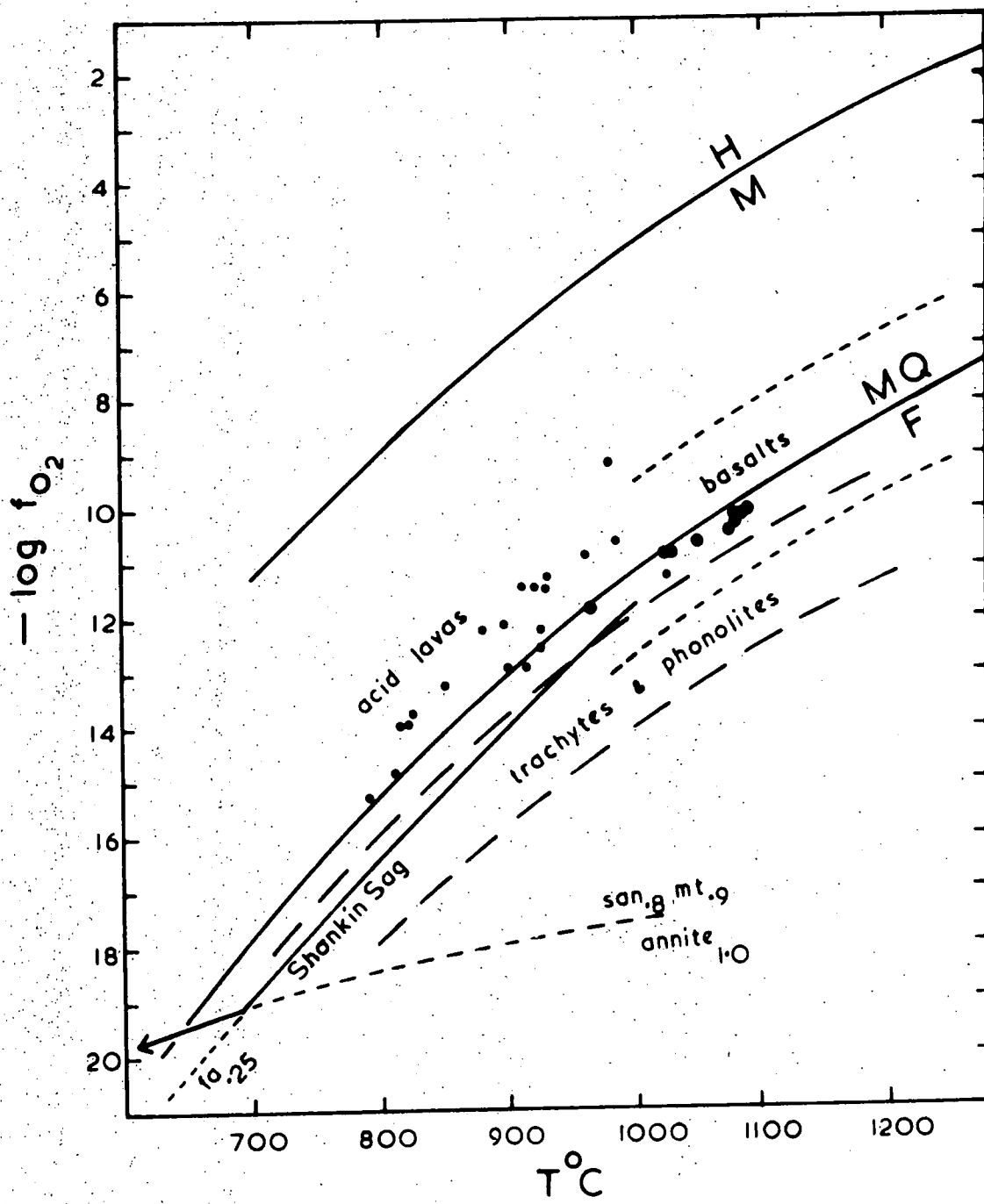


Fig. 4.10

Variation of oxygen fugacity with temperature in natural rock suites with reference to the synthetic buffer curves haematite - magnetite (HM) and fayalite - magnetite - quartz (FMQ) (Eugster & Wones, 1962; Wones & Gilbert, 1969). Theoretical limits of oxygen fugacity for basalts and phonolites from Carmichael & Nicholls, 1967 and Nash et al., 1969, respectively. Acid lava (small dots) and basalt (large dots) temperatures and oxygen fugacities are determined from coexisting iron - titanium oxides using the curves of Buddington & Lindsley (1964) and published by Carmichael & Nicholls (1967).

The general crystallisation path for Shonkin Sag (Nash & Wilkinson, 1970) is shown as a solid line, parallel to FMQ in the early stages, but running along the annite - alkali feldspar - magnetite buffer in the final stages after the disappearance of olivine, when oxygen fugacity decreases at a lesser rate. It is possible that the crystallisation path in the South Qôroq Centre is similar (see text).



small amounts (ca. 0.03 Wt.% Ti) and Al is occasionally detected in trace amounts. However, Cr and Ni were not detected in any samples.

Zoning is usually present to a small extent in most grains (Fig. 4.9) with an increase in  $\text{Fe}^{2+}$  and Mn, and decrease in Mg towards the rims, although this is not optically detectable. Ca shows no systematic distribution. As in the pyroxenes, zoning is least well developed in olivines from mafic bands in SS4b. Occasionally in the foyaites fairly homogeneous cores have a thin rim of very manganiferous olivine as in sample 127021 (SS2).

Olivine appears to be an early, cumulus phase in all the syenites, and the high Fe contents are thus attributable to a fairly advanced fractionation state in the immediate parental magma. The end of the olivine fractionation trend seems to be related to oxygen fugacity during the later stages of crystallisation, and evidence of instability is seen in the rims and exsolved lamellae of iron ore. It therefore seems pertinent at this stage to discuss the effects of  $f_{\text{O}_2}$  on crystallising alkaline magmas.

Unfortunately it is not possible to obtain quantitative estimates of the physical conditions of crystallisation by using the iron-titanium oxide geothermometer and oxygen barometer of Buddington and Lindsley (1964). This is because, as in most plutonic rocks, the magnetite-ulvospinel and ilmenite-haematite solid solutions do not coexist as primary phases, and usually only magnetite with exsolved ilmenite is present. However, several workers have calculated ranges of  $f_{\text{O}_2}$  for natural rock suites using synthetic buffer curves and thermodynamic considerations (Carmichael & Nicholls, 1967; Nash et al., 1969; Nash & Wilkinson, 1970).

From the synthetic buffer curves haematite - magnetite (HM) and fayalite - magnetite - quartz (FMQ) (Eugster & Wones, 1962; Wones & Gilbert, 1969) it is seen that  $f_{\text{O}_2}$  decreases with decreasing temperature (Fig. 4.10). These curves are displaced in natural systems if the phases

involved are not pure end members, and are similarly affected by the silica activity of the magma (Carmichael et al., 1970). A decrease in silica activity will decrease  $f_{O_2}$  for a given temperature etc., thus producing a set of parallel curves.

In many alkaline lavas olivine and magnetite coexist at least during the early stages of crystallisation, so conditions must approximate to those of the FMQ synthetic buffer curve. Nash et al. (1969) substituted the actual compositions of the phases in Mt. Suswa trachytes and phonolites, and for the maximum possible range of silica activity, found that they crystallised with  $f_{O_2}$  less than the synthetic FMQ values (Fig. 4.10). Nash and Wilkinson (1970) found a similar effect in the Shonkin Sag laccolith, but also took into account the effect of biotite later in the crystallisation sequence. The appropriate biotite - magnetite - alkali feldspar buffer curve cuts across the corresponding FMQ curve so that in the later stages the magma, following this curve, has an  $f_{O_2}$  greater than that of FMQ for any given temperature. Thus olivine is unstable and disappears at the point where the two curves cross (Fig. 4.10). Nash and Wilkinson (op. cit.) consider this to be most likely due to a new internal silicate - oxygen buffer taking over from FMQ (i.e. biotite - magnetite - alkali feldspar) but it could also represent the point at which a gas phase suddenly begins to control the silicate mineralogy with an external buffering effect.

Several workers have shown that acmite can be stable under quite a low  $f_{O_2}$  (Bailey, 1969) and it is therefore stable at low temperatures above the FMQ buffer curve, after the disappearance of olivine. This is seen in Shonkin Sag and also in the South Qôroq Centre. It would seem reasonable to suggest that  $f_{O_2}$  buffering in South Qôroq follows a similar course to that of Shonkin Sag, since olivine and magnetite appear as early phases and other mafic silicates including biotite appear

later in the crystallisation. Where  $f_{O_2}$  has been above the appropriate FMQ buffer curve during most of the crystallisation (i.e. in lower temperature rocks such as SS3 and in pegmatites), acmitic pyroxene is common but fayalite is unstable and does not occur. This adds support to the concept of recrystallisation under an  $f_{O_2}$  above the particular FMQ buffer around the Igdlarfigssalik Centre (possibly at a fairly low temperature - see also nepheline data 4f; or with external buffering from a gas phase), since within a wide zone (about 1.5 km.) olivine is not present. However, moving outwards through the zone one eventually finds olivine pseudomorphs and finally normal olivine.

#### (4e) Iron-Titanium Oxides

Iron-titanium oxide minerals occur in all units of the centre, and usually take the form of titaniferous magnetite with exsolution lamellae of ilmenite. They frequently appear to be an early phase present as rounded or subhedral grains in mafic aggregates or as inclusions in mafic minerals. However, in some samples, all or part of the oxides occur in distinctly interstitial areas. In reflected light the exsolved ilmenite lamellae have a higher reflectivity than the magnetite, are pleochroic from pale brown to white, and have a marked anisotropy. Fine, granular intergrowths of magnetite and haematite occur around the edges of grains where secondary oxidation has been intense.

Buddington and Lindsley (1964) reason that solid solutions between magnetite and ilmenite cannot exist, and therefore ilmenite lamellae cannot form by straightforward sub-solidus exsolution or oxidation. In the South Qôroq Centre, as in most plutonic rocks, the ilmenite lamellae are of the "trellis" type, parallel to the 111 plane of the host, and up to three sets intersecting each other at  $60^\circ$  can be seen depending on the orientation of the section. Duchesne (1972) interprets this texture as being indicative of direct oxidation - exsolution (mainly at supersolvus temperatures) of ulvospinel ( $2FeO \cdot TiO_2$ ) dissolved in the magnetite, to

form ilmenite lamellae ( $\text{FeO} \cdot 2\text{TiO}_2$ ). "Cloth" microtexture indicative of exsolution of ulvospinel followed by oxidation to ilmenite (Duchesne, *op cit.*) was not detected in any of the samples. Sometimes, particularly in SS2, the ilmenite lamellae are not very well developed and are only resolvable under very high power, but in most foyaite samples they become very broad.

Separate grains of magnetite and ilmenite are only found in samples which have been recrystallised near to the Igdlarfigssalik Centre, frequently with considerable amounts of associated sphene. Buddington and Lindsley (1964) suggest that coexisting separate phases are favoured by intense oxidation and high diffusion rates (implying a high temperature), with slow cooling and fluid phases also contributing to a certain extent. This supports the conditions of recrystallisation inferred from other mineralogical data, except that temperatures cannot have been very high.

The iron-titanium oxide analyses have not proved to be particularly informative, and consequently they have not been investigated as intensively as the other mafic minerals. Since only total Fe may be obtained from the electron probe analyses, the  $\text{Fe}_2\text{O}_3/\text{FeO}$  allocation has been made for both magnetite and ilmenite using the method of Carmichael (1967). The recalculated analyses are plotted in terms of molecular percent  $\text{RO}$ ,  $\text{RO}_2$  and  $\text{R}_2\text{O}_3$  in Fig. 4.11 with representative tie lines between coexisting magnetite and ilmenite.

Carmichael (*op cit.*) argues that all magnetite analyses should plot within the field magnetite - ulvospinel - ilmenite in the  $\text{RO} - \text{RO}_2 - \text{R}_2\text{O}_3$  diagram, and hence recalculations of electron probe analyses on the ilmenite basis (along the magnetite - ilmenite join) and ulvospinel basis (along the magnetite - ulvospinel join) should both have totals approaching 100%. This is seen to be true for most of the South Qôroq magnetites. There is little systematic compositional variation between magnetites from different units of the centre, such as was found for example by Lipman (1971) in

zoned ash flow sheets in southern Nevada. However, SS2 has a greater range of compositions than the other syenites, presumably owing to the fact that it is the outermost syenite, has cooled quicker, and hence exsolution - oxidation is generally less well developed. The more titanium-rich analyses are from magnetites having very little exsolution or extremely fine lamellae, unresolvable by the probe beam. In the other foyaites and SS4b, lamellae are better developed and the magnetite contains less Ti. Some of the magnetites from veins in metasomatised country rocks (127001) are almost stoichiometric.

Most natural ilmenites contain greater or lesser amounts of haematite in solid solution and hence plot along the ilmenite - haematite join. However, in all but one of the South Ooroo analyses, there is an excess of Ti over that necessary to make up stoichiometric ilmenite ( $\text{FeO} \cdot 2\text{TiO}_2$ ), and consequently the analyses fall along the ilmenite -  $\text{RO}_2$  join. Some of the analyses are clearly in error (due to practical difficulties encountered in analysing thin lamellae), as is seen by low FeO and low totals. However, others appear to be good analyses, and repeat determinations of Ti and Fe show reasonably good agreement precluding the possibility of random errors. Systematic errors due to electron - probe correction procedure are also considered to be too small to be responsible for the large excess of Ti encountered (e.g. fluorescence of Fe in the surrounding magnetite may slightly enhance the Ti peak in the ilmenite).

Buddington and Lindsley (1964) consider three possibilities for excess Ti in ilmenites:-

- (a) the original ilmenite may have contain  $\text{TiO}_2$  in solid solution when formed.
- (b) unreported elements in the RO group
- (c) alteration by oxidation to meta-ilmenite with exsolved rutile.

(a) is considered by Buddington and Lindsley (op cit.) to be impossible if the ilmenite has formed from titaniferous magnetite, and since the

Fig. 4.11

Compositions of iron-titanium oxides (magnetite and ilmenite) plotted in terms of Mol.%  $RO$ ,  $RO_2$ , and  $R_2O_3$ . The common end members are shown on the inset. Magnetites are plotted on the ulvospinel basis (along the magnetite - ulvospinel join) and ilmenites, owing to their excess of Ti, appear along the ilmenite -  $RO_2$  join. The analyses are recalculated from electron probe data using the method of Carmichael (1967) to estimate the  $Fe_2O_3/FeO$  ratio. Tie lines are between representative host magnetite and ilmenite lamellae in the same grain.

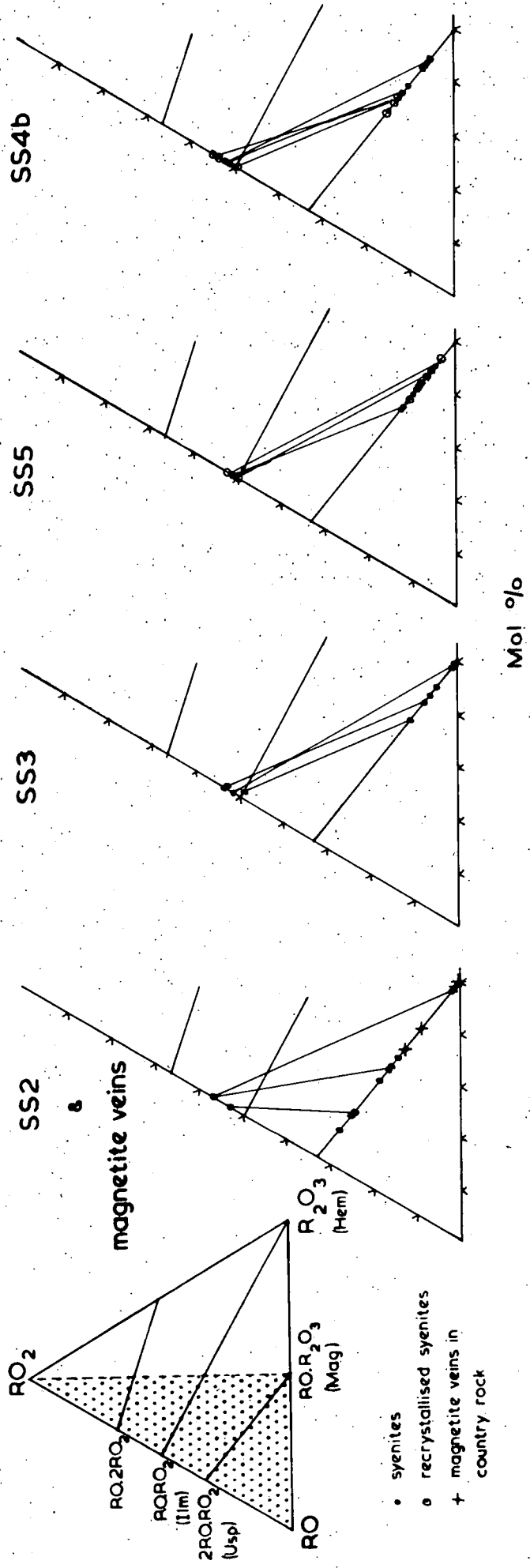
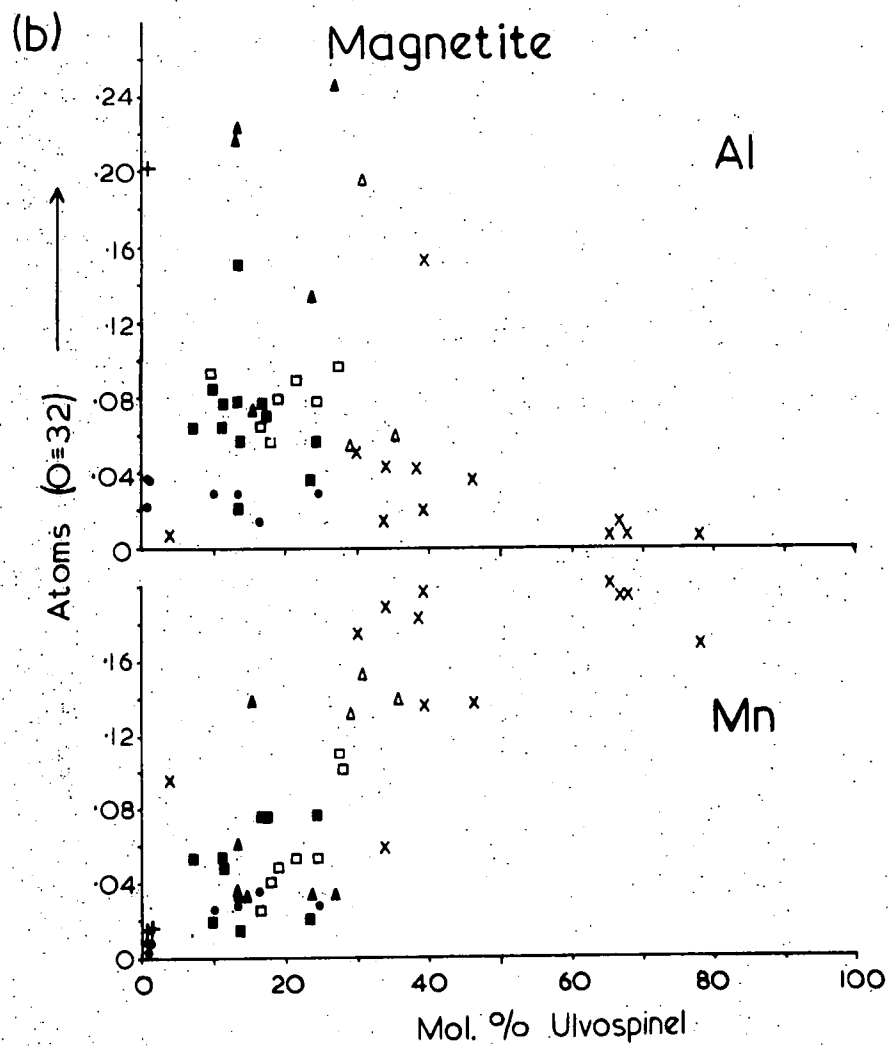
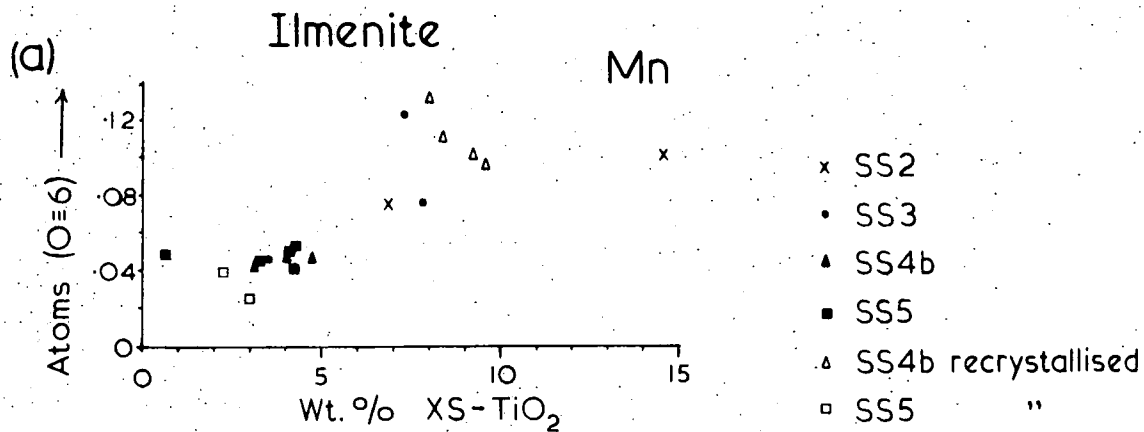


Fig. 4.12

Variation of the principal minor elements (Mn and Al) in the iron-titanium oxides. Magnetites are plotted against Mol.% of the ulvospinel end member (%Usp), corresponding to an increase in Ti. Ilmenites are plotted against Wt.% of excess  $\text{TiO}_2$  in the analysis, since this is the only variable suitable which also corresponds to an increase in  $\text{TiO}_2$ .



totals are good, (b) also seems unlikely. Thus the excess Ti is probably real and due to the exsolution of rutile during late stage oxidation. However, optical examination does not reveal any signs of further exsolution within the ilmenite lamellae even under the highest power available. Thus although the excess is considered to be real, its nature cannot be conclusively established.

The principal minor elements present in the oxides are Mn and Al with smaller amounts of Si (Fig. 4.12). Al is significant only in the magnetites and is higher in the augite syenites (about 0.1 - 0.6 Wt.%) than in the foyaites (about 0.02 - 0.10 Wt.%). Mn is considerably higher in the ilmenites (about 0.4 - 2.0 Wt.%) than in the magnetites (about 0.05 - 0.60 Wt.%) but shows a general increase with increasing Ti in both phases. These findings are consistent with those of Duchesne (1972).

Zoning is occasionally detected in magnetite grains, but in most cases it is obscured by the development of ilmenite lamellae. Duchesne (1972) reports considerable sub-solidus, deuteric adjustment in composition on both sides of magnetite/ilmenite boundaries owing to diffusion between the two phases. The irregular nature of element variation in the South Qôroq magnetites suggests that this has probably occurred, although sometimes an outwards increase of Ti and Mn is detectable.

Very few deductions can be made about the evolution of the South Qôroq Centre syenites from the iron-titanium oxides, since the geothermometer and oxygen barometer of Buddington and Lindsley (1964) is inapplicable where the magnetite and ilmenite do not exist as separate phases. In the recrystallised rocks, where two separate phases are present, the excess of Ti in the ilmenite places the compositions out of the range of Buddington and Lindsley's curves. However, the presence of separate phases does suggest a high  $f_{O_2}$  and high diffusion rates.

The veins in metasomatised country rocks contain near-stoichiometric magnetite and perovskite, an assemblage which is indicative of a relatively high  $f_{O_2}$  according to Carmichael (1967).

(4f) Nephelines

Nepheline is a major constituent of all the syenitic rocks in the centre, except in a few instances where contamination with country rock quartzite has occurred on the edge of SS2 (e.g. 52239, 126810). In the foyaites it has crystallised early along with the feldspar, and frequently shows euhedral tendencies (Plate 19). In SS4b and parts of SS4a, the nepheline occurs interstitially and is clearly later than the feldspars and certain mafics, (Plate 19). Similar relationships are found in the augite syenites and foyaites of the Hviddal dyke, Tugtutôq (Upton, 1964). In SS4a, SS4b and certain of the satellitic syenites it also occurs as rounded "blebs" within feldspar crystals in a manner which suggests an exsolution relationship (Widenfalk, 1972; see Chapter 3, Section 4g, Plate 23). In all rocks nepheline is the mineral most prone to deuteric alteration and weathering, generally to the micaceous mineral "gieseckite" which occurs as fine flakey aggregates, and gives the nepheline a pink colour in hand specimen. Such samples also have an increased  $H_2O$  and decreased  $Na_2O$  content in whole rock analyses, relative to the unaltered rocks (see Chapter 5). Reaction with  $CO_2$ -rich residua is seen as radiating rims of cancrinite on some nepheline grains, particularly near interstices filled by calcite (see Chapter 3, Plate 26).

The nepheline analyses listed in Appendix III show a general deficiency in the alkali sites when recalculated to 32 oxygen atoms, and the sum (Na + K + 2Ca) is less than the theoretical value of 8 atoms. This may represent vacant sites or may be due to the presence of the hydroxonium ion ( $H_3O^+$ ) (Heier, 1966), and is balanced, as in most natural nephelines, by an apparent excess of Si.

The analyses have been recalculated in terms of molecular weight percent nepheline ( $\text{NaAlSi}_3\text{O}_8$ ), kalsilite ( $\text{KAlSi}_3\text{O}_8$ ), anorthite ( $\text{CaAl}_2\text{Si}_2\text{O}_8$ ), and excess Si (expressed as  $\text{SiO}_2$ ), and are plotted in Fig. 4.13 in the system nepheline - kalsilite - quartz. Also shown on the diagram are the experimentally derived limits of nepheline solid - solution at 500, 700, 775 and 1068°C for nepheline in equilibrium with alkali feldspar, (Hamilton, 1961). The limits are determined at a  $P_{\text{H}_2\text{O}}$  of 15,000 p.s.i. (1.034 Kb), but they are not considered to be affected much by changes in pressure.

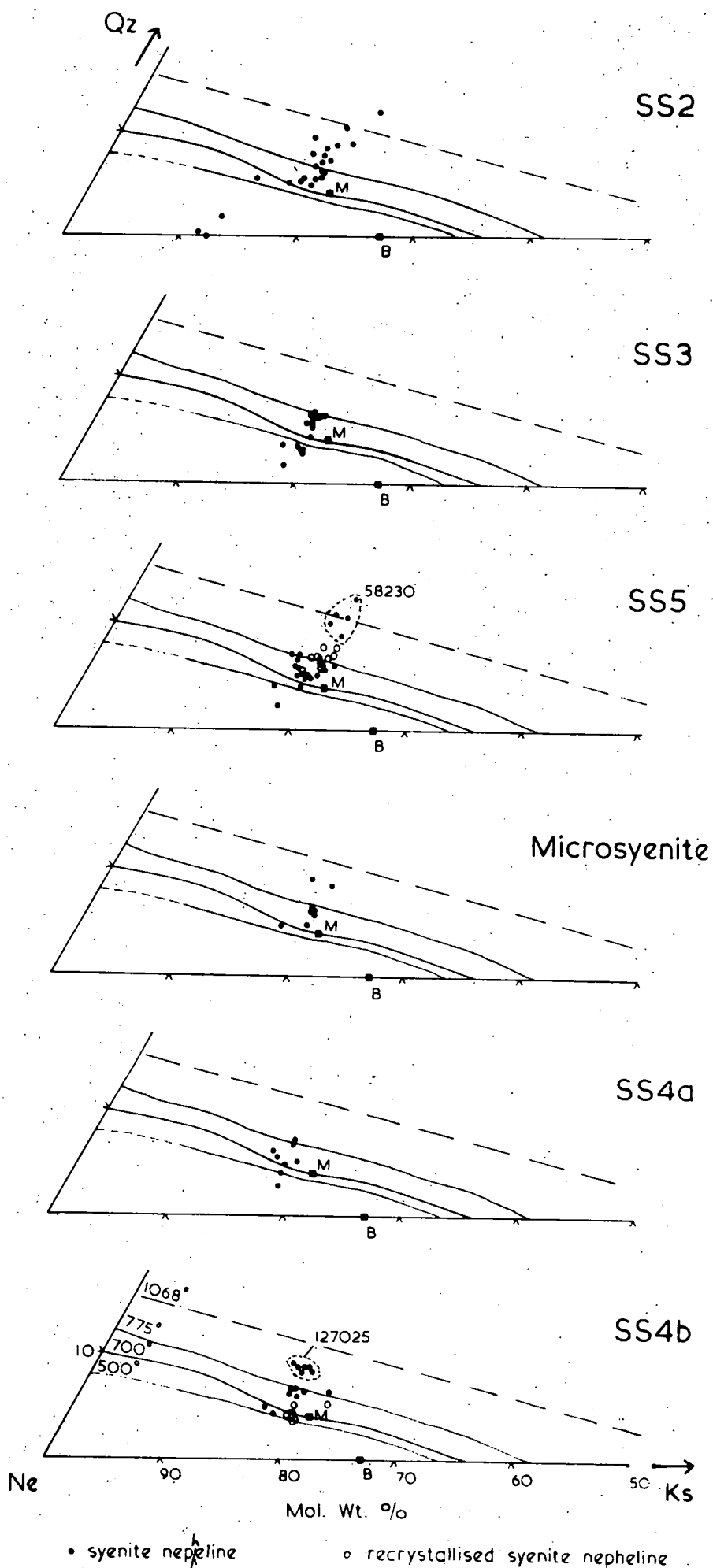
During crystallisation, nephelines change their composition in two ways: (a) The Si/Al ratio decreases with decreasing temperature, giving an indication of crystallisation temperature, particularly in rapidly cooled rocks. (b) Sub-solidus exchange of Na and K atoms frequently occurs between coexisting nepheline and feldspar. In the latter, nepheline compositions move towards an ideal Na:K ratio of 3:1, bringing them into a field between the ideal Morozewicz and Buerger compositions marked 'M' and 'B' in Fig. 4.13). Most plutonic nephelines are found within this field, and the nepheline geothermometer becomes inapplicable.

The South Qorroq Centre nephelines do not fall within the Morozewicz - Buerger convergence field, a feature which is also found in the plutonic nepheline syenites of Kangerdlugssuaq (Kempe & Deer, 1970). This suggests that sub-solidus exchange of Na and K has been minimal, and therefore the compositions do reflect crystallisation temperature. Most of the analyses (for both foyaites and augite syenites) fall between the 700°C and 775°C limits of solid solution. If this indicates the nepheline crystallisation temperature, it would appear that the foyaites (with early crystallising nepheline) commenced crystallisation within this range of temperature, whereas the augite syenites (with interstitial nepheline) commenced crystallisation at a higher temperature, but in this case nepheline did



Fig. 4.13

South Qoroq Centre nepheline compositions plotted in terms of molecular weight percent nepheline ( $\text{NaAlSi}_3\text{O}_8$ ), kalsilite ( $\text{KAlSi}_3\text{O}_8$ ) and excess Si (expressed as  $\text{SiO}_2$ ). Also shown are the experimentally determined limits of solid solution at 500, 700, 775 and  $1068^\circ\text{C}$  of nepheline in equilibrium with alkali feldspar ( $P_{\text{H}_2\text{O}} = 15,000$  p.s.i., 1.034Kb) taken from Hamilton (1961); the theoretical Morozewicz composition 'M' ( $\text{Na}_{6.1}\text{K}_{1.52}\text{Al}_{0.38}\text{Si}_{7.62}\text{O}_{32}$ ); and the theoretical Buerger composition 'B' ( $\text{Na}_3\text{KAl}_4\text{Si}_4\text{O}_{16}$ ). Sp. No. 127025 (SS4b) probably contains a systematic error in the  $\text{SiO}_2$  determination, and Sp. No. 58230 (SS5) may be slightly altered, although it is possible that these are relic high temperature compositions. The three analyses from SS2 with only slight excess  $\text{SiO}_2$  are nepheline grains completely surrounded by interstitial sodalite and have probably lost  $\text{SiO}_2$  to the later mineral.



not crystallise until later. Thus nepheline appears in the same temperature range irrespective of magma type. (Experimental work by Sood and Edgar (1970) at  $P_{H_2O} = 1Kb$  and  $f_{O_2}$  between the "haematite - magnetite" and "Ni - NiO" buffers shows an appearance of nepheline at about  $800^{\circ}C$  in Ilímaussaq foyaite and green lujauvrite.)

As has been found in several other mineral groups, the range in composition in SS2 is greater than in the other syenites, owing to it being the outer syenite, chilled against country rocks. Many grains within SS2 show slight zoning with Na and Al increasing and Si decreasing towards the rims, K remaining constant throughout. This was not generally detected in the other syenites, and can also be attributed to slightly faster cooling in SS2 allowing less time for equilibration with the liquid. Thus, individual grains reflect a temperature range of 1,000 to  $700^{\circ}C$ . A few grains in SS2, which are completely surrounded by interstitial sodalite (Sp. No. 127075, Plate 24), have virtually no excess  $SiO_2$  and plot near the base line of Fig. 4.13. Other grains in the same slide have normal compositions, so it appears that Si has entered the late sodalite. Nash et al. (1969) suggest that coexisting sodalite may invalidate the nepheline geothermometer (in Mt. Suswa lavas with sodalite phenocrysts, Si is higher than expected in nephelines), but in the South Qoqroq Centre sodalite crystallises much later, and only appears to have an effect where it is in direct contact with nepheline. No significant compositional differences have been detected in SS4b between the normal nepheline and that contained within feldspar.

Nephelines from the recrystallised syenite in SS5 indicate slightly higher temperatures than normal, but this is not noticeable in SS4b. Thus recrystallisation does not appear to have involved re-equilibration at a significantly higher temperature. There does not appear to be a change in the Na:K ratio in such nephelines (c.f. increase in Na in pyroxenes from recrystallised rocks).

Two samples give anomalously high temperatures. Sp. No. 127025 (SS4b) appears to have a systematic error in the  $\text{SiO}_2$  determination since both  $\text{SiO}_2$  and the totals are higher than normal. However, Sp. No. 58230 (SS5) has slightly higher  $\text{SiO}_2$ , higher  $\text{Al}_2\text{O}_3$  and lower  $\text{Na}_2\text{O}$  than normal, but reasonable totals. Hence the differences appear to be real and could be due to slight alteration, decreasing Na/Al, although this is not apparent in thin section. Alternatively, the grains could have relic high temperature compositions as is found in cores of SS2 grains.

The only significant minor elements present in the nephelines are Ca and Fe. As in most plutonic rocks, Ca is very low, being generally between 0.0 and 0.05 Wt.% in the foyaites, and only slightly higher (0.05 - 0.30 Wt.%) in the augite syenites. Fe (probably present as  $\text{Fe}^{3+}$  substituting for Al) is always present, but is low in the augite syenites (0.20 - 0.35 Wt.%) and tends to increase in the foyaites (0.45 - 0.60 Wt.%).

Although the compositional range of South Qôroq Centre nephelines is not great, and they are therefore less useful than mafic minerals for differentiating between syenites, they can be used as a guide to crystallisation temperature. However, care must be exercised in interpreting the results since exchange of Na and K with feldspar is possible, and also other effects, such as the presence of sodalite, and secondary alteration can affect  $\frac{\text{Fe}}{\text{Si/Al}}$  ratio.

#### (4g) Alkali Feldspars.

Alkali feldspar is the most abundant mineral in all the South Qôroq Centre rocks, constituting 40 - 60% of the foyaites and 50 - 70% of the augite syenites, according to the amount of coexisting nepheline. In the foyaites the feldspar usually occurs as tabular crystals, flattened parallel to 010, and reaching up to 30 x 7 x 2 mm in size in SS3 and SS5, where they commonly show a pronounced lamination. Some of the augite

syenites also contain tabular feldspar, but more commonly a rhombic habit is indicated by rectangular crystals up to 15 x 5 x 5 mm in size.

Most of the feldspars have perthitic textures, showing varying degrees of sub-solidus unmixing even within individual grains. In the foyaites the perthites are generally better developed and the Na and K - rich phases occur in almost equal proportions, but in parts of SS4b the texture is antiperthitic. Thin, irregular rims of albite are found in many samples of both foyaite and augite syenite, but separate grains are not found. Some of the augite syenite feldspars are microperthitic or occasionally cryptoperthitic, and have a characteristic blue schiller in hand specimen, similar to those of the Oslo larvikites (Muir and Smith, 1956). Recrystallised samples of the syenites have particularly coarse perthites.

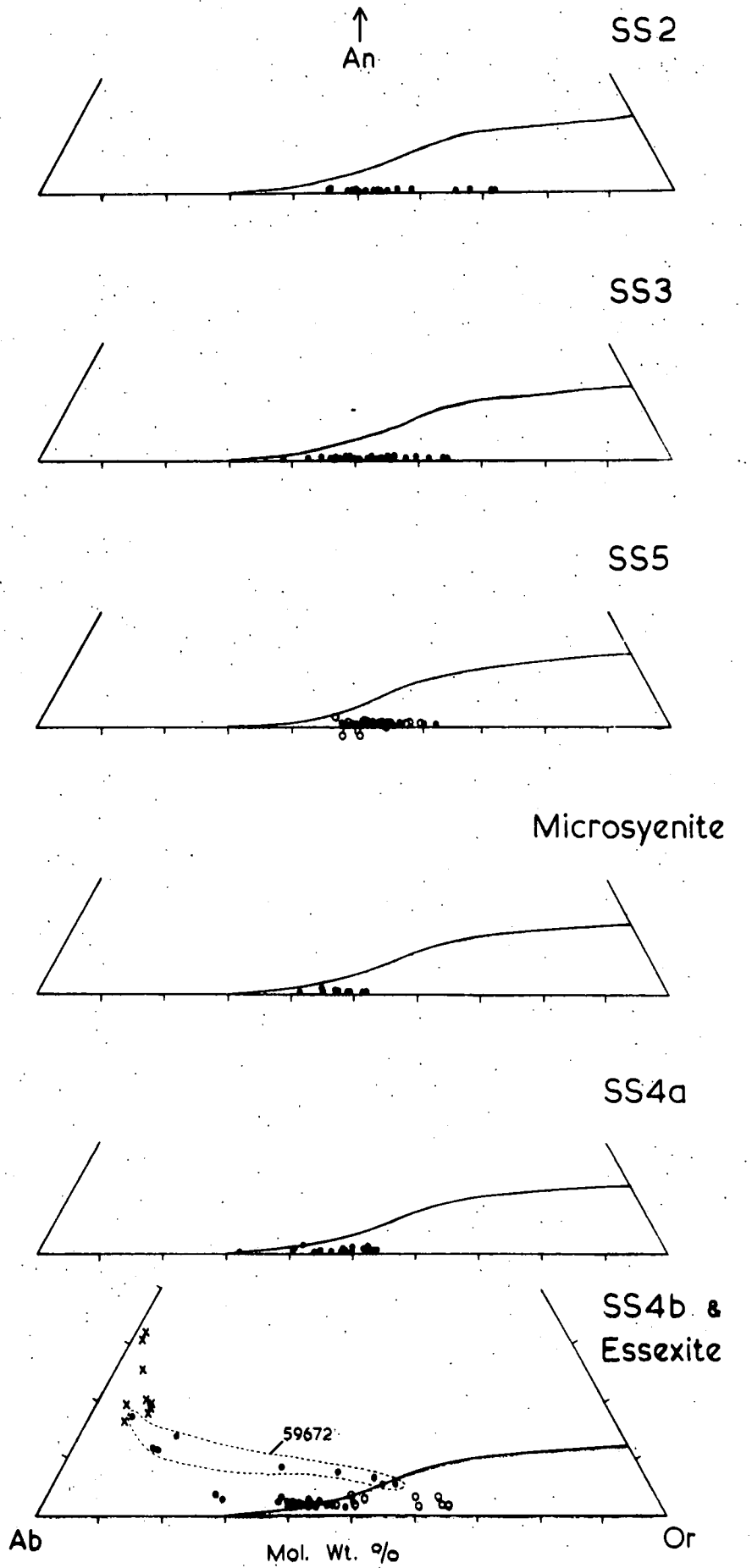
Twinning is normally of Carlsbad type (parallel to 010), with simple twins in the augite syenites and frequently multiple twins of up to six individuals in the foyaites. Manebach twins (parallel to 001) are scarce, but are sometimes seen creating a 'herringbone' effect of perthite lamellae. Albite twinning occurs in the plagioclase rims, but is seldom observed in the perthites. Albite - Pericline combinations of the microcline type were not detected.

Bulk electron - probe analyses of the feldspars were obtained by using a broad, defocussed beam (Ca. 50 $\mu$ ), and by concentrating on grains which were less coarsely exsolved. This is not entirely satisfactory since, even with a broad beam, slight fluctuations in Na/K ratio occur, and concentration on microperthitic areas may create a slight bias. However, the analyses give a useful indication of fractionation trends and are shown on Fig. 4.14 plotted in terms of molecular percent Or - Ab - An.

The compositions from the Essexite dyke and SS4b augite syenites fall on a trend from sodic andesine to a calcium-bearing alkali feldspar of composition Or<sub>49</sub>. The trend ends in the region of the 5Kb cotectic

Fig. 4.14

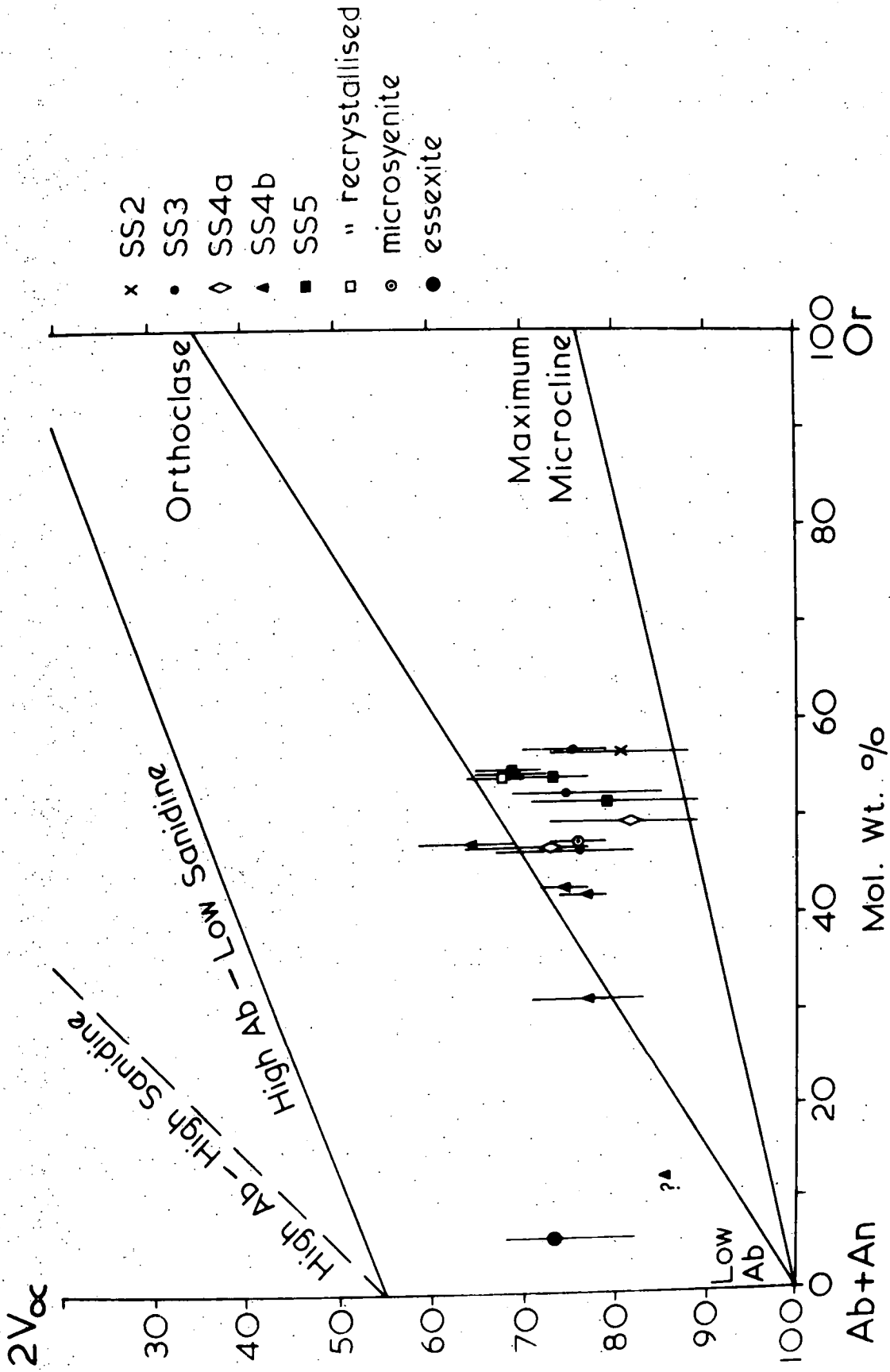
Compositions of South Qôroq Centre feldspar bulk analyses in the system Albite - Orthoclase - Anorthite (Ab - Or - An) - molecular weight percent. Also shown is the ternary cotectic at 5Kb (Yoder et al., 1957) which separates feldspars from the augite syenites and essexite from those of the foyaites. The more calcic analyses of 59672 are feldspars from a mafic band within SS4b. Feldspars from recrystallised rocks all fall on the K - rich side of the cotectic.



• syenite feldspar    ◦ recrystallised syenite feldspar    x essexite feldspar

Fig. 4.15

Average  $2V_{oc}$  values for unmixed feldspars as a function of the mean bulk feldspar composition in each electron-probe slide. The vertical lines indicate the range of  $2V$  values obtained in each sample. The foyaite feldspars lie in a field between the low albite - orthoclase and low albite - maximum microcline joins and thus correspond to type (e) in the cooling sequence of MacKenzie and Smith (1962). The augite syenite feldspars lie nearer to the low albite - orthoclase join indicating a lower degree of Al - Si ordering - type (d) of MacKenzie and Smith (op cit.). Increased Ca content in the essexite and SS4b mafic band feldspars has probably increased the  $2V$ , and these samples should lie nearer the high albite - sanidine join. (Diagram constructed as in Emeleus and Smith, 1959).



(Yoder et al., 1957) and is comparable with other Gardar trends from Kúngnát and Tugtutôq (Upton, 1960, 1964a, b, c). The SS4b compositions are similar to those from the Oslo larvikites (Muir and Smith, 1956). Feldspars from a mafic band in SS4b (i.e. 59672), which probably crystallised later than some of the mafics (see Chapter 3), are considerably more calcic than those of the normal augite syenite, and even at the cotectic contain 4% An.

Without exception, the foyaites lie on the K - rich side of the 5Kb cotectic, and contain no appreciable Ca. Compositions of Or<sub>38</sub> to Or<sub>72</sub> occur, but the spread is probably enhanced due to the perthitic nature of some of the grains. There are no significant differences between compositions from different foyaites. SS4a and microsyenite feldspars have similar compositions to those of the foyaites, although the range is more restricted (probably because they are less coarsely exsolved).

Feldspars from the recrystallised rocks of SS5 show no change in composition compared with unrecrystallised rocks, but in SS4b the change is very apparent. Whereas all normal SS4b feldspars fall on the Na - rich side of the 5Kb cotectic, in the recrystallised samples they fall on the K - rich side and have a similar range to the foyaites feldspars. However, they still retain a higher Ca content. This decrease in Na/K in the feldspars compliments the increased Na found in pyroxenes from recrystallised rocks (see Section 4b).

In many of the feldspar grains, chemical zoning is detected, although the effect is often confused by sub-solidus exsolution. In the essexite and augite syenite feldspars the zoning is initially a depletion of CaAl, followed by an increase in K. This produces, as would be expected, a trend towards a minimum - melt composition near the 5Kb cotectic. However, in the foyaites the zoning is also usually towards K - enrichment,

producing a trend away from the cotectic. This effect will be discussed in more detail below.

The only significant minor element present in the feldspars is Fe, which from the formula balance appears to be present as  $Fe^{3+}$  substituting for Al. There is little variation between feldspars from different rock types, and values range from 0.1 to 0.2 Wt.% Fe. However, feldspars from the mafic band (59672) have a very low Fe content. Ba was not detected in any of the samples.

Universal stage measurements of  $2V_{\infty}$  plotted against the average feldspar compositions of the probe samples are shown in Fig. 4.15. The  $2V$  values represent the average for the 2-phase feldspar within the field of the objective, since measurement of individual phases is impracticable. Limitations of the method are outlined by Parsons (1965), and in the South Qôroq samples  $2V$  values were unobtainable from very coarsely perthitic feldspars which may produce a slight bias towards higher structural states. From Fig. 4.15 it can be seen that the foyaite feldspars lie in a field between the low albite - orthoclase and low albite - maximum microcline joins, and thus correspond to type (e) in the cooling sequence of MacKenzie and Smith (1962), as do most of the Kûngnât and Tugtutôq feldspars investigated by these authors. The augite syenite feldspars plot closer to the low albite - orthoclase join (type (d) of MacKenzie and Smith, op cit), indicating a lower degree of Al-Si ordering. The essexite and SS4b mafic band feldspars are difficult to evaluate since their high Ca content will increase the  $2V$ , but they probably belong to the high albite (anorthoclase) - sanidine series.

Textural and mineralogical evidence suggests that the South Qôroq Centre magmas were below their liquidus temperatures on emplacement (see Chapter 6), and that feldspar fractionation had already occurred giving a range of compositions in the various rock types. Since all the rocks

contained essentially one feldspar phase, which has subsequently unmixed to a greater or lesser extent, the crystallisation must have been hypersolvus and is outlined as follows:-

The early stages of fractionation from andesine, through progressively more K - rich oligoclase, are seen in the essexite and in cores of feldspars from SS4b mafic bands. In the augite syenites it is difficult to tell, in the absence of diffraction data, whether initial feldspar crystallisation was monoclinic or triclinic. However, the bulk compositions suggest that they were on the monoclinic side of the monoclinic/triclinic inversion curve at crystallisation temperatures, and hence appeared as soda - sanidine rather than anorthoclase. The rhombic habit is characteristic of feldspars of a similar composition from Tugtutôq Central Complex described by Upton (1964a). With continued feldspar fractionation in foyaites of the Hviddal dyke, Tugtutôq, the 010 face becomes increasingly developed and eventually very thin, tabular feldspars are produced (Upton, 1964a, c). This also clearly occurs in the South Qôroq Centre in the more fractionated, Ca - free, K - rich alkali feldspars of the foyaites. Changes from a rhombic anorthoclase (triclinic) or soda - sanidine (monoclinic) to a tabular form with fractionation are also recorded from the Kangerdlugssuaq intrusion (Kempe and Deer, 1970), and the lavas of Mount Suswa (Nash et al., 1969). MacKenzie and Smith (1961) note that the very flat, tabular habit is characteristic of feldspars crystallising from undersaturated magmas, and suggest that it is due to the metastable crystallisation of sanidine cryptoperthite with subsequent preservation of the sanidine habit. Thus it would appear from their composition and habit that the foyaite feldspars first crystallised as sanidine,

In order that K - rich alkali feldspars can be precipitated in the foyaites it is necessary for feldspar compositions to cross the ternary cotectic (Fig. 4.14) and, as is seen from the zoning, fractionation then proceeds in the direction of further K - enrichment. (From the experimental work of Bowen and Tuttle, (1950) and Yoder et al. (1959) it is unlikely

that the effect of varying water pressure is capable of moving the cotectic sufficient for all the feldspars to lie on one side). In view of the "flat" nature of the solidus curve in the region of the cotectic (Bowen and Tuttle, 1950), it is possible that in the foyaites coprecipitation of nepheline, into which Na enters preferentially, causes late stage K - enrichment in the feldspars. Similar K - rich feldspars are found in undersaturated late fractions of the Hvíddal dyke, Tugtutôq (Upton, 1964c), the Ilímaussaq intrusion (Ferguson, 1970) and the Kangerdlugssuaq intrusion (Kempe and Deer, 1970). However, feldspars from oversaturated alkaline complexes, with no coexisting feldspathoids, and from augite syenites with only interstitial nepheline are seldom seen to cross the cotectic, although they frequently move down the cotectic curve towards a minimum - melt composition on the Ab - Or join (Kúngnât - Upton, 1960; Tugtutôq Central Complex - Upton, 1964a; Loch Ailsh - Parsons, 1965).

Continued cooling of the feldspars under sub-solidus conditions resulted in unmixing into separate Na and K - rich phases with increase Al - Si ordering and the development of a perthitic texture. Emeleus and Smith (1959) demonstrate that volatile fluxes have a considerable influence on the degree of ordering in feldspars, and Ferguson (1970) indicates marked structural differences between feldspars of Ilímaussaq augite syenites and agpaites, attributable to higher volatile pressure in the latter. Similarly, in the South Qôroq Centre the augite syenite feldspars are less coarsely perthitic and are of a higher structural state than those of the foyaites, which presumably reflects a higher volatile content in the foyaites, coupled with lower crystallisation temperatures and slower cooling. The very coarse perthites invariably found in the recrystallised rocks suggest a high volatile pressure during recrystallisation.

The feldspars of initial soda - sanidine composition in the augite syenites resemble those of the Oslo larvikites in many features, and hence

their sub-solidus crystallisation was probably similar to that described by Smith and Muir (1958). However, Widenfalk (1972) has pointed out that in addition to unmixing and ordering of feldspar phases, exsolution of nepheline also occurs, due to the initial feldspars having a slight deficiency of  $\text{SiO}_2$ . This is also seen in the South Qôroq Centre augite syenites as rounded 'blebs' of nepheline within the feldspar, and appears to have occurred quite early in the sub-solidus crystallisation, since the surrounding feldspar is often quite a fine microperthite. Some of the feldspars do recalculate to give a slight  $\text{SiO}_2$  deficiency, but this cannot be correlated with the exsolution features in any regular manner. The restriction of exsolved nepheline to augite syenite feldspars can probably be correlated with their higher Ca content, which reduces the amount of nepheline which can be held in solid solution (Widenfalk, op cit.).

Consideration of the experimental data in the system Ab - Or (Bowen and Tuttle, 1950; Yoder et al., 1957) enables broad estimates of crystallisation temperature and pressure to be made. Since the feldspars are all hypersolvus, they must have crystallised at a  $P_{\text{H}_2\text{O}}$  of less than 5Kb, since at this pressure the solidus and solvus intersect resulting in two separate feldspar phases (Yoder et al., 1957). Parsons (1965) considers by extrapolating the data, that 3Kb is a reasonable upper limit to  $P_{\text{H}_2\text{O}}$  in the Loch Ailsh intrusion, and his arguments can be applied to the South Qôroq Centre. From other mineralogical and petrographic data it is clear that the rocks crystallised under hydrous conditions, and considering a possible basalt cover of up to 3Km, it seems reasonable to suggest a lower limit of  $P_{\text{H}_2\text{O}}$  of about 1Kb. Thus the temperatures of initial crystallisation were within a range determined by the solidus curve at 1Kb (upper limit), and the top of the solvus at 3Kb (lower limit). For the foyaites this gives a range of  $850^\circ\text{C}$  to about  $700^\circ\text{C}$  (the temperature

of the top of the solvus is not accurately known at 3Kb, but is  $680^{\circ}\text{C}$  at 2Kb and  $715^{\circ}\text{C}$  at 5Kb in the Ca - free system). In the augite syenites the estimates are complicated by the effect of the An content. Assuming 1% An the lower limit will be raised to about  $750^{\circ}\text{C}$  (Parsons, 1965). In view of the relatively flat nature of the solidus curve in the system Ab - Or over the observed range of feldspar compositions, crystallisation must have been completed over a temperature range of less than  $20^{\circ}\text{C}$  assuming constant pressure, and the feldspars then remained stable until they had cooled to the solvus temperature appropriate to their bulk composition. Since no data is available on the compositions of separate phases from the perthites, it is not possible to give estimates of the lower temperature limit of sub-solidus exsolution.

Assuming a  $P_{\text{H}_2\text{O}}$  of between 1 and 3Kb, the South Qôroq feldspars commenced crystallisation around  $850^{\circ}\text{C}$  (possibly slightly higher in the augite syenites), completed crystallisation within about  $20^{\circ}\text{C}$  and remained stable down to ca.  $750^{\circ}\text{C}$  (augite syenites) or ca.  $700^{\circ}\text{C}$  (foyaïtes) before commencing sub-solidus unmixing. (Compositions further away from that of the solvus peak would remain stable to lower temperatures). During most of their crystallisation the foyaïte feldspars would have been coprecipitating with nephelines, which in Section 4f were seen to commence crystallisation between about 900 and  $850^{\circ}\text{C}$  (cores in SS2) and finally stabilise between 775 and  $700^{\circ}\text{C}$ .

#### (4h) Other Minerals

##### Sodalite:-

Sodalite is present in all the foyaïtes and in many samples of SS4a, as grey interstitial areas. Under ultra-violet light the sodalite fluoresces bright orange and is seen to be concentrated in areas up to 5 cm. across within individual hand specimens. In SS4b, thin rims of sodalite are occasionally found around nepheline, but no large areas occur. Disseminated

	<u>127075</u>	<u>58230</u>	<u>58164</u>
	SS2	SS5	SS4b (recrystallised)
SiO <sub>2</sub>	37.50	38.00	37.04
Al <sub>2</sub> O <sub>3</sub>	30.58	34.41	32.50
Fe <sub>2</sub> O <sub>3</sub>	0.60	0.53	0.40
CaO	0.13	0.19	0.27
Na <sub>2</sub> O	26.36	22.75	24.75
K <sub>2</sub> O	-	-	0.06
S	0.08	0.06	-
Cl	6.62	6.76	6.53
	<u>101.87</u>	<u>102.70</u>	<u>101.55</u>
O = S, Cl	1.52	1.54	1.48
TOTAL	<u>100.35</u>	<u>101.16</u>	<u>100.07</u>

Cations to 26 (O, S, Cl) :-

Si	5.054	} 11.946	5.973	} 12.411	5.951	} 12.154
Al	5.819		6.376		6.154	
Fe <sup>3+</sup>	0.073		0.062		0.048	
Ca	0.022	} 8.277	0.031	} 6.963	0.047	} 7.872
Na	8.255		6.932		7.709	
K	-		-		0.116	
S	0.025	} 1.834	0.017	} 1.817	-	} 1.776
Cl	1.809		1.800		1.776	

Table 2

South Qorroq Centre sodalite analyses

Perovskite -  $(\text{Ca}, \text{Fe}^{2+}, \text{Na}, \text{Ce})(\text{Ti}, \text{Nb})\text{O}_3$ 

	<u>127003</u>
SiO <sub>2</sub>	0.13
TiO <sub>2</sub>	48.21
Nb <sub>2</sub> O <sub>5</sub>	4.08
FeO	2.05
MnO	0.11
CaO	36.04
Na <sub>2</sub> O	1.18
CeO <sub>2</sub>	<u>7.71</u>
TOTAL	100.51

## Cations to 24 Oxygens :-

Si	0.026	}	7.372
Ti	6.990		
Nb	0.356		
Fe <sup>2+</sup>	0.331	}	8.773
Mn	0.019		
Ca	7.460		
Na	0.442		
Ce	0.521		

Table 3

Electron - microprobe analysis of perovskite, from a magnetite-rich, metasomatic vein, cutting Julianehåb Granite near the SS2 margin on the east side of Tunugdliarfik Fjord.

blue sodalite occurs in a single pegmatite vein cutting SS3. This variety has a pale purple fluorescence under ultra-violet light.

Three electron - probe analyses of sodalites (one each from SS2, SS5 and recrystallised SS4b) are given in Table 2. The two foyaite analyses are from interstitial areas and the SS4b analysis is of a thin rim around nepheline. All the analyses are rich in Cl but contain little S, and are very similar to those from the Ilímaussaq naujaite (Sørensen, 1962). However, Deer et al. (1966) point out that sodalite varies very little in major element composition (apart from volatiles) over a wide range of environments, so few conclusions may be made from the analyses, except that a build up in Cl in the late residua is indicated. There is very slight substitution of  $Fe^{3+}$  for Al, and Ca for Na, but no appreciable K is detected.

The differences in colour and fluorescence in natural sodalites are not fully understood and seem to be associated with little chemical variation (Deer et al., 1966). In the Ilímaussaq Intrusion, orange fluorescing sodalite occurs in the sodalite foyaite, but that from the naujaite fluoresces pale purple and only rims and small interstitial areas show orange. However, sulphur-bearing hackmanite from the Lovozero Intrusion, Kola Peninsula is orange fluorescing (Vlasov et al., 1966).

Perovskite:-

Perovskite does not occur in the South Qôroq Centre syenites, but is found in metasomatic veins, cutting Julianehåb Granite around the margin of the centre (see Chapter 2). The mineral is unusual in that it is completely opaque, unlike most other quoted examples which are weakly birefringent (Deer et al., 1966). However, the electron - probe analysis confirms the identification (Table 3) and indicates a high content of Na and Ce (substituting for Ca), and Nb (substituting for Ti) in the ideal formula of  $CaTiO_3$ . The sample analysed contains magnetite (see Section 4e)

and perovskite in an approximate 1:1 ratio, and an X.R.F. trace element analysis indicates high values of Ba, Sr, Y and La which are presumably concentrated in the perovskite along with the Ce and Nb. The analysis is of the subhedral grains of perovskite which form most of the sample, but a second generation also occurs as rims around these grains and these are found to be even higher in Ce and Nb.

Metasomatising solutions from the syenites are thus inferred to contain a high proportion of rare earths and other residual elements, as is also seen in the varied mineralogy of other metasomatic veins in the country rock (see Chapter 2).

#### Biotite:-

Biotite is the only major rock forming mineral in the syenites which, due to lack of time, was not subjected to electron-microprobe analysis. Its omission is unfortunate, since it is clearly a major factor in the later stages of crystallisation, frequently occurring in equal proportions with alkali amphibole. Occasionally it is the only hydrous mafic phase present, particularly in SS3. In Section 4d it was inferred, from comparison with the data of Nash et al. (1971), that the later stages of crystallisation in the South Qoroq Centre could have been under the influence of the "sanidine - magnetite - annite" oxygen fugacity buffer and/or an external buffer due to the separation of a gas phase. Thus biotite analyses could give an indication of crystallisation conditions, and of factors influencing the relative proportions of alkali amphibole and biotite.

Optical examinations suggest that the biotites in the foyaites, which have a strong absorption and are intensely pleochroic from yellow - brown to almost black, are probably lepidomelane (high  $Fe^{3+}$  content). This would fit in with data obtained from the other mafics and is in common with alkali undersaturated rocks elsewhere. However, in the augite syenites, the essexite and the problematic south-eastern extension of SS2, the biotite is a very reddish - brown, possibly suggesting a higher Ti content.

### Eucolite - Eudialyte:-

Members of this series occur only in marginal pegmatites in SS3, and reflect the agpaitic nature of the final residua from this, the most differentiated of the foyaites. They usually occur as dark red, subhedral grains, up to 1 cm. in diameter, but are also found interstitially. No probe analyses were made, but optical examination reveals strong zoning (Plates 44, 45, 46, 47) with cores of eucolite (uniaxial -ve) and rims of mesodialyte (isotropic). Thin outer rims of eudialyte (uniaxial +ve) rarely occur. This zoning contrasts with that found in the agpaitic intrusions of Ilímaussaq (Sørensen, 1962) and Lovozero (Vlasov et al., 1966), where eudialyte zones outwards to mesodialyte, and eucolite is less abundant. Sørensen, (op cit.) suggests that both physical conditions and chemical environment control the composition of members of this series. Thus the prevalence of the calcic end-member (eucolite) over the sodic (eudialyte) in the South Qôroq Centre could reflect the more calcic nature of the magma.

Other less abundant minerals which were not analysed are aenigmatite (found occasionally in SS2 mafic aggregates); apatite (ubiquitous in all rocks); zircon, sphene and <sup>o</sup>lavénite (occasionally present in accessory amounts).

5 ROCK GEOCHEMISTRY(5a) Introduction

Samples from all units of the South Qôroq Centre were analysed by X-Ray Fluorescence techniques for 10 major elements (Si, Ti, Al,  $\Sigma$ Fe, Mn, Mg, Ca, Na, K, P) and 14 trace elements (Ba, Nb, Zr, Y, Sr, Rb, Pb, Zn, Cu, Ni, La, Th, U, V). Details of sample preparation, analytical methods and correction procedures are given in Appendix II. A total of 128 analyses with C.I.P.W. norms are listed in Appendix IV, including 90 representative samples analysed for FeO (method of Wilson, 1955) and H<sub>2</sub>O<sup>-</sup>, H<sub>2</sub>O<sup>+</sup>, CO<sub>2</sub> (method of Riley, 1958). Details of the sampling have been given in Section 1e, and locations are shown on Plate 1A.

The rocks are all silica-undersaturated, containing both normative and modal nepheline. The peralkalinity index (atomic ratio (Na + K)/Al) is between 0.7 - 0.95 in the augite syenites but rises to values close to unity (0.95 - 1.10) in the foyaites (Fig. 5.1). The centre is thus only mildly peralkaline and lacks the agpaitic geochemical and petrographic features of the Ilímaussaq Intrusion (Sørensen, 1960). In variation diagrams (Figs. 5.1, 5.2, 5.4, 5.5) the analyses form a smooth, continuous trend from the essexite, through mafic bands in the augite syenites, to the augite syenites and foyaites.

(5b) Major Element Variation

The major element variation diagrams are shown in Fig. 5.1 using the "Fractionation Index" (F.I.) of Macdonald (1969) as an abscissa. This index is a modification of the "Differentiation Index" of Thornton and Tuttle (1960) and consists of the sum of all the normative components in the "residua system" + ac + ns (i.e. in the South Qôroq Centre, F.I. = or + ab + ne + ac). The modification is essential in peralkaline rocks, since the appearance of ac in the norm tends to

progressively decrease the "Differentiation Index" of Thornton and Tuttle with progressive fractionation. (N.B. the index listed in Table IV.2 is that of Thornton and Tuttle (op cit.) and not the one used in the variation diagrams.) Since in most cases it is impossible to distinguish between individual foyaites from their geochemical features, SS2, SS3 and SS5 are plotted with the same symbol for clarity.

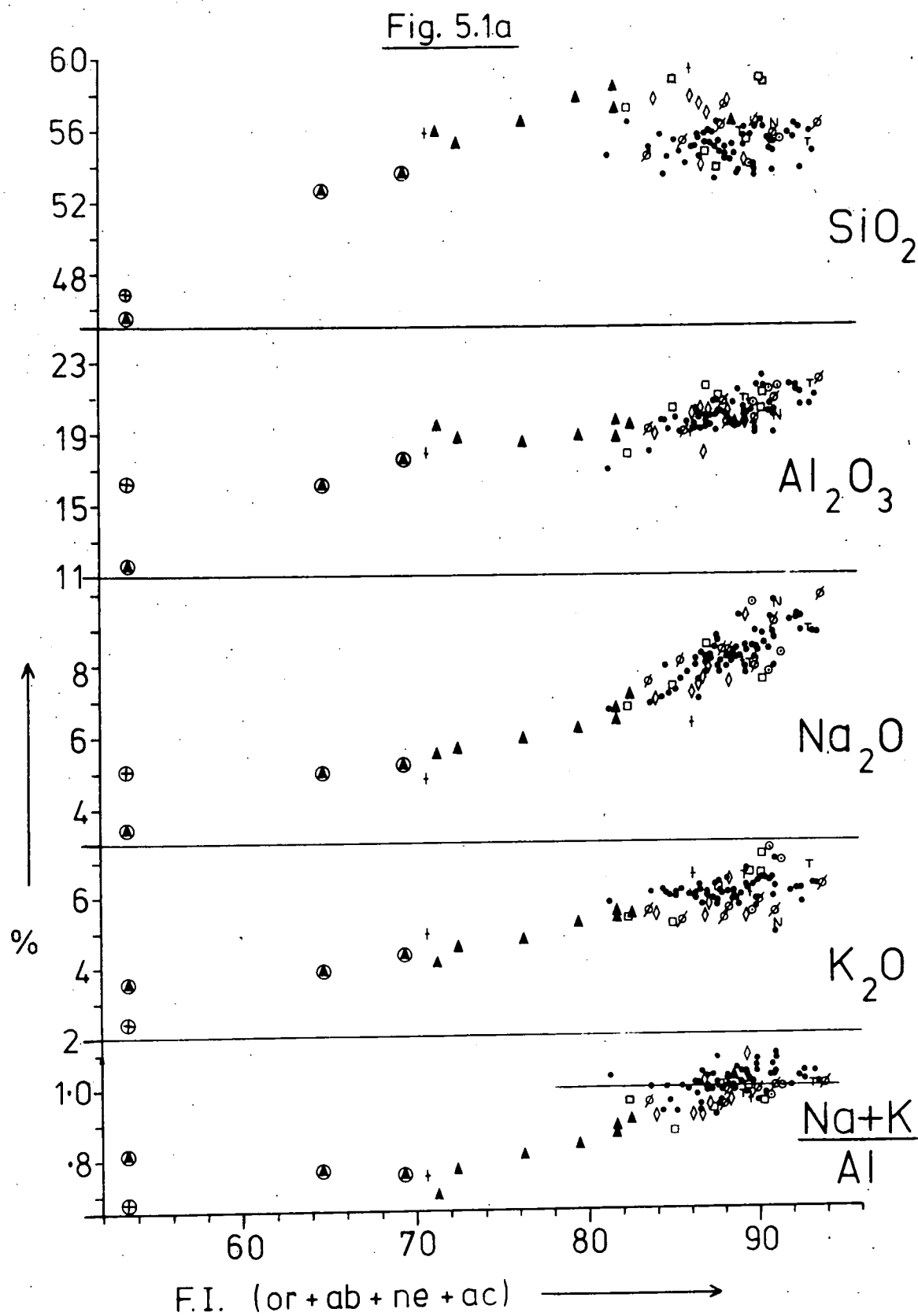
The analyses listed in Table IV.1 include a group in which the nepheline is pseudomorphed by aggregates of micaceous material (probably gieseckite). Such rocks have a reduced content of  $\text{Na}_2\text{O}$  and slightly higher  $\text{Al}_2\text{O}_3$  compared with unaltered equivalents, with the result that they have anomalously low values of Fractionation Index and peralkalinity, and frequently show normative corundum. These analyses cause considerable distortion in the variation diagrams and hence have been omitted. The loss in  $\text{Na}_2\text{O}$  is accompanied by a considerable increase in  $\text{H}_2\text{O}+$  (2.0 - 2.5% as opposed to 0.5 - 1.5% in unaltered rocks) and hence appears to be due to hydrothermal alteration of nepheline. Many of the altered samples are from the vicinity of faults or marginal areas of intrusions, but are also found elsewhere.

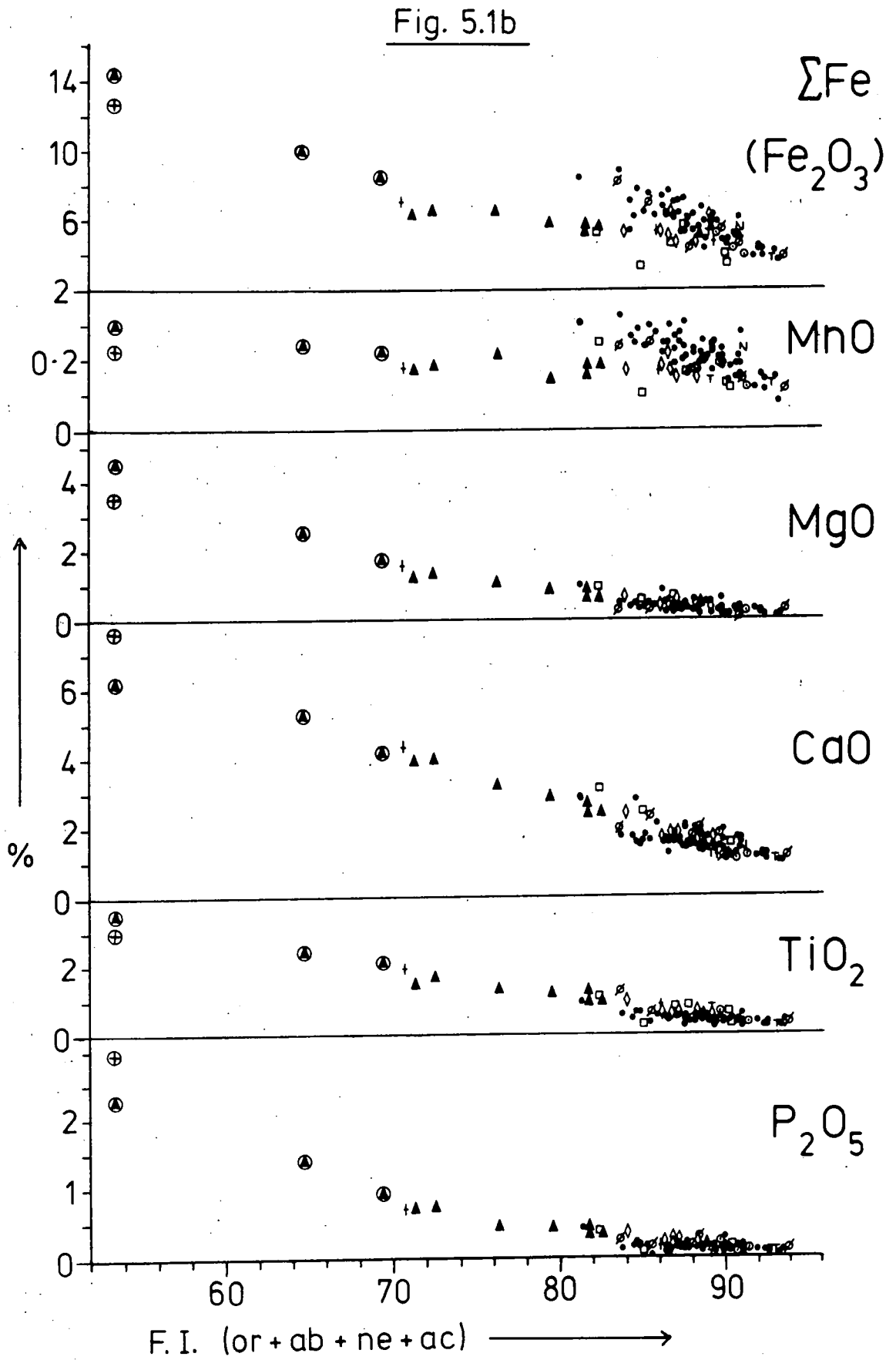
In Fig. 5.1 most elements are seen to follow a smooth, continuous trend through the augite syenites and foyaites, with the exception of  $\text{SiO}_2$ . The latter shows an increase with fractionation in the least fractionated augite syenites, followed by scattering and vague decrease in the more fractionated augite syenites and foyaites.  $\text{Al}_2\text{O}_3$  and  $\text{K}_2\text{O}$  increase steadily through the series, but  $\text{Na}_2\text{O}$  shows an increase with a pronounced kink towards the end of the augite syenite part of the trend, followed by a steep rise in the foyaites. This is even more pronounced in the normative nepheline content and reflects the point at which nepheline appears as an early-crystallising phase with alkali feldspar, rather than interstitially.  $\text{CaO}$ ,  $\text{MgO}$ ,  $\text{TiO}_2$  and  $\text{P}_2\text{O}_5$  decrease steadily through the series but total iron (as  $\text{Fe}_2\text{O}_3$ ) and  $\text{MnO}$ , although

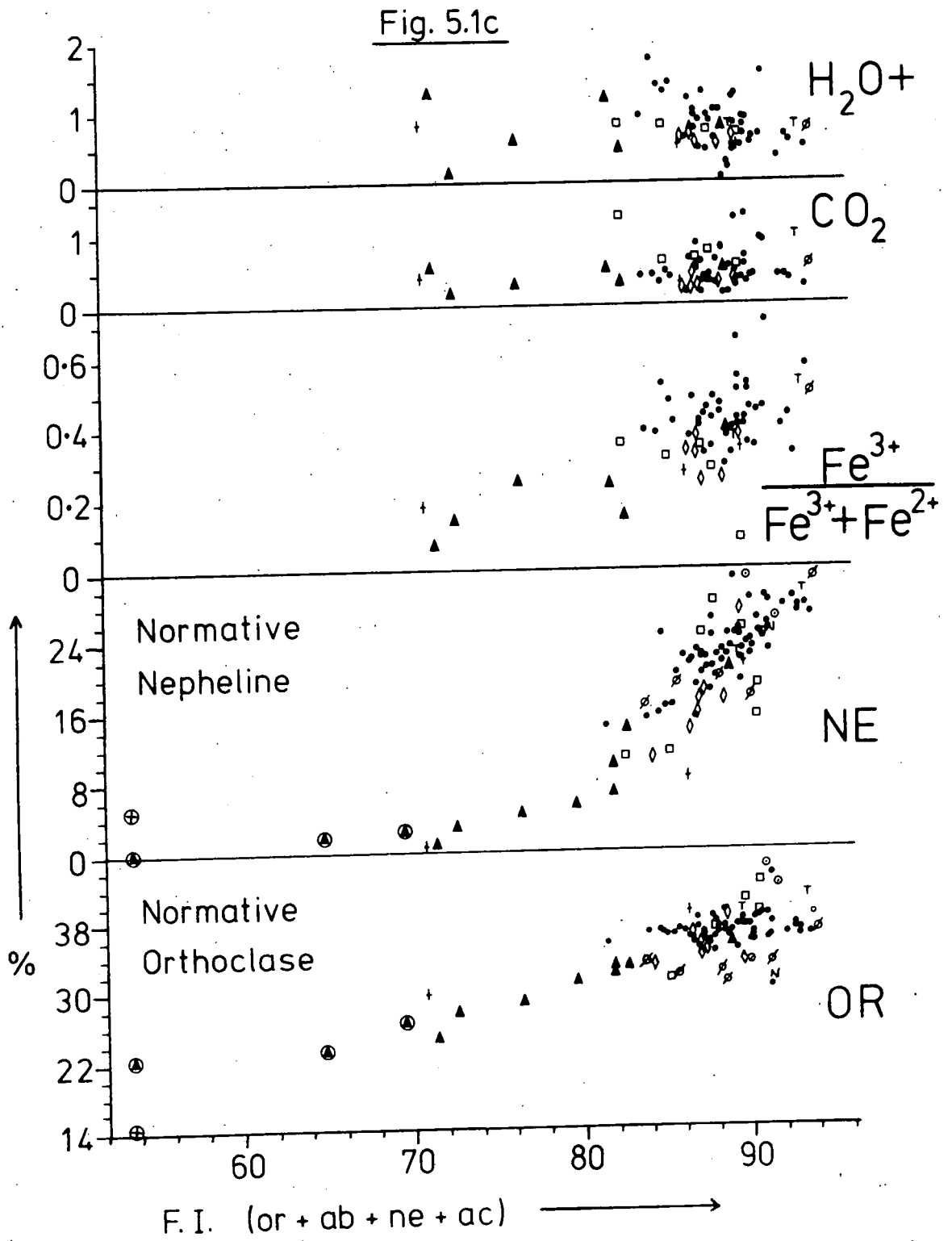
Fig. 5.1 (Three pages)

Variation of major elements and major element ratios with the "Fractionation Index" (F.I.) of Macdonald (1969) i.e.  $F.I. = or + ab + ne + ac$  (see text). N.B. The index listed in Table IV.2 (DIFIX) is the "Differentiation Index" of Thornton and Tuttle (1960) and is converted to F.I. by the addition of normative ac i.e.  $F.I. = DIFIX + ac$ .

- Foyaites SS2, SS3 and SS5
- ◇ SS4a
- ▲ Augite syenites of SS4b
- ⊕ Essexite
- ⊙ Microsyenite sheets
- † SS1
- N Narssarssuaq Syenite
- T Tunugdliarfik Syenite
- ∅ Østfjordsdal Syenite
- recrystallised syenites near to the Igdlarfigssalik Centre
- ⊕ ⊕ accumulative rocks







decreasing, show a slight suggestion of a separate, convergent trend in the foyaïtes. The iron oxidation ration ( $\text{Fe}^{3+}/(\text{Fe}^{3+}+\text{Fe}^{2+})$ ) shows a general increase with fractionation.  $\text{H}_2\text{O}+$  and  $\text{CO}_2$  show a considerable scatter, but there is a suggestion that  $\text{H}_2\text{O}+$  increases throughout the augite syenites but decreases in the later stages of foyaïte fractionation.

The three analyses from mafic bands in SS4b, and the essexite dyke, all of which show accumulation of olivine, iron-titanium oxides and possibly clinopyroxene, lie on smooth, backward extensions of the trends for all elements. Extreme late fractionates such as pegmatite veins have not been analysed, but a eucolite-bearing rock from marginal SS3 (59664) is included in Tables IV.1 and IV.2.

Recrystallised rocks near to the Igdlarfigssalik Centre show little deviation from normal values in most major elements. In the area around Niaqornarssuk, where the recrystallisation is most intense (see Chapter 2), samples of SS3 and SS4a have a slight depletion in total Fe, and samples of SS4b have a slightly increased iron oxidation ratio. However, further to the northeast, samples of SS5 show a marked reduction of oxidation ratio. It has been seen (Chapter 4) that clinopyroxenes from recrystallised rocks are more sodic than those from unrecrystallised equivalents. This is particularly noticeable in SS4b where there is a corresponding decrease in Na/K in the alkali feldspars. However, there is no apparent increase in the whole-rock content of  $\text{Na}_2\text{O}$  and  $\text{K}_2\text{O}$ , and some samples of SS3 and SS4a from Niaqornarssuk actually show a depletion.

Analyses from the microsyenite sheets and satellitic intrusions are also plotted on Fig. 5.1, apart from the Narssarssuaq Syenite where no fresh samples are available. In general they are seen to fall on the same trends as the larger intrusive units. However, the Østfjordsdal Syenite, which conforms to the foyaïte part of the trend in most elements, has a lower  $\text{K}_2\text{O}$  content and slightly higher  $\text{Na}_2\text{O}$ .

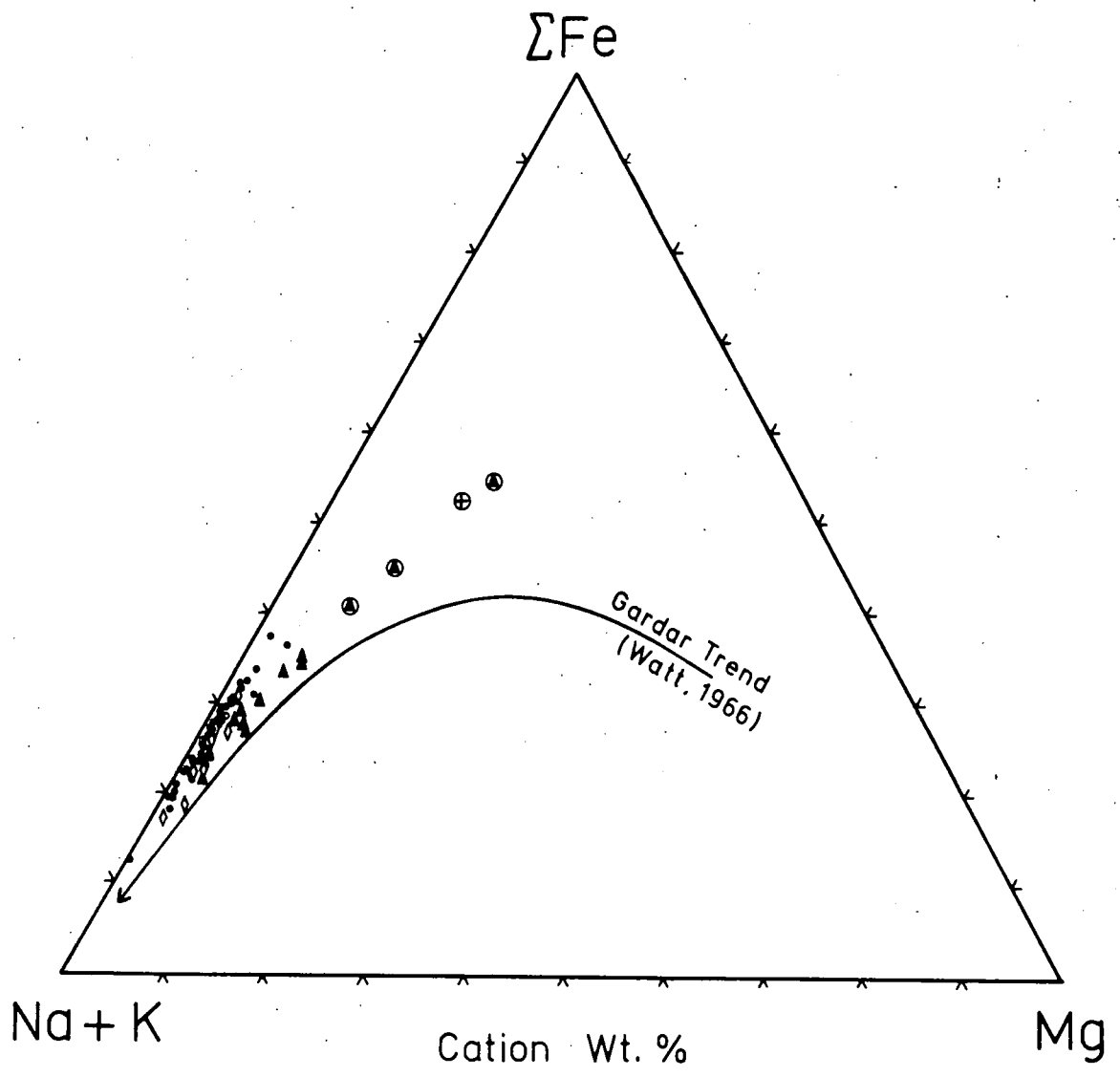
Analyses from the major units of the centre are plotted on a cation Wt.% A - F - M diagram (Na + K,  $\Sigma$ Fe, Mg) in Fig. 5.2, with the general Gardar Province trend of Watt (1966) for comparison. The enrichment of alkalis relative to iron in the later stages of fractionation, and the steady depletion of Mg from the mafic accumulates through the augite syenites are clearly demonstrated.

Since a vertical section of almost 1,000 m. is represented in the centre, the possibility of cryptic, geochemical variation was investigated by plotting the analyses against height above sea level. No systematic variation in a vertical sense was detected.

Slight variations in a horizontal sense, across the outcrops of the syenites are detectable, and are best seen in the outer syenite SS2 and the ring-dyke rocks of SS4a and SS4b (Fig. 5.3). Although SS5 is the most complete separate intrusion, mafic bands and igneous lamination are usually developed and probably mask any slight horizontal variations. For many elements the scatter masks the systematic variation, but representative elements from SS2 and SS4 are shown on Fig. 5.3, where slight trends outwards towards more fractionated rocks are seen. Normal centripetal cooling, as described by Kempe et al. (1970) for the Kangerdlugssuaq Intrusion, would result in a trend inwards to more fractionated rocks. Hence in the South Qôroq Centre the variation is more likely due to volatile transfer of alkali elements outwards along a thermal diffusion gradient during cooling. Alkali elements would thus be concentrated towards the margins producing more fractionated rocks.  $H_2O+$  is plotted on Fig. 5.3, but if anything shows a decrease towards the margins, probably reflecting loss into country rock. Accumulation of volatiles in other areas of the intrusions could account for some of the slight variations in composition and fractionation state seen on the variation diagrams.

Fig. 5.2

A - F - M (Na + K -  $\Sigma$ Fe - Mg) diagram for the South Qôroq Centre major intrusive units. (Cation Wt. %). Also shown is the mean trend for rocks of the Gardar Province taken from Watt (1966).

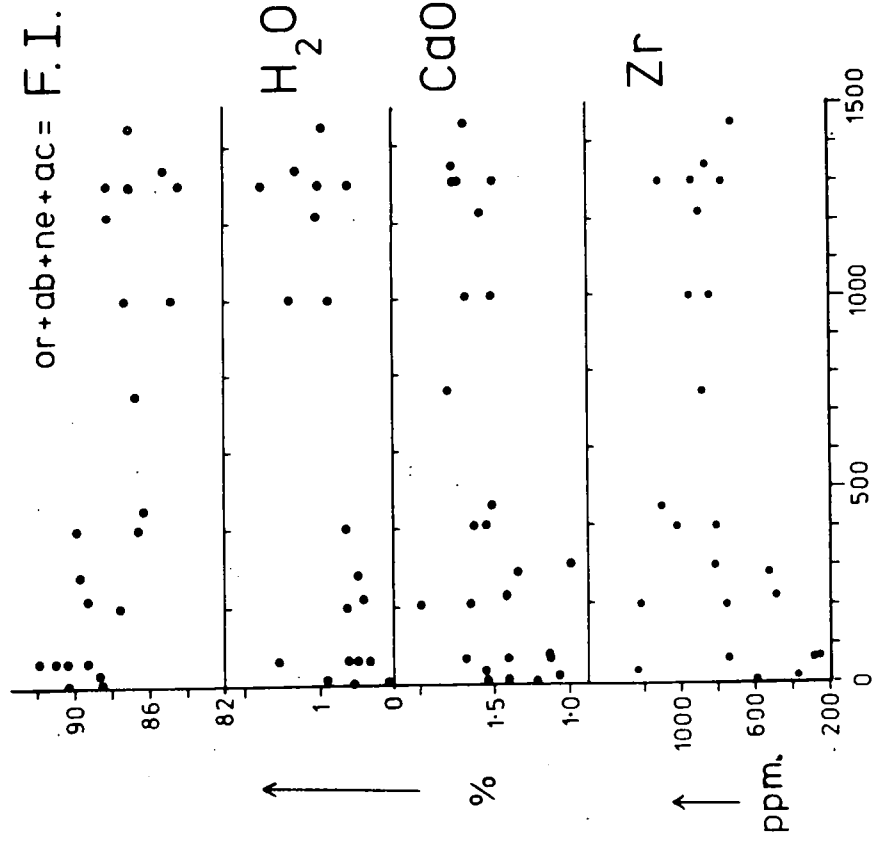


- Foyaites SS2, SS3 & SS5.
- ◊ SS4a.
- ▲ Augite syenites SS4b.
- + Essexite.
- accumulative rocks

Fig. 5.3

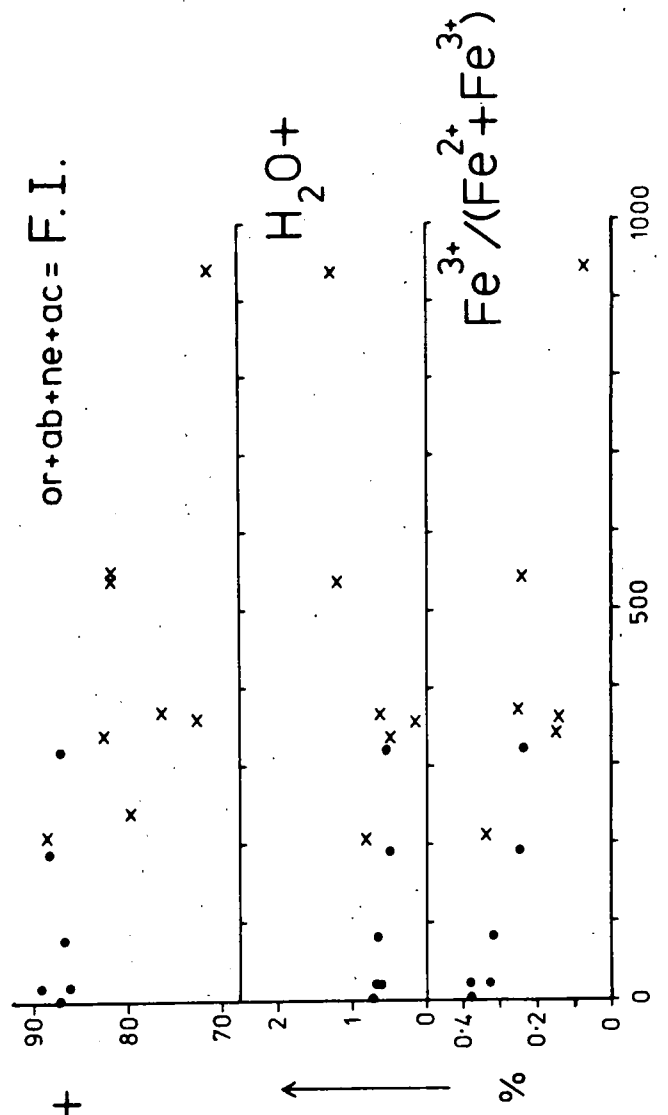
Variations in selected element concentrations horizontally, across the outcrops of SS2 and SS4. Only the most instructive elements are shown plotted against distance from the outer contacts of the respective units. In the case of SS4, both SS4a and SS4b are plotted against distance from the outer contact of SS4a. Despite considerable scatter the rocks are seen to generally become more fractionated outwards with an increase in F.I. and iron oxidation ratio, and a decrease in CaO,  $\text{TiO}_2$ ,  $\text{P}_2\text{O}_5$  etc.

SS2



SS4

• SS4a x SS4b



	<u>Ba</u>	<u>Sr</u>	<u>Rb</u>	<u>Zr</u>	<u>Nb</u>	<u>Y</u>	<u>La</u>	<u>Zn</u>	<u>Pb</u>	<u>Th</u>	<u>U</u>	<u>V</u>	<u>Cu</u>	<u>Ni</u>
<u>Ba</u>	-													
<u>Sr</u>	0.603	-												
<u>Rb</u>	-0.719	-0.478	-											
<u>Zr</u>	-0.247	-0.161	0.260	-										
<u>Nb</u>	-0.341	-0.238	0.325	0.917	-									
<u>Y</u>	-0.154	-0.111	0.097	0.759	0.730	-								
<u>La</u>	-0.187	-0.132	0.082	0.630	0.647	0.773	-							
<u>Zn</u>	-0.246	-0.146	0.215	0.725	0.788	0.682	0.579	-						
<u>Pb</u>	0.025	-0.032	0.044	0.473	0.460	0.432	0.365	0.457	-					
<u>Th</u>	-0.202	-0.240	0.090	0.499	0.560	0.758	0.562	0.671	0.439	-				
<u>U</u>	-0.274	-0.393	0.294	0.521	0.562	0.430	0.382	0.531	0.297	0.378	-			
<u>V</u>	-0.362	-0.233	0.309	0.241	0.325	0.005	0.033	0.230	0.215	0.154	0.248	-		
<u>Cu</u>	0.432	0.294	-0.432	-0.026	-0.040	-0.003	0.081	0.169	0.074	-0.067	0.030	-0.128	-	
<u>Ni</u>	0.120	0.086	-0.071	-0.015	-0.019	-0.006	-0.016	-0.035	-0.029	-0.053	-0.014	-0.013	-0.026	-

Table 4

Correlation coefficients between trace elements in the South Qôroq Centre Syenites (including hydrothermally altered rocks, accumulative rocks and recrystallised rocks). Values greater than 0.600 are underlined. The enclosed area includes all elements which appear to behave in a "residual" manner and hence show reasonably high correlations.

Fig. 5.4 (Two pages)

Trace element variation in the South Qoroq Centre rocks.

"Fractionation Index" (F.I.) and symbols as in Fig. 5.1.

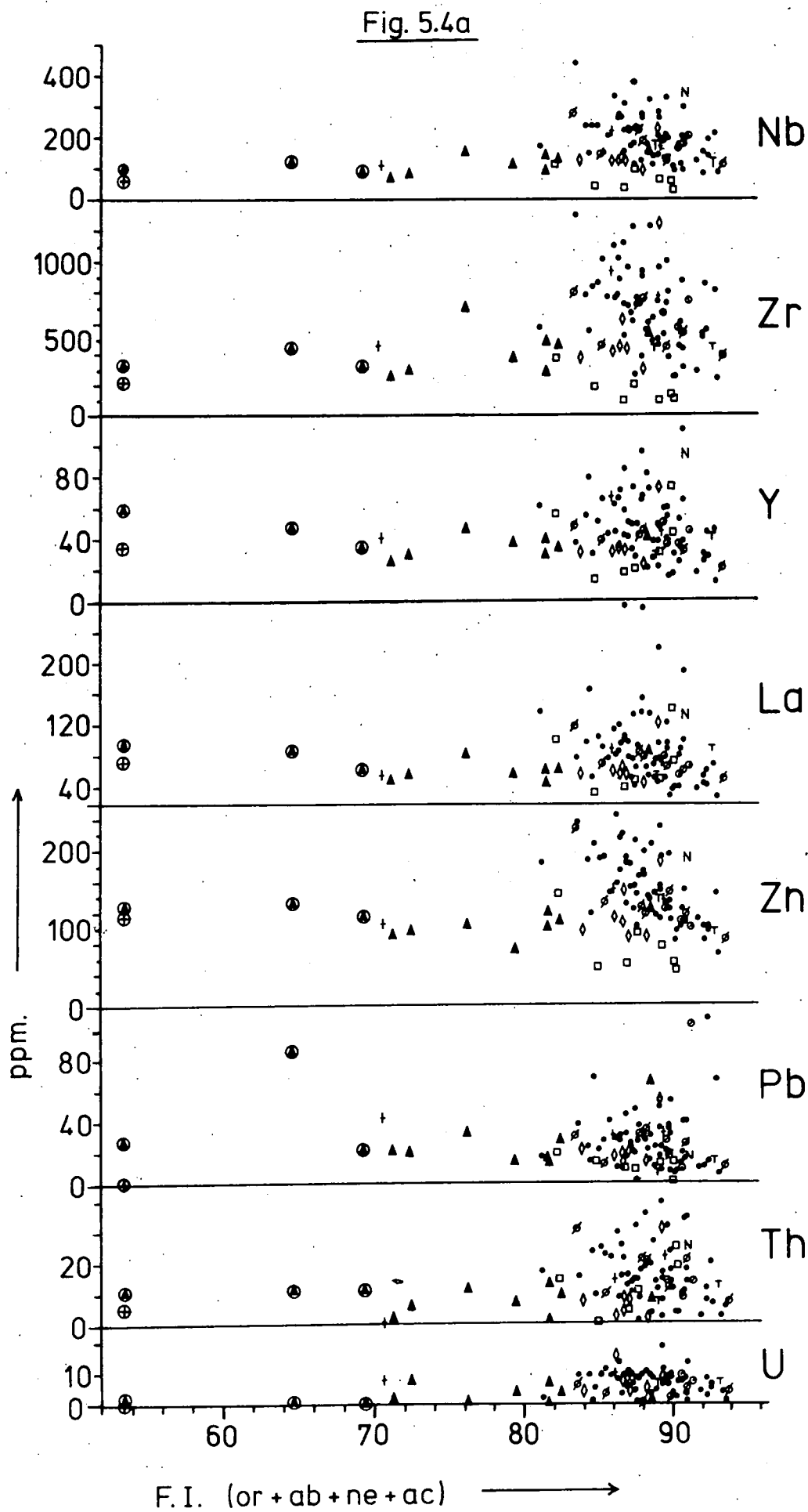


Fig. 5.4b

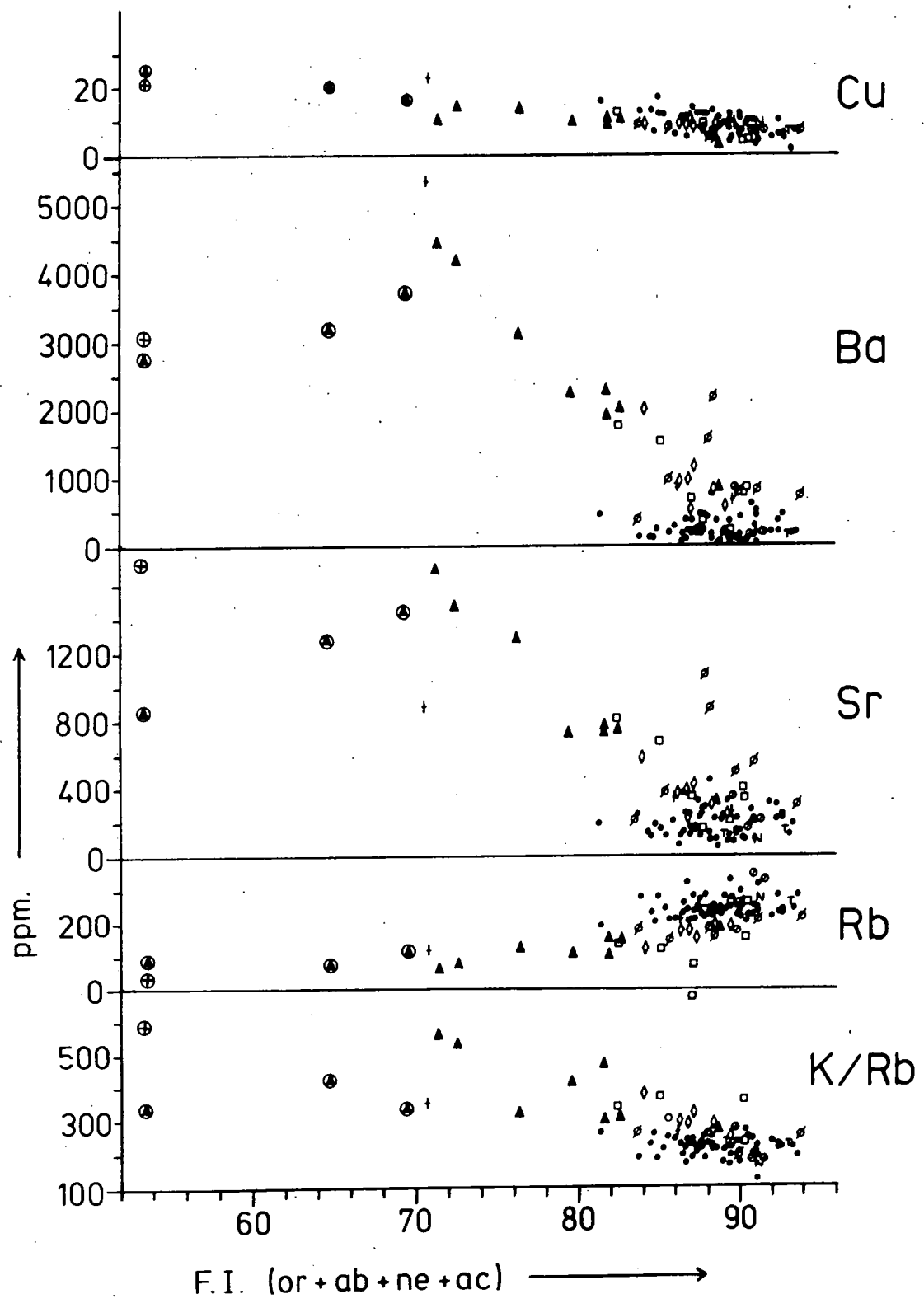


Fig. 5.5

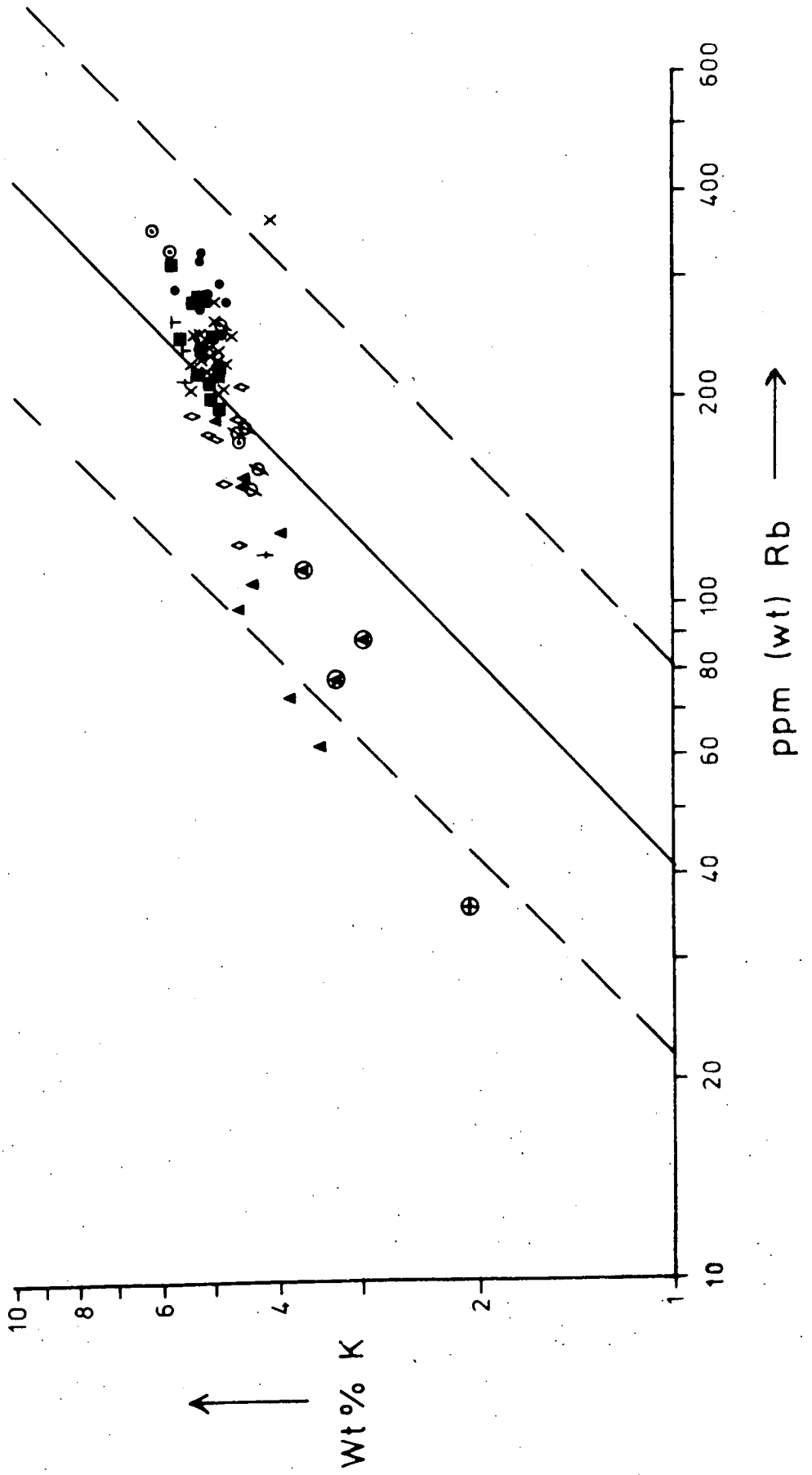
Potassium (Cation Wt. %) versus Rubidium (Wt. ppm.) diagram for the South Qoroq Centre rocks. Average K:Rb curve and normal limits of scattering taken from Ahrens et al. (1952).

x SS2

● SS3

■ SS5

Other symbols as in Fig. 5.1



### (5c) Trace Element Variation

Trace element variation is shown in Fig. 5.4, in which the elements are plotted against the same "Fractionation Index" (F.I.) as in Fig. 5.1. The ranges of most elements are similar to those found in highly fractionated rocks elsewhere in the Gardar Province (Upton 1960, 1964c; Macdonald and Edge, 1970; Gill, 1972) but do not reach the extreme values found in the Ilímaussaq Intrusion (Hamilton, 1964; Ferguson, 1970). The variation patterns are generally typical of highly differentiated magmas of alkaline affinities (Nockolds and Allen, 1954). Correlation coefficients for the trace elements are given in Table 4.

#### Barium and Strontium:-

These two elements have a strong positive correlation (Table 4) and both show a rapid depletion through the augite syenites of SS4b and SS4a, so that low concentrations with a slight spread are found in the foyaites. Slight variations can be detected between individual foyaites, with SS5 having generally higher values and SS2 having low values. Ba and Sr usually concentrate with fractionation in more basic magmas until the point where alkali feldspar begins to crystallise, but then decreases rapidly in late differentiates due to fractionation of the feldspar (Taylor, 1965). Alkali feldspar fractionation is thus strongly implicated during the evolution of the South Qôroq Centre (see Chapter 6). The essexite and accumulative rocks from SS4b lie on a separate, rising trend, which could represent the concentration of Ba and Sr in the liquid prior to alkali feldspar fractionation.

#### Rubidium:-

Rb shows a steady increase through the series, having a negative correlation with Ba and Sr. The K/Rb ratio drops considerably with increasing F.I. from 550 in the most basic augite syenite, to 150 in some of the foyaites. This behaviour is usual in alkaline complexes

where fractionation is dominated by alkali feldspar crystallisation, since size differences lead to an enrichment of Rb ( $1.47\text{\AA}$ ) relative to K ( $1.33\text{\AA}$ ) in the liquid (Taylor, 1965). The strong Rb enrichment is evident from the K - Rb diagram (Fig. 5.5) in which the South Qôroq trend is very oblique to the average K:Rb curve of Ahrens et al. (1952). Differences between individual syenites can be recognised on this trend, and the more differentiated nature of SS3 is particularly well seen. The essexite and two of the augite syenites lie outside the normal limits of scatter (Ahrens et al., op cit.) on the Rb deficient side. Rb deficiency also occurs in several less fractionated rocks from the Kûngnât Complex (Upton, 1960) and is correlated with an increased Ca and/or Ba content in the crystallising feldspar restricting the entry of Rb (Heier and Taylor, 1959).

Zirconium, Niobium, Yttrium, Lanthanum and Zinc:-

These elements do not substitute readily for major elements in the rock forming minerals and are concentrated in residual liquids (Taylor, 1965). In strongly differentiated series they therefore increase with fractionation. In the South Qôroq Centre values tend to be fairly constantly low, or increase slightly with F.I. in the augite syenites, but show a wide scatter over much higher values in the foyaites and related rocks. Within the scatter the five elements behave almost identically as is demonstrated by their high correlation coefficients given in Table 4. In some elements there is a suggestion, particularly within individual intrusions that values are highest in foyaites with a lower F.I. and that there is then a rapid decrease with fractionation. Zircon and zirconium silicates are not common in the rocks, but recent data shows that Zr can enter aegirine and alkali amphibole to a large extent (e.g. Bowden, 1966; Ferguson, 1970). It is therefore possible that the residual elements may enter late-crystallising sodic clinopyroxene and/or alkali amphibole (c.f. high

contents of these elements in amphiboles - Section 4c) and are thus subsequently reduced during the final stages of crystallisation. The wide scatter may then be attributed to the irregular development of amphibole and/or biotite as late stage hydrous minerals. However, Macdonald and Parker (1969) found that Zr concentrations in aegirine and alkali amphibole are unable to account for whole rock content in Tugtutôq alkaline dykes, and tentatively suggest the presence of sub-microscopic, Zr-rich accessory minerals.

Lead, Thorium and Uranium:-

The heavy elements appear from Fig. 5.4 to have a similar residual behavior <sup>u</sup> to the previous group, although they do not show quite such strong correlations (Table 4). Radioactive minerals are not detected in the centre and (Th + U) never exceeds 60 ppm. In many samples they are near or below the detection limits.

Copper, Nickle and Vanadium:-

Cu shows a steady decrease from the essexite through accumulative augite syenites and augite syenites to the foyaites, where concentrations are less than 10 ppm. Ni and V values are close to or below the detection limits and are thus not included in Fig. 5.4.

The hydrothermal alteration of nepheline does not alter the trace element content of the rocks appreciably, but recrystallised rocks near to the Igdlérfigssalik Centre show a marked depletion of residual elements. In such rocks amphibole is usually absent or considerably reduced and biotite is the main hydrous mafic. Hence the depletion could be due to the inability of these elements to enter any other phase after the disappearance of amphibole. However, it is also possible that they were "sweated out" along with volatiles during reheating.

Microsyenite sheets and satellitic syenites generally conform to the trends as in the major elements. However, the Østfjordsdal Syenite, having a lower  $K_2O$  content, is correspondingly depleted in Rb and

Fig. 5.6

Analyses from the main units of the South Qôroq Centre (excluding hydrothermally altered rocks) plotted in the Q - Ne - Ks "Residua System". Phase equilibria relationships at 1 Atm., 1kb P<sub>H<sub>2</sub>O</sub>, and 5 kb P<sub>H<sub>2</sub>O</sub> :-

1 Atm. - after Schairer (1950)

1 kb - " Hamilton and MacKenzie (1965)

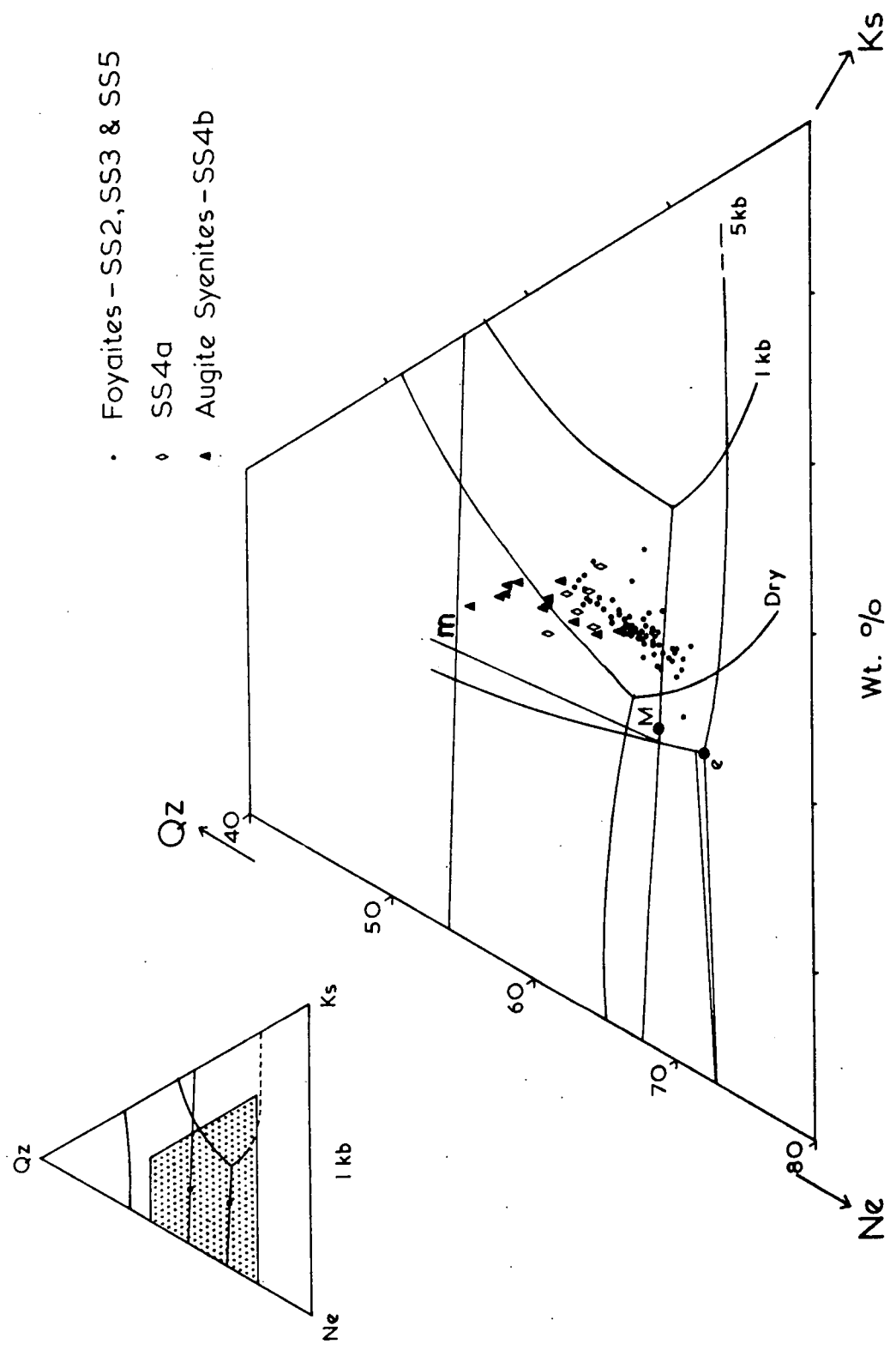
5 kb - " Morse (1969)

m = feldspar binary minimum at 1 kb

M = "nepheline syenite" ternary minimum at 1 kb

e = 5 kb eutectic

Unique fractionation paths at 1 and 5 kb are also shown.



enriched in Ba and Sr relative to the other rocks.

In general the accumulative rocks do not lie on the same trace element trends as normal rocks, as they do in major element content. They are usually displaced slightly upwards in the residual elements and Rb and, as explained above, may reflect an earlier stage of fractionation prior to alkali feldspar crystallisation.

Variations with height in the intrusion are not detected, and trace elements show less systematic variation towards the edges of intrusions than the major elements due to scattering, probably acquired during the late stages of crystallisation. However, some elements have fairly constant values in the centres of intrusions, but show increased scatter towards the margins. This is demonstrated in Fig. 5.3 by the Zr content of SS2.

#### (5d) Normative Mineralogy and Comparisons with Experimental Systems

With the exception of accumulative rocks and two less fractionated samples from SS4b, all the unaltered South Qôroq Centre rocks have normative (Ab + Or + Ne) greater than 80% and have been plotted in "Petrogeny's Residua System" (Q - Ne - Ks) (Bowen, 1937). The peralkalinity index is very close to 1.0 for most of the foyaites and only the more fractionated rocks are peralkaline. Hence the analyses lie close to the Q - Ne - Ks plane, and distortions due to the normative allocation of the excess alkalis over aluminium are only significant in the most fractionated samples (Bailey and Schairer, 1964; Thompson and MacKenzie, 1967).

Rocks from the main intrusive units (with the exception of hydrothermally altered rocks) are shown in Fig. 5.6 in relation to phase equilibrium relationships in the Q - Ne - Ks system at 1 atmosphere (Schairer, 1950); at 1 kb  $P_{H_2O}$  (Hamilton and MacKenzie, 1965); and at 5 kb  $P_{H_2O}$  (Morse, 1969). It has already been seen from Section 4g that  $P_{H_2O}$  was most likely between 1 and 3 kb during crystallisation of

the South Qôroq magmas, so the analyses will be related principally to the 1 kb phase equilibria.

The rocks lie on a curving trend (concave towards the Ne - Q join) from the least fractionated augite syenites of SS4b near to the Or - Ab thermal divide, through SS4a and the foyaites, to a minimum in the region of the feldspar - nepheline phase boundary. Several analyses fall just inside the nepheline field at 1 kb, but are well within the feldspar field at 5 kb. If this trend represents a fractionation curve then, by comparison with the experimentally derived curves of liquid descent (Hamilton and MacKenzie, *op cit.*), the foyaites would appear to lie in the low temperature thermal trough, and are derived via the augite syenites from the sodic side of the trough. The shape of the fractionation curve conforms to that of experimental equivalents and the foyaites lie along a line parallel to the unique fractionation curve in the experimental thermal trough. However, there is a considerable overall displacement towards Ks in the South Qôroq rocks compared with both the experimental data and the density distribution of natural rocks from Washington's tables (Hamilton and MacKenzie, *op cit.*). It is not unusual for such a displacement to occur in natural rock series, due to the presence of other phases not represented in the "Residua System", and the trend is similar to natural fractionation curves derived by Nash et al. (1969) for Mt. Suswa lavas. Peralkaline rocks (with normative acmite) are particularly prone to displacement and the apparent South Qôroq minimum is considerably more K-rich than the 1 kb nepheline syenite minimum ('M') since it is defined by the more peralkaline rocks of the centre.

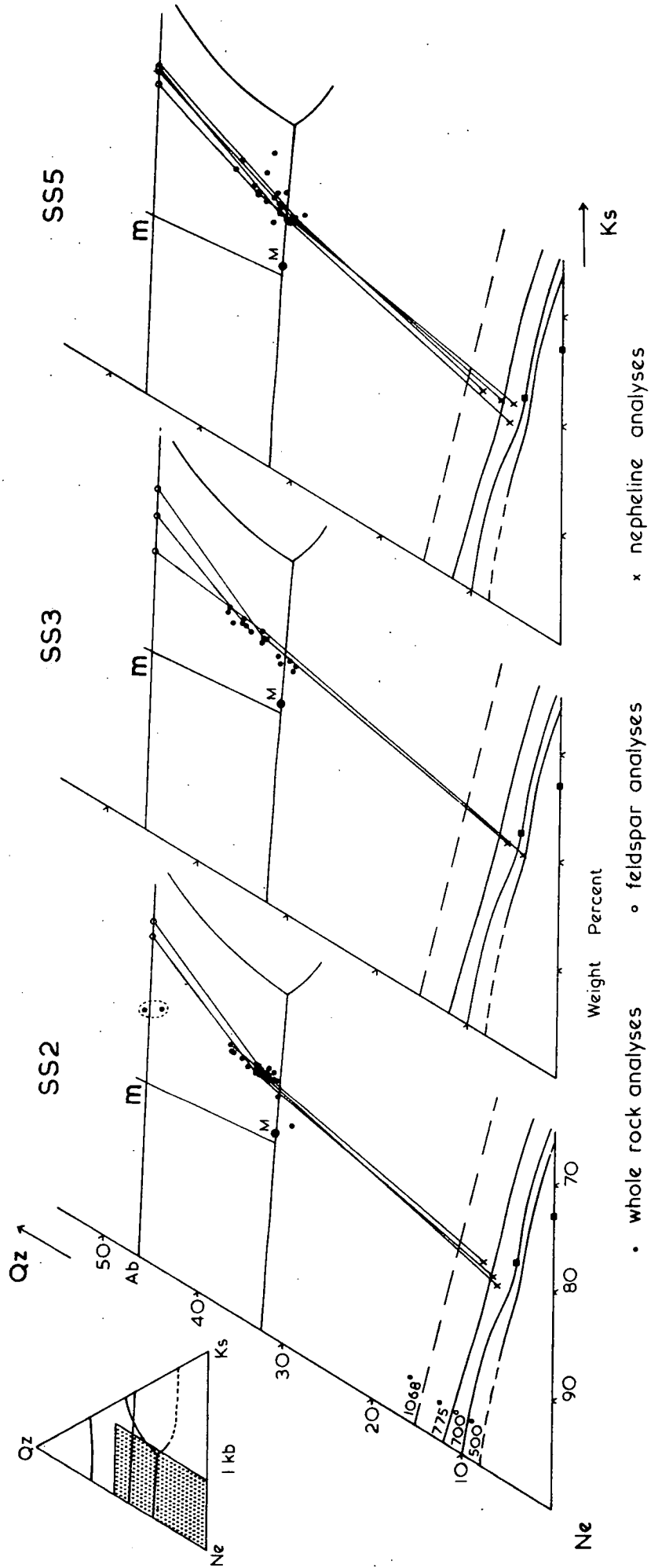
In Fig. 5.7, analyses from the various units of the centre are plotted with tie lines to average feldspar and nepheline compositions (where available) from individual samples. Phase equilibrium relationships at 1 kb (Hamilton and MacKenzie, *op cit.*), and limits of nepheline solid solution (Hamilton, 1961) are also shown. Regular

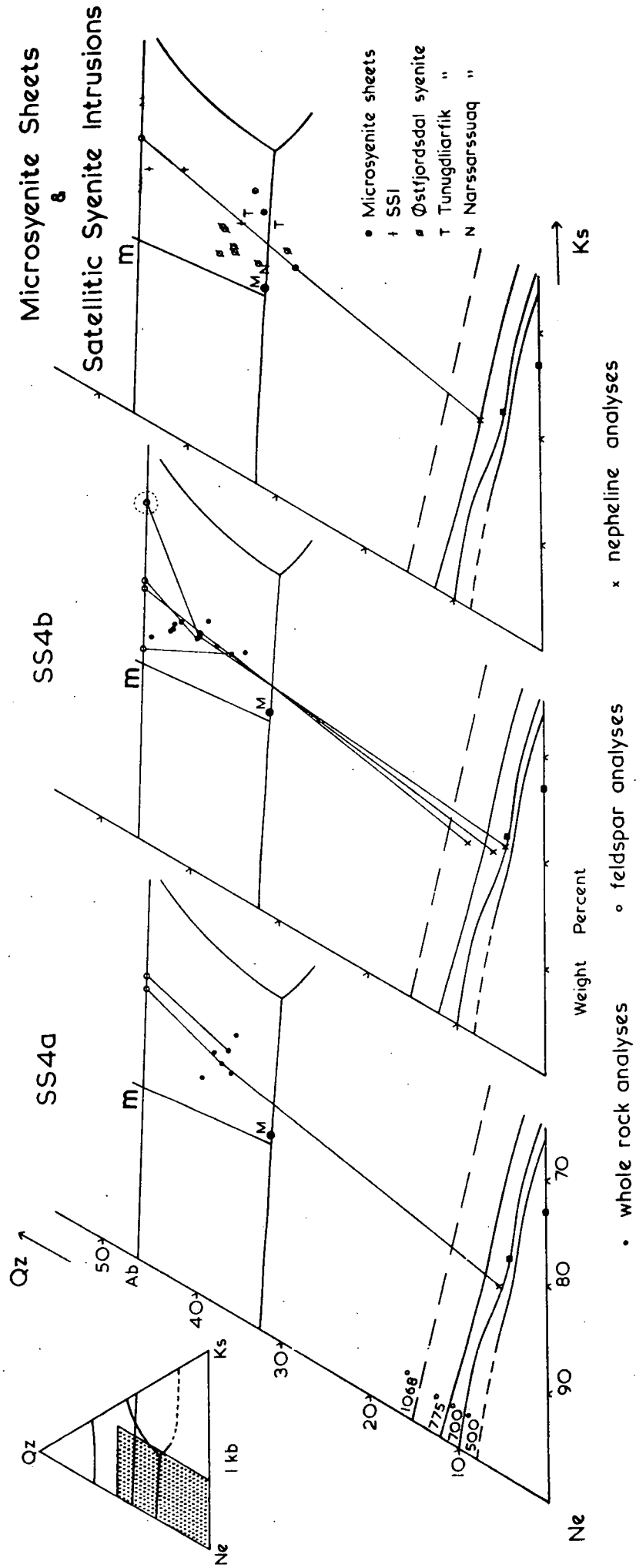
Fig. 5.7 (Two pages)

Analyses from individual units of the South Qôroq Centre (excluding hydrothermally altered rocks) together with coexisting average feldspar and nepheline analyses where available, plotted in the "Residua System" Q - Ne - Ks. Phase relationships at 1 kb  $P_{H_2O}$  after Hamilton and MacKenzie (1965). Limits of nepheline solid solution after Hamilton (1961).

N.B. i) two analyses from rocks contaminated by country rock in SS2 (circled).

ii) extreme potassium enrichment in the feldspar from a recrystallised rock in SS4b (circled).





relationships between whole rock analyses and the felsic phases suggest that the whole rock compositions are little modified by accumulative development of these phases and hence represent true bulk liquid compositions.

Fractionation of a relatively sodic alkali feldspar is seen in SS4b, and feldspar compositions become more potassic as the liquid moves towards the thermal trough. (SS4b feldspars project on the K-rich side of the experimental feldspar minimum ('m') as a result of their Ca content.) Straight tie lines in several analyses particularly in SS4a and SS5 between nepheline, rock and feldspar compositions (i.e. there is no three phase triangle) suggest that the particular liquids have reached the unique fractionation curve (Hamilton and MacKenzie, op cit.). In SS2 and SS3 it can generally be seen that feldspar compositions become more potassic and even cross over the projection of the thermal trough on the Ab - Or join as liquids become more fractionated. This reflects the trend towards K - enrichment and crossing of the feldspar ternary cotectic, probably due to the coprecipitation of nepheline, discussed in Section 4g. There is no indication that feldspars become more sodic with fractionation in the foyaites and in Fig. 5.1, normative Or is seen to increase constantly with F.I.

The departure of peralkaline liquids from the plane of the Q - Ne - Ks "Residua System", and the enrichment of late fractionates in other alkali silicates (notably acmite), led Bailey and Schairer (1966) to postulate a "Peralkaline Residua System" based on the system  $\text{Na}_2\text{O} - \text{Fe}_2\text{O}_3 - \text{Al}_2\text{O}_3 - \text{SiO}_2$  at 1 Atm. and  $P_{\text{O}_2} = \text{air}$ . The components of this system account for well over 90% of the South Qôroq Centre rocks, with the exception of the accumulative rocks in which they account for 80 - 90%. It is thus pertinent and instructive to consider the centre in relation to this system.

Engell (in press; and personal communication, 1972) has projected the phase relationships onto the plane  $\text{Na}_2\text{O} - \text{Fe}_2\text{O}_3 - \text{Al}_2\text{O}_3$ , in which he has plotted the Ilímaussaq rocks (Fig. 5.8). A large part of the diagram is dominated by the acmite - iron oxide incongruent melting relationships, but the most significant feature is the cotectic line E - A, along which Ab, Ne, Ac and liquid coexist. (E = reaction point where Ab, Ne, Ac, He and liquid coexist; A = the Ab, Ne, Ac, Ds, liquid eutectic). Assuming a closed system, liquids such as those of the Ilímaussaq Intrusion, precipitating feldspar, nepheline and acmite should follow this curve towards alkali enrichment and iron depletion. The proposed trend of Ilímaussaq liquid compositions (Engell, in press), although parallel to the cotectic, is considerably displaced towards the  $\text{Al}_2\text{O}_3$  corner. However, the intrusion probably fractionated at a higher  $P_{\text{H}_2\text{O}}$  (1 - 3 kb) and a lower  $P_{\text{O}_2}$  ( $\approx$ QFM) than those under which the phase equilibria were determined, so a direct comparison is not relevant.

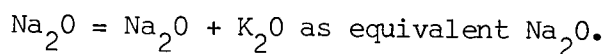
Using phase relationships in the system Ab - Ne - Ac (Nolan, 1966) and the stability relations of acmite (Bailey, 1969), Engell calculates the effect of increasing  $P_{\text{H}_2\text{O}}$  to 1 and 2 kb and decreasing the  $P_{\text{O}_2}$  below the NNO buffer. The former tends to increase the stability field of acmite relative to albite and nepheline, and the latter reduces the acmite stability field. Hence the variance of these two factors tend to have a cancelling effect. However, Nolan (op cit.) found that the addition of even small amounts of diopside to the system considerably increased the stability field of acmite. The Ilímaussaq pyroxenes do have a diopside component in their early stage of fractionation (L. Melchior - unpublished data), and Engell considers that this is responsible for the apparent shift of the cotectic towards  $\text{Al}_2\text{O}_3$ .

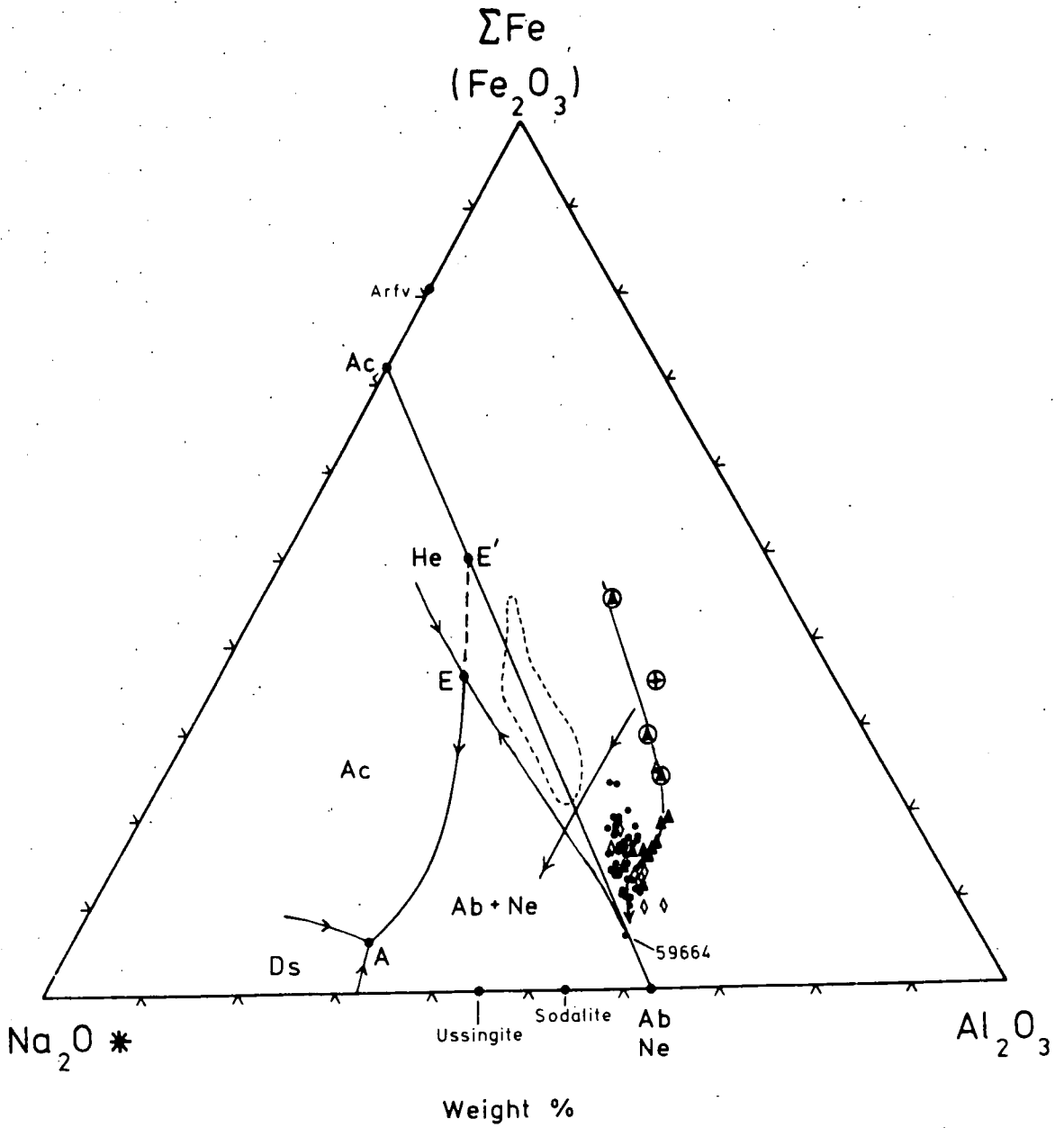
Fig. 5.8

South Qôroq Centre and Ilímaussaq Intrusion analyses (excluding hydrothermally altered rocks) plotted in the  $\text{Na}_2\text{O} - \text{Fe}_2\text{O}_3 - \text{Al}_2\text{O}_3$  plane of the "Peralkaline Residua System"  $\text{Na}_2\text{O} - \text{Fe}_2\text{O}_3 - \text{Al}_2\text{O}_3 - \text{SiO}_2$  (Bailey and Schairer, 1966). Phase relationships adapted from Bailey and Schairer (1966) by Engell (in press). Ilímaussaq plots also from Engell (in press).

- † = South Qôroq Centre essexite
- ▲ = " SS4b
- ◇ = " SS4a
- = " foyaites SS2, SS3 and SS5
- ⊕ = " accumulative rocks
- ⊕ = field of Ilímaussaq kakortokites and lujauvrites
- ↖ = Ilímaussaq proposed liquid trend
- E = reaction point where Ab, Ne, Ac, He and liquid coexist.
- A = eutectic point where Ab, Ne, Ac, Ds and liquid coexist.

\* N.B.  $\Sigma\text{Fe}$  is expressed as  $\text{Fe}_2\text{O}_3$





The South Qôroq analyses are plotted on Fig. 5.8 along with the Ilímaussaq data. A trend, parallel to the Ilímaussaq liquid trend, occurs in the augite syenites and probably turns downwards in the foyaites towards Ab and Ne on the Ac - Ab - Ne plane (see below). The foyaites exhibit a spread parallel to the Ac - Ab - Ne plane, similar to the Ilímaussaq lujavrites and kakortokites, which Engell (in press) considers to be modified from original magma compositions by cumulus effects and possible alkali loss. Part of the spread in South Qôroq foyaites may be due to slight accumulation of mafic minerals (c.f. slight enrichment in Fe and Mn in foyaites - Fig. 5.1). The turning down of the trend towards Ab + Ne is to be expected, since these are end products of solid solution series, and a liquid may only cross the Ac - Ab - Ne plane by precipitating a peralkaline mineral such as sodalite (Engell, personal communication, 1972). This occurs in the Ilímaussaq sodalite foyaite and naujaite but not in the South Qôroq Centre, where sodalite only occurs as a late, interstitial mineral.

The South Qôroq Centre accumulative rocks lie on an earlier part of the trend, which is approximately parallel to the Ac - He cotectic in the synthetic system. Thus they probably represent the early fractionation path of the liquid, prior to the appearance of feldspar and nepheline at the reaction point E. At the  $P_{O_2}$  expected in the magma, acmite would thus be precipitating with magnetite and/or olivine ( $P_{O_2} \approx \text{FMQ}$  - see Section 4d) rather than haematite ( $P_{O_2} = \text{air}$ ). This is consistent with textural and mineralogical evidence presented in earlier chapters. Since in general the South Qôroq Centre clinopyroxenes are more diopsidic than those from Ilímaussaq, it is to be expected <sup>that</sup> the acmite stability field will be further enlarged and the cotectic trend displaced even further towards  $\text{Al}_2\text{O}_3$  as is in fact observed in Fig. 5.8.

Thus comparison of the South Qôroq Centre analyses with both the "Peralkaline Residua System" and the conventional "Residua System"

enables a more complete interpretation to be made than with the Q<sub>c</sub>-Ne-Ks system alone. The evolution of the centre can be explained in terms of fractional crystallisation in a closed system of clinopyroxene and olivine/magnetite in the early stages, followed by alkali clinopyroxene, alkali feldspar and nepheline fractionation in the later stages.

## 6 CONCLUSIONS

### (6a) Intrusive Mechanisms

The major intrusive units comprising the South Qôroq Centre are concentric stocks and ring intrusions with steep, outward dipping contacts and elliptical cross sections. The north-west - south-east elongation conforms to the regional stress pattern of maximum north-east - south-west stress and minimum north-west - south-east stress deduced from faulting and direction of dyke emplacement. The centre was emplaced at a relatively high structural level, and cuts through the Eriksfjord basalt/sandstone succession, which has a maximum known thickness of 3 km. Contacts with country rock are usually sharp, and the outer syenite SS2 frequently shows a marked chill. Angular xenoliths are usually restricted to the immediate vicinity of the contact and shearing is seen along the contact at one locality. Metamorphism of country rock is not very widespread, although certain areas are heavily metasomatised. In the area around Narssarssuaq, the inward dip of the basalt succession is seen to increase towards the intrusion which, together with the above evidence suggests a permissive intrusion by ring fracture and block subsidence.

Three similar foyaitic magmas were emplaced in the order SS2, SS3, SS5. Internal contacts between these intrusions are usually diffuse or gradational, marked only by zones of marginal pegmatites, suggesting three pulses of magma from a common source in fairly rapid succession (Harry and Richey, 1963). It is likely that the magmas were below their liquidus on emplacement and in the chill of SS2, small feldspar phenocrysts are present, laminated parallel to the contact. In Chapter 4, variation in several mineral groups has been interpreted in terms of fractionation prior to emplacement. This is best demonstrated by the clinopyroxenes which show different compositional ranges in successive intrusions.

Igneous lamination of platy feldspar is found in all the foyaites, but is best developed in SS5 where slight accumulation of mafic minerals is also occasionally seen in mafic banding. The syenite SS4 has in general sharper contacts, often with associated minor crushing, and field relationships suggest that it is younger than both SS3 and SS5. The magma is an augite syenite, less differentiated than the foyaites and in places well developed mafic banding is observed. These features suggest that it is probably a later ring dyke. Internal contacts within SS4 suggest that it consists of at least two pulses, SS4a and SS4b. Thus the original order of intrusion, as deduced by Emeleus and Harry (1970), has been modified to :- SS2, SS3, SS5, SS4a, SS4b.

The inclined microsyenite sheets which cut SS3 and dip inwards towards SS4 have many mineralogical and geochemical features in common with SS4a. They would thus seem to be associated with the period of late ring dyke intrusion, as could the essexite giant dyke since basic rocks elsewhere in the Igaliko Complex are mostly associated with arcuate intrusions (Emeleus and Harry, 1970). Small, satellitic intrusions around the periphery of SS2 predate the main units and appear to be related bodies.

The centre was cut by the Mid-Gardar dyke swarm and was affected by transcurrent faulting, some of which appears to have been contemporaneous with dyke emplacement. Some of the transcurrent stress appears to have been taken up in the contemporaneous dykes by an apparent sinistral rotation on the Narssarssuaq - Qôroq peninsula, producing an 'S' shaped deflection of the dykes (Emeleus and Stephenson, 1970, see Section 2e).

#### (6b) Source and Primary Evolution of the South Qôroq Centre Magmas

Field relationships show that the South Qôroq Centre is made up of a series of concentric, high level intrusions emplaced in fairly rapid succession. The trend towards successively less fractionated magmas with time can be seen from the petrography and geochemistry, but is

particularly well demonstrated by the clinopyroxene trends.

Upton et al. (1971) describe similar situations in the Gardar silica-oversaturated syenite complexes of Kûngnât and Central Tugtutôq. At Kûngnât, later intrusions became successively less fractionated, culminating in an alkali gabbro ring dyke. The two earlier intrusions of quartz syenite crystallised under conditions of slow cooling to give an accumulative sequence with considerable cryptic layering. At Central Tugtutôq, which is a higher level intrusion, a succession of magma batches already below their liquidus temperatures were intruded in rapid succession. Cooling was faster than at Kûngnât and in situ fractionation was negligible, although deeper levels may have similar accumulative sequences to those at Kûngnât. In both cases Upton et al. (op cit.) consider that the complexes were derived from a deeper magma chamber which had already differentiated giving trachytic compositions overlying more basic magma at depth. It is suggested that the South Qôroq Centre is analogous to the Central Tugtutôq Complex and that separate intrusions were derived from some form of differentiated chamber at depth, from which progressively deeper fractions worked up to the surface separated by short time intervals.

#### Partial Melting:-

In recent years several authors (Bailey, 1964; Bailey and Schairer, 1966; Wright, 1971) have presented convincing evidence for the derivation of trachytic and phonolitic magmas by melting of mantle material in areas of high geothermal gradients such as are found in rift environments. Therefore, an alternative hypothesis is that the successive intrusions in the South Qôroq Centre are produced by successive stages in partial melting of crustal or upper mantle material. The early, lower temperature melts would form first, followed by more basic members as higher temperature melts formed. Since there is little material of more basic composition than augite syenite, it may be that temperatures never rose

above the augite syenite liquidus. This apparent lack of basic material would tend to favour a partial melting hypothesis, but it is highly likely that large volumes of basic material are present at greater depths (see below).

The smooth, continuous major element trends from augite syenite to foyaite seen in Chapter 5, are suggestive of fractional crystallisation of a common magma source. During partial melting, major and trace elements of the early melting phases would form the first melts, probably with some diffusion out of intergranular areas, and ultimately the magma should have a composition equal to that of the parent. However, immediate removal of earlier formed magma to higher crustal levels could result in successive batches lying along similar variation curves to those produced by fractional crystallisation.

The trace element distribution observed in the South Qôroq Centre may be possible with the above mechanism, but the highly ordered enrichment and depletion of elements is more consistent with fractional crystallisation (Taylor, 1965; Taylor et al., 1968). Ba and Sr decrease rapidly to low levels of concentration as is usually observed in the late stages of evolution of a basaltic magma in which feldspar fractionation has played a major part. K enters preferentially over Rb into alkali feldspar and hence in successive liquids the K/Rb ratio is progressively reduced (Taylor, 1965). These features are well illustrated in the centre, implying a considerable amount of feldspar fractionation. Crystal fractionation would also lead to a build up in residual elements (Zr, Nb, Y, La, Zn, Pb, Th, U) in late liquids and this too is well seen.

Comparisons with the systems Q - Ne - Ks and  $\text{Na}_2\text{O} - \text{Fe}_2\text{O}_3 - \text{Al}_2\text{O}_3 - \text{SiO}_2$  are consistent with feldspar fractionation, and data on individual mineral phases clearly demonstrates continuous crystallisation trends. Although it is recognised that comparative data is unavailable for magma series with a proven origin by progressive partial melting, the evidence strongly

suggests evolution of the South Qôroq Centre by fractionation of a common magma source.

#### Fractional Crystallisation:-

Bridgwater and Harry (1968) present convincing evidence for the presence of layered gabbro - anorthosite bodies beneath much of the Gardar Province. During the early stages of crystallisation in these bodies, fractionation of plagioclase and mafic minerals occurred. The early plagioclase was less dense than the liquid at this stage and tended to accumulate in suspension at high levels where it was incorporated in rising batches of magma and hence can be seen in the "Big Feldspar Dykes" (BFD's) of the province (see Section 2b). Mafic minerals would sink to lower levels of the chamber and hence the overall effect of removing these phases would be to deplete the liquid in Ca, Al and Mg to produce an alkali-enriched residua. Bridgwater and Harry (op cit.) calculate that when the liquid reached an  $\text{SiO}_2$  content of about 53% (about the content of an augite syenite), the fractionating plagioclase would be more dense than the liquid and hence would sink. As a result of this, very few anorthosite xenoliths are present in the more differentiated Gardar intrusions, although they are found sporadically in certain units of the Igdlérfigssalik Centre (Emeleus and Harry, 1970), in the nearby Klokken intrusion and in several other complexes.

Continued feldspar fractionation and removal of Ca + Al results in a trend towards increasing peralkalinity of successive residua. In the South Qôroq Centre the feldspars are seen to range from a sodic oligoclase, through Ca-bearing soda-sanidines in the augite syenites, to K-rich alkali feldspars in the foyaites. On reaching the feldspar/nepheline phase boundary, nepheline began to coprecipitate with alkali feldspar. Since Na is preferentially incorporated into nepheline, marked changes in the chemical trends of the rocks are seen at this

point, and feldspar compositions are "forced" across the ternary cotectic becoming enriched in potassium.

In order that the fractionation processes should be effective, it is necessary that some of the early formed feldspar crystals be removed from the liquid by crystal settling. It is therefore possible that a series of layered cumulates is present below the South Qôroq Centre in a situation analagous to the Kûngnât/Central Tugtutôq relationship (Upton et al., 1971). Cryptic layering is present in unit SI4 and possibly other units of the Igdlérfigssalik Centre, but little is known yet of the other Igaliko intrusions (C. H. Emeleus, personal communication, 1972).

The South Qôroq element variation cannot be entirely explained by feldspar fractionation and a considerable contribution has also been made by fractionating mafic phases. Fayalitic olivine, iron-titanium oxide, apatite and titanaugite are usually present as early phases, particularly in the less differentiated augite syenites. The reductions in Mg, Fe and P in the augite syenites and low concentrations in the foyaites may be attributed to fractionation of these phases. Alkali clinopyroxene, alkali amphibole and biotite continue crystallising throughout the series, further depleting the liquid in Fe and Ca. The fractionation of certain of the mafics in terms of phase equilibria is well seen in the projection of the system  $\text{Na}_2\text{O} - \text{Fe}_2\text{O}_3 - \text{Al}_2\text{O}_3 - \text{SiO}_2$  (Engell, in press).

The few available analyses from SS4b mafic bands lie on smooth backward extensions of the major element trends in non-accumulative rocks, and can also be related to the phase equilibria in the  $\text{Na}_2\text{O} - \text{Fe}_2\text{O}_3 - \text{Al}_2\text{O}_3$  system (see Chapter 5). This suggests that they lie on or close to the liquid line of descent and emphasises the importance of fractionating mafic minerals, particularly in the earlier evolution of the augite syenite magma. Slight deviations in the Fe

and Mn content of several foyaite samples suggest that mafic accumulation probably also occurred in the foyaites, particularly in SS5 where definite mafic bands are observed.

It has already been suggested that the South Qôroq magmas were below their liquid<sup>(ii)</sup> on emplacement and hence were in a partially crystalline state. Feldspar and nepheline were the principal phases at the liquidus, but it is also likely that small amounts of apatite, magnetite, olivine and clinopyroxene had also started to nucleate. Clinopyroxene in particular commonly occurs as phenocrysts in the Igaliko trachytic dykes. Melting experiments on similar undersaturated rocks from the province by Piotrowski and Edgar (1970) and Sood and Edgar (1970) have shown that under most conditions of  $P_{H_2O}$  and  $P_{O_2}$ , clinopyroxene is either the primary liquidus phase (excluding high temperature phases such as apatite and magnetite) or appears within  $20^{\circ}C$  of the liquidus after feldspar and/or nepheline. Thus, in each of the South Qôroq intrusions, the starting point of the respective pyroxene trend probably reflects the composition of the pyroxene on intrusion, and hence the depth of origin in the underlying magma chamber.

The earliest syenite (SS2) has a trend which starts fairly early in the pyroxene series, probably due to intrusion before much differentiation had taken place at depth. Pyroxenes from this syenite also show considerable zoning which reflects the relatively rapid cooling against country rock, preventing continuous reaction with liquid. (This is also seen in several other minerals.) The next syenite (SS3) contains the most fractionated pyroxenes, with a considerably advanced starting point, indicating an origin near the top of the differentiated chamber which had now formed. Successive intrusions (SS5, SS4a, SS4b) then show a continuous regression of starting point due to tapping from deeper levels (Fig. 4.1).

The satellitic syenite stocks around the periphery of SS2 would in general appear to be derived from the same or a similar source to the rest of the centre. They lie on the same major and trace element trends with the exception of the Østfjordsdal Syenite which is slightly less potassic and is correspondingly depleted in Rb and enriched in Ba and Sr relative to the other syenites. All the satellites were emplaced earlier than the main centre and hence may represent small batches of magma which separated at an early stage and subsequently evolved along slightly different lines.

#### Liquid Fractionation:-

Objections may be raised to a model invoking tapping of a differentiated magma chamber on the grounds that lower levels would be largely crystalline long before they could be emplaced. The syenites were emplaced over a short time interval, and it could be significant that there is very little material more basic than augite syenite in all the Gardar major intrusions. Thus it is possible that the higher levels of the magma chambers were tapped off, forming intrusions of syenite, nepheline syenite and augite syenite, but that the lower, more basic levels were too highly crystallised to rise to higher levels. Alternatively a residual magma of augite syenite composition may have become compositionally zoned through some form of liquid fractionation, to act as a largely liquid parent body for the higher level intrusions.

Liquid fractionation involving a vertical column of magma, more salic in composition in higher levels and more basic towards the base, is envisaged by Bridgwater and Harry (1968) as the principal source of high level Gardar dykes involving pulses of magma with widely varying composition. Thus the primary compositions of the feldspars and other minerals in each magma batch would reflect the composition of the liquid at the depth of origin. A similar mechanism is proposed by Lipman et al. (1966) and Lipman (1967) for the source of compositionally zoned

salic ash flow sheets in Southern Nevada and South-western Japan. It is also implied by Gibson (1970) for similar welded ash flows from Fantale volcano, Ethiopia.

Although this hypothesis is perhaps the simplest way of explaining compositional differences in successive magma pulses, and particularly such mineralogical variations as are seen in South Qôroq clinopyroxenes, it is difficult to envisage a mechanism whereby such a column of liquid may be generated, and perpetuated on such a large scale. Problems of degree of solidification are avoided if the column remains largely liquid prior to emplacement. However, it is clear that many Gardar high level intrusions were partly crystalline on emplacement, and at crustal levels one would expect considerable crystallisation of at least the higher temperature mineral phases such as olivine and plagioclase.

The most likely mechanism of liquid fractionation is an upward diffusion of alkalis in the liquid, aided by volatile transfer (Kennedy, 1955). The South Qôroq magmas are seen to have had a reasonably high volatile content, and volatile transfer under a thermal diffusion gradient after emplacement has been demonstrated in Section 5b. The presence of volatiles would tend to lower the liquidus temperature of the magma which would preserve the liquid state for longer than in a dry magma. However, it is unlikely that such a process is capable of producing variation on such a large scale as is seen in the Gardar major intrusions without some fractional crystallisation occurring. Most of the variation in the South Qôroq Centre can be explained on a crystal fractionation hypothesis, but it is likely that upward volatile transfer could also have played a significant part, particularly in the development of the residual liquids. However, it is difficult to assess the relative influence of the two mechanisms.

Summary:-

The interpretations on the magmatic and structural evolution of the South Qôroq Centre presented in this thesis, add considerable support to the conclusions of many workers in the Gardar Province, that the differentiated alkaline complexes can be derived from alkali olivine basalt, largely by processes of fractional crystallisation (Upton, in press). Progressive partial melting and removal of early melts to higher levels, although still feasible, seems to be an unlikely mechanism, particularly in view of the trace element evidence. Large, layered intrusions of gabbro - anorthosite postulated by Bridgwater and Harry (1968) probably gave rise to residua of augite syenite composition by fractionation and subsequent removal of plagioclase feldspar and mafic phases. Further feldspar and mafic fractionation, possibly in conjunction with a certain amount of liquid fractionation through upward volatile transfer of alkalis, produced stratified magma chambers with an upward increase in salic constituents. Tapping of such a magma chamber from successively lower levels produced a series of concentric, high level stocks of foyaite and a later ring dyke of augite syenite to form the South Qôroq Centre.

The source of the primary alkali olivine basalt is beyond the scope of this thesis, but it is probably closely related to a rift valley environment, since many features of modern rift systems can be identified in the Gardar Province (Gill, 1972; Upton, in press). In such an environment, partial melting of upper mantle material occurs in areas of high geothermal gradient, producing large volumes of magma of both tholeiitic and alkaline affinities, within and on the flanks of the rifts. Models to explain the generation of the various magma types have been proposed by Bailey (1964), Bailey and Schairer (1966) and Harris (1969, 1970), and a review of the application of these

models has been given by Gill (1972). Recent isotopic work on the Kūngnât and Tugtutôq rocks has shown that initial  $\text{Sr}^{87}/\text{Sr}^{86}$  ratios are consistent with a lower crustal or upper mantle origin (Van Breeman and Upton, 1972).

(6c) Conditions of Crystallisation and Late-Stage Evolution of the South Qôroq Magmas

Estimates of liquidus temperatures of natural magmas from experimental phase equilibria are usually unreliable due to the presence of additional components; inaccuracies in estimating  $P_{\text{H}_2\text{O}}$  and  $P_{\text{O}_2}$  in the magma; and the inability to take into account variations of  $P_{\text{H}_2\text{O}}$  and  $P_{\text{O}_2}$  during crystallisation. However, in the South Qôroq Centre data is available on alkali feldspar and nepheline, both of which appeared at or close to liquidus temperatures.

Nepheline provides the most reliable geothermometer (assuming no sub-solidus adjustments) since compositions are almost independent of other variables (Hamilton, 1961). Cores of zoned nepheline in SS2 suggest that the phase commenced crystallisation between 900 and 850°C and most grains appear to have stabilised between 775 and 700°C. Assuming a  $P_{\text{H}_2\text{O}}$  of between 1 and 3 kb (see below), the alkali feldspars probably commenced crystallisation around 850°C in the foyaites and completed crystallisation within 20°C. There is thus reasonable agreement between the methods. Feldspar in the augite syenites probably commenced crystallisation at temperatures slightly above 850°C, but nepheline appeared at similar temperatures irrespective of magma composition.

Melting relationships determined by Sood and Edgar (1970) for similar Gardar rocks at controlled  $P_{\text{H}_2\text{O}}$  and  $P_{\text{O}_2}$  give liquidus temperatures (excluding high temperature phases such as apatite and

magnetite) in the same range. However, detailed comparisons of temperature and order of crystallisation are not relevant, since only two samples were investigated under controlled  $P_{O_2}$ , and the buffer conditions used were higher than those expected in the South Qôroq Centre (see below).

From comparisons with calculations of oxygen fugacity in other alkaline rock series' (see Section 4d), the early stages of crystallisation in the South Qôroq magmas were controlled by the fayalite - magnetite - quartz (FMQ) buffer. However, in later stages, olivine became unstable and hydrous alkali amphibole and biotite started to precipitate, suggesting either a new internal buffer above the FMQ (such as the annite - magnetite - sanidine buffer), or an external buffer due to the separation of a volatile phase. The nature of the clinopyroxene fractionation trend (i.e. the state at which enrichment in  $NaFe^{3+}$  commences) may be related to  $f_{O_2}$  and differences in trends from oversaturated and undersaturated alkaline complexes could be due to different oxidation conditions.

From phase relationships in the Ab - Or system it is deduced that  $P_{H_2O}$  was between 1 and 3 kb during the crystallisation of the foyaite alkali feldspar. The normative rock compositions have been related to the 1 kb phase equilibria in the Q - Ne - Ks system and considering the possible thickness of basalt/sandstone cover, 1 kb seems to be a reasonable estimate. However,  $P_{H_2O}$  may have been initially lower in the augite syenites and probably built up in the later stages of foyaite crystallisation to values above 1 kb. As a result of increased  $P_{H_2O}$  (and the gradually decreasing  $f_{O_2}$ ) during the later stages, alkali amphibole became stable in place of alkali clinopyroxene, and in many samples, biotite formed as a second hydrous mafic phase. The hydrous phases are always interstitial relative to the other phases, suggesting a separate stage

of crystallisation. It is possible that their precipitation is controlled by a rapid decrease in load pressure as the magma was emplaced to its present level, causing  $P_{H_2O}$  to exceed  $P_{total}$ , but there is insufficient evidence to determine the extent of this influence. Other volatile fractions in the magma which became active during the later stages are F which entered alkali amphibole and occasional fluorite; Cl which resulted in the precipitation of interstitial sodalite; and  $CO_2$  which entered secondary cancrinite and interstitial calcite.

Since the South Qôroq Centre is composed of batches of magma which were already below their liquidus temperatures and highly differentiated on emplacement into a fairly cool, high structural level, further differentiation after emplacement has been minimal (c.f. Central Tugtutôq, Upton et al., 1971). Occasional mafic bands, concordant with igneous lamination have produced local variations. However, the main effect has been the volatile transfer of alkalis outwards under a thermal diffusion gradient established during cooling. This is seen in slight variations in element content across the intrusion, with an increase in differentiation outwards. Marginal pegmatites, suggesting local accumulation of trapped volatiles, are common and there is often a zone of alkali metasomatism in the country rocks around the centre. Pegmatite veins representing the final magmatic residua, and composed essentially of the low temperature phases albite, aegirine and carbonate, cut the outer syenite SS2.

Sub-solidus exsolution, commencing in the temperature range 750 - 700°C, occurred to a greater or lesser extent in all alkali feldspars. The exsolution was probably enhanced in rocks with a high volatile content. Exsolution - oxidation ordering of the iron-titanium oxides probably occurred at super-solvus temperatures.

Hydrothermal alteration of the rocks occurred in several areas, but was particularly active in the vicinity of faults, in shear zones

and in marginal areas. The alteration principally involved hydration of the nepheline to produce giesseckite pseudomorphs, thus increasing  $H_2O$  and decreasing  $Na_2O$  in the affected rocks.

#### (6d) Effects of Recrystallisation Around the Igdlarfigssalik Centre

It has been seen in Chapter 3 that marked textural and mineralogical changes occur in the South Qóroq Centre rocks in a wide zone around the later Igdlarfigssalik Centre. The effect is most pronounced in the area around Niaqornarssuk, where remobilisation has occurred in certain rocks. In most recrystallised samples there is no systematic change in major element content, although the iron oxidation ratio  $Fe^{3+}/(Fe^{3+} + Fe^{2+})$  is increased in some samples (SS4b) and reduced in others (SS5). Alkali metasomatism has not occurred and some samples even show a slightly reduced alkali content. However, all the samples show a marked depletion in residual trace elements.

Increased oxidation and high diffusion rates in recrystallised rocks are suggested by the fact that, in more extreme examples, ilmenite and magnetite occur as discrete phases instead of in the normal exsolution relationship. The pyroxene trends of such rocks suggest some form of constant  $f_{O_2}$  buffering, at least during part of their crystallisation. Fayalite is absent from the recrystallised zone, and the hydrous mafic mineral tends to be biotite rather than amphibole. Both features suggest that  $f_{O_2}$  had been raised above the FMQ buffer. (see Section 4d).

The increase in  $f_{O_2}$  caused more  $NaFe^{3+}$  to be taken into the pyroxenes, and in the SS4b sample investigated (58164) there is a corresponding decrease in Na/K in the alkali feldspars. The alkali feldspars themselves are very coarsely exsolved perthites, indicating a high degree of sub-solidus ordering. Emeleus and Smith (1959) have shown that this is favoured by a fairly high  $P_{H_2O}$  and slow cooling rates. Nepheline temperatures do not indicate any significant rise in temperature during recrystallisation, so it is suggested that the temperatures were sustained for a longer period in recrystallised rocks, enabling increased

feldspar ordering. This was probably aided by an increase in  $P_{H_2O}$  which probably also contributed to a general increase in  $f_{O_2}$ . Although no large systematic changes occurred in the major elements, it appears that residual elements were removed, possibly with the aid of volatile solutions.

APPENDICES

APPENDIX IELECTRON MICROPROBE ANALYSIS(techniques and analytical conditions)

The samples for analysis were prepared as polished thin sections, and whenever possible, samples and standards were carbon-coated simultaneously to ensure a uniform thickness of carbon. The samples were cleaned and recoated frequently since the coating deteriorates with time, particularly if the samples are not stored in a dessicator.

The instrument used in the University of Durham is a Cambridge Instrument Company "Geoscan", and the general techniques employed are those suggested by Sweatman and Long (1969). The standards used for the analyses in this thesis are listed in Table I.1, together with the analysing conditions. Most of the mineral groups were analysed with an accelerating voltage of 15KV, except for nephelines, which were analysed at 12KV in order to minimise volatilisation of alkali elements. A lower voltage was found to be unnecessary for the feldspars, since a defocussed beam was used in order to obtain bulk analyses of microperthitic intergrowths.

The "Geoscan" has two spectrometers and four pre-set spectrometer positions. In general, two elements were determined simultaneously with pre-set peaks and backgrounds for each element. However, in strongly zoned minerals such as the pyroxenes and amphiboles it is desirable to ensure that the four most variable elements (in this case Na, Ca, Fe and Mg) are analysed on exactly the same spot. Hence, four elements were determined simultaneously using the pre-set spectrometer positions for the four peaks (backgrounds were determined separately). For the remaining elements, a return to the same spot was facilitated by the use of sketches, and the recognition of burn marks on the carbon coating.

Since many analyses were usually being performed in the pair of slides loaded in the machine at any one time, analysis was usually performed in the following order:-

3 x 10 second counts on each standard

2 x 10 second counts on each of 9 unknowns

3 x 10 second counts on each standard

Backgrounds as appropriate (usually 4 x 10 seconds on standards)

Repeat for next 9 unknowns

Thus, for each run, nine unknowns were each counted for 20 seconds and each standard was counted for 60 seconds. The data was processed (taking into account drift and counter dead-time) using the computer program "SORT", provided by F.B. Frost. The uncorrected analyses were then corrected for mass-absorption, secondary fluorescence and atomic number effect (stopping power and electron back-scatter) using the program "ABFAN" (Boyd et al., 1969).

Although the smallest possible diameter for the electron beam is theoretically  $1\mu\text{m}$ , the excited area in the sample is somewhat greater than this. Other factors such as dirt in the electron-optical system also inhibit precise focussing of the beam, but in general the resolution is considered to be between 2 and  $5\mu\text{m}$ . Detection limits (calculated from the formula  $\frac{3}{m}\sqrt{\frac{R_b}{T_b}}$ , where  $m$  = mean peak counts/sec/%,  $R_b$  = mean background c.p.s.,  $T_b$  = counting time on background) for most elements are in the order of .01%, but some are slightly higher, the worst being Si at .04%. Overall accuracy, taking into account counting precision and uncertainties in the correction procedure, is in the order of  $\pm 2\%$  of the amount present for the major constituents. Elements present in quantities below about 3 - 5% and certain volatile elements, notably F, Cl and S have a somewhat lower accuracy.

Z	Element	Line	Analyzing Crystal	Counter	2θ (peak)	2θ (background)	Standard
9	F	K $\alpha_1$	K.A.P.	Flow	87°01'	+ 3°	CaF <sub>2</sub>
11	Na	"	"	"	53°14'	+ 1°30'	Jadeite (JD-1) *
12	Mg	"	"	"	43°42'	- 2°	Olivine (OL-GB)/MgO
13	Al	"	"	"	36°32'	+2° - 2°	Bytownite (M-11) * /Al <sub>2</sub> O <sub>3</sub>
14	Si	"	"	"	31°02'	-1° + 1°30'	Wollastonite (WO-2) *
16	S	"	Quartz	"	106°56'	+ 2°	Pyrite
17	Cl	"	"	"	89°58'	+ 2°	NaCl
19	K	"	"	"	67°58'	- 2°	Orthoclase (AF-15)
20	Ca	"	Quartz/LiF	"	60°18' / 113°02'	- 2°	Wollastonite (WO-2) *
22	Ti	"	LiF	"	86°05'	+ 2°	TiO <sub>2</sub>
24	Cr	"	"	Sealed	69°16'	+ 2°	Cr <sub>2</sub> O <sub>3</sub>
25	Mn	"	"	"	62°48'	+ 2°	Mn
26	Fe	"	"	Sealed/Flow +	57°20'	+ 2°	Fe
28	Ni	"	"	Sealed	48°34'	+ 2°	Ni
40	Zr	La <sub>1</sub>	Mica	"	35°15'	+ 2°	Zr
41	Nb	"	Quartz	Flow	117°44'	+ 2°	NaNbO <sub>3</sub>
56	Ba	"	"	"	48°59'	- 1°30'	BaSO <sub>4</sub>
58	Ce	"	"	"	44°58'	+ 2°	CeO <sub>2</sub>

Accelerating voltage 15KV/12KV - (see text). Specimen current .06 mA on copper Faraday cage.

+ Flow counter usually used to reduce count rate on Fe-metal standard to within the limits of dead-time corrections.

\* Standards analysed by Sweatman and Long (1969)

Names in brackets are University of Durham standard names.

TABLE I.1 Optimum analysing conditions and standards used for electron-microprobe analysis

APPENDIX IIX-RAY FLUORESCENCE - WHOLE ROCK ANALYSIS(IIa) Sample Preparation

Rock samples selected for analysis were split into fragments of less than 6 cm. in size using a Cutrock Engineering hydraulic splitter. Where possible up to 1 Kg. of coarse grained rock was used in order to gain a representative sample, but frequently the sample was smaller than the ideal. At this stage care was taken to exclude weathered edges, veins, inclusions, etc. and to remove all traces of paint and other superficial deposits. The fragments were then crushed to a coarse gravel using a Sturtevant 2" x 6" Roll Jaw Crusher, and  $\frac{1}{2}$ ,  $\frac{1}{4}$  or  $\frac{1}{8}$  fractions were taken to reduce the sample to a representative 100 - 200 gm. This fraction was then ground to a fine powder using a Tema Laboratory Disc Mill, model T-100 with a tungsten-carbide Widia grinding barrel.

Work by Fitton and Gill (1970) has shown that considerable atmospheric oxidation of ferrous iron occurs in hydrous igneous rocks during continued grinding in the disc mill. Thus a small sample of powder was withdrawn from the mill after 30 seconds for the determination of FeO by the method of Wilson (1955), and the remainder was ground for a further 3 - 4 minutes until the powder was sufficiently fine.

In the Durham University Geology Department, the X-Ray Fluorescence procedure is based on the use of rock-powder bricquettes, largely because of the great saving in preparation time compared to fusion techniques. The powders were pressed into bricquettes (with a few drops of Mowiol as a binding agent) using a hydraulic press operating at 5 - 6 tons/sq.in, (800 - 900 Kg/cm<sup>2</sup>).

The analyses were then carried out on a Philips PW1212 automatic spectrometer equipped with a vacuum path. Most of the routine running conditions used on this particular machine are given by Reeves (1971), but details relevant to the present work will be given in the following sections.

### (IIb) Major Element Analysis

The elements Si, Al, Fe (total), Mg, Ca, Na, K, Ti and P were determined using a Cr target and an evacuated X-Ray path. Mn was determined separately using a W target. In order to minimise systematic and random errors due to electronic instability etc. the method of "fixed counts" was used, together with a monitor for all the major elements and certain traces. In this method the time (T) taken to accumulate a pre-determined 'N' counts on a monitor for a particular element is automatically recorded. The next three samples are then counted over the same time interval (T) for the same element, and hence an allowance is made for irregularities in the count rate as detected by the monitor.

The standards used were of similar composition to the unknowns to minimise mass absorption differences and matrix effects, and were found to cover the range of most elements satisfactorily. Most of them were Gardar samples provided by Dr. B. G. J. Upton and the geochemical laboratory of Grønlands Geologiske Undersøgelse (G.G.U.), but international standards G-1, W-1, and S-1 were also used (Table II.1).

It is usual to correct the analytical data for mass absorption differences between standards and unknowns as described by Holland and Brindle (1966) and Reeves (1971). However, this procedure depends considerably upon a normalisation of the analysis to a total of 100% in order to produce realistic analyses, and hence is open to much criticism. The reasons for the dependency upon normalisation are not entirely understood, and it is found that for compositions of standards and unknowns which are very similar, there is considerable over-correction for certain elements, which is very noticeable in un-normalised analyses. Gill (1972), using the same set of standards as in the present work, has observed the same effect and gives a full critical evaluation of the correction procedure as applied to standards and unknowns of similar composition.

For syenites and nepheline syenites, the most realistic analyses are obtained by direct comparison of the unknown with the uncorrected standard calibration, except in the case of  $\text{SiO}_2$ , where an empirical correction is necessary if the total Fe (expressed as  $\text{Fe}_2\text{O}_3$ ) exceeds 11%. This correction is dependant entirely on the Fe content of the unknown, and full details of its derivation and application are given by Gill (op cit.). All analyses quoted in the present work are derived by this method.

The totals for those samples which have been analysed wet chemically for  $\text{FeO}$ ,  $\text{H}_2\text{O}$  and  $\text{CO}_2$ , although showing a greater variation than is normal for complete wet chemical analyses, are mostly within the range 98.0 to 100.5%, which is considered satisfactory for the present work (see histogram - Fig. II.1). Internal consistency, as with most X.R.F. analyses, is extremely good, which makes the method ideal for the present work, where many analyses are required to establish quite subtle variations in composition. Analyses which have been performed on different occasions are shown in Table II.2 as an indication of precision.

#### (II.c) Trace Element Analysis

The elements Ba, Nb, Zr, Y, Sr, Rb, Pb, Zn, Cu, Ni, La, Th, U and V were determined using a W target and an evacuated X-Ray path. For most of the samples the usual counting time was halved and the machine set to recycle twice. The data was then processed using the program "COMPARE" developed by Gill (1972) which enables random errors due to stray counts etc. to be detected. The main calculation was then performed by the program "TRATIO" (Gill, op cit.) using the count-rate function (peak intensity/background intensity - 1). This function enables scattered background radiation to be used as an internal standard to compensate for matrix and mass absorption effects. The programme enables corrections for blank/contamination and  $K_\beta$  interference (e.g. interference of  $\text{SrK}_\beta$  on  $\text{ZrK}_\alpha$ ) to be included. It also calculates the nominal detection limit

of each element from the formula  $3(\bar{B}^2)^{1/2}$ , where  $\bar{B}$  is the mean background-under-peak in counts averaged over all the determinations processed.

Certain elements need special procedures:-

(i) La values are calculated from the count rate function (peak - background) since this gives a more reliable standard calibration. It is also necessary to use a monitor for the count rate (see II.b).

(ii) Because of the serious interference of  $TiK_{\beta}$  upon  $VK_{\alpha}$  it is necessary to analyse Ti and V simultaneously during V determinations. A special procedure and computer program has been developed by J. G. Fitton for this purpose.

For most of the elements the standards used were synthetic, spiked glasses prepared by the Pilkington Research Laboratory (Lathom, England) for use in lunar investigations (Brown et al., 1970). These standards are in two sets in order to avoid interelement interferences as much as possible. International standards G-1, G-2, W-1, S-1, GSP-1, and AGV-1 were also run for most elements, and in certain cases they were used exclusively due either to interferences in the Pilkington standards (i.e. Pb and Th) or the element not being present (i.e. La). Certain heavy metals (i.e. Cu and Ni) gave count rates which seemed too high at low concentrations in the Pilkington standards. This was interpreted as due to lack of mass absorption and matrix effects for heavy metals in the synthetic glasses, compared with natural samples. Consequently, only the natural international standards were used for low concentrations of these elements.

As in the major elements, precision between runs is extremely good and therefore the results are internally consistent (Table II.3). To enable a better comparison to be made with analyses from other laboratories, the analysed values for the common international standards are tabulated in Table II.4 along with the accepted values.

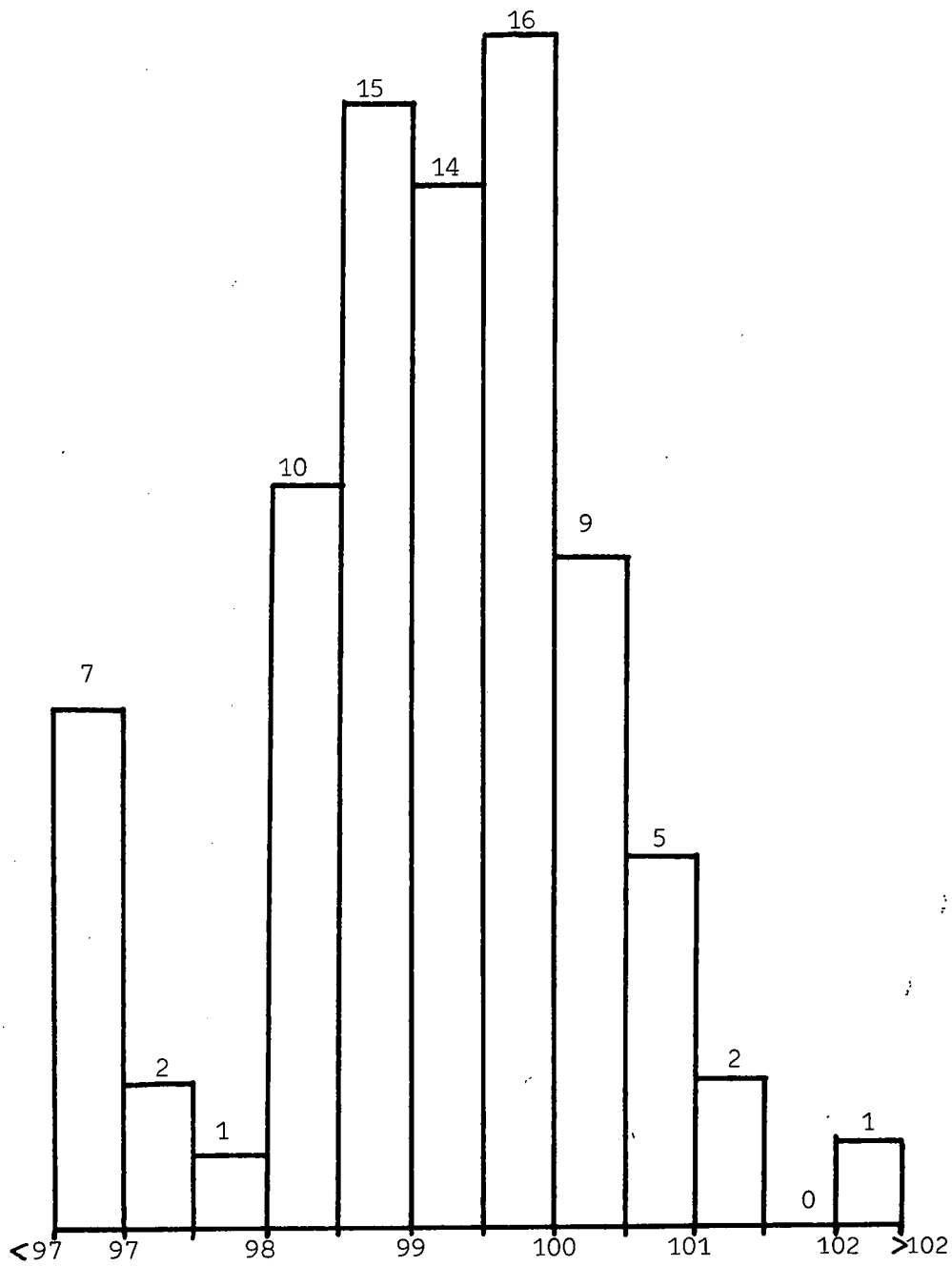


Fig. II.1

Histogram of totals for 82 South Qoroq Centre Analyses including FeO, H<sub>2</sub>O+ and CO<sub>2</sub>

Table II.1 Standards used for major element analyses of South Qôroq Centre rocks

Standard	Type	Locality	Analysis Published
27099	Nepheline syenite	Grønmedal-Íka	Watt (1966, p.48)
27137	Nepheline syenite	Grønmedal-Íka	----- (-----, p.46)
27159	Nepheline syenite	Grønmedal-Íka	----- (-----, p.50)
27182	Mafic nepheline syenite	Grønmedal-Íka	----- (-----, p.48)
30681	Nepheline syenite	Hviddal, Tugtutôq	----- (-----, p.48)
30684	Syenogabbro	Hviddal, Tugtutôq	----- (-----, p.62)
40452	Gabbro	Giant dyke Tugtutôq	----- (-----, p.62)
40551	Gabbro	Krydssø syenogabbro, Tugtutôq	----- (-----, p.54)
50216	Quartz syenite	Assorutit intrusion, Tugtutôq	----- (-----, p.38)
50262	Quartz syenite	Ring-dyke, Tugtutôq	----- (-----, p.38)
50345	Microsyenite	Unit 1, Tugtutôq	----- (-----, p.38)
48004	Naujaite	Ilímaussaq	Ferguson (1964, p.56)
G-1	Granite	U.S.G.S.	Fleischer (1969)
W-1	Dolerite	U.S.G.S.	
S-1	Syenite	C.A.A.S.	Sine et al. (1969)

Sp. No. 58281

Syenite SI4 - Igdlerfigssalik Centre

	<u>Feb/March, 1970</u>				<u>March 1971</u>	
SiO <sub>2</sub>	59.47	58.91	59.05	58.60	58.81	59.18
TiO <sub>2</sub>	0.47	0.47	0.47	0.47	0.45	0.45
Al <sub>2</sub> O <sub>3</sub>	19.40	19.23	19.46	19.15	19.42	19.32
Fe <sub>2</sub> O <sub>3</sub> (T)	5.64	5.62	5.61	5.60	5.56	5.56
MnO	0.17	0.16	0.16	0.17	0.17	0.16
MgO	0.33	0.31	0.30	0.31	0.22	0.23
CuO	1.66	1.63	1.63	1.64	1.64	1.67
Na <sub>2</sub> O	6.54	7.19	7.18	7.25	5.87	7.28
K <sub>2</sub> O	5.80	5.76	5.80	5.81	5.73	5.73
P <sub>2</sub> O <sub>5</sub>	0.11	0.10	0.11	0.11	0.12	0.13
TOTAL	99.60	99.40	99.78	99.11	97.99	99.71

Table II.2

Repeat analyses of Sp. No. 58281 from two separate X.R.F. runs, giving an indication of the precision of the method. For most elements precision is high, but Na<sub>2</sub>O is prone to occasional low values and MgO shows a marked difference between the two runs.

## INTERNATIONAL STANDARD G-1 (ppm)

Ba	-	-		-	-	-	-
Nb	20	21		20	21	20	-
Zr	186	186		197	198	195	-
Y	13	10		11	12	10	-
SR	264	260		238	237	238	-
Rb	233	231		233	233	235	-
Pb	34	32		35	30	-	-
Zn <sup>1</sup>	63	60		71	71	73	-
Cu	29	24		21	21	22	21
Ni	11	10		10	-	-	-
La	82	84		83	84	81	84
Th	53	62		64	70	-	-
U	6	4		3	4	-	-
V	18	-		-	-	-	-

Table II.3 Repeat trace element analyses of international standard G-1 by X.R.F. Vertical lines separate values obtained in different runs with a different standard calibration curve.

	(ppm)					
	<u>G-1</u>	<u>G-2</u>	<u>W-1</u>	<u>S-1</u>	<u>GSP-1</u>	<u>AGV-1</u>
Ba	- 1200	- 1950	- 180	- 282	1254 1360	- 1410
Nb	20 20	13 16	10 10	- 75	22 28	15 22
Zr	192 210	356 316	95 100	- 3030	644 544	270 227
Y	11 13	13 12	21 25	- 441	41 37	19 25
Sr	247 250	562 463	184 180	- 286	271 247	765 657
Rb	233 220	199 -	22 22	- -	250 -	80 -
Pb	33 49	46 29	26 8	276 495	67 52	47 35
Zn	72 45	96 75	96 82	246 219	111 143	91 112
Cu	23 13	12 11	116 110	24 25	32 35	60 64
Ni	9 1	10 6	76 78	35 43	14 11	22 18
La	81 97	77 82	10 10	114 180	111 173	32 33
Th	62 52	25 25	2 4	1100* 1100	110 110	7 7
U	4 4	3 <2	0 <2	2698* 2700	0 <2	6 <2
V	18 10	33 37	246 240	73 89	45 52	100 121

Table II.4 Averages of X.R.F. determinations for trace elements in International standards, compared with quoted values. Top line - X.R.F. average. Bottom line - quoted average (less optical spectrometry results) - Flanagan (1969), Fleischer (1969), Sine et al. (1969)

\* Close comparison due to S-1 being the only available standard with high concentrations in the calibration.

## APPENDIX III

ELECTRON-MICROPROBE MINERAL ANALYSESTable III.1

The South Qôroq Centre mineral analyses arranged in the order of mineral groups as found in Chapter 4, i.e. pyroxene, amphibole, olivine, magnetite, ilmenite, nepheline, feldspar. Within each mineral group the analyses are arranged in the order:- SS2, SS3, SS4a, SS4b, SS5, pegmatites, microsyenite sheet, essexite. The digits following each specimen number refer to the index number of a particular grain or group of grains in the section, and where photographs of analysed grains occur, these numbers are referred to in the caption. Analysed points are also marked 'x' on some photographs.

Recalculations of complete analyses to an appropriate number of oxygens to make up the unit cell are given, together with end-member compositions. Details of end-member calculations and estimates of  $Fe_2O_3/FeO$  ratio (where appropriate) are given in the relevant sections of Chapter 4.

The sample numbers used for each rock unit are as follows:-

SS2 - 58231	SS5 - 46243
127021	46244
127075	58230
	recrystallised SS5 - 58154
SS3 - 46269	
58229	peg. vein in SS2 - 127071
58236	" patch in SS3 - 59663
127015	
127038	Microsyenite sheet - 127027
SS4a - 58150	Essexite - 58150
58228	
SS4b - 58221	Magnetite veins
59676	cutting Jhb. Gr. - 127001
127025	127003
Mafic band	
in SS4b - 59672	
Recrystallised	
SS4b - 58164	

- \* 59676 has several mineralogical similarities to SS4a and may be associated with this syenite.

SOUTH QOROO CENTRE PYROXENE ANALYSES

	1	2	3	4	5	6	7	8	9	10
	58231.1	58231.1	58231.1	58231.1	58231.2	58231.2	58231.2	58231.2	58231.2	127021.1
OXIDE WEIGHT PERCENTAGE										
SI02	51.83	52.67	52.88	52.45	51.81	52.96	52.40	53.70	53.45	50.98
AL2O3	0.83	0.87	0.74	0.81	0.76	0.81	1.04	1.44	1.68	0.77
TI02	0.30	0.30	0.41	0.28	0.28	0.35	0.45	0.45	0.49	0.39
FE2O3	14.04	13.30	15.07	14.79	13.19	11.54	2.86	2.11	2.24	13.24
FE0	11.71	12.68	10.64	10.32	12.36	14.25	16.53	14.43	14.28	9.59
MGO	1.48	1.30	1.84	2.15	1.40	1.32	5.20	7.16	6.76	3.85
CAO	13.96	14.23	14.02	13.34	13.90	15.91	21.16	21.33	21.47	13.32
NA2O	5.45	5.16	5.85	5.74	5.12	4.48	1.11	0.82	0.87	5.14
MNO	1.04	1.10	1.15	1.19	1.13	1.03	0.96	0.93	0.84	0.97
TOTAL	100.64	101.60	102.60	101.06	99.95	102.65	101.71	102.37	102.08	98.25

ATOMIC PROPORTIONS ON THE BASIS OF 6 OXYGENS

SI	2.012	2.024	2.008	2.015	2.024	2.023	2.006	2.011	2.007	2.003
AL	0.038	0.039	0.033	0.037	0.035	0.036	0.047	0.064	0.074	0.036
TI	0.009	0.009	0.012	0.008	0.008	0.010	0.013	0.013	0.014	0.012
FE3	0.410	0.385	0.431	0.428	0.388	0.332	0.082	0.060	0.063	0.392
FE2	0.380	0.408	0.338	0.331	0.404	0.455	0.529	0.452	0.449	0.315
MG	0.086	0.074	0.104	0.123	0.082	0.075	0.297	0.400	0.378	0.225
CA	0.581	0.586	0.570	0.549	0.582	0.651	0.868	0.856	0.864	0.561
NA	0.410	0.385	0.431	0.428	0.388	0.332	0.082	0.060	0.063	0.392
MN	0.034	0.036	0.037	0.039	0.037	0.033	0.031	0.030	0.027	0.032

END MEMBER COMPOSITIONS

AC	45.08	42.62	47.35	46.44	42.60	37.07	8.77	6.33	6.91	40.62
DI	9.41	8.25	11.44	13.37	8.95	8.39	31.58	42.48	41.25	23.37
HD	45.51	49.13	41.20	40.19	48.45	54.54	59.65	51.19	51.83	36.01

SOUTH QORQQ CENTRE PYROXENE ANALYSES

	11	12	13	14	15	16	17	18	19	20
	127021.1	127021.1	127021.1	127021.5	127021.5	127021.5	127021.5	127075.0	127075.0	127075.0
OXIDE WEIGHT PERCENTAGE										
SI02	49.66	50.05	49.40	50.42	50.28	50.62	49.67	49.63	49.53	49.83
AL2O3	1.55	1.33	1.48	0.75	0.53	0.75	0.72	0.68	0.87	0.81
TiO2	0.49	0.41	0.45	0.35	0.30	0.21	0.37	0.80	0.46	0.32
FE2O3	2.91	3.17	3.14	11.49	9.20	14.35	4.15	9.77	5.10	7.73
FeO	14.49	14.86	14.54	11.97	14.28	11.66	17.69	13.70	18.15	14.87
MgO	8.32	7.55	8.63	3.93	3.86	1.59	4.93	3.29	4.15	4.44
CaO	21.67	21.22	21.34	15.51	16.60	12.89	20.45	16.87	19.93	18.17
Na2O	1.13	1.23	1.22	4.46	3.57	5.57	1.61	3.79	1.98	3.00
MnO	0.91	0.87	0.81	0.83	0.97	1.03	0.88	1.26	0.95	1.03
TOTAL	101.13	100.69	101.02	99.71	99.59	98.67	100.47	99.79	101.12	100.20

ATOMIC PROPORTIONS ON THE BASIS OF 6 OXYGENS

SI	1.913	1.937	1.907	1.974	1.983	2.007	1.957	1.960	1.948	1.959
AL	0.070	0.061	0.067	0.035	0.025	0.035	0.033	0.032	0.040	0.038
TI	0.014	0.012	0.013	0.010	0.009	0.006	0.011	0.024	0.014	0.009
FE3	0.084	0.092	0.091	0.339	0.273	0.428	0.123	0.290	0.151	0.229
FE2	0.467	0.481	0.470	0.392	0.471	0.387	0.583	0.453	0.597	0.489
Mg	0.478	0.435	0.496	0.229	0.227	0.094	0.290	0.194	0.243	0.260
CA	0.895	0.880	0.883	0.651	0.702	0.548	0.864	0.714	0.840	0.765
NA	0.084	0.092	0.091	0.339	0.273	0.428	0.123	0.290	0.151	0.229
MN	0.030	0.029	0.026	0.028	0.032	0.035	0.029	0.042	0.032	0.034

END MEMBER COMPOSITIONS

AC	7.98	8.90	8.43	34.30	27.21	45.40	12.01	29.66	14.77	22.61
DI	45.12	41.98	45.81	23.22	22.61	9.96	28.25	19.78	23.78	25.70
HD	46.91	49.12	45.76	42.48	50.18	44.64	59.75	50.56	61.46	51.69

SOUTH QOROO CENTRE PYROXENE ANALYSES

	21	22	23	24	25	26	27	28	29	30
	127075.0	127075.1	127075.1	127075.2	46269.2	46269.2	46269.2	46269.2	46269.2	46269.3
OXIDE WEIGHT PERCENTAGE										
SI02	50.07	50.07	49.40	50.67	50.79	50.36	50.33	50.48	50.39	50.95
AL2O3	0.75	0.81	0.90	0.87	0.96	0.94	1.05	0.97	0.88	0.99
TI02	0.25	0.26	0.23	0.37	0.51	0.49	0.56	0.46	0.48	0.34
FE2O3	10.87	15.92	16.00	9.92	12.26	12.60	13.53	13.60	13.55	11.41
FEO	13.66	10.96	10.04	13.21	12.85	12.97	12.06	11.97	11.74	13.21
MGO	2.93	0.66	0.99	3.85	2.20	2.05	2.14	2.26	2.53	3.04
CAD	15.36	11.53	11.43	16.00	15.23	14.66	14.86	14.45	14.57	15.45
NA2O	4.22	6.18	6.21	3.85	4.76	4.89	5.25	5.28	5.26	4.43
MND	1.40	1.25	1.15	0.98	1.09	1.00	1.15	1.13	0.92	1.04
TOTAL	99.51	97.64	96.35	99.72	100.65	99.95	100.93	100.61	100.32	100.87

ATOMIC PROPORTIONS ON THE BASIS OF 6 OXYGENS

SI	1.981	2.009	2.003	1.985	1.981	1.980	1.962	1.971	1.970	1.980
AL	0.035	0.038	0.043	0.040	0.044	0.044	0.048	0.045	0.041	0.045
TI	0.007	0.008	0.007	0.011	0.015	0.014	0.016	0.014	0.014	0.010
FE3	0.324	0.481	0.488	0.292	0.360	0.373	0.397	0.400	0.399	0.334
FE2	0.452	0.368	0.340	0.433	0.419	0.426	0.393	0.391	0.384	0.429
MG	0.173	0.039	0.060	0.225	0.128	0.120	0.124	0.131	0.147	0.176
CA	0.651	0.496	0.497	0.672	0.637	0.618	0.621	0.605	0.610	0.643
NA	0.324	0.481	0.489	0.293	0.360	0.373	0.397	0.400	0.399	0.334
MN	0.047	0.042	0.040	0.033	0.036	0.033	0.038	0.037	0.030	0.034

END MEMBER COMPOSITIONS

AC	32.53	51.69	52.63	29.78	38.19	39.14	41.68	41.67	41.53	34.30
DI	17.35	4.24	6.45	22.88	13.56	12.61	13.05	13.70	15.35	18.08
HD	50.11	44.07	40.93	47.35	48.26	48.25	45.27	44.63	43.13	47.62

SOUTH QOROQ CENTRE PYROXENE ANALYSES

31 32 33 34 35 36 37 38 39 40  
 46269.3 46269.3 46269.3 127038.0 127038.0 127038.0 127038.0 127038.1 127038.1 127038.1

OXIDE WEIGHT PERCENTAGE

SiO2	49.63	50.87	49.94	51.38	51.68	51.34	50.09	52.25	52.32	51.78
Al2O3	0.94	0.85	1.03	0.86	0.62	0.75	1.30	1.32	0.85	1.11
TiO2	0.30	0.32	0.41	0.30	0.37	0.37	0.33	0.22	0.26	0.24
Fe2O3	10.80	9.51	13.97	20.05	19.17	18.29	21.10	32.54	32.65	24.09
FeO	13.68	12.35	10.95	6.86	7.94	8.96	5.80	-	-	6.24
MgO	2.83	5.07	2.17	2.04	2.01	1.83	1.45	0.09	0.02	0.32
CaO	15.62	17.49	13.57	8.35	10.09	9.93	8.71	0.29	0.39	7.98
Na2O	4.19	3.69	5.42	7.78	7.44	7.10	8.19	12.63	12.67	9.35
MnO	1.12	0.91	1.36	0.81	0.66	0.92	0.92	0.15	0.12	0.24
TOTAL	99.10	101.05	98.81	98.42	99.98	99.50	97.89	99.49	99.28	101.35

ATOMIC PROPORTIONS ON THE BASIS OF 6 OXYGENS

Si	1.972	1.963	1.978	2.010	2.002	2.003	1.979	2.000	2.009	1.984
Al	0.044	0.039	0.048	0.040	0.028	0.035	0.061	0.060	0.038	0.050
Ti	0.009	0.009	0.012	0.009	0.011	0.011	0.010	0.006	0.008	0.007
Fe3	0.323	0.276	0.416	0.590	0.559	0.537	0.627	0.937	0.943	0.695
Fe2	0.455	0.399	0.363	0.224	0.257	0.293	0.192	0.000	0.000	0.200
Mg	0.168	0.292	0.128	0.119	0.116	0.106	0.085	0.005	0.001	0.018
Ca	0.665	0.723	0.576	0.350	0.419	0.415	0.369	0.012	0.016	0.328
Na	0.323	0.276	0.417	0.591	0.559	0.537	0.628	0.938	0.944	0.695
Mn	0.038	0.030	0.046	0.027	0.022	0.030	0.031	0.005	0.004	0.008

END MEMBER COMPOSITIONS

AC	32.86	27.73	43.71	61.47	58.59	55.59	67.10	98.95	99.47	75.46
DI	17.05	29.27	13.44	12.38	12.16	11.01	9.13	0.54	0.12	1.98
HD	50.09	43.00	42.85	26.15	29.25	33.40	23.77	0.51	0.41	22.55

SOUTH QOROO CENTRE PYROXENE ANALYSES

	41	42	43	44	45	46	47	48	49	50
	127038.1	127038.1	58228.3	58228.3	58228.3	58228.4	58228.4	58228.4	58228.4	58228.4
OXIDE WEIGHT PERCENTAGE										
SiO2	52.30	51.95	49.33	50.82	50.65	50.46	50.88	52.20	52.24	53.58
Al2O3	0.92	1.32	0.94	1.67	1.06	1.00	0.85	1.21	0.81	1.27
TiO2	0.28	0.22	0.46	0.74	0.63	0.57	0.50	0.66	0.28	0.59
Fe2O3	30.95	28.88	4.23	4.30	3.99	4.33	10.72	3.86	14.92	2.81
FeO	-	1.76	17.14	13.66	14.39	15.17	12.54	15.08	9.71	14.29
MgO	0.68	0.25	4.83	7.32	6.32	5.96	3.52	6.14	3.00	6.57
CaO	1.13	2.26	19.90	21.61	20.85	21.00	16.77	21.17	14.68	21.60
Na2O	12.01	11.21	1.64	1.67	1.55	1.68	4.16	1.50	5.79	1.09
MnO	0.30	0.35	0.97	0.72	0.91	0.84	1.20	0.85	1.30	0.84
TOTAL	98.57	98.20	99.43	102.51	100.35	101.00	101.14	102.68	102.73	102.64

ATOMIC PROPORTIONS ON THE BASIS OF 6 OXYGENS

Si	2.015	2.016	1.959	1.926	1.964	1.955	1.971	1.975	1.981	2.007
Al	0.042	0.060	0.044	0.075	0.048	0.046	0.039	0.054	0.036	0.056
Ti	0.008	0.006	0.014	0.021	0.018	0.017	0.015	0.019	0.008	0.017
Fe3	0.897	0.843	0.126	0.123	0.117	0.126	0.312	0.110	0.426	0.079
Fe2	0.000	0.057	0.569	0.433	0.467	0.491	0.406	0.477	0.308	0.448
Mg	0.039	0.014	0.286	0.413	0.365	0.344	0.203	0.346	0.170	0.367
Ca	0.047	0.094	0.847	0.878	0.866	0.872	0.696	0.858	0.596	0.867
Na	0.898	0.844	0.126	0.123	0.117	0.126	0.313	0.110	0.426	0.079
Mn	0.010	0.012	0.033	0.023	0.030	0.028	0.039	0.027	0.042	0.027

END MEMBER COMPOSITIONS

AC	94.84	91.05	12.46	12.37	11.92	12.76	32.51	11.46	45.06	8.60
DI	4.13	1.56	28.19	41.66	37.33	34.78	21.14	36.03	17.94	39.85
HD	1.03	7.39	59.35	45.96	50.75	52.46	46.35	52.51	37.00	51.55

## SOUTH QORQQ CENTRE PYROXENE ANALYSES

	51	52	53	54	55	56	57	58	59	60
	58228.4	59676.1	59676.1	59676.1	59676.1	59676.2	59676.2	59676.2	59676.2	59676.2
OXIDE WEIGHT PERCENTAGE										
SiO2	52.91	50.40	49.99	50.53	50.88	49.76	50.85	50.39	51.43	49.98
Al2O3	1.23	2.04	2.35	2.52	2.39	1.96	2.45	2.54	2.24	2.02
TiO2	0.65	0.85	0.96	1.16	1.06	0.65	0.96	0.93	1.07	0.69
Fe2O3	3.86	2.53	2.55	2.09	2.65	3.35	2.83	2.76	2.19	2.63
FeO	13.54	13.21	12.75	10.55	9.27	13.09	11.74	10.50	9.40	13.93
MgO	6.36	8.16	8.45	10.71	11.51	7.97	9.47	10.04	11.38	7.85
CaO	21.37	21.94	22.11	22.20	21.89	21.60	22.16	21.65	21.77	21.62
Na2O	1.50	0.98	0.99	0.81	1.03	1.30	1.10	1.07	0.85	1.02
MnO	0.81	0.66	0.63	0.58	0.58	0.72	0.64	0.67	0.58	0.75
TOTAL	102.24	100.76	100.78	101.15	101.27	100.40	102.20	100.55	100.91	100.48

## ATOMIC PROPORTIONS ON THE BASIS OF 6 OXYGENS

Si	1.994	1.929	1.911	1.901	1.902	1.918	1.907	1.909	1.924	1.926
Al	0.055	0.092	0.106	0.112	0.105	0.089	0.108	0.113	0.099	0.092
Ti	0.018	0.024	0.028	0.033	0.030	0.019	0.027	0.027	0.030	0.020
Fe3	0.110	0.073	0.073	0.059	0.075	0.097	0.080	0.079	0.062	0.076
Fe2	0.427	0.423	0.408	0.332	0.290	0.422	0.368	0.333	0.294	0.449
Mg	0.357	0.465	0.481	0.600	0.641	0.458	0.529	0.567	0.634	0.451
Ca	0.863	0.900	0.906	0.895	0.877	0.892	0.891	0.879	0.873	0.893
Na	0.110	0.073	0.073	0.059	0.075	0.097	0.080	0.079	0.062	0.076
Mn	0.026	0.021	0.020	0.018	0.018	0.024	0.020	0.022	0.018	0.024

## END MEMBER COMPOSITIONS

AC	11.92	7.41	7.47	5.85	7.29	9.72	8.02	7.87	6.12	7.62
DI	38.84	47.38	48.99	59.45	62.61	45.76	53.04	56.70	62.90	45.06
HD	49.23	45.22	43.54	34.70	30.10	44.52	38.94	35.43	30.98	47.31

SOUTH QORQQ CENTRE PYROXENE ANALYSES

	61	62	63	64	65	66	67	68	69	70
	58164.1	58164.1	58164.1	58164.2	58164.2	58164.2	58164.3	58164.3	58164.3	58221.1
OXIDE WEIGHT PERCENTAGE										
SiO2	51.26	52.41	52.06	52.51	52.74	52.62	52.37	51.41	51.95	52.59
Al2O3	0.92	1.76	1.07	1.18	1.83	1.83	0.77	0.90	0.96	1.98
TiO2	0.37	0.65	0.55	0.52	0.76	0.78	0.34	0.39	0.34	1.11
Fe2O3	14.25	2.76	15.49	10.59	5.57	2.73	14.74	13.42	13.22	2.22
FeO	8.61	10.36	7.46	9.06	8.21	10.42	8.61	8.11	9.20	9.79
MGD	3.84	11.30	2.98	6.42	11.27	11.45	3.62	4.66	3.98	12.56
CAO	13.40	22.07	11.76	15.98	19.90	21.46	13.42	14.54	14.25	22.73
NA2O	5.53	1.07	6.01	4.11	2.16	1.06	5.72	5.21	5.13	0.86
MNO	1.62	0.74	1.48	1.35	0.67	0.77	1.69	1.74	1.62	0.49
TOTAL	99.80	103.12	98.85	101.72	103.11	103.12	101.28	100.39	100.65	104.32

ATOMIC PROPORTIONS ON THE BASIS OF 6 OXYGENS

SI	1.986	1.931	2.019	1.978	1.931	1.934	1.998	1.977	1.994	1.908
AL	0.042	0.076	0.049	0.052	0.079	0.079	0.035	0.041	0.043	0.085
TI	0.011	0.018	0.016	0.015	0.021	0.022	0.010	0.011	0.010	0.030
FE3	0.416	0.076	0.452	0.300	0.153	0.076	0.423	0.389	0.382	0.060
FE2	0.279	0.319	0.242	0.286	0.252	0.320	0.275	0.261	0.295	0.297
MG	0.222	0.620	0.172	0.360	0.615	0.627	0.206	0.267	0.228	0.679
CA	0.556	0.871	0.489	0.645	0.781	0.845	0.549	0.599	0.586	0.884
NA	0.416	0.076	0.452	0.300	0.153	0.076	0.423	0.389	0.382	0.061
MN	0.053	0.023	0.049	0.043	0.021	0.024	0.055	0.057	0.053	0.015

END MEMBER COMPOSITIONS

AC	42.86	7.36	49.42	30.35	14.74	7.22	44.16	39.93	39.89	5.76
DI	22.87	59.70	18.82	36.43	59.09	59.89	21.47	27.44	23.77	64.57
HD	34.27	32.94	31.76	33.22	26.17	32.89	34.37	32.63	36.34	29.67

SOUTH QOROO CENTRE PYROXENE ANALYSES

	71	72	73	74	75	76	77	78	79	80
58221.1	58221.1	58221.1	58221.1	58221.1	58221.3	58221.3	58221.3	58221.3	58221.3	59672.2
OXIDE WEIGHT PERCENTAGE										
SiO2	51.92	51.31	50.84	52.73	51.34	51.38	50.85	49.62	52.71	51.94
Al2O3	1.95	1.93	1.82	1.98	1.41	1.83	1.67	1.89	2.10	1.95
TiO2	0.69	0.85	0.74	1.08	0.76	0.79	0.65	0.50	1.19	1.13
Fe2O3	3.04	1.86	2.47	2.50	3.12	2.58	2.89	2.68	2.06	1.57
FED	12.83	13.62	12.87	8.94	14.27	13.47	14.72	14.85	8.90	9.41
MgO	9.32	9.85	8.48	13.03	8.35	9.69	8.21	7.71	11.47	11.62
CaO	22.02	22.02	21.58	22.04	21.73	21.52	21.20	21.14	21.91	21.75
Na2O	1.18	0.72	0.96	0.97	1.21	1.00	1.12	1.04	0.80	0.61
MnO	0.72	0.63	0.69	0.49	0.85	0.64	0.69	0.82	0.54	0.54
TOTAL	103.68	102.79	100.46	103.76	103.03	102.90	102.00	100.25	101.68	100.52

ATOMIC PROPORTIONS ON THE BASIS OF 6 OXYGENS

Si	1.926	1.920	1.944	1.914	1.932	1.922	1.933	1.925	1.946	1.943
Al	0.085	0.085	0.082	0.085	0.063	0.081	0.075	0.086	0.091	0.086
Ti	0.019	0.024	0.021	0.029	0.022	0.022	0.019	0.015	0.033	0.032
Fe3	0.085	0.052	0.071	0.068	0.088	0.073	0.083	0.078	0.057	0.044
Fe2	0.398	0.426	0.412	0.271	0.449	0.421	0.468	0.482	0.275	0.294
Mg	0.515	0.549	0.483	0.705	0.468	0.540	0.465	0.446	0.631	0.648
Ca	0.875	0.883	0.884	0.857	0.876	0.863	0.863	0.879	0.867	0.872
Na	0.085	0.052	0.071	0.068	0.088	0.073	0.083	0.078	0.057	0.044
Mn	0.023	0.020	0.022	0.015	0.027	0.020	0.022	0.027	0.017	0.017

END MEMBER COMPOSITIONS

AC	8.32	4.99	7.20	6.45	8.55	6.88	7.96	7.58	5.85	4.41
DI	50.46	52.42	48.88	66.52	45.35	51.23	44.81	43.16	64.40	64.56
HD	41.22	42.59	43.91	27.04	46.10	41.89	47.24	49.26	29.75	31.03

SOUTH QOROO CENTRE PYROXENE ANALYSES

81 82 83 84 85 86 87 88 89 90

59672.2 59672.2 59672.2 59672.2 59672.3 59672.3 59672.3 59672.4 59672.4 59672.4

OXIDE WEIGHT PERCENTAGE

SiO2	51.12	50.73	51.83	51.39	52.22	52.56	52.27	52.55	53.20	52.50
Al2O3	2.68	2.38	2.49	2.31	2.07	2.14	2.14	2.44	2.16	2.08
TiO2	1.26	1.22	1.51	1.28	0.95	1.11	1.46	1.08	1.15	1.19
Fe2O3	1.78	1.91	2.78	2.73	2.19	2.55	1.44	2.83	2.96	2.37
FeO	9.34	10.14	8.02	8.45	9.47	8.86	9.41	8.79	8.76	8.66
MgO	11.45	10.31	11.31	10.96	10.66	11.55	11.32	10.43	10.67	11.38
CaO	21.95	21.52	21.82	21.46	21.74	21.96	21.55	22.30	22.23	21.75
Na2O	0.69	0.74	1.08	1.06	0.85	0.99	0.56	1.10	1.15	0.92
MnO	0.51	0.48	0.55	0.52	0.43	0.57	0.61	0.49	0.55	0.61
TOTAL	100.78	99.43	101.39	100.16	100.58	102.29	100.76	102.01	102.84	101.46

ATOMIC PROPORTIONS ON THE BASIS OF 6 OXYGENS

Si	1.912	1.930	1.920	1.930	1.954	1.934	1.947	1.940	1.947	1.943
Al	0.118	0.107	0.109	0.102	0.091	0.093	0.094	0.106	0.093	0.091
Ti	0.035	0.035	0.042	0.036	0.027	0.031	0.041	0.030	0.032	0.033
Fe3	0.050	0.055	0.078	0.077	0.062	0.071	0.040	0.079	0.082	0.066
Fe2	0.292	0.323	0.248	0.265	0.296	0.272	0.293	0.271	0.268	0.268
Mg	0.638	0.584	0.624	0.613	0.595	0.633	0.628	0.574	0.582	0.628
Ca	0.880	0.877	0.866	0.864	0.872	0.866	0.860	0.882	0.872	0.863
Na	0.050	0.055	0.078	0.077	0.062	0.071	0.040	0.079	0.082	0.066
Mn	0.016	0.015	0.017	0.017	0.014	0.018	0.019	0.015	0.017	0.019

END MEMBER COMPOSITIONS

AC	5.02	5.59	8.02	7.94	6.39	7.11	4.12	8.39	8.60	6.73
DI	64.04	59.80	64.53	63.06	61.53	63.70	64.03	61.09	61.33	63.99
HD	30.94	34.61	27.45	29.00	32.09	29.20	31.84	30.53	30.07	29.27

SOUTH QOROQ CENTRE PYROXENE ANALYSES

	91	92	93	94	95	96	97	98	99	100
	59672.4	59672.4	46243.1	46243.1	46243.1	46243.1	46243.2	46243.2	46243.2	46243.2
OXIDE WEIGHT PERCENTAGE										
SI02	50.79	53.19	50.42	50.05	49.85	49.46	50.77	51.42	51.37	51.17
AL2O3	2.17	2.22	1.07	0.81	0.92	0.94	0.89	0.82	1.11	0.91
TIO2	1.33	1.20	0.27	0.39	0.30	0.28	0.32	0.34	0.43	0.36
FE2O3	3.07	2.76	9.48	7.11	11.75	6.96	7.11	6.18	4.59	4.95
FE0	8.34	9.11	14.00	16.35	11.94	15.75	15.51	15.69	15.93	15.95
MGO	11.31	10.10	3.05	2.85	2.81	3.37	3.29	3.76	4.66	4.37
CAO	21.68	22.17	17.99	19.37	19.15	19.46	19.16	19.55	20.18	20.11
NA2O	1.19	1.07	3.68	2.76	4.56	2.70	2.76	2.40	1.78	1.92
MNO	0.55	0.55	1.36	1.38	1.42	1.47	1.38	1.33	1.11	1.08
TOTAL	100.43	102.37	101.32	101.07	102.70	100.39	101.19	101.49	101.16	100.82

ATOMIC PROPORTIONS ON THE BASIS OF 6 OXYGENS

SI	1.909	1.956	1.963	1.966	1.925	1.955	1.979	1.991	1.987	1.990
AL	0.096	0.096	0.049	0.038	0.042	0.044	0.041	0.037	0.051	0.042
TI	0.038	0.033	0.008	0.012	0.009	0.008	0.009	0.010	0.013	0.011
FE3	0.087	0.076	0.278	0.210	0.341	0.207	0.209	0.180	0.134	0.145
FE2	0.262	0.280	0.456	0.537	0.386	0.521	0.506	0.508	0.515	0.519
MG	0.634	0.553	0.177	0.167	0.162	0.199	0.191	0.217	0.269	0.253
CA	0.873	0.874	0.751	0.816	0.792	0.824	0.800	0.811	0.836	0.838
NA	0.087	0.076	0.278	0.210	0.342	0.207	0.209	0.180	0.134	0.145
MN	0.018	0.017	0.045	0.046	0.046	0.049	0.046	0.044	0.036	0.036

END MEMBER COMPOSITIONS

AC	8.68	8.23	29.08	21.90	36.52	21.22	21.94	19.00	14.00	15.21
DI	63.35	59.70	18.52	17.37	17.29	20.35	20.09	22.87	28.16	26.59
HD	27.97	32.07	52.40	60.73	46.19	58.43	57.96	58.14	57.85	58.20

SOUTH QOROQ CENTRE PYROXENE ANALYSES

	101	102	103	104	105	106	107	108	109	110
	46243.2	46243.2	46243.3	46243.3	46243.3	46244.1	46244.1	46244.1	46244.1	46244.2
OXIDE WEIGHT PERCENTAGE										
SiO2	51.41	51.94	51.48	51.70	51.83	48.51	48.10	47.97	47.89	48.82
Al2O3	1.04	0.95	0.85	0.72	0.82	0.90	0.85	0.85	0.79	0.90
TiO2	0.48	0.41	0.27	0.34	0.25	0.32	0.37	0.30	0.41	0.35
Fe2O3	4.46	4.38	5.95	7.34	6.78	9.69	8.14	7.06	7.50	7.45
FeO	15.76	16.10	16.72	16.07	16.44	15.18	15.78	16.35	15.94	15.90
MgO	4.87	4.61	3.10	2.74	2.66	3.34	3.78	4.16	3.73	4.51
CaO	20.63	20.21	19.37	18.68	18.85	17.46	17.40	18.38	18.02	17.29
Na2O	1.73	1.70	2.31	2.85	2.63	3.76	3.16	2.74	2.91	2.89
MnO	0.90	1.09	1.50	1.39	1.35	0.92	1.04	1.15	1.03	0.89
TOTAL	101.28	101.39	101.55	101.84	101.61	100.08	98.62	98.96	98.22	99.00

ATOMIC PROPORTIONS ON THE BASIS OF 6 OXYGENS

Si	1.984	2.001	1.999	2.001	2.009	1.929	1.938	1.930	1.939	1.949
Al	0.047	0.043	0.039	0.033	0.037	0.042	0.040	0.040	0.038	0.042
Ti	0.014	0.012	0.008	0.010	0.007	0.010	0.011	0.009	0.012	0.011
Fe3	0.129	0.127	0.174	0.214	0.198	0.290	0.247	0.214	0.228	0.224
Fe2	0.509	0.519	0.543	0.520	0.533	0.505	0.532	0.550	0.540	0.531
Mg	0.280	0.265	0.179	0.158	0.154	0.198	0.227	0.249	0.225	0.268
Ca	0.853	0.834	0.806	0.775	0.783	0.744	0.751	0.793	0.782	0.740
Na	0.130	0.127	0.174	0.214	0.198	0.290	0.247	0.214	0.229	0.224
Mn	0.029	0.036	0.049	0.046	0.044	0.031	0.036	0.039	0.035	0.030

END MEMBER COMPOSITIONS

AC	13.67	13.43	18.40	22.81	21.29	28.32	23.72	20.31	22.21	21.25
DI	29.55	27.98	18.97	16.85	16.54	19.33	21.80	23.70	21.87	25.48
HD	56.78	58.59	62.63	60.34	62.17	52.35	54.47	55.99	55.91	53.27

## SOUTH QOROQ CENTRE PYROXENE ANALYSES

	111	112	113	114	115	116	117	118	119	120
	46244.2	46244.3	46244.3	46244.3	58154.1	58154.1	58154.1	58154.2	58154.2	58154.2
OXIDE WEIGHT PERCENTAGE										
SI02	48.05	48.63	48.06	48.45	50.23	49.97	50.73	49.98	49.84	50.21
AL2O3	0.90	0.85	1.00	1.07	1.11	1.05	0.79	1.11	1.33	1.16
TIO2	0.43	0.39	0.30	0.39	0.36	0.30	0.34	0.34	0.50	0.37
FE2O3	5.69	5.87	4.69	3.89	7.99	8.12	7.47	3.53	4.84	9.02
FEO	16.83	16.22	14.79	15.98	12.41	13.43	14.59	14.47	14.02	11.62
MGO	4.46	4.28	5.35	5.96	5.27	5.58	4.91	6.38	6.43	5.38
CAO	20.95	19.72	19.99	20.36	17.49	18.03	18.31	21.13	20.27	16.71
NA2O	2.21	2.28	1.82	1.51	3.10	3.15	2.90	1.37	1.88	3.50
MNO	1.15	1.08	1.00	0.99	0.97	0.83	0.83	0.87	0.84	0.85
TOTAL	100.67	99.32	97.00	98.60	98.93	100.45	100.87	99.18	99.96	98.82

## ATOMIC PROPORTIONS ON THE BASIS OF 6 OXYGENS

SI	1.908	1.942	1.948	1.936	1.972	1.946	1.970	1.963	1.944	1.969
AL	0.042	0.040	0.048	0.050	0.051	0.048	0.036	0.051	0.061	0.054
TI	0.013	0.012	0.009	0.012	0.011	0.009	0.010	0.010	0.015	0.011
FE3	0.170	0.177	0.143	0.117	0.236	0.238	0.218	0.104	0.142	0.266
FE2	0.559	0.542	0.501	0.534	0.408	0.437	0.474	0.475	0.457	0.381
MG	0.264	0.255	0.323	0.355	0.308	0.324	0.284	0.373	0.374	0.314
CA	0.892	0.844	0.868	0.872	0.736	0.752	0.762	0.889	0.847	0.702
NA	0.170	0.177	0.143	0.117	0.236	0.238	0.218	0.104	0.142	0.266
MN	0.039	0.037	0.034	0.034	0.032	0.027	0.027	0.029	0.028	0.028

## END MEMBER COMPOSITIONS

AC	16.50	17.50	14.28	11.26	23.98	23.18	21.76	10.63	14.21	26.89
DI	25.58	25.23	32.25	34.14	31.32	31.55	28.31	38.02	37.33	31.76
HD	57.92	57.27	53.47	54.60	44.69	45.27	49.93	51.36	48.46	41.34

## SOUTH QOROO CENTRE PYROXENE ANALYSES

	121	122	123	124	125	126	127	128	129	130
	58154.2	58230.4	58230.4	58230.4	58230.4	58230.4	58230.4	58230.4	58230.4	58230.4
OXIDE WEIGHT PERCENTAGE										
SI02	50.53	49.70	52.16	52.17	51.79	52.25	50.83	50.39	50.21	50.84
AL2O3	1.02	0.83	0.93	0.97	0.78	0.83	0.87	0.89	1.13	0.83
TIO2	0.32	0.25	0.23	0.41	0.46	0.37	0.34	0.34	0.23	0.27
FE2O3	7.65	7.81	6.60	3.86	8.14	7.83	3.97	4.92	6.18	5.98
FEO	11.52	14.39	15.13	16.29	13.62	15.53	19.14	17.26	15.57	16.40
MGO	5.96	3.63	3.66	4.66	3.84	3.04	3.17	3.56	3.80	3.49
CAO	17.59	18.80	20.18	21.19	18.50	17.55	20.63	20.18	19.93	19.46
NA2O	2.97	3.03	2.56	1.50	3.16	3.04	1.54	1.91	2.40	2.32
MND	0.76	1.15	0.94	0.91	0.97	0.92	0.83	0.97	1.02	0.98
TOTAL	98.32	99.58	102.38	101.97	101.26	101.37	101.32	100.42	100.47	100.57

## ATOMIC PROPORTIONS ON THE BASIS OF 6 OXYGENS

SI	1.983	1.967	1.996	1.999	1.996	2.017	1.990	1.983	1.969	1.991
AL	0.047	0.039	0.042	0.044	0.035	0.038	0.040	0.041	0.052	0.038
TI	0.009	0.007	0.007	0.012	0.013	0.011	0.010	0.010	0.007	0.008
FE3	0.226	0.233	0.190	0.111	0.236	0.228	0.117	0.146	0.182	0.176
FE2	0.378	0.476	0.484	0.522	0.439	0.501	0.627	0.568	0.511	0.537
MG	0.349	0.214	0.209	0.266	0.221	0.175	0.185	0.209	0.222	0.204
CA	0.740	0.797	0.828	0.870	0.764	0.726	0.866	0.851	0.838	0.817
NA	0.226	0.233	0.190	0.112	0.236	0.228	0.117	0.146	0.183	0.176
MN	0.025	0.039	0.030	0.030	0.032	0.030	0.028	0.032	0.034	0.033

## END MEMBER COMPOSITIONS

AC	23.12	24.19	20.81	12.00	25.47	24.37	12.23	15.27	19.24	18.56
DI	35.64	22.27	22.85	28.63	23.78	18.72	19.34	21.86	23.40	21.45
HD	41.24	53.54	56.34	59.37	50.74	56.91	68.43	62.88	57.37	60.00

SOUTH QORQQ CENTRE PYROXENE ANALYSES

	131	132	133	134	135	136	137	138	139	140
127071.0	127071.0	127071.0	127071.0	127071.0	127071.0	127071.0	127071.1	127071.1	127071.2	127071.2
OXIDE WEIGHT PERCENTAGE										
SI02	51.94	51.98	52.19	51.64	51.75	52.65	52.54	51.42	51.81	51.57
AL2O3	1.10	1.40	0.91	0.92	0.86	1.30	1.47	0.84	1.25	1.08
TIO2	0.21	0.16	0.16	0.26	0.31	0.21	0.43	0.28	0.31	0.10
FE2O3	36.90	37.18	35.82	30.87	31.00	37.26	37.52	30.40	33.37	39.09
FE0	-	-	-	0.14	-	-	-	0.73	-	-
MGO	-	-	-	0.12	0.04	-	-	-	-	0.26
CAD	0.41	0.55	0.44	3.48	3.44	0.47	0.48	3.94	2.09	0.14
NA2O	14.32	14.43	13.90	11.98	12.03	14.46	14.56	11.80	12.95	15.17
MNO	0.14	0.08	0.24	0.38	0.48	0.06	0.06	0.47	0.32	0.06
TOTAL	105.02	105.78	103.66	99.79	99.91	106.41	107.06	99.88	102.10	107.47

ATOMIC PROPORTIONS ON THE BASIS OF 6 OXYGENS

SI	1.921	1.910	1.947	1.984	1.986	1.919	1.906	1.981	1.954	1.879
AL	0.048	0.061	0.040	0.042	0.039	0.056	0.063	0.038	0.056	0.046
TI	0.006	0.004	0.004	0.008	0.009	0.006	0.012	0.008	0.009	0.003
FE3	1.027	1.028	1.006	0.893	0.895	1.022	1.024	0.881	0.947	1.072
FE2	0.000	0.000	0.000	0.005	0.000	0.000	0.000	0.023	0.000	0.000
MG	0.000	0.000	0.000	0.007	0.002	0.000	0.000	0.000	0.000	0.014
CA	0.016	0.022	0.018	0.143	0.141	0.018	0.019	0.163	0.084	0.005
NA	1.027	1.028	1.006	0.893	0.896	1.023	1.025	0.882	0.948	1.072
MN	0.004	0.002	0.008	0.012	0.016	0.002	0.002	0.015	0.010	0.002

END MEMBER COMPOSITIONS

AC	99.57	99.76	99.25	97.41	98.04	99.82	99.82	95.78	98.93	98.53
DI	0.00	0.00	0.00	0.75	0.25	0.00	0.00	0.00	0.00	1.30
HD	0.43	0.24	0.75	1.84	1.71	0.18	0.18	4.22	1.07	0.17

SOUTH QOROO CENTRE PYROXENE ANALYSES

	141	142	143	144	145	146	147	148	149	150
	59663.1	59663.2	59663.2	59663.2	59663.3	59663.4	59663.4	59663.4	127027.0	127027.0
OXIDE WEIGHT PERCENTAGE										
SiO2	49.05	51.29	52.86	52.65	53.10	51.44	49.72	49.52	50.53	51.94
Al2O3	1.04	6.40	0.88	1.20	1.38	1.11	1.09	0.90	0.92	0.78
TiO2	1.45	1.60	1.21	1.15	2.04	0.44	0.45	0.37	0.36	0.43
Fe2O3	39.06	37.72	36.30	34.30	37.41	27.26	27.13	25.51	8.19	6.88
FeO	-	-	-	-	-	2.32	2.05	3.01	14.31	14.41
MgO	0.16	-	0.38	0.54	0.26	0.55	0.59	0.81	4.25	4.72
CaO	0.18	0.14	1.71	2.71	0.28	6.46	7.59	7.54	17.63	18.89
Na2O	15.16	14.64	14.09	13.31	14.52	10.58	10.53	9.90	3.18	2.67
MnO	0.14	0.15	0.45	0.69	0.42	0.68	0.92	0.90	1.36	1.27
TOTAL	106.24	111.94	107.88	106.54	109.41	100.84	100.07	98.46	100.73	101.99

ATOMIC PROPORTIONS ON THE BASIS OF 6 OXYGENS

Si	1.822	1.775	1.904	1.913	1.884	1.968	1.932	1.952	1.969	1.989
Al	0.046	0.261	0.037	0.051	0.058	0.050	0.050	0.042	0.042	0.035
Ti	0.041	0.042	0.033	0.031	0.054	0.013	0.013	0.011	0.011	0.012
Fe3	1.092	0.982	0.984	0.938	0.999	0.785	0.793	0.757	0.240	0.198
Fe2	0.000	0.000	0.000	0.000	0.000	0.074	0.067	0.099	0.466	0.462
Mg	0.009	0.000	0.020	0.029	0.014	0.031	0.034	0.048	0.247	0.269
Ca	0.007	0.005	0.066	0.106	0.011	0.265	0.316	0.319	0.736	0.775
Na	1.093	0.983	0.985	0.938	0.999	0.785	0.794	0.757	0.240	0.198
Mn	0.004	0.004	0.014	0.021	0.013	0.022	0.030	0.030	0.045	0.041

END MEMBER COMPOSITIONS

AC	98.80	99.55	96.65	94.89	97.43	86.03	85.82	81.05	24.07	20.44
DI	0.80	0.00	2.00	2.96	1.34	3.44	3.69	5.09	24.72	27.76
HD	0.40	0.45	1.35	2.15	1.23	10.54	10.49	13.85	51.21	51.81

SOUTH QDROQ CENTRE      PYROXENE ANALYSES

	151	152	153	154	155	156	157	158	159	160
	127027.0	127027.1	127027.1	127027.1	127027.2	127027.2	127027.2	58130.1	58130.1	58130.1
OXIDE WEIGHT PERCENTAGE										
SiO2	51.61	51.92	52.24	51.44	51.81	51.47	50.97	49.70	51.33	51.17
Al2O3	1.13	1.39	1.49	0.89	1.50	1.45	0.80	4.50	3.34	3.21
TiO2	0.56	0.87	0.72	0.41	0.69	0.63	0.46	1.90	1.57	1.68
Fe2O3	3.17	3.99	2.60	6.85	3.53	4.35	4.59	2.22	2.06	2.42
FeO	13.26	12.02	12.92	15.27	12.48	15.02	17.30	7.75	7.62	8.30
MgO	8.24	8.44	8.52	4.88	8.44	5.94	4.39	10.96	12.40	12.28
CaO	21.43	21.63	21.92	19.06	21.93	21.64	20.08	22.67	23.46	22.60
Na2O	1.23	1.55	1.01	2.66	1.37	1.69	1.78	0.86	0.80	0.94
MnO	0.95	0.81	0.83	1.21	0.82	0.76	1.15	0.29	0.31	0.34
TOTAL	101.58	102.62	102.25	102.68	102.57	102.96	101.52	100.84	102.89	102.94

ATOMIC PROPORTIONS ON THE BASIS OF 6 OXYGENS

Si	1.960	1.945	1.961	1.967	1.944	1.951	1.979	1.853	1.874	1.872
Al	0.051	0.061	0.066	0.040	0.066	0.065	0.037	0.198	0.144	0.138
Ti	0.016	0.025	0.020	0.012	0.019	0.018	0.013	0.053	0.043	0.046
Fe3	0.091	0.113	0.074	0.197	0.100	0.124	0.134	0.062	0.057	0.067
Fe2	0.421	0.377	0.406	0.488	0.392	0.476	0.562	0.242	0.233	0.254
Mg	0.466	0.471	0.477	0.278	0.472	0.335	0.254	0.609	0.675	0.670
Ca	0.872	0.868	0.882	0.781	0.882	0.879	0.836	0.906	0.918	0.886
Na	0.091	0.113	0.074	0.197	0.100	0.124	0.134	0.062	0.057	0.067
Mn	0.031	0.026	0.026	0.039	0.026	0.024	0.038	0.009	0.010	0.011

END MEMBER COMPOSITIONS

AC	8.98	11.42	7.49	19.67	10.08	12.94	13.57	6.75	5.82	6.67
DI	46.23	47.79	48.53	27.72	47.69	34.94	25.71	66.06	69.31	66.90
HD	44.78	40.79	43.98	52.61	42.23	52.13	60.71	27.20	24.87	26.43

## SOUTH QOROO CENTRE PYROXENE ANALYSES

	161	162	163	164	165	166
	58130.1	58130.2	58130.2	58130.2	58130.2	58130.2
OXIDE WEIGHT PERCENTAGE						
SiO2	50.64	50.83	50.45	51.34	51.27	50.62
Al2O3	3.24	2.84	3.55	3.13	2.86	3.48
TiO2	1.54	1.55	1.84	1.48	1.52	1.37
Fe2O3	1.96	1.96	2.73	2.24	1.42	1.26
FeO	7.99	8.40	7.42	7.97	8.58	9.16
MgO	12.18	11.90	11.70	12.03	12.19	11.45
CaO	23.09	22.53	22.17	22.70	22.62	22.99
Na2O	0.76	0.76	1.06	0.87	0.55	0.49
MnO	0.31	0.38	0.35	0.32	0.40	0.31
TOTAL	101.71	101.15	101.27	102.09	101.40	101.14

## ATOMIC PROPORTIONS ON THE BASIS OF 6 OXYGENS

Si	1.874	1.892	1.871	1.889	1.899	1.886
Al	0.141	0.125	0.155	0.136	0.125	0.153
Ti	0.043	0.043	0.051	0.041	0.042	0.038
Fe3	0.055	0.055	0.076	0.062	0.040	0.035
Fe2	0.247	0.261	0.230	0.245	0.266	0.286
Mg	0.672	0.660	0.647	0.660	0.673	0.636
Ca	0.916	0.899	0.881	0.895	0.898	0.918
Na	0.055	0.055	0.076	0.062	0.040	0.035
Mn	0.010	0.012	0.011	0.010	0.013	0.010

## END MEMBER COMPOSITIONS

AC	5.55	5.55	7.91	6.35	3.99	3.66
DI	68.32	66.78	67.07	67.51	67.93	65.78
HD	26.13	27.66	25.02	26.13	28.08	30.56

## SOUTH QOROQ CENTRE PYROXENE PARTIAL ANALYSES

	1	2	3	4	5	6	7	8	9	10
	127021.2	127021.2	127021.3	127021.3	127021.5	127021.5	127021.5	127021.5	127021.6	127021.6

## OXIDE WEIGHT PERCENTAGE

FE2O3	3.86	2.55	15.61	19.12	18.63	18.19	12.26	23.34	4.69	13.63
FEO	14.61	13.55	9.43	6.01	8.89	8.77	13.05	3.53	17.28	11.84
MGO	6.55	9.30	2.86	0.93	0.92	0.91	2.80	1.61	5.00	2.43
CAO	21.04	20.99	12.36	9.61	10.12	10.34	15.05	5.45	19.83	13.42
NA2O	1.50	0.99	6.06	7.42	7.23	7.06	4.76	9.06	1.82	5.29

TOTAL	47.57	47.38	46.33	43.09	45.79	45.27	47.92	42.99	48.62	46.61
-------	-------	-------	-------	-------	-------	-------	-------	-------	-------	-------

## END MEMBER COMPOSITIONS

AC	11.69	7.08	49.17	69.18	61.42	61.19	37.97	76.66	13.88	43.14
DI	39.21	51.13	17.83	6.66	6.00	6.06	17.16	10.47	29.30	15.23
HD	49.10	41.79	33.00	24.16	32.57	32.75	44.87	12.88	56.83	41.63

## SOUTH QOROQ CENTRE PYROXENE PARTIAL ANALYSES

	11	12	13	14	15	16	17	18	19	20
	127075.1	127075.1	127075.1	127075.1	127075.1	127075.2	127075.2	127075.2	127075.3	127075.3
OXIDE WEIGHT PERCENTAGE										
FE2O3	7.94	5.90	7.45	3.01	11.47	16.93	14.87	15.28	13.42	12.88
FEO	15.44	16.72	13.70	17.60	12.96	10.44	12.59	11.13	12.60	13.53
MGO	4.02	4.22	5.87	5.87	2.87	0.54	0.61	1.22	1.66	1.60
CAO	18.26	19.28	18.40	20.88	15.58	11.27	11.94	12.23	14.20	14.00
NA2O	3.08	2.29	2.89	1.17	4.45	6.57	5.77	5.93	5.21	5.00
TOTAL	48.74	48.41	48.31	48.53	47.32	45.75	45.77	45.79	47.10	47.01
END MEMBER COMPOSITIONS										
AC	24.01	17.97	21.72	8.82	36.35	57.20	49.46	50.82	43.71	41.45
DI	24.08	25.44	33.89	33.99	18.01	3.61	4.02	8.03	10.70	10.19
HD	51.91	56.58	44.39	57.19	45.63	39.19	46.52	41.15	45.59	48.36

SOUTH QORDO CENTRE PYROXENE PARTIAL ANALYSES

	21	22	23	24	25	26	27	28	29	30
	127075.3	46269.2	46269.2	46269.2	46269.2	46269.3	46269.3	46269.3	46269.3	58229.1

OXIDE WEIGHT PERCENTAGE

FE2O3	13.50	13.09	12.42	13.30	15.20	19.79	13.01	10.56	11.93	22.37
FEO	12.90	12.27	12.19	12.32	10.59	6.23	11.34	12.87	12.76	5.73
MGO	1.19	2.11	2.95	2.10	2.03	2.44	2.71	3.79	2.42	1.00
CAO	13.94	14.56	15.83	14.63	13.09	10.30	15.40	15.78	14.84	9.66
NA2O	5.24	5.08	4.82	5.16	5.90	7.68	5.05	4.10	4.63	8.68

TOTAL	46.78	47.11	48.21	47.50	46.82	46.44	47.52	47.10	46.58	47.44
-------	-------	-------	-------	-------	-------	-------	-------	-------	-------	-------

END MEMBER COMPOSITIONS

AC	44.72	42.36	39.06	42.70	49.05	62.74	42.00	32.64	38.61	72.82
DI	7.80	13.52	18.36	13.35	12.97	15.32	17.32	23.18	15.51	6.45
HD	47.48	44.13	42.58	43.95	37.98	21.94	40.68	44.17	45.88	20.73

## SOUTH QORQQ CENTRE PYROXENE PARTIAL ANALYSES

	31	32	33	34	35	36	37	38	39	40
58229.1	58229.1	58229.1	58229.1	58229.1	58229.2	58229.2	58229.2	58229.2	58236.1	58236.1

## OXIDE WEIGHT PERCENTAGE

FE2O3	19.20	22.11	17.60	14.71	20.54	19.38	18.55	18.78	16.95	15.72
FEO	8.90	6.25	9.50	10.81	8.20	8.70	9.12	8.95	10.27	11.31
MGO	1.27	1.00	1.69	2.09	0.76	0.98	1.01	0.86	1.26	1.30
CAO	10.85	9.66	12.35	13.44	10.72	10.93	11.95	11.88	14.11	13.33
NA2O	7.45	8.58	6.83	5.71	7.97	7.52	7.20	7.29	6.58	6.10

TOTAL	47.67	47.60	47.97	46.77	48.18	47.51	47.83	47.77	49.17	47.76
-------	-------	-------	-------	-------	-------	-------	-------	-------	-------	-------

## END MEMBER COMPOSITIONS

AC	60.75	71.24	55.87	47.67	65.93	62.54	60.46	61.72	54.95	50.94
DI	7.96	6.38	10.62	13.40	4.83	6.26	6.52	5.59	8.08	8.34
HD	31.30	22.38	33.50	38.93	29.24	31.20	33.02	32.68	36.97	40.72

## SOUTH QORQQ CENTRE PYROXENE PARTIAL ANALYSES

	41	42	43	44	45	46	47	48	49	50
58236.1	58236.2	58236.2	58236.2	58236.2	58236.2	58236.2	58236.2	127015.0	127015.0	127015.1

## OXIDE WEIGHT PERCENTAGE

FE2O3	13.86	11.52	12.06	10.62	13.66	11.80	13.97	16.59	16.85	20.84
FEO	13.05	14.96	12.91	13.09	13.18	13.07	12.98	10.44	9.49	6.00
MGO	1.29	1.73	2.52	3.39	1.54	2.50	1.02	1.95	2.14	1.28
CAO	14.53	16.09	16.32	16.64	14.97	16.14	14.19	13.22	12.98	10.69
NA2O	5.38	4.47	4.68	4.12	5.30	4.58	5.42	6.44	6.54	8.09

TOTAL	48.11	48.77	48.49	47.86	48.65	48.09	47.57	48.65	48.00	46.90
-------	-------	-------	-------	-------	-------	-------	-------	-------	-------	-------

## END MEMBER COMPOSITIONS

AC	44.84	36.49	38.41	33.31	43.56	37.73	45.94	51.77	53.27	69.39
DI	8.26	10.85	15.89	21.06	9.72	15.82	6.64	12.04	13.39	8.43
HD	46.90	52.66	45.70	45.63	46.72	46.44	47.42	36.19	33.33	22.18

SOUTH QOROO CENTRE PYROXENE PARTIAL ANALYSES

51 52 53 54 55 56 57 58 59 60  
 127015.1 127015.1 127015.2 127015.2 127015.2 127015.2 127038.1 127038.1 127038.1 127038.1

OXIDE WEIGHT PERCENTAGE

FE2O3	21.85	21.64	21.95	22.73	12.37	27.67	18.09	18.19	20.25	15.85
FEO	4.96	1.66	5.70	5.86	18.44	3.02	9.25	8.68	6.99	11.01
MGO	1.68	1.53	0.39	0.37	1.89	0.66	1.77	2.16	1.34	1.68
CAO	9.45	7.03	8.40	8.79	7.64	5.43	9.90	11.04	9.82	11.75
NA2O	8.48	8.40	8.52	8.82	4.80	10.74	7.02	7.06	7.86	6.15
TOTAL	46.42	40.26	44.96	46.56	45.14	47.52	46.03	47.13	46.26	46.44

END MEMBER COMPOSITIONS

AC	71.19	81.63	75.55	75.84	33.79	85.60	56.76	56.66	66.03	50.45
DI	10.84	11.42	2.66	2.44	10.22	4.04	11.00	13.32	8.65	10.59
HD	17.97	6.95	21.80	21.71	55.99	10.36	32.24	30.02	25.32	38.96

## SOUTH QORQQ CENTRE PYROXENE PARTIAL ANALYSES

	61	62	63	64	65	66	67	68	69	70
127038.2	127038.2	127038.2	127038.2	58150.1	58150.1	58150.1	58150.1	58150.1	58150.2	58150.2

## OXIDE WEIGHT PERCENTAGE

FE2O3	32.52	30.56	33.47	4.48	4.33	3.94	4.17	5.05	4.15	4.10
FEO	-	0.75	-	15.39	14.65	11.79	11.09	14.02	14.52	14.31
MGO	-	0.29	-	5.02	5.35	7.57	7.72	5.92	5.83	6.15
CAO	0.48	2.33	0.27	20.23	20.97	21.85	21.56	21.21	21.40	21.50
NA2O	12.62	11.86	12.99	1.74	1.68	1.53	1.62	1.96	1.61	1.59
TOTAL	45.62	45.79	46.73	46.86	46.97	46.69	46.17	48.16	47.51	47.65

## END MEMBER COMPOSITIONS

AC	100.00	95.60	100.00	14.23	13.88	12.31	13.13	15.61	13.04	12.73
DI	0.00	1.80	0.00	31.53	33.95	46.79	48.08	36.24	36.27	37.84
HD	0.00	2.60	0.00	54.24	52.17	40.91	38.78	48.15	50.69	49.43

SOUTH QOROQ CENTRE PYROXENE PARTIAL ANALYSES

	71	72	73	74	75	76	77	78	79	80
58150.2	58150.2	58164.1	58164.1	58164.1	58164.1	58164.1	58164.1	58164.2	58164.2	58164.2

OXIDE WEIGHT PERCENTAGE

FE2O3	2.86	3.99	8.76	3.50	2.60	6.31	8.58	2.63	2.32	6.67
FEO	12.05	13.45	10.25	10.80	10.92	9.48	10.45	11.89	12.42	10.68
MGO	8.21	6.49	6.58	10.90	11.22	9.69	6.43	10.49	9.99	8.03
CAO	21.86	21.36	17.75	21.44	22.19	19.61	17.37	21.15	21.18	19.41
NA2O	1.11	1.55	3.40	1.36	1.01	2.45	3.33	1.02	0.90	2.59

TOTAL	46.09	46.84	46.74	48.00	47.94	47.54	46.16	47.17	46.81	47.38
-------	-------	-------	-------	-------	-------	-------	-------	-------	-------	-------

END MEMBER COMPOSITIONS

AC	8.80	12.57	26.41	9.45	7.04	17.52	26.06	7.18	6.46	19.38
DI	50.01	40.43	39.27	58.20	60.12	53.24	38.67	56.74	55.09	46.17
HD	41.19	47.01	34.33	32.35	32.84	29.24	35.27	36.08	38.45	34.45

SOUTH QOROQ CENTRE PYROXENE PARTIAL ANALYSES

	81	82	83	84	85	86	87	88	89	90
	58164.2	58164.2	58164.3	58164.3	58164.3	58164.3	58164.3	58164.3	58221.1	58221.1

OXIDE WEIGHT PERCENTAGE

FE2O3	21.51	4.17	14.33	12.68	12.75	11.72	13.73	13.84	3.27	2.42
FEO	-	11.05	8.37	8.86	8.42	10.76	9.21	8.88	11.95	9.63
MGO	6.20	8.32	3.74	4.37	4.51	3.75	3.36	3.51	9.16	13.65
CAO	9.45	20.53	14.05	14.83	15.71	15.72	14.04	14.28	21.98	22.03
NA2O	8.35	1.62	5.56	4.92	4.95	4.55	5.33	5.37	1.27	0.94
TOTAL	45.51	45.70	46.05	45.65	46.34	46.51	45.67	45.88	47.63	48.67

END MEMBER COMPOSITIONS

AC	63.68	12.68	46.17	40.68	41.10	37.69	44.86	45.14	9.44	6.03
DI	36.32	50.02	23.86	27.76	28.77	23.87	21.73	22.67	52.29	67.31
HD	0.00	37.30	29.97	31.57	30.13	38.44	33.41	32.19	38.27	26.65

SOUTH QOROQ CENTRE PYROXENE PARTIAL ANALYSES

91	92	93	94	95	96	97	98	99	100
58221.1	58221.1	58221.3	58221.3	58221.3	58221.3	58221.3	127025.0	127025.0	127025.0

OXIDE WEIGHT PERCENTAGE

FE2O3	3.12	3.17	2.24	2.24	2.76	2.86	4.02	3.84	2.68
FEO	11.54	12.46	13.55	13.52	14.74	14.83	13.01	12.89	11.92
MGO	10.55	8.91	9.89	9.67	8.16	7.69	6.59	7.15	8.72
CAO	22.11	21.49	21.68	21.05	21.14	21.09	21.24	20.62	22.21
NA2O	1.21	1.23	0.87	0.93	1.07	1.11	1.56	1.49	1.04
TOTAL	48.52	47.26	48.24	47.71	47.87	47.58	46.42	45.99	46.57

END MEMBER COMPOSITIONS

AC	8.47	9.15	6.08	6.09	7.81	8.28	12.75	11.88	8.08
DI	56.72	50.90	53.09	52.10	45.78	44.05	41.38	43.81	52.02
HD	34.81	39.95	40.83	41.81	46.41	47.67	45.87	44.31	39.91

SOUTH QOROQ CENTRE PYROXENE PARTIAL ANALYSES

	101	102	103	104	105	106	107	108	109	110
	127025.0	127025.1	127025.1	127025.1	127025.1	127025.1	46244.1	46244.1	46244.2	46244.2
OXIDE WEIGHT PERCENTAGE										
FE2O3	5.23	3.84	3.35	2.78	3.68	5.02	7.81	10.74	8.17	8.30
FEO	10.98	15.28	14.54	10.82	12.28	11.80	16.20	13.16	15.84	14.85
MGO	6.74	5.27	6.31	9.55	7.54	6.84	2.95	3.75	4.15	4.41
CAO	20.85	21.56	21.60	22.28	21.63	21.31	17.43	15.81	17.57	17.24
NA2O	2.03	1.49	1.30	1.08	1.43	1.95	3.03	4.17	3.17	3.22
TOTAL	45.84	47.44	47.10	46.51	46.56	46.92	47.41	47.64	48.90	48.01

END MEMBER COMPOSITIONS

AC	17.00	12.29	10.47	8.26	11.43	15.86	24.67	32.76	24.03	24.75
DI	43.35	33.39	39.05	56.09	46.28	42.75	18.46	22.64	24.17	26.04
HD	39.65	54.32	50.48	35.65	42.29	41.39	56.87	44.60	51.79	49.21

## SOUTH QOROQ CENTRE

	111	112	113	114	115	116	117
	46244.3	46244.3	46244.3	46244.3	46244.3	58154.1	58154.2

## OXIDE WEIGHT PERCENTAGE

FE2O3	4.53	3.84	4.48	4.64	6.42	8.84	8.17
FEO	15.94	16.39	15.54	17.52	15.49	11.95	11.24
MGO	5.51	5.26	5.45	3.78	4.39	6.03	5.41
CAO	20.17	20.81	20.52	19.08	18.57	17.47	17.93
NA2O	1.76	1.49	1.74	1.80	2.49	3.43	3.17
TOTAL	47.92	47.79	47.73	46.82	47.35	47.72	45.92

## END MEMBER COMPOSITIONS

AC	13.68	11.83	13.78	14.68	19.85	25.96	26.04
DI	32.90	32.08	33.16	23.69	26.89	35.06	34.14
HD	53.42	56.09	53.06	61.62	53.25	38.99	39.82

SOUTH QORQQ CENTRE - AMPHIBOLE PARTIAL ANALYSES

	1	2	3	4	5	6	7	8	9	10
	58231.1	58231.1	58231.1	58231.1	58231.1	58231.2	58231.2	58231.2	58231.2	127038.1
OXIDE WEIGHT PERCENTAGE										
SiO2	44.89	45.77	45.99	45.56	44.96	46.29	46.27	46.29	45.62	45.40
FeO T	26.05	29.02	28.02	27.59	28.07	28.05	28.01	27.04	27.05	29.81
MgO	2.53	2.24	2.69	2.51	2.41	2.72	2.27	2.56	2.56	2.52
CaO	4.84	6.06	5.67	5.37	6.20	6.23	6.24	5.48	5.52	5.90
Na2O	6.26	5.84	6.09	5.75	5.47	5.38	5.37	5.42	5.61	5.75
K2O	1.86	1.92	1.97	1.81	2.03	1.89	1.91	1.87	1.85	1.94
TOTAL	86.43	90.85	90.43	88.59	89.14	90.56	90.07	89.56	88.22	91.32

END MEMBER COMPOSITIONS

Ca	15.87	19.04	18.13	17.67	19.71	19.53	19.96	17.77	18.31	18.06
Mg	12.26	9.79	11.96	11.48	10.65	11.86	10.10	11.54	11.79	10.73
Fe	70.87	71.17	69.91	70.85	69.64	68.62	69.94	70.69	69.90	71.21
Na+K	26.22	33.29	34.30	33.42	32.78	31.83	32.41	32.18	33.37	32.21
Mg	9.41	8.07	9.60	9.29	8.92	10.04	8.53	9.52	9.61	8.87
Fe	54.37	58.64	56.10	57.29	58.30	58.13	59.06	58.30	57.01	58.92

SOUTH QORQQ CENTRE - AMPHIBOLE PARTIAL ANALYSES

	11	12	13	14	15	16	17	18	19	20
127038.1	127038.1	127038.1	127038.1	127038.1	127038.1	127038.5	127038.5	127038.5	58228.7	58228.7
OXIDE WEIGHT PERCENTAGE										
SiO2	45.03	46.05	44.49	47.59	46.59	44.52	45.19	45.32	44.61	45.27
FeO T	28.83	29.10	28.84	29.63	29.71	31.86	31.62	31.84	29.71	27.49
MgO	2.91	2.60	2.84	2.53	2.54	1.08	0.91	0.94	1.84	3.97
CaO	6.52	5.25	7.55	3.97	5.15	5.99	6.11	5.88	6.55	8.51
Na2O	5.69	6.13	4.81	7.12	6.02	5.95	5.59	6.28	5.27	4.79
K2O	1.81	2.04	1.85	1.75	2.06	1.93	1.92	1.86	1.85	1.80
TOTAL	90.79	91.17	90.38	92.59	92.07	91.33	91.34	92.12	89.83	91.83

END MEMBER COMPOSITIONS

CA	19.72	16.63	22.20	12.97	16.16	18.51	19.06	18.35	20.28	23.98
Mg	12.24	11.45	11.61	11.49	11.08	4.64	3.95	4.08	7.92	15.56
FE	68.05	71.92	66.19	75.54	72.76	76.85	76.99	77.57	71.80	60.46
NA+K	31.93	33.94	29.19	35.98	33.32	33.14	32.35	34.18	31.32	28.62
Mg	10.38	9.07	10.57	8.45	8.82	3.81	3.30	3.29	5.83	14.61
FE	57.69	56.99	60.24	55.57	57.87	63.05	64.35	62.53	61.85	56.78

## SOUTH QOROO CENTRE - AMPHIBOLE PARTIAL ANALYSES

	21	22	23	24	25	26	27	28	29	30
	58228.7	58228.7	58228.7	58228.7	58228.7	58228.7	58228.7	58221.1	58221.1	58221.1
OXIDE WEIGHT PERCENTAGE										
SiO <sub>2</sub>	47.10	45.44	46.23	45.79	45.18	45.93	44.29	40.46	40.58	40.66
FeO T	26.47	27.58	31.58	26.54	26.12	26.20	26.76	23.08	20.63	22.31
MgO	5.09	3.60	1.55	4.38	4.35	4.57	3.89	6.08	7.18	6.50
CaO	6.58	8.36	2.73	8.11	8.29	7.51	8.61	10.70	10.95	10.80
Na <sub>2</sub> O	5.12	4.27	2.45	5.04	4.57	5.20	4.57	3.18	3.18	3.35
K <sub>2</sub> O	1.79	1.84	2.02	1.80	1.77	1.77	1.77	2.03	1.68	1.76
TOTAL	92.15	91.09	86.56	91.66	90.28	91.28	89.89	85.53	84.20	85.38
END MEMBER COMPOSITIONS										
Ca	19.17	23.96	9.24	23.23	23.87	21.80	24.67	28.79	29.57	28.99
Mg	20.63	14.35	7.30	17.45	17.42	18.85	15.50	22.75	26.96	24.27
Fe	60.20	61.69	83.46	59.33	58.71	59.35	59.84	48.46	43.47	46.74
Na+K	29.13	27.21	20.33	29.59	28.19	29.95	28.30	23.59	22.92	23.57
Mg	18.09	13.72	6.41	16.00	16.43	16.98	14.75	24.41	29.50	26.12
Fe	52.79	59.05	73.26	54.41	55.37	53.16	56.95	52.00	47.58	50.31

## SOUTH QORQQ CENTRE - AMPHIBOLE PARTIAL ANALYSES

	31	32	33	34	35	36	37	38	39	40
	58221.1	58221.3	58221.3	58221.3	58221.3	58221.3	59672.1	59672.1	59672.8	59672.8
OXIDE WEIGHT PERCENTAGE										
SiO2	40.47	43.55	43.88	42.87	44.34	43.71	45.57	43.33	45.38	43.66
FeO T	22.64	21.79	21.49	24.37	17.51	21.63	13.87	15.85	13.69	16.26
MgO	6.79	6.53	6.41	4.77	6.46	5.31	8.02	10.16	7.22	9.27
CaO	11.03	10.79	10.85	10.70	21.55	10.68	9.52	11.16	9.03	11.38
Na2O	3.32	3.08	3.13	3.11	1.43	3.27	3.74	3.39	5.52	3.77
K2O	1.67	1.74	1.76	1.95	1.81	1.62	2.52	1.68	1.81	1.85
TOTAL	85.92	87.48	87.52	87.77	93.10	87.22	83.24	85.57	82.65	86.19

## END MEMBER COMPOSITIONS

Ca	28.92	29.26	29.70	29.43	48.76	29.39	30.22	29.63	30.35	30.79
Mg	24.76	24.62	24.40	18.25	20.33	24.15	35.41	37.52	33.74	34.88
Fe	46.33	46.12	45.91	52.32	30.92	46.45	34.37	32.85	35.91	34.33
Na+K	22.78	22.67	23.20	23.66	17.32	23.42	30.77	23.49	36.95	26.08
Mg	25.89	26.92	26.65	19.74	32.79	26.19	35.13	40.79	30.54	37.25
Fe	50.33	50.41	50.15	56.60	49.89	50.39	34.10	35.72	32.50	36.67

SOUTH QOROO CENTRE - AMPHIBOLE PARTIAL ANALYSES

	41	42	43	44	45	46	47	48	49	50
	59672.8	59672.8	59672.8	59672.8	59672.8	45243.2	46243.2	46243.2	46243.2	46243.2
OXIDE WEIGHT PERCENTAGE										
SiO2	43.50	45.34	45.54	43.12	43.79	44.59	44.13	43.85	44.49	45.88
FeO T	16.05	14.52	15.71	16.45	15.60	26.94	26.69	25.89	27.10	26.07
MgO	9.61	7.85	8.43	9.31	9.37	4.04	4.24	4.67	4.28	4.18
CaO	11.49	10.36	10.67	11.33	11.06	8.17	9.26	9.11	9.24	8.24
Na2O	3.30	3.69	3.37	3.38	3.16	4.49	3.62	3.60	3.80	3.70
K2O	1.80	2.28	2.45	1.83	1.93	1.81	1.87	1.74	1.63	1.87
TOTAL	85.75	84.04	86.17	85.42	84.91	90.04	89.81	88.85	90.54	89.94

END MEMBER COMPOSITIONS

CA	30.74	31.77	30.79	30.53	30.50	23.47	25.73	25.44	25.42	23.95
MG	35.75	33.48	33.83	34.88	35.93	16.14	16.38	18.14	16.38	16.90
FE	33.51	34.75	35.38	34.59	33.57	60.40	57.88	56.43	58.20	59.15
NA+K	23.87	29.69	27.32	24.34	24.13	27.85	24.73	24.34	24.55	25.44
MG	39.30	34.50	35.52	37.99	39.22	15.21	15.61	18.40	15.57	16.57
FE	36.84	35.81	37.15	37.67	36.65	56.94	58.67	57.26	58.88	58.00

## SOUTH QOROO CENTRE - AMPHIBOLE PARTIAL ANALYSES

	51	52	53	54	55	56	57	58	59	60
	46243.3	46243.3	46243.3	46243.3	58230.1	58230.1	58230.1	58230.1	58230.1	58230.1
OXIDE WEIGHT PERCENTAGE										
SiO <sub>2</sub>	44.87	45.48	44.90	43.71	44.68	44.50	44.04	44.56	44.68	44.43
FeO T	26.32	28.49	28.05	28.26	27.19	26.95	28.10	28.46	28.42	27.61
MgO	4.42	3.10	3.35	3.51	3.23	2.91	3.51	3.18	3.69	3.15
CaO	9.17	8.54	8.45	8.37	8.57	7.98	8.29	8.70	7.77	8.51
Na <sub>2</sub> O	3.73	4.17	4.18	4.12	4.62	5.05	4.43	3.73	4.79	4.16
K <sub>2</sub> O	1.69	1.85	1.69	1.77	2.00	1.90	1.85	1.87	1.79	1.89
TOTAL	90.20	91.63	90.62	89.74	90.29	89.29	90.22	90.50	91.14	89.75
END MEMBER COMPOSITIONS										
Ca	25.57	24.34	24.14	23.71	25.00	24.14	23.62	24.62	22.15	24.71
Mg	17.14	12.29	13.31	13.82	13.10	12.24	13.91	12.52	14.63	12.72
Fe	57.29	63.37	62.55	62.47	61.90	63.62	62.48	62.86	63.23	62.57
Na+K	24.72	26.86	26.51	26.20	29.47	31.26	27.60	25.21	28.34	27.39
Mg	17.34	11.88	12.89	13.37	12.32	11.09	13.18	12.42	13.46	12.27
Fe	57.94	61.26	60.59	60.42	58.21	57.65	59.22	62.37	58.20	60.34

## SOUTH OOROO CENTRE - AMPHIROLE PARTIAL ANALYSES

	61	62	63	64	65	66	67	68	69	70
	58230.1	58230.3	58230.3	127027.3	127027.3	127027.3	127027.3	127027.3	127027.3	127027.3
OXIDE WEIGHT PERCENTAGE										
SiO2	44.45	52.90	52.56	43.67	44.30	43.94	53.32	44.22	43.98	44.05
FeO T	28.20	24.88	23.57	25.37	25.61	25.39	16.47	26.05	25.60	26.28
MgO	3.10	1.61	1.60	3.96	4.13	4.00	6.88	4.18	3.77	3.95
CaO	7.95	15.10	15.71	9.03	8.74	8.29	21.84	8.99	8.62	8.71
Na2O	4.24	4.68	4.59	3.66	3.64	4.45	1.22	4.05	3.63	3.72
K2O	1.88	0.05	0.21	1.71	1.56	1.81	-	1.83	1.73	1.77
TOTAL	89.82	99.22	98.24	87.40	87.98	88.88	99.73	89.32	87.33	88.48

## END MEMBER COMPOSITIONS

CA	23.20	41.08	43.24	26.30	25.35	24.06	49.34	25.59	25.47	25.09
Mg	12.58	6.09	6.12	16.04	16.66	16.15	21.62	16.54	15.49	15.82
FE	64.22	52.83	50.63	57.66	57.98	59.79	29.04	57.87	59.04	59.09
NA+K	27.36	28.26	29.33	25.50	24.71	28.07	8.97	26.67	25.49	25.37
Mg	11.90	7.42	7.63	16.21	16.80	15.29	38.85	15.30	15.49	15.76
FE	60.74	64.32	63.04	58.29	58.48	56.63	52.19	57.02	59.02	58.86

SOUTH QOROO CENTRE - AMPHIBOLE PARTIAL ANALYSES

71 72

127027.2 127027.2

OXIDE WEIGHT PERCENTAGE

SiO2	45.46	46.46
FeO T	26.40	26.41
MgO	4.02	3.95
CaO	7.70	7.33
Na2O	4.34	4.58
K2O	1.89	1.82
TOTAL	90.81	90.55

END MEMBER COMPOSITIONS

Ca	22.72	21.92
Mg	16.49	16.43
Fe	60.79	61.65
Na+K	27.84	28.60
Mg	15.40	15.02
Fe	55.76	56.38

## SOUTH QOROQ CENTRE OLIVINE ANALYSES

	1	2	3	4	5	6	7	8	9	10
	127021.1	127021.1	127021.1	127021.1	127021.1	127021.4	127021.4	127021.4	127021.4	58150.3
OXIDE WEIGHT PERCENTAGE										
SiO2	30.28	30.43	29.92	30.01	30.28	29.76	29.97	29.69	30.58	29.34
TiO2	0.05	0.06	0.05	0.05	0.05	0.03	0.03	0.03	0.02	0.02
Al2O3	-	-	-	-	-	-	-	-	-	-
FeO	57.00	60.61	60.44	60.53	59.92	58.94	61.34	61.30	60.14	62.13
MnO	11.08	5.49	6.86	6.83	7.25	7.34	5.79	6.23	6.14	5.49
MgO	0.74	1.91	1.95	1.39	1.65	1.02	1.30	0.87	1.45	1.74
CaO	0.73	0.70	0.79	0.65	0.85	0.65	0.74	0.76	0.80	0.50
TOTAL	99.88	99.20	100.01	99.46	100.00	97.74	99.17	98.88	99.13	99.22

## ATOMIC PROPORTIONS ON THE BASIS OF 4 OXYGENS

Si	1.613	1.015	0.997	1.006	1.007	1.015	1.008	1.005	1.022	0.991
Ti	0.001	0.002	0.001	0.001	0.001	0.001	0.001	0.001	0.001	0.001
Al	0.000	0.000	0.000	0.000	0.000	0.000	0.000	0.000	0.000	0.000
Fe2	1.594	1.691	1.684	1.698	1.667	1.681	1.725	1.736	1.680	1.754
Mn	0.314	0.155	0.194	0.194	0.204	0.212	0.165	0.179	0.174	0.157
Mg	0.037	0.095	0.097	0.069	0.082	0.052	0.065	0.044	0.072	0.088
Ca	0.026	0.025	0.028	0.023	0.030	0.024	0.027	0.028	0.029	0.018

## END MEMBER COMPOSITIONS

FO	1.90	4.89	4.90	3.54	4.19	2.67	3.33	2.24	3.75	4.38
FA	81.97	87.12	85.29	86.56	85.35	86.43	88.23	88.63	87.23	87.77
TE	16.14	7.99	9.81	9.89	10.46	10.90	8.44	9.12	9.02	7.86

## SOUTH QOROO CENTRE OLIVINE ANALYSES

	11	12	13	14	15	16	17	18	19	20
58150.3	58150.3	58150.3	58150.3	58150.3	58150.3	58150.3	58150.4	58150.4	58228.1	58228.1
OXIDE WEIGHT PERCENTAGE										
SiO2	29.73	29.30	29.88	29.51	29.77	29.45	29.51	29.71	29.56	29.45
TiO2	0.02	0.02	0.02	0.06	0.03	0.02	0.02	0.02	0.05	0.05
Al2O3	-	-	-	-	-	-	-	-	-	-
FeO	61.20	60.66	60.03	60.70	61.62	61.57	62.12	61.66	60.40	59.76
MnO	5.15	5.17	6.28	6.51	6.20	6.02	5.74	5.63	8.18	8.20
MgO	2.30	2.21	1.95	1.87	1.37	1.81	1.05	1.07	0.76	0.65
CaO	0.58	0.62	0.45	0.44	0.54	0.28	0.52	0.67	0.50	0.66
TOTAL	98.98	97.98	98.61	99.09	99.53	99.15	98.96	98.76	99.45	98.77

## ATOMIC PROPORTIONS ON THE BASIS OF 4 OXYGENS

Si	0.998	0.995	1.007	0.995	1.000	0.994	1.000	1.006	0.999	1.002
Ti	0.001	0.001	0.001	0.002	0.001	0.001	0.001	0.001	0.001	0.001
Al	0.000	0.000	0.000	0.000	0.000	0.000	0.000	0.000	0.000	0.000
Fe2	1.719	1.724	1.692	1.711	1.732	1.738	1.761	1.746	1.708	1.700
Mn	0.147	0.149	0.179	0.186	0.177	0.172	0.165	0.162	0.234	0.236
Mg	0.115	0.112	0.098	0.094	0.069	0.091	0.053	0.054	0.038	0.033
Ca	0.021	0.023	0.016	0.016	0.019	0.010	0.019	0.024	0.018	0.024

## END MEMBER COMPOSITIONS

FO	5.81	5.64	4.97	4.72	3.47	4.55	2.68	2.75	1.93	1.67
FA	86.79	86.86	85.92	85.95	87.60	86.85	88.99	89.02	86.24	86.33
TE	7.40	7.50	9.10	9.34	8.93	8.60	8.33	8.23	11.83	12.00

SOUTH QORQQ CENTRE OLIVINE ANALYSES

21 22 23 24 25 26 27 28 29 30

58228.1 58228.1 58228.2 58228.2 58228.2 58228.2 58228.2 58221.2 58221.2 58221.2

OXIDE WEIGHT PERCENTAGE

SiO2	29.42	29.20	28.81	29.07	29.15	28.92	29.63	29.48	29.33
TiO2	0.05	0.03	0.06	0.05	0.06	0.06	0.05	0.05	0.06
Al2O3	-	-	-	-	-	-	-	-	-
FeO	59.75	59.43	58.78	58.73	59.17	59.17	60.98	62.05	61.56
MnO	8.93	9.19	8.77	9.24	8.64	8.74	6.06	5.98	5.44
MgO	0.85	0.76	0.87	0.65	0.72	0.70	1.35	0.89	1.31
CaO	0.46	0.39	0.58	0.55	0.41	0.57	0.28	0.25	0.56
TOTAL	99.46	99.00	97.87	98.29	98.15	98.16	98.35	98.70	98.26

ATOMIC PROPORTIONS ON THE BASIS OF 4 OXYGENS

Si	0.995	0.994	0.991	0.996	0.999	0.993	1.006	1.003	0.999
Ti	0.001	0.001	0.002	0.001	0.002	0.002	0.001	0.001	0.002
Al	0.000	0.000	0.000	0.000	0.000	0.000	0.000	0.000	0.000
Fe2	1.691	1.692	1.692	1.683	1.696	1.699	1.732	1.765	1.754
Mn	0.256	0.265	0.256	0.268	0.251	0.254	0.174	0.172	0.157
Mg	0.043	0.039	0.045	0.033	0.037	0.036	0.068	0.045	0.067
Ca	0.017	0.014	0.021	0.020	0.015	0.021	0.010	0.009	0.020

END MEMBER COMPOSITIONS

FO	2.15	1.93	2.24	1.67	1.85	1.80	3.46	2.28	3.36
FA	84.98	84.79	84.93	84.81	85.50	85.42	87.71	89.03	88.70
TE	12.86	13.28	12.83	13.52	12.65	12.78	8.83	8.69	7.94

## SOUTH QOROQ CENTRE OLIVINE ANALYSES

	31	32	33	34	35	36	37	38	39	40
58221.2	58221.2	59672.1	59672.1	59672.1	59672.1	59672.1	59672.1	59672.1	59672.1	59672.3

## OXIDE WEIGHT PERCENTAGE

SiO2	29.96	30.21	32.70	32.53	32.31	32.35	32.48	32.33	32.44	32.21
TiO2	0.08	0.05	0.05	0.08	0.07	0.07	0.07	0.08	0.05	0.05
Al2O3										
FeO	60.30	61.03	51.52	51.34	50.89	51.81	51.36	51.79	51.62	51.72
MnO	5.60	5.34	2.24	2.16	2.38	2.52	2.45	2.46	2.58	2.48
MgO	1.28	1.19	13.01	13.35	13.00	13.03	13.24	13.31	12.64	12.89
CaO	0.28	0.62	0.25	0.28	0.28	0.33	0.29	0.29	0.29	0.25
TOTAL	97.50	98.44	99.77	99.74	98.93	100.11	99.89	100.26	99.62	99.60

## ATOMIC PROPORTIONS ON THE BASIS OF 4 OXYGENS

Si	1.020	1.020	1.005	1.000	1.002	0.995	0.998	0.992	1.002	0.996
Ti	0.002	0.001	0.001	0.002	0.002	0.002	0.002	0.002	0.001	0.001
Al	0.000	0.000	0.000	0.000	0.000	0.000	0.000	0.000	0.000	0.000
Fe2	1.718	1.723	1.324	1.319	1.320	1.333	1.320	1.329	1.334	1.338
Mn	0.162	0.153	0.058	0.056	0.063	0.066	0.064	0.064	0.068	0.065
Mg	0.065	0.060	0.596	0.611	0.601	0.597	0.606	0.609	0.582	0.594
Ca	0.010	0.022	0.008	0.009	0.009	0.011	0.010	0.010	0.010	0.008

## END MEMBER COMPOSITIONS

FO	3.34	3.09	30.12	30.77	30.29	29.93	30.47	30.41	29.34	29.75
FA	88.35	89.12	66.94	66.40	66.55	66.78	66.33	66.40	67.25	67.00
TE	8.31	7.89	2.95	2.83	3.15	3.29	3.20	3.19	3.40	3.25

## SOUTH QOROO CENTRE OLIVINE ANALYSES

	41	42	43	44	45	46	47	48	49	50
	59672.4	59672.5	59672.5	59672.5	59676.3	59676.3	59676.3	127025.3	127025.3	127025.3
OXIDE WEIGHT PERCENTAGE										
SiO2	31.42	32.27	32.83	32.23	30.57	30.66	30.53	29.95	30.18	29.80
TiO2	0.05	0.05	0.03	0.07	0.08	0.11	0.05	0.06	0.03	0.02
Al2O3	-	-	-	-	0.05	0.02	0.02	-	-	-
FeO	52.87	51.81	51.94	52.01	60.68	60.54	60.78	60.90	60.63	60.88
MnO	2.69	2.37	2.36	2.39	4.06	4.03	3.86	5.20	4.93	4.63
MgO	11.54	12.73	12.48	12.90	3.56	3.81	3.94	3.33	3.46	3.61
CaO	0.34	0.21	0.29	0.26	0.56	0.86	0.77	0.31	0.26	0.40
TOTAL	98.91	99.44	99.93	99.86	99.56	100.03	99.95	99.75	99.49	99.34

## ATOMIC PROPORTIONS ON THE BASIS OF 4 OXYGENS

Si	0.990	0.999	1.009	0.995	1.007	1.004	1.001	0.993	1.000	0.991
Ti	0.001	0.001	0.001	0.002	0.002	0.003	0.001	0.001	0.001	0.001
Al	0.000	0.000	0.000	0.000	0.002	0.001	0.001	0.000	0.000	0.000
Fe2	1.393	1.342	1.336	1.342	1.671	1.658	1.667	1.689	1.680	1.693
Mn	0.072	0.062	0.061	0.062	0.113	0.112	0.107	0.146	0.138	0.130
Mg	0.542	0.587	0.572	0.593	0.175	0.186	0.193	0.165	0.171	0.179
Ca	0.011	0.007	0.010	0.009	0.020	0.030	0.027	0.011	0.009	0.014

## END MEMBER COMPOSITIONS

FO	27.00	29.50	29.04	29.69	8.92	9.51	9.79	8.23	8.59	8.93
FA	69.42	67.38	67.84	67.18	85.30	84.78	84.76	84.47	84.46	84.55
TE	3.58	3.12	3.12	3.13	5.78	5.72	5.45	7.31	6.96	6.51

## SOUTH QOROQ CENTRE OLIVINE ANALYSES

	51	52	53	54	55	56	57	58	59	60
	127025.3	127025.4	127025.4	46243.1	46243.1	46243.1	46243.1	46243.1	58230.1	58230.1
OXIDE WEIGHT PERCENTAGE										
SiO <sub>2</sub>	30.21	29.92	30.22	29.42	29.62	29.76	29.81	29.59	29.73	29.36
TiO <sub>2</sub>	0.05	0.02	0.02	0.05	0.03	0.06	0.02	0.02	0.05	0.06
Al <sub>2</sub> O <sub>3</sub>	-	-	-	-	-	-	-	-	-	-
FeO	61.25	60.30	59.23	58.80	58.98	59.32	59.35	59.06	61.26	61.48
MnO	4.59	4.83	4.54	9.58	7.80	8.46	8.85	8.98	6.32	5.61
MgO	3.61	3.84	4.15	0.63	1.22	1.28	1.28	1.07	1.50	1.91
CaO	1.02	0.48	0.64	0.18	0.26	0.31	0.18	0.24	0.48	0.58
TOTAL	100.73	99.39	98.80	98.66	97.91	99.19	99.49	98.96	99.34	99.00

## ATOMIC PROPORTIONS ON THE BASIS OF 4 OXYGENS

Si	0.990	0.992	1.001	1.003	1.010	1.003	1.003	1.002	1.000	0.991
Ti	0.001	0.000	0.000	0.001	0.001	0.002	0.001	0.001	0.001	0.002
Al	0.000	0.000	0.000	0.000	0.000	0.000	0.000	0.000	0.000	0.000
Fe <sub>2</sub>	1.678	1.672	1.641	1.676	1.682	1.673	1.670	1.673	1.724	1.736
Mn	0.127	0.136	0.127	0.277	0.225	0.242	0.252	0.258	0.180	0.160
Mg	0.176	0.190	0.205	0.032	0.062	0.064	0.064	0.054	0.075	0.096
Ca	0.036	0.017	0.023	0.007	0.009	0.011	0.006	0.009	0.017	0.021

## END MEMBER COMPOSITIONS

FO	8.89	9.50	10.38	1.61	3.15	3.25	3.23	2.72	3.80	4.82
FA	84.68	83.71	83.16	84.45	85.41	84.54	84.07	84.30	87.10	87.12
TE	6.43	6.79	6.46	13.94	11.44	12.21	12.70	12.98	9.10	8.05

## SOUTH QOROO CENTRE OLIVINE ANALYSES

	61	62	63	64	65	66	67	68	69	70
58230.1	58230.1	58230.1	58230.1	58230.1	58230.2	58230.2	58230.2	58230.2	58230.2	58230.2

## OXIDE WEIGHT PERCENTAGE

SI02	29.30	29.28	29.04	29.00	29.70	29.46	29.64	29.19	29.37	29.55
TIO2	0.03	0.02	0.03	0.05	0.05	0.05	0.03	0.05	0.05	0.05
AL2O3	-	-	-	-	-	-	-	-	-	-
FE0	61.45	61.68	60.75	60.82	61.39	61.33	61.08	60.70	60.95	60.80
MNO	5.69	5.26	5.82	6.25	5.89	5.78	5.98	5.91	6.86	6.53
MGO	1.98	2.07	1.72	1.41	1.26	1.57	1.59	1.80	0.89	1.35
CAO	0.50	0.48	0.81	0.58	0.31	0.50	0.35	0.48	0.31	0.71
TOTAL	98.95	98.79	98.17	98.11	98.60	98.69	98.67	98.13	98.43	98.99

## ATOMIC PROPORTIONS ON THE BASIS OF 4 OXYGENS

SI	0.990	0.990	0.990	0.992	1.006	0.998	1.003	0.994	1.002	0.999
TI	0.001	0.001	0.001	0.001	0.001	0.001	0.001	0.001	0.001	0.001
AL	0.000	0.000	0.000	0.000	0.000	0.000	0.000	0.000	0.000	0.000
FE2	1.737	1.745	1.732	1.739	1.740	1.738	1.728	1.729	1.739	1.719
MN	0.163	0.151	0.168	0.181	0.169	0.166	0.171	0.171	0.198	0.187
MG	0.100	0.104	0.087	0.072	0.064	0.079	0.080	0.091	0.045	0.068
CA	0.018	0.017	0.030	0.021	0.011	0.018	0.013	0.018	0.011	0.026

## END MEMBER COMPOSITIONS

FO	4.99	5.22	4.40	3.61	3.23	4.00	4.05	4.59	2.28	3.45
FA	86.87	87.25	87.15	87.31	88.20	87.64	87.29	86.85	87.72	87.08
TE	8.15	7.54	8.46	9.09	8.57	8.37	8.66	8.56	10.00	9.47

## SOUTH QOROQ CENTRE OLIVINE ANALYSES

	71	72	73	74	75	76	77	78	79
58230.3	58230.3	58230.3	58230.3	58130.3	58130.3	58130.3	58130.3	58130.3	58130.3
OXIDE WEIGHT PERCENTAGE									
SiO2	28.59	28.25	28.52	33.02	33.42	33.33	33.59	32.88	33.49
TiO2	0.06	0.05	0.03	0.11	0.10	0.07	0.10	0.10	0.10
Al2O3	-	-	-	0.02	0.02	0.02	0.02	0.02	0.02
FeO	59.09	60.45	60.36	51.17	50.31	50.41	49.29	51.40	50.62
MnO	8.36	6.58	6.01	1.39	1.37	1.18	1.33	1.37	1.43
MgO	0.96	1.59	1.50	15.08	15.74	15.75	16.45	15.14	16.31
CaO	0.36	0.80	0.81	0.17	0.32	0.16	0.31	0.25	0.24
TOTAL	97.42	97.72	97.23	100.96	101.28	100.92	101.09	101.16	102.21

## ATOMIC PROPORTIONS ON THE BASIS OF 4 OXYGENS

Si	0.989	0.974	0.985	0.994	0.997	0.998	0.998	0.989	0.990
Ti	0.002	0.001	0.001	0.002	0.002	0.002	0.002	0.002	0.002
Al	0.000	0.000	0.000	0.001	0.001	0.001	0.001	0.001	0.001
Fe2	1.710	1.744	1.744	1.288	1.255	1.262	1.225	1.293	1.252
Mn	0.245	0.192	0.176	0.035	0.035	0.030	0.033	0.035	0.036
Mg	0.049	0.082	0.077	0.676	0.700	0.703	0.729	0.679	0.719
Ca	0.013	0.030	0.030	0.005	0.010	0.005	0.010	0.008	0.008

## END MEMBER COMPOSITIONS

FO	2.47	4.05	3.87	33.82	35.17	35.23	36.66	33.82	35.82
FA	85.31	86.42	87.33	64.41	63.09	63.27	61.65	64.44	62.39
TE	12.22	9.53	8.81	1.77	1.74	1.50	1.69	1.74	1.79

SOUTH AFRICAN CENTRE MAGNETITE ANALYSES

	1	2	3	4	5	6	7	8	9	10
	127021.3	127021.3	127021.3	127021.3	127021.7	127021.7	127021.7	127075.3	127075.3	127075.3
OXIDE WEIGHT PERCENTAGE										
SiO2	0.11	0.13	0.13	0.09	0.09	0.09	0.13	0.11	0.13	0.13
TiO2	27.32	23.32	22.89	22.63	13.72	1.27	11.74	15.80	13.23	10.27
Al2O3	0.02	0.04	0.02	0.02	0.43	0.02	0.04	0.10	0.12	0.14
CR2O3	0.03	0.03	0.02	0.02	-	0.01	0.03	-	-	0.02
FeO	69.76	73.27	73.88	72.54	81.46	94.75	84.46	78.30	81.31	84.19
MnO	0.66	0.76	0.79	0.76	0.53	0.38	0.23	0.53	0.71	0.68
MgO	-	-	-	-	-	-	-	-	-	-
CaO	0.02	0.01	0.01	-	-	0.05	-	0.06	-	0.05
TOTAL	97.92	97.56	97.74	97.06	96.23	96.57	96.63	94.90	95.50	95.48

CORRECTED ANALYSES (AFTER CARMICHAEL, 1967)

ILMENITE BASIS

FE2O3	32.88	39.18	39.96	38.47	51.30	69.59	54.78	47.79	51.78	55.89
FeO	39.27	38.01	37.92	37.92	35.29	32.13	35.17	35.29	34.71	33.89
TOTAL	101.31	101.48	101.74	100.91	101.27	103.54	102.11	99.68	100.68	101.08

ULVOSPINEL BASIS

FE2O3	15.58	23.53	24.59	22.65	42.08	68.67	46.84	37.16	42.85	48.94
FeO	55.74	52.10	51.75	52.16	43.59	32.96	42.31	44.86	42.75	40.15
TOTAL	90.48	99.91	100.20	99.33	100.44	103.44	101.32	98.62	99.79	100.38
% USP	77.83	66.53	65.16	67.65	39.28	3.89	33.66	46.06	38.36	29.80

SOUTH AOROO CENTPE MAGNETITE ANALYSES

	11	12	13	14	15	16	17	18	19	20
	127075.3	127075.4	46269.5	46269.5	46269.6	127038.3	127038.3	127038.4	127038.4	58164.4
OXIDE WEIGHT PERCENTAGE										
SiO2	0.16	0.13	0.14	0.25	0.20	0.13	0.11	0.16	0.14	0.20
TiO2	13.58	11.61	0.10	0.10	0.07	8.41	4.51	3.28	5.46	10.91
Al2O3	0.05	0.12	0.06	0.10	0.10	0.08	0.08	0.08	0.04	0.57
CR2O3	0.02	0.02	0.01	0.01	0.01	0.05	0.08	0.06	0.08	0.06
FeO	81.88	82.50	92.70	93.61	91.96	86.38	89.52	91.25	88.27	86.79
MnO	0.77	0.73	0.03	0.03	0.01	0.11	0.11	0.10	0.14	0.62
MgO	-	-	-	0.02	-	-	-	-	-	-
CaO	0.01	-	-	-	-	-	-	-	-	0.05
TOTAL	96.48	95.11	93.04	94.12	92.35	95.15	94.51	94.93	94.13	99.20

CORRECTED ANALYSES (AFTER CARMICHAEL, 1967)

ILMENITE BASIS

Fe2O3	52.02	53.75	68.48	69.06	67.86	58.30	63.31	65.29	61.69	57.05
FeO	35.07	34.13	31.08	31.46	30.89	33.91	32.65	32.50	32.75	35.45
TOTAL	101.69	100.49	99.90	101.03	99.14	101.00	100.95	101.47	100.31	104.91

ULVO SPINEL BASIS

Fe2O3	42.83	45.90	68.29	68.77	67.64	52.58	60.21	62.96	57.93	49.60
FeO	43.33	41.10	31.25	31.72	31.10	39.06	35.44	34.59	35.14	42.15
TOTAL	100.77	99.70	99.88	101.00	99.12	100.42	100.54	101.23	99.93	104.17
% USP	39.09	33.81	0.83	1.24	0.98	24.54	13.35	9.95	16.27	30.64

SOUTH QOROO CENTRE MAGNETITE ANALYSES

	21	22	23	24	25	26	27	28	29	30
58164.4	58164.4	58221.1	58221.1	58221.1	58221.1	58221.1	58221.1	58221.3	58221.3	46244.1
OXIDE WEIGHT PERCENTAGE										
SiO2	0.18	0.13	0.18	0.20	0.18	0.22	0.20	0.23	0.18	0.09
TiO2	10.45	11.61	4.21	4.99	7.94	9.00	4.46	4.35	4.89	4.55
Al2O3	0.16	0.16	0.59	0.20	0.37	0.58	0.53	1.06	0.96	0.22
CR2O3	0.06	0.03	0.03	-	0.06	0.08	0.05	0.06	0.05	0.05
FeO	88.88	79.13	87.18	87.13	85.50	84.09	89.86	90.35	89.38	91.02
MNO	0.54	0.52	0.13	0.53	0.13	0.13	0.24	0.14	0.13	0.14
MGO	0.11	-	-	-	-	-	-	-	-	-
CAO	0.01	0.01	0.02	-	0.05	-	-	0.01	-	-
TOTAL	100.39	91.59	92.34	93.05	94.23	94.20	95.44	96.20	95.59	96.07

CORRECTED ANALYSES (AFTER CARMICHAEL, 1967)

	21	22	23	24	25	26	27	28	29	30
ILMENITE RASTS										
FE2O3	59.18	51.08	61.42	61.24	57.83	55.82	63.26	63.38	62.38	64.30
FeO	35.62	33.16	31.91	31.93	33.46	23.85	32.93	33.32	33.24	33.16
TOTAL	106.31	96.70	98.49	99.19	100.02	99.79	101.77	102.54	101.83	102.51

ULVOSPINEL BASIS

FE2O3	52.06	43.23	58.46	57.84	52.38	49.53	60.11	60.27	58.96	61.19
FeO	42.03	40.23	34.57	35.08	38.27	39.43	35.77	36.11	36.32	35.96
TOTAL	105.60	95.92	98.19	98.84	99.47	99.17	101.46	102.23	101.49	102.20
% USP	28.97	35.12	13.02	15.30	23.57	26.78	13.38	13.05	14.49	13.16

## SOUTH QOROO CENTRE MAGNETITE ANALYSFS

	31	32	33	34	35	36	37	38	39	40
	46244.1	46244.1	46244.1	46244.1	46244.1	46244.1	46244.1	46244.1	46244.4	46244.5
OXIDE WEIGHT PERCENTAGE										
SiO2	0.14	0.16	0.14	0.11	0.09	0.13	0.07	0.16	0.09	0.14
TiO2	2.29	3.24	3.88	4.61	4.60	8.01	3.83	8.32	4.61	6.05
Al2O3	0.18	0.24	0.22	0.43	0.06	0.10	0.18	0.16	0.16	0.20
CR2O3	0.03	0.05	0.03	0.06	0.02	0.05	0.03	0.06	0.02	0.05
FeO	92.13	92.05	92.35	90.59	89.95	86.85	91.45	86.46	89.67	90.40
MnO	0.21	0.08	0.19	0.14	1.36	0.08	0.21	0.30	0.06	0.30
MgO	-	-	-	-	-	-	-	-	-	-
CaO	-	-	-	-	0.02	0.06	-	-	0.02	-
TOTAL	94.98	95.82	96.81	95.94	96.10	95.28	95.77	95.46	94.63	97.14

## CORRECTED ANALYSES (AFTER CARMICHAEL, 1967)

## ILMENEITE BASIS

FF2O3	65.66	65.81	65.73	63.81	64.50	58.94	65.19	58.49	63.26	62.92
FeO	32.14	32.82	33.20	33.17	31.91	33.81	32.78	33.82	32.75	33.78
TOTAL	101.65	102.41	103.39	102.33	102.56	101.18	102.30	101.32	100.96	103.44

## ULVOSPINEL BASIS

FE2O3	65.01	63.51	63.02	60.64	61.35	53.49	62.58	52.81	60.11	58.77
FeO	33.63	34.89	35.64	36.02	34.74	38.72	35.14	38.94	35.58	37.51
TOTAL	101.49	102.18	103.12	102.01	102.74	100.63	102.03	100.75	100.65	103.02
% HSP	7.04	9.74	11.36	13.41	13.30	23.35	11.09	24.30	13.54	17.41

SOUTH QOROO CENTRE MAGNETITE ANALYSES

	41	42	43	44	45	46	47	48	49	50
	46244.5	58154.5	58154.3	58154.3	58154.4	58154.4	58154.5	58154.5	58154.5	127001.1
OXIDE WEIGHT PERCENTAGE										
SiO2	0.14	0.16	0.20	0.16	0.11	0.11	0.07	0.13	0.09	0.16
TiO2	5.78	6.44	5.60	3.14	9.50	9.50	6.28	8.47	7.46	0.07
Al2O3	0.22	0.22	0.18	0.26	0.68	0.27	0.16	0.22	0.25	0.57
CR2O3	0.03	0.05	0.03	0.03	0.05	0.05	0.08	0.09	0.06	0.04
FeO	90.09	87.97	89.96	91.31	83.47	85.36	90.04	87.65	88.11	93.67
MnO	0.30	0.19	0.10	0.08	0.39	0.43	0.16	0.21	0.21	0.06
MgO	-	-	-	-	-	-	-	-	-	0.26
CaO	-	0.01	0.01	0.01	-	-	-	-	-	0.04
TOTAL	95.56	95.04	96.08	94.99	94.20	95.72	96.79	96.77	96.18	94.87

CORRECTED ANALYSES (AFTER CARMICHAEL, 1967)

ILMENITE BASIS

Fe2O3	62.87	60.76	62.72	65.34	55.33	56.98	62.47	59.19	60.23	69.32
FeO	33.51	33.29	33.52	32.51	33.68	34.09	33.82	34.38	33.91	31.29
TOTAL	102.85	101.12	102.36	101.53	99.74	101.42	103.04	102.70	102.21	101.81

ULVOSPINEL BASIS

Fe2O3	58.90	56.33	58.81	63.11	48.91	50.55	58.22	53.43	55.18	69.14
FeO	37.09	37.28	37.03	34.52	39.46	39.87	37.64	39.57	38.45	31.46
TOTAL	102.46	100.68	101.97	101.31	99.10	100.78	102.62	102.12	101.70	101.79
% USP	16.75	18.99	16.55	9.54	27.82	27.42	17.87	24.28	21.40	0.80

## SOUTH GORROQ CENTRE      MAGNETITE ANALYSES

51                      52                      53

127001.2 127003.1 127003.2

## OXIDE WEIGHT PERCENTAGE

SIO <sub>2</sub>	0.32	0.11	0.11
TIO <sub>2</sub>	0.08	6.97	10.31
AL <sub>2</sub> O <sub>3</sub>	1.54	1.86	1.85
CR <sub>2</sub> O <sub>3</sub>	0.04	0.08	0.08
FEO	90.89	81.55	77.80
MNO	0.06	1.36	1.16
MGO	0.04	1.53	1.30
CAO	0.23	0.02	0.01
TOTAL	93.20	93.48	92.62

## CORRECTED ANALYSES (AFTER CARMICHAFL, 1967)

## ILMENITE BASIS

FE <sub>2</sub> O <sub>3</sub>	66.50	57.74	52.28
FEO	31.05	29.59	30.76
TOTAL	99.86	99.26	97.85

## ULVOSPINEL BASIS

FE <sub>2</sub> O <sub>3</sub>	66.16	53.00	45.31
FEO	31.35	33.86	27.03
TOTAL	99.82	98.79	97.16
% USP	1.45	20.26	30.21

SOUTH 30000 CENTRF ILMENITE ANALYSES

	1	2	3	4	5	6	7
	127021.3	127021.7	46269.5	127038.3	127038.4	127038.4	58164.1
OXIDE WEIGHT PERCENTAGE							
SiO2	0.09	0.09	0.17	0.13	0.15	0.34	0.17
TiO2	55.93	58.71	50.57	49.91	55.26	52.18	53.53
Al2O3	0.02	0.02	0.13	0.02	-	0.24	0.02
CR2O3	-	-	-	0.02	0.02	0.04	0.04
FFO	42.36	37.33	41.48	45.51	41.03	37.94	37.69
MNO	1.81	2.45	1.03	1.55	1.80	2.78	2.32
MGO	-	-	-	-	-	-	-
CAO	0.01	0.01	-	0.47	-	-	0.01
TOTAL	100.22	98.61	93.38	97.61	98.26	93.52	93.78

CORRECTED ANALYSES (AFTER CARMICHAEL, 1967)

FF2O3	0.0	0.0	0.0	2.94	0.0	0.0	0.0
FFO	42.36	37.33	41.48	42.86	41.03	37.94	37.69
TOTAL	100.22	98.61	93.38	97.90	98.26	93.52	93.78
% P2O3	0.03	0.03	0.20	2.90	0.02	0.40	0.07
%XS TiO2	6.89	14.54	3.51	-0.00	7.81	7.31	9.22

## SOUTH OROO CFNTRE ILMENITE ANALYSES

	8	9	10	11	12	13	14
	58164.1	58164.1	58164.4	58164.4	58221.1	58221.1	58221.3
OXIDE WEIGHT PERCENTAGE							
SiO2	0.15	0.13	0.11	0.34	0.13	0.17	0.17
TiO2	54.68	54.43	54.43	54.04	54.27	54.93	54.06
Al2O3	0.02	0.02	0.02	0.02	0.15	0.02	0.06
CR2O3	-	0.04	-	-	-	-	0.02
FeO	39.17	38.78	46.99	37.87	44.13	44.17	44.96
MnO	2.60	3.07	2.02	2.20	1.15	1.15	1.04
MgO	-	-	-	-	-	-	-
CaO	-	0.01	-	0.23	-	0.01	-
TOTAL	96.62	96.48	103.57	94.70	99.83	100.45	100.31

## CORRECTED ANALYSES (AFTEP CARMICHAEL, 1967)

FE2O3	0.0	0.0	0.0	0.0	0.0	0.0	0.0
FeO	39.17	38.78	46.99	37.87	44.13	44.17	44.96
TOTAL	96.62	96.48	103.57	94.70	99.83	100.45	100.31
% P2O3	0.03	0.07	0.03	0.03	0.22	0.03	0.11
%XS TiO2	8.39	8.01	0.05	9.57	4.07	4.73	3.12

## SOUTH 00800 CENTRE ILMENITE ANALYSES

	15	16	17	18	19	20	21
	46244.1	46244.1	46244.4	46244.4	58154.3	58154.4	58154.5
OXIDE WEIGHT PERCENTAGE							
SiO2	0.13	0.13	0.11	0.09	0.09	0.13	0.06
TiO2	54.06	52.57	55.01	55.18	54.61	50.53	54.02
Al2O3	0.07	0.06	0.05	0.04	0.09	0.16	0.04
Cr2O3	0.02	0.02	0.02	0.02	0.02	0.04	0.02
FeO	43.82	45.65	44.79	44.68	45.15	42.28	45.68
MnO	1.20	1.17	1.01	1.25	1.09	0.58	0.95
MgO	-	0.02	-	-	-	-	-
CaO	-	-	-	-	-	0.02	-
TOTAL	99.30	99.62	100.99	101.26	101.05	93.74	100.77

## CORRECTED ANALYSES (AFTER CARMICHAEL, 1967)

Fe2O3	0.0	0.0	0.0	0.0	0.0	0.0	0.0
FeO	43.82	45.65	44.79	44.68	45.15	42.28	45.58
TOTAL	99.30	99.62	100.99	101.26	101.05	93.74	100.77
% R2O3	0.12	0.11	0.09	0.08	0.15	0.29	0.08
%XS TiO2	4.15	0.62	4.21	4.21	3.29	3.00	2.23

SOUTH QORQO CENTRE - NEPHELINE ANALYSES

	1	2	3	4	5	6	7	8	9	10
	58231.3	58231.3	58231.3	58231.3	58231.3	58231.4	58231.4	58231.4	58231.4	127021.8
OXIDE WEIGHT PERCENTAGE										
SiO2	46.24	45.69	46.28	45.96	45.84	44.86	45.27	44.96	45.78	46.24
Al2O3	33.29	32.02	31.07	31.78	32.33	31.92	32.17	31.27	31.95	31.59
Fe2O3	1.01	0.76	0.37	0.63	0.72	0.91	0.76	0.64	0.63	0.61
CaO	0.79	0.01	0.13	0.01	0.10	0.07	0.24	2.16	1.41	0.23
Na2O	16.48	15.99	16.66	15.73	16.26	15.18	16.43	15.81	16.11	14.83
K2O	5.58	5.46	5.76	4.88	5.54	5.47	5.77	3.70	5.38	5.41
TOTAL	103.39	99.93	100.27	98.99	100.79	98.41	100.64	98.54	101.26	98.91

ATOMIC PROPORTIONS ON THE BASIS OF 32 OXYGENS

Si	8.559	8.710	8.821	8.796	8.676	8.675	8.615	8.670	8.651	8.854
Al	7.265	7.197	6.982	7.171	7.214	7.278	7.218	7.109	7.118	7.132
Fe3	0.141	0.109	0.053	0.091	0.103	0.132	0.109	0.093	0.090	0.088
Ca	0.157	0.002	0.027	0.002	0.020	0.015	0.049	0.446	0.286	0.047
Na	5.917	5.913	6.160	5.840	5.970	5.694	6.065	5.914	5.906	5.509
K	1.318	1.328	1.401	1.192	1.338	1.350	1.401	0.910	1.297	1.322

END MEMBER COMPOSITIONS (MOL WT %)

QZ	5.47	7.73	6.20	9.41	7.00	8.60	5.51	5.50	4.81	10.47
NE	75.75	73.81	74.84	73.82	74.43	72.31	75.16	80.67	75.49	70.65
KS	18.78	18.46	18.95	16.77	18.57	19.08	19.33	13.83	18.71	18.88

## SOUTH QORQQ CENTRE - NEPHELINE ANALYSES

	11	12	13	14	15	16	17	18	19	20
127021.8	127021.8	127021.8	127021.8	127021.8	127021.9	127021.9	127021.9	127021.9	127021.9	127075.1

## OXIDE WEIGHT PERCENTAGE

SiO2	52.21	47.51	50.07	44.28	44.56	45.18	43.06	44.38	46.39	44.85
Al2O3	27.70	31.33	28.12	32.59	31.97	32.48	31.92	32.21	28.08	24.70
Fe2O3	0.51	0.68	0.72	0.69	0.75	0.67	0.79	0.78	4.32	7.15
CaO	0.09	0.04	0.16	0.10	0.03	0.03	0.04	0.01	2.18	2.36
Na2O	11.83	13.32	11.81	14.68	15.64	16.33	14.82	16.58	15.96	14.08
K2O	7.25	5.17	6.44	5.73	5.57	5.72	5.04	5.25	4.64	4.47
TOTAL	99.59	98.05	97.32	98.07	98.52	100.41	95.67	99.21	101.57	97.61

## ATOMIC PROPORTIONS ON THE BASIS OF 32 OXYGENS

Si	9.817	9.079	9.628	8.589	8.629	8.602	8.554	8.553	8.831	8.942
Al	6.141	7.059	6.375	7.453	7.299	7.291	7.476	7.319	6.303	5.807
Fe3	0.072	0.098	0.104	0.101	0.109	0.096	0.118	0.113	0.619	1.073
Ca	0.018	0.008	0.033	0.021	0.006	0.006	0.009	0.002	0.445	0.504
Na	4.315	4.938	4.405	5.524	5.875	6.031	5.711	6.199	5.894	5.446
K	1.740	1.261	1.580	1.418	1.376	1.390	1.278	1.291	1.127	1.137

## END MEMBER COMPOSITIONS (MOL WT %)

QZ	20.14	16.04	19.71	8.73	7.23	6.12	8.41	5.54	5.17	7.85
NE	55.12	65.37	57.38	70.98	73.58	74.71	73.33	76.67	78.18	74.77
KS	24.74	18.58	22.92	20.29	19.19	19.17	18.26	17.78	16.65	17.39

SOUTH QORDQ CENTRE - NEPHELINE ANALYSES

	21	22	23	24	25	26	27	28	29	30
127075.5	127075.5	127075.5	127075.5	127075.5	127075.6	127075.6	127075.6	46269.4	46269.4	46269.4
OXIDE WEIGHT PERCENTAGE										
SiO2	57.80	45.52	45.07	48.90	42.54	43.39	42.24	43.89	43.70	42.65
Al2O3	24.10	31.93	31.96	29.25	31.61	31.91	31.56	31.86	31.17	31.09
Fe2O3	0.54	0.88	0.61	0.76	0.79	0.59	0.68	0.59	0.76	0.81
CaO	0.24	0.07	0.03	0.11	0.07	0.01	0.07	0.01	0.01	0.01
Na2O	13.80	16.37	16.96	14.77	19.54	18.86	19.24	15.96	16.11	16.67
K2O	4.10	5.41	5.29	6.38	3.88	3.78	3.37	5.22	5.51	5.60
TOTAL	100.58	100.18	99.92	100.17	98.43	98.54	97.16	97.53	97.26	96.83

ATOMIC PROPORTIONS ON THE BASIS OF 32 OXYGENS

Si	10.563	8.676	8.626	9.265	8.333	8.436	8.347	8.585	8.604	8.480
Al	5.193	7.175	7.212	6.534	7.300	7.315	7.353	7.347	7.236	7.288
Fe3	0.074	0.126	0.088	0.108	0.116	0.086	0.101	0.087	0.113	0.121
Ca	0.047	0.014	0.006	0.022	0.015	0.002	0.015	0.002	0.002	0.002
Na	4.892	6.052	6.297	5.428	7.425	7.113	7.375	6.056	6.153	6.430
K	0.956	1.316	1.292	1.542	0.970	0.938	0.850	1.303	1.384	1.421

END MEMBER COMPOSITIONS (MOL WT %)

QZ	24.71	6.71	5.31	11.75	-0.46	1.94	0.47	6.44	5.52	3.20
NE	61.84	75.11	77.08	67.04	87.70	85.51	88.22	75.48	75.55	77.69
KS	13.46	18.18	17.61	21.21	12.75	12.55	11.32	18.08	18.93	19.11

SOUTH QOROOQ CENTRE - NEPHELINE ANALYSES

	31	32	33	34	35	36	37	38	39	40
	46269.4	46269.7	46269.7	46269.7	46269.7	46269.7	127038.5	127038.5	127038.5	127038.5
OXIDE WEIGHT PERCENTAGE										
SiO2	43.20	43.30	44.31	42.74	43.24	43.03	43.86	44.49	43.77	44.48
Al2O3	31.20	31.14	31.58	31.57	31.48	31.14	31.12	31.89	31.35	30.90
Fe2O3	0.69	1.05	0.66	0.57	0.64	0.67	1.44	0.72	0.75	0.76
CaO	0.01	0.01	0.01	0.01	0.01	0.01	0.04	0.01	0.01	0.01
Na2O	16.86	16.90	16.43	16.90	16.95	17.66	15.66	16.50	17.26	16.01
K2O	5.54	5.52	5.60	5.08	5.68	5.51	5.62	5.40	5.89	5.37
TOTAL	97.50	97.92	98.59	96.87	98.00	98.02	97.74	99.01	99.03	97.53

ATOMIC PROPORTIONS ON THE BASIS OF 32 OXYGENS

Si	8.520	8.512	8.608	8.464	8.492	8.472	8.600	8.595	8.523	8.710
Al	7.255	7.218	7.233	7.371	7.289	7.228	7.195	7.264	7.198	7.134
Fe3	0.102	0.155	0.096	0.085	0.095	0.099	0.213	0.105	0.110	0.112
Ca	0.002	0.002	0.002	0.002	0.002	0.002	0.008	0.002	0.002	0.002
Na	6.451	6.445	6.191	6.492	6.457	6.745	5.957	6.183	6.520	6.081
K	1.394	1.385	1.388	1.284	1.423	1.384	1.406	1.331	1.464	1.342

END MEMBER COMPOSITIONS (MOL WT %)

QZ	3.43	3.47	5.30	3.52	3.09	1.70	6.42	5.61	2.71	6.68
NE	77.84	77.90	75.78	79.07	77.81	80.02	74.10	76.14	77.84	74.91
KS	18.73	18.63	18.92	17.41	19.10	18.28	19.48	18.25	19.46	18.40

SOUTH QORQQ CENTRE - NEPHELINE ANALYSES

	41	42	43	44	45	46	47	48	49	50
	127038.5	127038.6	127038.6	127038.6	127038.6	58228.5	58228.5	58228.5	58228.5	58228.5
OXIDE WEIGHT PERCENTAGE										
SiO2	44.61	43.78	43.87	44.19	44.31	44.24	44.42	44.22	44.52	45.24
Al2O3	30.94	31.87	32.15	31.82	31.62	30.89	31.55	31.96	31.63	31.50
Fe2O3	0.73	0.95	0.50	0.63	0.66	0.86	0.72	0.72	0.69	0.66
CaO	0.01	0.01	0.01	0.01	0.01	0.13	0.11	0.63	0.11	0.01
Na2O	16.21	15.71	15.92	16.17	16.78	15.92	17.59	16.63	16.58	16.25
K2O	5.44	5.54	5.51	5.42	5.72	5.07	5.54	5.12	4.64	5.11
TOTAL	97.94	97.86	97.96	98.24	99.10	97.11	99.93	99.28	98.17	98.77

ATOMIC PROPORTIONS ON THE BASIS OF 32 OXYGENS

Si	8.707	8.554	8.554	8.596	8.582	8.691	8.555	8.533	8.639	8.723
Al	7.120	7.342	7.391	7.298	7.221	7.155	7.164	7.271	7.236	7.161
Fe3	0.107	0.140	0.073	0.092	0.096	0.127	0.104	0.105	0.101	0.096
Ca	0.002	0.002	0.002	0.002	0.002	0.027	0.023	0.130	0.023	0.002
Na	6.137	5.955	6.021	6.101	6.305	6.067	6.572	6.225	6.241	6.078
K	1.355	1.381	1.371	1.345	1.414	1.271	1.361	1.261	1.149	1.257

END MEMBER COMPOSITIONS (MOL WT %)

QZ	6.28	6.42	6.09	5.99	4.41	6.84	2.93	4.18	6.34	7.26
NE	75.23	74.37	74.92	75.48	76.49	75.54	78.88	78.19	77.73	75.38
KS	18.49	19.21	18.99	18.53	19.10	17.62	18.20	17.63	15.93	17.36

SOUTH QORQQ CENTRE - NEPHELINE ANALYSES

	51	52	53	54	55	56	57	58	59	60
	58228.6	58228.6	58164.6	58164.5	58164.5	58164.5	58164.5	58164.5	58164.5	58221.4
OXIDE WEIGHT PERCENTAGE										
SiO2	43.90	44.12	44.77	43.65	44.55	43.42	44.25	43.78	43.64	43.67
Al2O3	31.95	31.84	32.26	32.25	32.26	31.86	33.38	32.66	32.11	31.16
Fe2O3	0.53	0.69	0.50	0.54	0.57	0.57	0.54	0.57	0.54	0.31
CaO	0.07	0.07	0.10	0.01	0.10	0.09	0.04	0.01	0.14	0.70
Na2O	16.62	16.61	16.63	16.61	17.10	16.55	16.96	16.60	15.59	15.19
K2O	5.19	4.85	5.58	5.71	5.90	5.41	5.95	5.65	6.28	5.27
TOTAL	98.26	98.18	99.84	98.77	100.48	97.90	101.12	99.27	98.30	96.30

ATOMIC PROPORTIONS ON THE BASIS OF 32 OXYGENS

Si	8.545	8.577	8.581	8.481	8.524	8.502	8.407	8.456	8.518	8.646
Al	7.332	7.298	7.291	7.388	7.278	7.355	7.478	7.438	7.389	7.273
Fe3	0.078	0.101	0.072	0.079	0.082	0.084	0.077	0.083	0.079	0.046
Ca	0.015	0.015	0.021	0.002	0.021	0.019	0.008	0.002	0.029	0.149
Na	6.275	6.264	6.183	6.260	6.347	6.286	6.251	6.220	5.903	5.834
K	1.289	1.203	1.365	1.416	1.441	1.352	1.443	1.393	1.564	1.331

END MEMBER COMPOSITIONS (MOL WT %)

QZ	4.96	5.67	5.17	4.14	3.57	4.29	3.62	4.37	5.21	6.41
NE	77.35	77.71	76.13	76.58	76.98	77.22	76.68	76.55	73.20	74.63
KS	17.69	16.62	18.71	19.28	19.45	18.49	19.70	19.08	21.60	18.96

SOUTH QOROO CENTRE - NEPHELINE ANALYSES

	61	62	63	64	65	66	67	68	69	70
	58221.4	58221.4	58221.4	58221.4	58221.6	58221.6	58221.6	58221.6	127025.6	127025.6
OXIDE WEIGHT PERCENTAGE										
SiO2	43.96	44.37	44.28	44.03	44.24	43.54	44.35	43.82	46.53	45.39
Al2O3	30.74	30.97	30.57	31.22	31.24	31.34	31.36	30.16	31.67	32.19
Fe2O3	0.24	0.31	0.28	0.24	0.35	0.35	0.42	0.42	0.36	1.22
CaO	0.24	0.44	0.14	0.22	0.33	0.33	0.33	0.34	0.09	0.33
Na2O	15.79	16.75	17.04	16.53	15.74	15.01	16.00	15.83	16.00	15.27
K2O	5.05	4.83	5.23	5.61	5.17	5.97	5.38	5.06	4.92	5.24
TOTAL	96.02	97.67	97.54	97.85	97.07	96.54	97.84	95.63	99.57	99.64

ATOMIC PROPORTIONS ON THE BASIS OF 32 OXYGENS

Si	8.719	8.676	8.696	8.624	8.683	8.621	8.657	8.743	8.851	8.667
Al	7.188	7.140	7.078	7.209	7.229	7.316	7.217	7.094	7.103	7.247
Fe3	0.036	0.046	0.041	0.035	0.052	0.052	0.062	0.063	0.052	0.175
Ca	0.051	0.092	0.029	0.046	0.069	0.070	0.069	0.073	0.018	0.068
Na	6.075	6.353	6.491	6.280	5.993	5.765	6.059	6.127	5.904	5.656
K	1.278	1.205	1.311	1.402	1.295	1.508	1.340	1.288	1.194	1.277

END MEMBER COMPOSITIONS (MOL WT %)

QZ	6.65	4.88	4.25	4.38	6.67	6.42	5.91	6.21	9.12	8.72
NE	75.63	78.54	78.17	76.58	75.23	72.47	75.50	76.00	74.17	72.94
KS	17.72	16.59	17.57	19.04	18.10	21.11	18.59	17.79	16.71	18.33

## SOUTH QOROO CENTRE - NEPHELINE ANALYSES

	71	72	73	74	75	76	77	78	79	80
	127025.6	127025.7	127025.7	127025.7	46243.4	46243.4	46243.4	46243.4	46243.4	46243.5

## OXIDE WEIGHT PERCENTAGE

SiO2	46.30	45.36	46.11	45.65	44.72	44.72	44.15	43.97	44.25	42.54
Al2O3	32.52	32.21	32.52	32.60	31.24	31.39	31.07	31.68	31.40	29.82
Fe2O3	0.43	0.36	0.42	0.36	0.63	0.78	0.57	0.63	0.61	0.64
CaO	0.13	0.29	0.17	0.20	0.03	0.01	0.01	0.01	0.09	0.01
Na2O	15.94	15.38	15.95	15.59	16.65	16.65	15.90	16.41	15.85	15.39
K2O	5.13	5.42	5.29	5.18	5.42	5.66	5.77	5.70	5.58	5.72
TOTAL	100.45	99.02	100.46	99.58	98.69	99.21	97.47	98.40	97.78	94.12

## ATOMIC PROPORTIONS ON THE BASIS OF 32 OXYGENS

Si	8.743	8.704	8.719	8.696	8.671	8.642	8.668	8.567	8.648	8.664
Al	7.240	7.287	7.250	7.321	7.142	7.152	7.192	7.278	7.235	7.161
Fe3	0.061	0.052	0.060	0.052	0.092	0.113	0.084	0.092	0.090	0.098
Ca	0.026	0.060	0.034	0.041	0.006	0.002	0.002	0.002	0.019	0.002
Na	5.839	5.725	5.851	5.761	6.263	6.241	6.055	6.202	6.009	6.080
K	1.236	1.327	1.276	1.259	1.341	1.396	1.445	1.417	1.392	1.487

## END MEMBER COMPOSITIONS (MOL WT %)

QZ	8.65	8.26	8.14	8.61	5.44	5.15	6.03	4.88	6.34	5.64
NE	73.92	72.92	73.91	73.51	76.35	75.94	74.24	75.83	74.46	74.17
KS	17.42	18.82	17.95	17.89	18.20	18.91	19.73	19.29	19.20	20.19

SOUTH QOROQ CENTRE - NEPHELINE ANALYSES

	81	82	83	84	85	86	87	88	89	90
	46243.5	46243.5	46243.5	46244.6	46244.6	46244.6	46244.6	46244.6	46244.7	46244.7

OXIDE WEIGHT PERCENTAGE

SiO2	43.83	44.04	44.40	43.35	44.01	43.71	44.24	44.65	44.14	44.51
Al2O3	32.01	31.17	31.19	31.60	31.48	31.91	31.04	31.19	30.17	31.42
Fe2O3	0.64	0.61	0.66	0.83	0.91	0.73	0.73	0.78	0.78	0.78
CaO	0.01	0.01	0.01	0.01	0.01	0.01	0.01	0.04	0.07	0.01
Na2O	15.59	16.23	16.98	16.13	17.30	16.45	16.19	16.53	15.93	16.52
K2O	6.00	5.77	5.65	5.29	4.90	5.26	5.03	5.12	4.92	5.23
TOTAL	98.08	97.83	98.89	97.21	98.61	98.07	97.24	98.31	96.01	98.47

ATOMIC PROPORTIONS ON THE BASIS OF 32 OXYGENS

Si	8.555	8.629	8.622	8.534	8.555	8.529	8.679	8.676	8.764	8.641
Al	7.366	7.201	7.141	7.335	7.214	7.341	7.180	7.146	7.062	7.192
Fe3	0.094	0.090	0.096	0.123	0.133	0.107	0.108	0.114	0.117	0.114
Ca	0.002	0.002	0.002	0.002	0.002	0.002	0.002	0.008	0.015	0.002
Na	5.903	6.169	6.397	6.160	6.523	6.227	6.161	6.231	6.135	6.221
K	1.494	1.443	1.400	1.329	1.215	1.310	1.259	1.270	1.246	1.296

END MEMBER COMPOSITIONS (MOL WT %)

QZ	6.06	5.23	4.19	5.45	4.18	5.16	6.56	6.03	7.07	5.82
NE	73.28	75.19	77.04	76.24	79.36	76.84	76.12	76.60	75.79	76.45
KS	20.66	19.58	18.78	18.31	16.46	18.00	17.32	17.38	17.14	17.73

SOUTH QOROO CENTRE - NEPHELINE ANALYSES

	91	92	93	94	95	96	97	98	99	100
	46244.7	46244.7	58154.3	58154.3	58154.3	58154.3	58154.6	58154.6	58154.6	58154.6
OXIDE WEIGHT PERCENTAGE										
SI02	43.79	43.78	44.41	45.12	44.39	44.55	44.99	44.35	44.50	44.35
AL2O3	31.17	31.79	32.04	31.73	31.12	32.18	32.69	31.44	32.11	31.32
FE2O3	0.89	0.73	0.78	0.51	0.50	0.59	0.53	0.56	0.57	0.59
CAO	0.01	0.01	0.06	0.01	0.01	0.06	0.01	0.01	0.01	0.01
NA2O	15.98	16.48	15.98	16.08	15.51	15.25	15.66	16.06	15.71	16.48
K2O	4.68	5.53	5.82	5.48	5.78	5.70	5.45	5.76	5.76	5.32
TOTAL	96.52	98.32	99.09	98.93	97.31	98.33	99.33	98.18	98.66	98.07

ATOMIC PROPORTIONS ON THE BASIS OF 32 OXYGENS

SI	8.639	8.536	8.580	8.696	8.708	8.631	8.618	8.644	8.612	8.646
AL	7.250	7.308	7.298	7.210	7.198	7.351	7.383	7.224	7.327	7.199
FE3	0.132	0.107	0.113	0.074	0.074	0.086	0.076	0.082	0.083	0.087
CA	0.002	0.002	0.012	0.002	0.002	0.012	0.002	0.002	0.002	0.002
NA	6.116	6.233	5.989	6.012	5.902	5.732	5.819	6.072	5.898	6.233
K	1.178	1.376	1.435	1.348	1.447	1.409	1.332	1.432	1.422	1.323

END MEMBER COMPOSITIONS (MOL WT %)

QZ	7.10	4.79	5.93	6.98	7.09	7.83	7.81	5.89	6.79	5.63
NE	76.50	76.43	74.26	74.44	72.99	72.36	73.46	74.53	73.48	76.33
KS	16.41	18.78	19.81	18.58	19.92	19.81	18.73	19.58	19.73	18.05

## SOUTH QOROQ CENTRE - NEPHELINE ANALYSES

	101	102	103	104	105	106	107	108	109	110
	58154.6	58230.5	58230.5	58230.5	58230.5	58230.5	58230.5	58230.6	58230.6	127027.4
OXIDE WEIGHT PERCENTAGE										
SiO2	44.77	46.09	45.21	44.84	44.95	45.28	44.94	54.90	44.70	44.39
Al2O3	30.95	32.38	32.17	32.12	31.79	32.12	32.63	33.07	30.95	32.48
Fe2O3	0.61	1.07	0.86	0.69	0.75	0.75	0.64	0.22	0.88	0.42
CaO	0.01	0.07	0.09	0.13	0.04	0.09	0.01	0.11	0.24	0.01
Na2O	16.07	14.10	14.44	15.86	14.47	18.32	14.95	13.67	14.59	16.35
K2O	5.31	5.45	5.49	5.54	5.14	5.53	5.71	3.21	5.13	5.35
TOTAL	97.72	99.16	98.26	99.18	97.14	102.09	98.88	105.18	96.49	99.00

## ATOMIC PROPORTIONS ON THE BASIS OF 32 OXYGENS

Si	8.739	8.785	8.721	8.628	8.754	8.544	8.639	9.550	8.786	8.559
Al	7.123	7.277	7.317	7.286	7.299	7.145	7.396	6.782	7.172	7.383
Fe3	0.090	0.153	0.125	0.100	0.110	0.107	0.093	0.029	0.130	0.061
Ca	0.002	0.014	0.019	0.027	0.008	0.018	0.002	0.021	0.051	0.002
Na	6.085	5.214	5.404	5.920	5.466	6.705	5.575	4.613	5.563	6.115
K	1.323	1.326	1.351	1.360	1.277	1.331	1.401	0.713	1.287	1.316

## END MEMBER COMPOSITIONS (MOL WT %)

QZ	6.92	12.30	10.56	6.86	10.91	2.37	8.96	24.66	9.99	5.90
NE	74.95	68.35	69.96	74.17	70.70	79.95	71.14	64.28	71.58	75.91
KS	18.14	19.35	19.48	18.97	18.39	17.68	19.90	11.06	18.43	18.19

SOUTH QORQQ CENTRE - NEPHELINE ANALYSES

	111	112	113	114	115	116	117	118
	127027.4	127027.4	127027.4	127027.4	127027.4	127027.5	127027.5	127027.5
OXIDE WEIGHT PERCENTAGE								
SiO2	45.57	45.11	45.16	43.97	44.33	44.75	44.24	43.45
Al2O3	32.71	32.57	32.27	32.29	24.99	32.38	32.82	32.81
Fe2O3	0.53	0.66	0.35	0.57	0.29	0.47	0.54	0.51
CaO	0.04	0.03	0.04	0.03	0.01	0.01	0.03	0.04
Na2O	16.37	15.49	15.26	16.86	10.26	16.18	15.91	15.75
K2O	5.65	4.86	5.65	5.05	6.66	5.64	5.59	5.60
TOTAL	100.87	98.72	98.73	98.77	86.54	99.43	99.13	98.16

ATOMIC PROPORTIONS ON THE BASIS OF 32 OXYGENS

SI	8.623	8.659	8.694	8.513	9.624	8.596	8.520	8.458
AL	7.298	7.371	7.324	7.371	6.397	7.333	7.452	7.530
FE3	0.075	0.095	0.051	0.083	0.047	0.068	0.078	0.075
CA	0.008	0.006	0.008	0.006	0.002	0.002	0.006	0.008
NA	6.009	5.768	5.699	6.332	4.321	6.029	5.944	5.947
K	1.364	1.190	1.388	1.248	1.845	1.382	1.374	1.391

END MEMBER COMPOSITIONS (MOL WT %)

QZ	6.48	9.15	8.50	4.80	18.64	6.19	6.31	5.86
NE	74.65	73.88	71.98	78.07	55.14	74.73	74.51	74.69
KS	18.87	16.98	19.52	17.13	26.22	19.08	19.17	19.45

SOUTH QORDQ CENTRE FELDSPAR ANALYSES

	1	2	3	4	5	6	7	8	9	10
58231.5	58231.5	58231.5	58231.5	58231.6	58231.6	58231.6	58231.7	58231.7	58231.7	127075.7
OXIDE WEIGHT PERCENTAGE										
SiO2	67.15	65.56	65.08	63.90	64.97	64.67	65.68	66.98	68.02	64.82
Al2O3	18.47	18.69	18.87	18.79	18.87	18.59	18.04	18.71	18.56	18.41
Fe2O3	0.38	0.23	0.26	0.19	0.35	0.17	0.36	0.19	0.22	0.22
CaO	0.01	0.06	0.06	0.06	0.03	0.06	0.01	0.03	0.03	0.06
Na2O	5.41	6.10	6.10	4.89	5.75	5.69	3.38	6.03	5.77	3.68
K2O	8.78	8.66	8.44	9.93	9.13	9.01	11.96	8.69	8.70	11.17
TOTAL	100.20	99.30	98.81	97.76	99.10	98.19	99.43	100.63	101.30	98.36

ATOMIC PROPORTIONS ON THE BASIS OF 32 OXYGENS

Si	12.053	11.923	11.886	11.860	11.869	11.910	12.036	11.993	12.071	11.974
Al	3.909	4.007	4.063	4.112	4.064	4.036	3.898	3.950	3.883	4.010
Fe3	0.051	0.031	0.036	0.027	0.048	0.024	0.050	0.026	0.029	0.031
Ca	0.002	0.012	0.012	0.012	0.006	0.012	0.002	0.006	0.006	0.012
Na	1.884	2.152	2.161	1.761	2.038	2.033	1.202	2.095	1.986	1.319
K	2.011	2.010	1.967	2.352	2.128	2.117	2.797	1.986	1.970	2.633

END MEMBER COMPOSITION (WEIGHT PERCENT)

AB	46.76	49.98	50.62	41.14	47.26	47.26	28.72	49.68	48.55	31.88
AN	0.05	0.29	0.29	0.30	0.14	0.29	0.05	0.14	0.15	0.30
OR	53.19	49.73	49.09	58.56	52.60	52.45	71.23	50.18	51.31	67.82

SOUTH QORQQ CENTRE FELDSPAR ANALYSES

	11	12	13	14	15	16	17	18	19	20
OXIDE WEIGHT PERCENTAGE										
SI02	69.23	67.46	67.71	66.63	66.19	65.88	67.40	69.41	66.93	68.73
AL2O3	18.57	18.48	18.56	18.70	18.75	18.38	18.69	18.73	18.64	18.73
FE2O3	0.30	0.51	0.35	0.30	0.22	0.30	0.23	0.30	0.20	0.13
CAO	0.03	0.03	0.01	0.09	0.09	0.01	0.06	0.09	0.04	0.04
NA2O	5.81	3.18	3.85	5.18	6.14	5.35	5.35	6.36	6.78	6.42
K2O	7.84	11.62	10.50	9.59	7.45	8.88	9.28	7.64	7.09	8.09
TOTAL	101.78	101.28	100.98	100.49	98.84	98.80	101.01	102.53	99.68	102.14

127075.7 127075.7 127075.7 127075.8 127075.8 127075.9 127075.9 127075.9 46269.8 46269.8 46269.8

ATOMIC PROPORTIONS ON THE BASIS OF 32 OXYGENS

SI	12.150	12.078	12.097	11.983	11.993	12.013	12.028	12.108	12.018	12.072
AL	3.843	3.901	3.910	3.965	4.005	3.951	3.933	3.852	3.946	3.879
FE3	0.040	0.069	0.047	0.041	0.030	0.041	0.031	0.039	0.027	0.017
CA	0.006	0.006	0.002	0.017	0.017	0.002	0.011	0.017	0.008	0.008
NA	1.978	1.104	1.334	1.807	2.158	1.892	1.852	2.152	2.362	2.187
K	1.756	2.655	2.394	2.201	1.722	2.066	2.113	1.701	1.624	1.813

END MEMBER COMPOSITION (WEIGHT PERCENT)

AB	51.31	28.04	34.33	43.33	53.79	46.20	45.00	54.04	57.59	53.00
AN	0.16	0.16	0.05	0.44	0.46	0.05	0.30	0.45	0.20	0.19
OR	48.53	71.81	65.62	56.23	45.75	53.75	54.71	45.51	42.21	46.81

SOUTH QOROQ CENTRE FELDSPAR ANALYSES

	21	22	23	24	25	26	27	28	29	30
	46269.8	46269.8	46269.8	46269.9	46269.9	46269.9	46269.9	58236.3	58236.3	58236.3
OXIDE WEIGHT PERCENTAGE										
SiO2	69.92	70.13	69.11	69.93	69.22	67.54	67.50	67.41	66.88	66.15
Al2O3	18.45	18.49	18.48	18.61	18.32	18.54	18.50	18.36	18.34	18.43
Fe2O3	0.19	0.23	0.25	0.15	0.26	0.19	0.25	0.19	0.22	0.19
CaO	0.03	0.03	0.04	0.03	0.03	0.06	0.03	0.03	0.01	0.01
Na2O	5.34	6.14	5.92	6.32	7.56	6.64	6.10	5.92	5.37	5.47
K2O	9.25	7.86	8.28	7.89	6.71	7.57	8.39	8.42	8.97	8.99
TOTAL	103.18	102.88	102.08	102.93	102.10	100.54	100.77	100.33	99.79	99.24

ATOMIC PROPORTIONS ON THE BASIS OF 32 OXYGENS

Si	12.172	12.180	12.133	12.151	12.117	12.045	12.045	12.073	12.063	12.015
Al	3.787	3.786	3.825	3.813	3.781	3.898	3.892	3.877	3.900	3.947
Fe3	0.025	0.030	0.033	0.020	0.034	0.026	0.034	0.026	0.030	0.026
Ca	0.006	0.006	0.008	0.006	0.006	0.011	0.006	0.006	0.002	0.002
Na	1.803	2.069	2.016	2.130	2.567	2.297	2.112	2.057	1.879	1.927
K	2.055	1.742	1.855	1.749	1.499	1.723	1.910	1.924	2.065	2.084

END MEMBER COMPOSITION (WEIGHT PERCENT)

Ab	45.10	52.63	50.39	53.25	61.56	55.42	50.84	50.00	46.04	46.45
An	0.15	0.15	0.20	0.15	0.14	0.29	0.15	0.15	0.05	0.05
Or	54.76	47.22	49.41	46.60	38.30	44.29	49.01	49.85	53.91	53.51

SOUTH QOROQ CENTRE FELDSPAR ANALYSES

	31	32	33	34	35	36	37	38	39	40
58236.3	58236.3	58236.4	58236.4	58236.4	58236.4	58236.4	127038.6	127038.6	127038.6	127038.6
OXIDE WEIGHT PERCENTAGE										
SiO2	67.18	66.88	66.80	66.74	66.63	67.05	65.79	66.46	66.52	66.16
Al2O3	18.28	18.48	17.91	18.02	17.91	18.14	18.35	18.24	18.50	18.41
Fe2O3	0.22	0.23	0.22	0.30	0.15	0.23	0.23	0.19	0.23	0.23
CaO	0.01	0.03	0.01	0.01	0.04	0.01	0.01	0.03	0.01	0.06
Na2O	5.42	6.72	5.79	4.21	6.12	5.86	4.40	6.10	4.98	5.10
K2O	9.03	8.11	8.45	10.66	8.21	8.96	10.03	8.36	9.78	9.25
TOTAL	100.14	100.45	99.18	99.94	99.06	100.25	98.81	99.38	100.02	99.21

ATOMIC PROPORTIONS ON THE BASIS OF 32 OXYGENS

Si	12.078	11.993	12.107	12.093	12.091	12.062	12.031	12.036	12.018	12.024
Al	3.875	3.907	3.827	3.850	3.832	3.848	3.956	3.895	3.941	3.945
Fe3	0.030	0.031	0.030	0.041	0.020	0.031	0.032	0.026	0.031	0.031
Ca	0.002	0.006	0.002	0.002	0.008	0.002	0.002	0.006	0.002	0.012
Na	1.890	2.338	2.036	1.480	2.154	2.045	1.561	2.143	1.745	1.798
K	2.072	1.856	1.954	2.465	1.901	2.057	2.340	1.932	2.255	2.145

END MEMBER COMPOSITION (WEIGHT PERCENT)

AB	46.11	54.10	49.41	36.02	51.44	48.24	38.47	50.93	42.06	43.89
AN	0.05	0.14	0.05	0.05	0.20	0.05	0.05	0.15	0.05	0.30
OR	53.84	45.76	50.54	63.93	48.37	51.71	61.47	48.92	57.89	55.80

## SOUTH QOROO CENTRE FELDSPAR ANALYSES

	41	42	43	44	45	46	47	48	49	50
	127038.6	127038.6	127038.7	127038.7	127038.7	58150.5	58150.5	58150.5	58150.6	58150.6
OXIDE WEIGHT PERCENTAGE										
SiO2	65.70	65.97	65.83	66.35	65.63	66.05	67.81	68.45	67.51	67.41
Al2O3	18.19	18.25	18.07	18.18	18.33	19.00	19.29	18.68	18.74	18.84
Fe2O3	0.23	0.26	0.20	0.23	0.30	0.20	0.12	0.15	0.13	0.26
CaO	0.06	0.01	0.01	0.04	0.07	0.20	0.28	0.06	0.20	0.16
Na2O	4.57	4.13	5.18	5.60	5.20	5.75	6.69	5.50	5.38	5.38
K2O	9.62	10.64	9.11	8.81	9.45	8.16	6.87	8.83	8.42	8.39
TOTAL	98.37	99.26	98.40	99.21	98.98	99.36	101.06	101.67	100.38	100.44

## ATOMIC PROPORTIONS ON THE BASIS OF 32 OXYGENS

Si	12.049	12.040	12.057	12.048	11.988	11.945	11.984	12.091	12.060	12.038
Al	3.933	3.927	3.902	3.892	3.948	4.051	4.019	3.890	3.947	3.967
Fe3	0.032	0.036	0.028	0.031	0.041	0.027	0.016	0.020	0.017	0.035
Ca	0.012	0.002	0.002	0.008	0.014	0.039	0.053	0.011	0.038	0.031
Na	1.626	1.462	1.840	1.973	1.843	2.017	2.294	1.885	1.864	1.864
K	2.251	2.478	2.129	2.041	2.203	1.883	1.549	1.990	1.919	1.912

## END MEMBER COMPOSITION (WEIGHT PERCENT)

AB	40.27	35.62	44.77	47.46	43.83	49.62	57.33	46.91	47.20	47.38
AN	0.31	0.05	0.05	0.20	0.35	1.01	1.41	0.30	1.03	0.83
OR	59.42	64.33	55.18	52.34	55.83	49.36	41.27	52.79	51.78	51.79

SOUTH QOROQ CENTRE FELDSPAR ANALYSES

	51	52	53	54	55	56	57	58	59	60
58150.6	58150.6	58150.7	58150.7	58150.7	58228.6	58228.6	58228.8	58228.8	58228.8	58228.8
OXIDE WEIGHT PERCENTAGE										
SiO2	67.42	68.28	67.41	67.75	65.30	67.49	66.92	66.97	66.51	66.85
Al2O3	18.73	18.85	18.60	18.64	18.68	18.82	18.75	18.90	18.68	18.74
Fe2O3	0.12	0.13	0.09	0.09	0.13	0.24	0.13	0.15	0.19	0.18
CaO	0.19	0.04	0.10	0.13	0.04	0.13	0.12	0.04	0.10	0.03
Na2O	5.74	7.96	5.73	5.95	7.16	11.44	7.08	6.91	5.51	5.75
K2O	8.83	5.32	7.77	8.00	6.69	0.85	6.89	7.73	9.12	9.38
TOTAL	101.03	100.58	99.70	100.56	98.00	98.97	99.89	100.70	100.11	100.93

ATOMIC PROPORTIONS ON THE BASIS OF 32 OXYGENS

Si	12.017	12.057	12.087	12.071	11.936	11.976	11.993	11.957	11.986	11.973
Al	3.936	3.924	3.932	3.916	4.026	3.938	3.962	3.978	3.969	3.957
Fe3	0.016	0.017	0.012	0.012	0.018	0.032	0.018	0.020	0.026	0.024
Ca	0.036	0.008	0.019	0.025	0.008	0.025	0.023	0.008	0.019	0.006
Na	1.985	2.727	1.993	2.056	2.539	3.938	2.461	2.393	1.926	1.998
K	2.098	1.199	1.778	1.819	1.560	0.192	1.576	1.761	2.097	2.144

END MEMBER COMPOSITION (WEIGHT PERCENT)

AB	47.67	67.96	51.00	51.14	60.31	94.45	59.10	55.94	46.07	46.59
AN	0.93	0.20	0.52	0.66	0.20	0.63	0.59	0.19	0.49	0.14
OR	51.40	31.84	48.48	48.20	39.50	4.92	40.31	43.87	53.44	53.27

SOUTH QOROO CENTRE FELDSPAR ANALYSES

	61	62	63	64	65	66	67	68	69	70
	58228.9	58228.9	58228.9	58228.9	58228.9	58164.6	58164.6	58164.6	58164.6	58164.6
OXIDE WEIGHT PERCENTAGE										
SI02	65.93	65.67	65.55	67.39	66.63	63.95	64.19	63.56	63.74	63.90
AL2O3	18.69	19.14	18.81	19.24	19.19	19.55	19.31	19.43	19.01	18.48
FE2O3	0.12	0.16	0.17	0.17	0.17	0.15	0.10	0.13	0.12	0.25
CAO	0.07	0.10	0.07	0.09	0.04	0.38	0.38	0.36	0.32	0.70
NA2O	6.11	6.70	5.87	6.88	6.41	6.29	6.41	3.93	4.75	4.96
K2O	8.10	7.78	8.29	6.68	7.91	9.17	8.33	10.82	10.52	10.82
TOTAL	99.02	99.55	98.76	100.45	100.35	99.49	98.72	98.23	98.46	99.11

ATOMIC PROPORTIONS ON THE BASIS OF 32 OXYGENS

SI	11.971	11.875	11.943	11.977	11.930	11.692	11.764	11.774	11.796	11.802
AL	4.001	4.081	4.041	4.032	4.051	4.214	4.173	4.243	4.148	4.024
FE3	0.016	0.022	0.023	0.023	0.023	0.021	0.014	0.018	0.017	0.035
CA	0.014	0.019	0.014	0.017	0.008	0.074	0.075	0.071	0.063	0.139
NA	2.152	2.350	2.075	2.372	2.226	2.231	2.279	1.412	1.705	1.777
K	1.877	1.795	1.927	1.515	1.807	2.139	1.948	2.558	2.484	2.550

END MEMBER COMPOSITION (WEIGHT PERCENT)

AB	51.65	54.86	50.08	59.23	53.52	48.61	51.40	33.52	38.58	38.29
AN	0.35	0.48	0.35	0.45	0.20	1.72	1.79	1.80	1.52	3.17
OR	48.00	44.66	49.57	40.31	46.29	49.67	46.82	64.68	59.89	58.54

SOUTH QORQQ CENTRE FELDSPAR ANALYSES

	71	72	73	74	75	76	77	78	79	80
	58164.7	58164.7	58164.7	58164.7	58221.7	58221.7	58221.7	58221.7	58221.7	58221.8
OXIDE WEIGHT PERCENTAGE										
SiO2	65.32	64.31	63.63	64.04	66.68	66.85	66.29	66.32	66.80	66.25
Al2O3	18.40	18.67	18.24	19.22	19.15	19.13	19.12	19.23	19.26	19.05
Fe2O3	0.29	0.15	0.13	0.15	0.13	0.13	0.12	0.19	0.10	0.12
CaO	0.39	0.60	0.66	0.70	0.31	0.33	0.38	0.38	0.41	0.42
Na2O	4.20	5.60	4.37	6.28	6.68	6.59	7.01	6.13	6.82	6.46
K2O	10.98	8.70	11.12	8.93	7.61	7.07	7.28	7.48	6.75	7.05
TOTAL	99.28	98.03	98.15	99.32	100.56	100.10	100.20	99.73	100.14	99.35

ATOMIC PROPORTIONS ON THE BASIS OF 32 OXYGENS

Si	11.928	11.864	11.857	11.724	11.916	11.954	11.890	11.922	11.931	11.939
Al	3.980	4.061	4.007	4.148	4.035	4.033	4.044	4.076	4.056	4.048
Fe3	0.040	0.021	0.018	0.021	0.017	0.017	0.016	0.026	0.013	0.016
Ca	0.077	0.119	0.132	0.137	0.059	0.063	0.073	0.073	0.078	0.081
Na	1.495	2.004	1.580	2.230	2.316	2.286	2.439	2.138	2.363	2.258
K	2.570	2.048	2.644	2.086	1.735	1.613	1.666	1.716	1.538	1.621

END MEMBER COMPOSITION (WEIGHT PERCENT)

AB	34.64	46.47	34.82	48.49	54.77	56.14	56.83	52.86	57.84	55.46
AN	1.89	2.92	3.08	3.17	1.49	1.65	1.81	1.92	2.04	2.11
OR	63.48	50.61	62.10	48.34	43.74	42.21	41.37	45.22	40.12	42.43

SOUTH QOROQ CENTRE FELDSPAR ANALYSES

	81	82	83	84	85	86	87	88	89	90
58221.8	58221.8	58221.8	58221.8	59672.6	59672.6	59672.6	59672.7	59672.7	59672.7	59672.8
OXIDE WEIGHT PERCENTAGE										
SiO2	66.19	66.56	66.30	64.17	63.20	63.61	64.45	64.97	65.78	65.65
Al2O3	19.18	18.95	19.33	21.14	21.55	22.21	20.80	20.07	20.76	19.81
Fe2O3	0.25	0.19	0.15	0.03	0.05	0.10	0.06	0.02	0.19	0.13
CaO	0.33	0.36	0.44	2.25	2.76	3.43	1.67	1.45	2.21	0.99
Na2O	7.01	6.50	6.89	8.70	8.21	8.90	6.67	5.38	8.50	4.51
K2O	6.65	7.30	6.77	2.28	2.56	1.16	5.85	6.99	2.12	8.65
TOTAL	99.61	99.86	99.88	98.57	98.33	99.41	99.50	98.88	99.56	99.74

ATOMIC PROPORTIONS ON THE BASIS OF 32 OXYGENS

Si	11.899	11.951	11.889	11.531	11.417	11.329	11.602	11.765	11.663	11.838
Al	4.065	4.012	4.087	4.479	4.590	4.664	4.415	4.285	4.340	4.212
Fe3	0.034	0.026	0.020	0.004	0.007	0.013	0.008	0.003	0.025	0.018
Ca	0.064	0.069	0.085	0.433	0.534	0.655	0.322	0.281	0.420	0.191
Na	2.445	2.264	2.397	3.033	2.877	3.075	2.329	1.890	2.924	1.578
K	1.526	1.673	1.549	0.523	0.590	0.264	1.344	1.615	0.480	1.990

END MEMBER COMPOSITION (WEIGHT PERCENT)

Ab	59.08	54.95	57.93	74.89	70.64	75.91	56.77	48.34	75.34	40.44
An	1.63	1.78	2.17	11.36	13.92	17.15	8.33	7.64	11.48	5.20
Or	39.29	43.26	39.90	13.76	15.44	6.94	34.90	44.02	13.17	54.36

SOUTH QOROO CENTRE FELDSPAR ANALYSES

	91	92	93	94	95	96	97	98	99	100
59672.8	59672.8	59676.4	59676.4	59676.4	59676.4	59676.5	59676.5	59676.5	59676.6	59676.6
OXIDE WEIGHT PERCENTAGE										
SiO2	65.66	66.25	66.76	66.39	67.17	66.31	65.82	65.88	66.33	67.44
Al2O3	19.88	20.00	19.12	19.14	19.45	19.13	19.38	19.30	19.17	19.16
Fe2O3	0.12	0.13	0.15	0.10	0.12	0.13	0.03	0.12	0.15	0.15
CaO	1.25	1.03	0.44	0.36	0.35	0.41	0.52	0.62	0.48	0.52
Na2O	4.82	4.65	7.11	6.13	6.58	5.46	6.26	7.15	7.32	6.44
K2O	7.96	8.20	7.21	7.72	6.52	7.84	6.76	6.37	6.44	7.45
TOTAL	99.69	100.26	100.79	99.84	100.19	99.28	98.77	99.44	99.89	101.16

ATOMIC PROPORTIONS ON THE BASIS OF 32 OXYGENS

Si	11.822	11.851	11.902	11.934	11.954	11.964	11.906	11.863	11.893	11.955
Al	4.220	4.218	4.019	4.056	4.081	4.069	4.133	4.097	4.052	4.005
Fe3	0.016	0.018	0.020	0.014	0.016	0.018	0.004	0.016	0.020	0.020
Ca	0.241	0.197	0.084	0.069	0.067	0.079	0.101	0.120	0.092	0.099
Na	1.683	1.614	2.459	2.137	2.272	1.911	2.197	2.497	2.546	2.215
K	1.829	1.872	1.640	1.771	1.481	1.805	1.560	1.464	1.473	1.685

END MEMBER COMPOSITION (WEIGHT PERCENT)

AB	43.30	42.27	57.24	52.16	57.95	48.77	55.38	59.69	60.42	53.82
AN	6.58	5.49	2.08	1.80	1.81	2.15	2.70	3.03	2.32	2.55
OR	50.12	52.24	40.69	46.04	40.25	49.08	41.92	37.28	37.26	43.64

## SOUTH QORQQ CENTRE FELDSPAR ANALYSES

	101	102	103	104	105	106	107	108	109	110
	59676.6	127025.5	127025.5	127025.5	46243.6	46243.6	46243.6	46243.7	46243.7	46243.7
OXIDE WEIGHT PERCENTAGE										
SiO2	66.47	66.98	67.30	67.14	66.91	67.62	67.39	67.18	67.09	67.16
Al2O3	19.09	19.63	19.57	19.36	19.05	18.87	18.96	18.93	18.68	18.89
Fe2O3	0.10	0.03	0.06	0.12	0.15	0.16	0.16	0.22	0.23	0.25
CaO	0.26	0.62	0.71	0.47	0.07	0.04	0.07	0.01	0.07	0.04
Na2O	5.96	8.48	7.99	7.15	6.05	5.83	6.18	5.56	5.33	4.89
K2O	8.16	4.93	4.40	6.74	7.92	8.35	8.67	8.92	8.91	9.40
TOTAL	100.04	100.67	100.03	100.98	100.15	100.87	101.43	100.82	100.31	100.63

## ATOMIC PROPORTIONS ON THE BASIS OF 32 OXYGENS

Si	11.943	11.857	11.924	11.909	11.982	12.032	11.973	11.996	12.032	12.019
Al	4.044	4.097	4.088	4.049	4.022	3.959	3.972	3.985	3.950	3.986
Fe3	0.014	0.004	0.008	0.016	0.020	0.021	0.021	0.030	0.031	0.034
Ca	0.050	0.118	0.135	0.089	0.013	0.008	0.013	0.002	0.013	0.008
Na	2.077	2.912	2.746	2.460	2.102	2.012	2.130	1.926	1.854	1.698
K	1.871	1.114	0.995	1.525	1.810	1.896	1.966	2.033	2.039	2.147

## END MEMBER COMPOSITION (WEIGHT PERCENT)

AB	50.37	68.95	69.54	58.85	51.96	49.80	50.25	47.05	45.88	42.51
AN	1.29	2.96	3.62	2.27	0.35	0.29	0.33	0.05	0.35	0.20
OR	48.34	28.10	26.84	38.88	47.68	50.00	49.42	52.90	53.76	57.28

## SOUTH QOROO CENTRE FELDSPAR ANALYSES

	111	112	113	114	115	116	117	118	119	120
	46243.8	46243.8	46243.8	46244.8	46244.8	46244.8	46244.9	46244.9	46244.9	46244.0

## OXIDE WEIGHT PERCENTAGE

SiO2	67.15	67.04	66.52	66.33	66.67	67.18	66.40	66.57	67.11	66.60
Al2O3	18.73	18.68	18.52	18.19	18.51	18.29	18.39	18.45	18.55	19.01
Fe2O3	0.13	0.22	0.25	0.26	0.15	0.20	0.17	0.19	0.12	0.19
CaO	0.09	0.03	0.04	0.03	0.13	0.04	0.15	0.09	0.15	0.10
Na2O	6.20	5.55	5.90	4.52	5.83	4.55	5.74	5.68	5.68	5.67
K2O	8.33	9.07	8.88	10.95	8.93	10.04	8.72	8.81	8.75	8.80

TOTAL	100.63	100.59	100.11	100.28	100.22	100.30	99.57	99.79	100.36	100.37
-------	--------	--------	--------	--------	--------	--------	-------	-------	--------	--------

## ATOMIC PROPORTIONS ON THE BASIS OF 32 OXYGENS

Si	12.003	12.012	11.990	12.022	12.002	12.090	12.016	12.019	12.035	11.954
Al	3.947	3.946	3.936	3.887	3.929	3.881	3.924	3.928	3.922	4.023
Fe3	0.017	0.030	0.034	0.035	0.020	0.027	0.023	0.026	0.016	0.026
Ca	0.017	0.006	0.008	0.006	0.025	0.008	0.029	0.017	0.029	0.019
Na	2.150	1.929	2.063	1.589	2.036	1.588	2.015	1.989	1.976	1.974
K	1.901	2.074	2.042	2.533	2.051	2.306	2.014	2.030	2.002	2.016

## END MEMBER COMPOSITION (WEIGHT PERCENT)

AB	51.28	46.54	48.57	37.01	47.92	39.19	48.07	47.70	47.73	47.66
AN	0.44	0.15	0.19	0.14	0.63	0.20	0.74	0.44	0.74	0.49
OR	48.29	53.31	51.24	62.85	51.45	60.61	51.19	51.86	51.53	51.85

## SOUTH QOROO CENTRE FELDSPAR ANALYSES

	121	122	123	124	125	126	127	128	129	130
	46244.0	46244.0	58154.0	58154.7	58154.7	58154.8	58154.8	58154.8	58154.9	58154.9
OXIDE WEIGHT PERCENTAGE										
SiO2	66.24	66.51	66.29	66.29	66.40	65.23	65.81	65.49	65.88	66.07
Al2O3	18.67	18.33	18.81	18.47	18.75	18.52	18.80	18.50	18.43	18.71
Fe2O3	0.10	0.26	0.17	0.19	0.28	0.52	0.17	0.23	0.17	0.26
CaO	0.15	0.10	0.01	0.03	0.04	0.07	0.10	0.04	0.04	0.32
Na2O	5.56	5.41	6.13	5.26	5.99	4.96	4.82	4.58	4.63	6.06
K2O	8.88	9.02	8.34	9.21	8.89	9.83	9.71	9.97	10.15	7.61
TOTAL	99.60	99.63	99.75	99.45	100.35	99.13	99.41	98.81	99.30	99.03

## ATOMIC PROPORTIONS ON THE BASIS OF 32 OXYGENS

Si	11.985	12.034	11.962	12.019	11.949	11.929	11.961	11.987	12.007	11.970
Al	3.983	3.910	4.002	3.948	3.978	3.993	4.029	3.992	3.960	3.997
Fe3	0.014	0.035	0.023	0.026	0.038	0.072	0.023	0.032	0.023	0.035
Ca	0.029	0.019	0.002	0.006	0.008	0.014	0.019	0.008	0.008	0.062
Na	1.952	1.899	2.146	1.850	2.091	1.760	1.699	1.626	1.637	2.130
K	2.050	2.083	1.920	2.131	2.041	2.294	2.252	2.329	2.361	1.759

## END MEMBER COMPOSITION (WEIGHT PERCENT)

Ab	46.83	45.88	51.16	44.83	48.92	41.71	41.25	39.51	39.34	52.32
An	0.74	0.50	0.05	0.15	0.19	0.35	0.50	0.20	0.20	1.62
Or	52.43	53.62	48.79	55.02	50.89	57.94	58.25	60.29	60.46	46.06

SOUTH QOROQ CENTRE FELDSPAR ANALYSES

	131	132	133	134	135	136	137	138	139	140
	58154.9	58230.8	58230.8	58230.8	58230.9	58230.9	58230.9	58230.0	58230.0	58230.0
OXIDE WEIGHT PERCENTAGE										
SI02	66.60	66.62	66.54	66.42	66.52	66.47	66.14	66.08	65.96	66.69
AL2O3	18.69	18.80	18.55	18.63	18.54	18.77	18.73	18.73	19.02	18.44
FE2O3	0.23	0.22	0.19	0.17	0.12	0.22	0.20	0.23	0.12	0.13
CAO	0.13	0.07	0.06	0.04	0.13	0.10	0.06	0.01	0.12	0.06
NA2O	6.19	4.95	5.09	5.24	5.20	5.40	5.26	5.12	5.39	5.69
K2O	8.40	9.44	8.94	9.26	8.91	9.12	9.27	9.24	9.06	8.61
TOTAL	100.24	100.10	99.37	99.76	99.42	100.08	99.66	99.41	99.67	99.62

ATOMIC PROPORTIONS ON THE BASIS OF 32 OXYGENS

SI	11.970	12.000	12.041	12.006	12.036	11.979	11.975	11.985	11.935	12.041
AL	3.961	3.992	3.958	3.970	3.955	3.988	3.998	4.005	4.058	3.925
FE3	0.031	0.030	0.026	0.023	0.016	0.030	0.027	0.031	0.016	0.018
CA	0.025	0.014	0.012	0.008	0.025	0.019	0.012	0.002	0.023	0.012
NA	2.158	1.730	1.787	1.837	1.825	1.888	1.847	1.801	1.892	1.993
K	1.927	2.170	2.064	2.136	2.057	2.097	2.142	2.138	2.092	1.984

END MEMBER COMPOSITION (WEIGHT PERCENT)

AB	50.93	42.64	44.68	44.58	45.13	45.56	44.60	44.13	45.64	48.38
AN	0.63	0.35	0.31	0.20	0.66	0.49	0.30	0.05	0.60	0.30
OR	48.44	57.00	55.01	55.22	54.21	53.94	55.10	55.82	53.77	51.32

SOUTH QOROQ CENTRE FELDSPAR ANALYSES

141 142 143 144 145 146 147 148 149 150  
 127027.6 127027.6 127027.6 127027.6 127027.7 127027.7 127027.8 127027.8 127027.8 58130.4

OXIDE WEIGHT PERCENTAGE

SiO2	66.84	66.96	66.60	66.95	66.53	66.40	66.27	66.69	66.90	63.15
Al2O3	18.56	18.65	18.53	18.73	18.68	18.43	18.68	18.12	18.73	22.65
Fe2O3	0.19	0.12	0.10	0.25	0.07	0.15	0.12	0.23	0.09	0.15
CaO	0.04	0.10	0.06	0.10	0.12	0.04	0.04	0.13	0.16	4.01
Na2O	5.90	6.09	6.01	6.55	6.61	5.89	5.65	6.12	6.53	8.40
K2O	8.21	7.90	8.32	7.67	7.88	9.05	8.63	7.80	7.63	1.24
TOTAL	99.74	99.82	99.62	100.25	99.89	99.96	99.39	99.09	100.04	99.60

ATOMIC PROPORTIONS ON THE BASIS OF 32 OXYGENS

Si	12.033	12.030	12.020	11.990	11.976	11.997	11.997	12.073	11.999	11.240
Al	3.940	3.950	3.943	3.955	3.965	3.926	3.987	3.868	3.961	4.753
Fe3	0.026	0.016	0.014	0.034	0.009	0.020	0.016	0.031	0.012	0.020
Ca	0.008	0.019	0.012	0.019	0.023	0.008	0.008	0.025	0.031	0.765
Na	2.060	2.122	2.104	2.275	2.308	2.064	1.984	2.149	2.272	2.900
K	1.886	1.811	1.916	1.753	1.810	2.086	1.994	1.802	1.746	0.282

END MEMBER COMPOSITION (WEIGHT PERCENT)

AB	50.52	52.11	50.60	54.65	54.16	48.05	48.20	52.47	54.54	72.29
AN	0.20	0.50	0.30	0.49	0.58	0.19	0.20	0.65	0.78	20.23
OR	49.28	47.39	49.10	44.86	45.26	51.75	51.60	46.88	44.67	7.48

## SOUTH QOROQ CENTRE FELDSPAR ANALYSES

	151	152	153	154	155	156	157	158
	58130.4	58130.4	58130.5	58130.5	58130.5	58130.6	58130.6	58130.6
OXIDE WEIGHT PERCENTAGE								
SiO <sub>2</sub>	64.07	61.26	60.50	63.36	62.38	64.34	63.78	64.17
Al <sub>2</sub> O <sub>3</sub>	21.83	24.24	24.60	22.57	23.62	22.46	22.40	22.47
Fe <sub>2</sub> O <sub>3</sub>	0.10	0.15	0.15	0.13	0.29	0.09	0.12	0.10
CaO	3.10	6.17	6.59	3.68	5.17	3.86	3.72	3.90
Na <sub>2</sub> O	8.70	7.88	8.03	8.70	8.25	8.26	8.22	8.84
K <sub>2</sub> O	0.96	0.27	0.24	1.53	0.69	1.43	1.44	0.80
TOTAL	98.76	99.97	100.11	99.97	100.40	100.44	99.68	100.28

## ATOMIC PROPORTIONS ON THE BASIS OF 32 OXYGENS

Si	11.438	10.890	10.774	11.254	11.037	11.339	11.326	11.315
Al	4.595	5.081	5.165	4.727	4.927	4.667	4.690	4.672
Fe <sub>3</sub>	0.013	0.020	0.020	0.017	0.039	0.012	0.016	0.013
Ca	0.593	1.175	1.258	0.700	0.980	0.729	0.708	0.737
Na	3.013	2.717	2.774	2.998	2.832	2.824	2.832	3.024
K	0.219	0.061	0.055	0.347	0.156	0.322	0.326	0.180

## END MEMBER COMPOSITION (WEIGHT PERCENT)

AB	77.75	67.43	66.57	72.93	70.12	71.67	72.04	75.64
AN	16.24	30.95	32.03	18.09	25.76	19.64	19.11	19.56
OR	6.01	1.62	1.39	8.99	4.11	8.70	8.85	4.80

APPENDIX IVWHOLE ROCK ANALYSES AND C.I.P.W. NORMSTable IV.1

List of G.G.U. sample numbers available for the South Qoroq Centre including dykes, country rocks etc. Also given are the name of the collector and references to the appropriate G.G.U. field diaries.

N.B. Not all of the samples have been analysed, and in general only analysed samples of syenites are indicated on Plate 1A.

<u>G.G.U. No's.</u>	<u>Collected by:-</u>	<u>Reference</u>
46202 - 05		
46286 - 88	C. H. Emeleus	G.G.U. Field Diary 1961
46298 - 300		
46237 - 84	W. T. Harry	G.G.U. Field Diary 1961
58118 - 22		
58130 - 69		
58191 - 94	C.H. Emeleus	G.G.U. Field Diary 1962
58200 - 77		
58327 - 34		
59640 - 90	W. T. Harry	G.G.U. Field Diary 1962
59721 - 34		
52201 - 07		
52229 - 40	C. H. Emeleus	G.G.U. Field Diary 1963
52254 - 300		
58346 - 51		
54113 - 21		
59865 - 76	W. T. Harry	G.G.U. Field Diary 1963
59883 - 89		
63892	C. H. Emeleus	G.G.U. Field Diary 1969
127001 - 100		
126801 - 15	D. Stephenson	G.G.U. Field Diary 1969

Table IV.2

Whole rock major and trace element analyses of the South Qorroq Centre rocks. Within each rock unit the analyses are arranged in numerical order in two groups. The first group are complete analyses including FeO, Fe<sub>2</sub>O<sub>3</sub>, H<sub>2</sub>O<sup>-</sup>, H<sub>2</sub>O<sup>+</sup> and CO<sub>2</sub>. These are followed by further analyses which are X.R.F. results only, in which total Fe is expressed as Fe<sub>2</sub>O<sub>3</sub> (Fe<sub>2</sub>O<sub>3</sub>T). The quoted total is exclusive of H<sub>2</sub>O<sup>-</sup>.

The trace elements are ppm cation Wt.%. Detection limits calculated as given in Appendix II and upper limits of standard calibration are:-

	<u>Detection Limit</u>	<u>Upper Limit of Standards</u>
Ba	8 ppm	5000 ppm
Nb	3 "	573 "
Zr	3 "	5000 "
Y	3 "	500 "
Sr	3 "	1100 "
Rb	3 "	1000 "
Pb	7 "	266 "
Zn	2 "	1000 "
Cu	2 "	1000 "
Ni	2 "	1000 "
La	3 "	272 "
Th	7 "	1100 "
U	5 "	2700 "
V	5 "	998 "

Also quoted are the height above sea level of the sample in metres (HT OD), and the distance in metres from the outer edge of the appropriate intrusion (DIST). In the case of SS4, distances for both SS4a and SS4b are quoted from the outer contact of SS4a.

Specimen localities are shown on Plate 1A.

[ ] = Samples with heavily altered nepheline, loss of Na and high H<sub>2</sub>O<sup>+</sup> (see Chapter 5).

□ = Samples with Si contamination by country-rock quartzite

R = Samples with pronounced recrystallisation near to the Igdlarfigssalik Centre

C = Samples with extensive development of cumulus mafic phases

## SOUTH QOROO CENTRE

58205

127011

## TUNUGDLIARFIK SYENITE

58205

127011

## PERCENT

SI02	55.87	55.13
TI02	0.74	0.23
AL203	20.81	21.54
FE203	1.98	1.96
FEO	3.04	1.64
MNO	0.14	0.13
MGO	0.17	0.19
CAO	1.20	1.09
NA2O	8.03	8.92
K2O	6.58	6.80
P2O5	0.02	0.07
H2O+	0.81	0.80
CO2	0.52	0.96
TOTAL	99.91	99.46
H2O-	0.23	0.31

## PPM

BA	116	114
NB	176	114
ZR	449	450
Y	30	41
SR	113	128
RB	238	260
PB	7	14
ZN	137	93
CU	8	7
NI	6	6
LA	53	89
TH	7	12
U	7	7
V	4	5
HT OD	40	1
DIST	50	150

SOUTH QOROQ CENTRE	OSTFJORDSDAL		SYENITE		52281	52288	52290
	52258	52278	52280	52288			
PERCENT							
SI02	56.18	56.31	55.29	54.49	54.49	55.61	57.40
TI02	0.34	0.56	0.63	1.29	1.29	0.37	0.64
AL203	21.78	19.51	18.97	19.08	19.08	20.76	19.49
FE203T	4.42	5.48	6.98	8.29	8.29	4.73	4.87
FE203	1.89						
FEO	1.79						
MNO	0.12	0.18	0.25	0.24	0.24	0.15	0.17
MGO	0.29	0.24	0.36	0.26	0.26	0.10	0.43
CAO	1.14	1.16	2.32	1.98	1.98	1.47	1.98
NA2O	9.90	7.92	8.09	7.50	7.50	9.16	8.33
K2O	6.23	5.86	5.28	5.53	5.53	5.50	5.13
P2O5	0.11	0.14	0.26	0.25	0.25	0.14	0.26
H2O+	0.72						
CO2	0.55						
TOTAL	101.04	97.90	98.43	98.91	98.91	97.99	98.70
H2O-	0.26						

PPM	OSTFJORDSDAL		SYENITE		52281	52288	52290
	52258	52278	52280	52288			
BA	735	760	961	362	362	821	2183
NB	111	127	149	280	280	181	188
ZR	382	442	451	799	799	530	754
Y	21	36	39	48	48	32	45
SR	283	482	360	195	195	541	855
RB	215	258	149	180	180	210	159
PB	10	18	12	30	30	25	33
ZN	83	144	131	227	227	110	116
CU	7	6	8	9	9	6	5
NI	13	5	4	7	7	6	6
LA	50	65	69	116	116	60	78
TH	6	11	9	30	30	20	19
U	4	0	3	6	6	5	4
V	4	5	6	3	3	6	4
HT OD	560	630	35	600	600	800	760
DIST	90	20	20	1500	1500	450	600

PERCENT	SOUTH QOROQ CENTRE [46298]		NARSSARSSUAQ [52204]		SYENITE [52240]	
		52203	55.83	59.64		
SI02	57.90	56.22	0.84	0.64		
TI02	1.14	0.29	18.63	19.69		
AL203	16.80	19.79	6.62	4.15		
FE203T	7.40	5.50	0.24	0.13		
MNO	6.36	0.23	2.31	1.51		
MGO	1.25	6.11	2.64	1.39		
CAO	2.46	1.35	5.12	4.44		
NA2O	5.61	9.70	5.57	7.27		
K2O	5.02	5.16	0.32	0.19		
P2O5	0.34	0.08	98.12	99.05		
TOTAL	98.28	98.43				

PPM	174	1344	1760
BA	174	1344	1760
NB	346	220	185
ZR	1599	905	586
Y	94	53	34
SR	73	321	454
RB	273	171	209
PB	18	28	4
ZN	187	195	111
CU	9	8	4
NI	6	8	6
LA	131	91	54
TH	24	27	12
U	4	8	2
V	7	14	10
HT OD	40	40	40
DIST	390	540	380

SOUTH QOROO CENTRE [58244]	MICROSyenite SHEETS AND ESSEXITE			58130
	127027 [127028]	127029	127030 [126811]	
PERCENT				C R
SiO2	56.62	54.00	55.01	46.83
TiO2	0.28	0.61	0.27	3.02
Al2O3	20.53	20.52	22.13	16.22
Fe2O3T	6.82	5.13	4.70	12.67
MnO	0.22	0.19	0.17	6.23
MgO	6.18	6.54	0.18	3.55
CaO	1.64	1.86	1.35	7.64
Na2O	6.27	9.70	6.92	5.09
K2O	5.79	5.50	7.07	2.47
P2O5	0.06	0.22	0.10	3.00
TOTAL	98.41	98.27	97.90	100.73

PPM	MICROSyenite SHEETS AND ESSEXITE			3071
	127027 [127028]	127029	127030 [126811]	
BA	144	849	130	454
NB	239	191	155	199
ZR	1289	666	565	707
Y	82	50	39	88
SR	433	334	191	2685
RB	300	173	330	175
PB	27	27	14	36
ZN	196	123	99	0
CU	9	7	13	115
NI	4	7	5	22
LA	106	78	72	4
TH	8	13	11	72
U	5	8	7	5
V		3	5	0
HT OD	690	750	780	1
DIST	1	1	1	1



SOUTH QOROO CENTRE		SYENITE SS2		[52299]					
PERCENT	46250	46255	46273	46276	52296	58202	58211	58231	58245
SI02	55.08	55.54	55.46	55.79	55.03	55.63	56.09	55.84	53.57
TI02	0.40	0.49	0.42	0.39	0.38	0.44	0.43	0.51	0.23
AL203	20.64	20.25	20.46	21.58	20.16	20.25	21.55	19.30	19.79
FE203	2.17	2.51	2.21	1.57	2.60	2.36	2.17	3.03	4.27
FEO	3.35	3.87	3.02	2.09	3.23	2.93	2.47	3.64	1.66
MNO	0.22	0.25	0.17	0.12	0.23	0.21	0.18	0.28	0.28
MGO	0.20	0.27	0.29	0.29	0.28	0.21	0.13	0.35	0.18
CAO	1.41	1.67	1.42	1.13	1.41	1.35	1.13	1.69	1.69
NA2O	8.43	8.12	8.42	9.18	8.52	8.37	8.55	8.19	9.76
K2O	6.09	5.93	6.22	6.07	6.25	6.21	6.47	5.89	4.93
P2O5	0.12	0.14	0.11	0.07	0.10	0.09	0.10	0.14	0.02
H2O+	0.05	0.62	0.41	0.33	0.49	0.49	0.61	0.86	1.54
CO2	0.10	0.16	0.47	0.40	0.25	0.36	0.40	0.60	0.89
TOTAL	98.26	99.82	99.08	99.01	98.93	98.90	100.28	100.32	98.81
H2O-	0.13	0.56	0.43	0.22	0.25	0.16	0.38	0.30	0.26

PPM	BA	NR	ZR	Y	SR	RB	PB	ZN	CU	NI	LA	TH	U	V	HT OD	DIST
	38	151	598	21	81	247	14	134	11	4	54	3	3	5	160	5
	154	204	757	44	108	260	9	155	10	7	80	8	13	4	500	200
	136	139	488	21	96	249	7	109	12	6	47	2	7	5	260	220
	204	127	284	18	302	219	9	110	5	5	36	2	4	6	240	60
	66	204	744	38	67	242	17	152	9	6	75	7	6	4	750	60
	189	235	891	43	720	230	32	189	14	7	87	10	13	4	660	170
	112	135	522	59	67	228	20	128	8	7	53	31	6	5	1	280
	93	93	254	30	80	223	7	94	10	6	38	3	7	6	20	60
	191	228	954	50	138	233	23	181	12	3	97	13	6	5	665	1000
	48	302	1580	110	78	364	53	281	4	5	189	34	13	5	690	60

SOUTH OOROO CENTRE  
[58256]

58266 SYENITE SS2  
58267

[127007]

[58274]

[58271]

[58268]

PERCENT	58269	58273	58275
SI02	55.13	56.52	56.14
TI02	0.56	0.41	0.36
AL203	19.55	22.14	21.59
FE203	2.55	1.57	2.20
FEO	3.35	2.71	2.43
MNO	0.23	0.14	0.19
MGO	0.29	0.12	0.16
CAO	1.69	1.22	1.07
NA2O	7.78	8.81	8.36
K2O	5.98	6.47	6.39
P2O5	0.13	0.08	0.11
H2O+	0.93	0.53	0.88
CO2	0.54	0.38	0.32
TOTAL	98.71	101.10	100.20
H2O-	0.36	0.30	0.32

55.47
0.52
20.37
1.90
3.69
0.19
0.31
1.70
5.34
6.17
0.11
2.42
0.70
98.89
0.30

55.86
0.47
21.97
2.41
2.52
0.22
0.54
1.63
4.94
6.79
0.11
1.85
0.21
99.52
0.54

56.36
0.39
21.88
2.40
1.72
0.13
0.16
4.52
4.66
6.23
0.11
2.34
0.58
101.48
0.47

55.40
0.70
20.29
3.03
3.49
0.24
0.21
1.66
5.93
6.25
0.11
1.76
0.37
99.44
0.29

PPM

BA	190	92	137	72	88	489
NR	310	265	98	106	136	116
ZR	1116	936	288	250	376	406
Y	58	65	19	17	16	16
SR	112	72	753	82	129	1827
RB	231	247	221	205	248	231
PB	31	28	8	5	31	26
ZN	187	166	97	81	109	122
CU	8	13	6	9	7	6
NI	5	5	7	7	0	4
LA	273	270	37	35	28	32
TH	15	18	4	3	11	3
U	10	10	2	2	3	0
V	7	5	6	7	5	3
HT OD	640	660	500	560	560	1
DIST	1300	1300	1	1	15	20

216
223
722
85
155
210
44
182
8
5
102
52
9
7
540
1450

177
357
1655
74
136
244
44
175
13
6
340
13
7
670
1400

216
223
722
85
155
210
44
182
8
5
102
52
9
7
540
1450

177
357
1655
74
136
244
44
175
13
6
340
13
7
670
1400



SOUTH QOROO CENTRE		SYENITE SS2	
	52234	52235	52237
PERCENT			
SiO2	54.46	54.63	54.99
TiO2	0.58	0.44	0.52
Al2O3	19.05	19.23	19.34
Fe2O3T	7.67	6.80	7.36
MNO	0.30	0.26	0.22
MGO	0.31	0.15	0.86
CaO	1.81	1.56	1.52
Na2O	8.29	8.39	7.97
K2O	5.78	5.88	6.01
P2O5	0.17	0.10	0.11
TOTAL	98.42	97.44	98.90

	52239	59726	[59728]	59730	59732
	56.30	55.15	57.27	55.88	55.02
	0.76	0.46	0.37	0.26	0.50
	17.04	19.97	22.20	20.50	19.03
	9.41	6.34	5.16	4.17	7.17
	0.32	0.25	0.20	0.15	0.31
	0.81	0.21	0.13	0.10	0.36
	2.17	1.56	1.32	0.99	2.00
	5.35	7.52	5.87	8.82	8.73
	5.56	6.12	6.84	6.23	5.70
	0.22	0.12	0.11	0.06	0.16
	97.94	97.70	99.47	97.16	98.98

PPM	52239	59726	[59728]	59730	59732
BA	264	108	172	195	187
NB	362	277	145	218	383
ZR	1223	1016	470	817	1220
Y	64	66	30	47	73
SR	848	128	324	109	97
RB	128	240	248	242	224
PB	32	30	3	66	47
ZN	239	173	116	142	211
CU	23	5	3	1	8
NI	9	6	6	5	2
LA	128	118	47	68	131
TH	20	25	6	20	31
U	6	3	3	4	8
V	7	7	5	6	5
HT OD	460	1	1	20	1
DIST	20	400	350	300	200

	SOUTH QOROO CENTRE		SYENITE SS3		52297	52300	[58234]	58236	58257	127015	[127016]
PERCENT	46269	46270	46271								
SI02	54.29	53.46	55.20		55.02	54.73	53.84	55.32	55.58	55.35	54.54
TI02	0.55	0.51	0.51		0.56	0.49	0.29	0.35	0.43	0.30	0.29
AL203	19.54	21.35	19.84		17.92	20.10	23.72	20.14	19.76	20.02	20.44
FE203	1.65	1.91	2.07		3.51	2.93	1.20	2.43	3.02	3.39	4.34
FEO	3.56	3.57	3.88		4.85	2.84	3.39	2.97	3.00	2.62	2.52
MNO	0.19	0.20	0.25		0.33	0.22	0.18	0.21	0.25	0.25	0.30
MGO	0.37	0.22	0.28		0.48	0.39	0.48	0.28	0.35	0.28	0.21
CAO	1.33	1.40	1.56		1.75	1.45	1.20	1.40	1.24	1.34	1.32
NA2O	8.03	9.37	8.12		6.89	8.07	3.02	7.73	7.03	8.33	5.48
K2O	5.83	5.71	5.87		6.06	6.03	8.33	6.09	6.27	6.22	6.09
P2O5	0.14	0.13	0.15		0.12	0.13	0.07	0.09	0.05	0.07	0.07
H2O+	1.02	0.25	0.47		0.94	0.85	2.41	0.94	1.18	1.22	2.53
CO2	0.78	0.15	0.16		0.42	0.31	0.87	0.42	0.65	0.31	0.45
TOTAL	97.28	98.21	98.36		98.85	98.54	99.00	98.37	98.81	99.70	98.58
H2O-	0.24	0.09	0.19		0.29	0.26	0.18	0.31	0.37	0.25	0.48

PPM	BA	NB	ZR	Y	SR	RB	PB	ZN	CU	NI	LA	TH	U	V	HT OD	DIST
	375	179	548	82	204	233	21	138	8	6	64	19	9	6	220	180
	168	110	473	27	203	279	10	143	10	5	51	13	4	4	280	180
	234	219	705	41	158	249	25	150	11	5	77	10	9	6	240	40
	136	443	1297	37	237	279	38	234	13	5	77	15	9	4	1050	180
	428	232	753	49	285	224	37	163	12	5	91	17	9	4	660	200
	370	112	475	37	235	332	17	114	8	4	60	6	6	5	770	1300
	454	230	711	28	280	283	26	142	12	5	63	8	8	6	840	800
	397	264	775	35	366	320	27	214	11	5	84	15	6	5	855	1000
	125	264	957	47	100	276	23	191	5	5	74	16	11	5	610	400
	65	396	1697	84	343	308	53	248	9	6	161	25	16	5	620	150

PERCENT	SOUTH QOROO CENTRE		SVENITE SS3		127038	59659	59664	58328
	127017	[127018]	[127033]	[127033]				
SI02	55.23	54.33	56.33	54.00		55.19	46.91	58.67
TI02	0.22	0.40	0.30	0.39		0.34	0.11	0.65
AL203	19.92	16.81	20.77	18.96		20.44	26.41	20.17
FE203T						5.16	2.85	3.95
FE203	3.76	6.50	2.18	3.12				
FEO	1.84	2.84	2.88	2.59				
MNO	0.23	0.44	0.20	0.18		0.21	0.08	0.13
MGO	0.15	0.38	0.27	0.19		0.19	0.02	0.20
CAO	1.49	3.26	1.44	1.41		1.34	0.38	1.54
NA2O	7.73	5.57	6.53	8.13		8.87	14.00	7.53
K2O	6.24	5.45	6.46	5.87		5.98	4.43	6.55
P2O5	0.04	0.04	0.08	0.07		0.11	0.03	0.13
H2O+	1.20	2.47	1.36	0.88				
CO2	0.35	0.40	0.32	0.66				
TOTAL	98.35	98.89	99.12	96.45		97.83	95.22	99.52
H2O-	0.42	0.39	0.39	0.34				
PPM								
BA	53	133	426	102		312	72	768
NB	577	779	201	330		206	454	58
ZR	1997	5242	650	1003		872	2193	125
Y	137	170	28	54		52	88	73
SR	70	564	304	121		201	62	399
RB	328	253	296	293		246	290	153
PB	49	87	18	36		39	5	0
ZN	228	419	130	193		147	81	52
CU	4	10	5	12		3	3	4
NI	5	5	0	6		5	6	0
LA	218	259	53	95		79	98	139
TH	39	34	8	23		33	5	24
U	18	17	2	9		8	3	0
V	6	5	5	5		9	6	
HT OD	650	680	930	630		10	10	180
DIST	40	1	1100	340		40	5	1350

SOUTH QOROQ CENTRE		SYENITE SS4A		[127024]		58258A		58258B		127025		127086		127093		59676		58327	
[58149]		58228		58258A		58258B		[127024]		127025		127086		127093		59676		58327	
PERCENT																			
SI02	54.94	57.58	57.35	57.91	54.38	54.99	56.92	58.74	54.01	57.70	58.57	57.70	54.01	57.70	58.57	57.70	54.01	57.70	58.57
TI02	0.22	0.62	0.59	0.56	0.46	0.60	0.58	0.29	0.56	0.94	0.36	0.29	0.56	0.94	0.36	0.29	0.56	0.94	0.36
AL203	22.49	20.13	20.31	20.06	19.49	19.73	20.19	20.30	17.78	18.93	21.07	20.30	17.78	18.93	21.07	20.30	17.78	18.93	21.07
FE203T																			
FE203	2.47	1.14	1.63	1.75	2.36	1.61	1.09	1.03	2.45	5.29	3.46	1.03	2.45	5.29	3.46	1.03	2.45	5.29	3.46
FEO	2.43	3.08	3.05	3.21	3.41	4.00	3.12	2.04	3.66			2.04	3.66			2.04	3.66		
MNO	0.20	0.15	0.17	0.18	0.24	0.23	0.15	0.10	0.22			0.10	0.22			0.10	0.22		
MGO	0.12	0.41	0.40	0.39	0.33	1.03	0.59	0.53	0.41			0.53	0.41			0.53	0.41		
CAO	0.91	1.59	1.71	1.76	1.73	1.31	1.82	2.48	1.80			2.48	1.80			2.48	1.80		
NA2O	6.54	7.49	7.53	7.20	9.31	5.59	7.90	7.34	7.49			7.34	7.49			7.34	7.49		
K2O	6.25	6.46	5.91	6.11	5.44	5.41	5.75	5.19	5.42			5.19	5.42			5.19	5.42		
P2O5	0.03	0.21	0.19	0.19	0.13	0.20	0.24	0.10	0.23			0.10	0.23			0.10	0.23		
H2O+	2.23	0.48	0.65	0.61	0.64	2.69	0.53	0.80	0.72			0.80	0.72			0.80	0.72		
CO2	0.42	0.31	0.24	0.24	0.33	0.69	0.28	0.61	0.46			0.61	0.46			0.61	0.46		
TOTAL	99.25	99.65	99.73	100.17	98.25	98.08	99.16	99.55	95.21			99.55	95.21			99.55	95.21		
H2O-	0.30	0.23	0.30	0.29	0.35	0.39	0.27	0.27	0.46			0.27	0.46			0.27	0.46		
PPM																			
BA	153	823	977	968	593	1161	1190	1518	568			1518	568			2033	811		
NB	246	94	126	123	228	124	120	40	129			40	129			128	29		
ZR	1252	297	443	409	1249	465	427	181	620			181	620			371	99		
Y	37	23	33	32	73	32	32	13	32			13	32			31	44		
SR	249	289	375	359	226	357	417	685	222			685	222			576	338		
RB	335	190	174	176	186	144	151	119	209			119	209			122	260		
PB	18	14	19	17	53	9	20	13	14			13	14			21	13		
ZN	160	86	105	111	184	120	85	47	145			47	145			95	43		
CU	0	9	9	9	8	27	9	11	11			11	11			9	4		
NI	7	6	6	7	5	0	6	7	6			7	6			8	6		
LA	50	43	55	59	122	54	55	31	62			31	62			55	72		
TH	7	1	8	2	30	5	7	0	4			0	4			7	18		
U	3	5	7	15	9	3	4	4	8			4	8			4	7		
V	4	0	3	4	5	3	3	7	4			7	4			5	7		
HT OD	40	40	780	860	860	790	820	150	1			150	1			1	180		
DIST	190	190	80	20	20	100	320	60	1			60	1			80	10		

SOUTH OOROO CENTRE

	SYENITE SS4B			
	58146	58147	58148	58164
PERCENT				
SiO2	53.54	55.32	56.49	57.10
TiO2	1.13	1.71	0.55	1.09
Al2O3	17.70	18.66	19.41	17.68
Fe2O3	2.92	0.97	2.06	1.89
FEO	5.49	5.19	2.91	3.11
MNO	0.32	0.19	0.20	0.25
MGO	1.49	1.36	0.48	0.96
CAO	2.83	4.02	1.84	3.11
NA2O	4.78	5.68	8.24	6.80
K2O	5.30	4.61	5.92	5.39
P2O5	0.33	0.76	0.20	0.37
H2O+	0.42	0.14	0.78	0.82
CO2	0.75	0.18	0.52	1.25
TOTAL	97.00	98.79	99.60	99.82
H2O-	0.38	0.28	0.14	0.28

	58165	58220	58221	58259
R	54.66	56.03	57.24	56.52
	0.79	1.50	0.98	0.97
	21.52	19.39	19.57	19.36
	1.56	0.42	1.42	0.83
	2.77	5.36	3.97	4.40
	0.16	0.18	0.19	0.19
	0.64	1.24	0.68	0.65
	1.70	3.96	2.43	2.48
	8.52	5.51	6.78	7.18
	5.76	4.14	5.40	5.44
	0.30	0.74	0.34	0.34
	0.66	1.28	1.20	0.49
	0.67	0.56	0.53	0.33
	99.71	100.31	100.73	99.18
	0.32	0.12	0.36	0.32

	58164	58148	58164	58165	58220	58221	58259
PPM							
BA	377	860	1779	659	4470	1946	2048
NB	234	156	115	34	71	146	132
ZR	802	543	366	89	259	483	460
Y	60	43	56	18	26	40	35
SR	318	318	807	349	1698	765	744
RB	159	185	135	72	62	152	150
PB	17	66	19	9	21	16	28
ZN	209	124	142	51	90	120	107
CU	13	3	12	9	11	11	11
NI	5	6	4	5	6	13	3
LA	107	85	99	38	49	61	62
TH	17	8	14	4	2	13	9
U	9	2	2	4	2	7	4
V	1	4	0	3	0	0	1
HT OD	10	1	140	140	860	790	855
DIST	380	210	470	470	940	540	340

SOUTH QDROQ CENTRE		SYENITE SS4B	
PERCENT	59671	59672	59673
SI02	45.62	52.71	53.69
TI02	3.54	2.48	2.17
AL203	11.76	16.20	17.60
FE203T	14.50	10.05	8.57
MNO	0.31	0.25	0.23
MGO	4.55	2.55	1.79
CAO	6.24	5.32	4.21
NA2O	3.49	5.03	5.23
K2O	3.60	3.94	4.42
P2O5	2.33	1.43	0.97
TOTAL	95.94	99.96	98.88

	58333
	58.38
	1.31
	18.68
	5.39
	0.16
	0.89
	2.75
	6.43
	5.54
	0.46
	99.99

PPM	2798	3205	3748	2271	2300
BA	107	126	92	116	91
NB	332	447	321	372	284
ZR	60	48	35	38	30
Y	864	1286	1455	728	729
SR	89	78	111	107	99
RB	28	86	22	14	14
PB	129	133	115	71	99
ZN	26	21	17	10	10
CU	5	5	6	7	6
NI	95	88	63	57	45
LA	11	11	11	7	1
TH	2	1	1	4	0
U	0	8	1	3	
V	1	1	1	1	
HT OD	380	380	380	1	590
DIST				240	550



SOUTH OOROO CENTRE PERCENT	SYENITE SS5		58348	[127026]		127091	127092
	58222	58230		57.89	55.79		
SI02	53.75	56.32	56.11	57.89	55.79	53.87	
TI02	0.85	0.30	0.43	0.22	0.27	0.28	
AL203	20.94	21.53	19.49	19.57	20.68	20.28	
FE203	1.60	1.92	2.78	1.57	2.41	1.25	
FEO	3.71	2.27	2.47	1.72	2.60	2.39	
MNO	0.16	0.16	0.24	0.11	0.20	0.12	
MGO	0.44	0.18	0.50	0.67	0.29	0.17	
CAO	1.58	1.23	1.71	1.32	1.39	1.04	
NA2O	8.64	9.34	7.90	5.83	7.45	8.85	
K2O	6.17	6.38	6.74	7.17	6.31	5.74	
P2O5	0.23	0.10	0.14	0.08	0.09	0.09	
H2O+	0.72	0.63	0.81	2.33	1.26	0.57	
CO2	0.75	0.42	1.24	0.81	0.39	0.35	
TOTAL	99.54	100.78	100.56	99.29	99.13	95.00	
H2O-	0.22	0.34	0.31	0.40	0.43	0.24	

PPM	58222	58230	58348	[127026]	127091	127092
BA	179	367	360	404	479	463
NB	283	85	150	111	173	141
ZR	1012	328	445	478	660	549
Y	66	25	49	43	33	28
SR	102	298	311	124	310	209
RB	210	279	245	252	274	224
PB	27	10	35	27	20	107
ZN	190	81	148	94	122	94
CU	9	10	10	8	12	6
NI	5	5	7	7	5	6
LA	89	53	95	58	50	40
TH	22	11	14	13	14	6
U	11	8	7	8	4	5
V	5	0	3	6	6	6
HT OD	800	780	110	870	1	1
DIST	560	170	1800	100	900	1000

SOUTH QOROO CENTRE		SYENITE SS5	
PERCENT	59643	59644	59649
SI02	54.14	53.23	55.19
TI02	0.51	0.44	0.41
AL203	19.38	19.86	20.09
FE203T	6.29	5.26	5.08
MNO	0.28	0.24	0.19
MGO	0.41	0.49	0.25
CAD	2.10	2.03	1.40
NA2O	7.77	8.39	8.68
K2O	6.00	5.82	6.18
P2O5	0.15	0.21	0.18
TOTAL	97.03	95.97	97.65

PPM	59651	59655	59667	59669	59678	58334	58351
BA	471	495	626	522	440	109	793
NB	176	194	177	97	152	149	123
ZR	574	859	451	316	520	546	387
Y	62	44	25	65	29	80	96
SR	181	227	172	184	205	105	445
RB	192	239	224	314	231	200	220
PB	17	13	12	15	7	14	28
ZN	183	100	100	104	99	117	196
CU	16	4	7	7	6	7	7
NI	5	6	5	7	31	5	12
LA	135	61	37	98	44	165	135
TH	17	19	9	17	7	23	35
U	2	6	1	1	2	1	1
V	6	7	5	6	8		
HT OD	15	1	1	1	1	250	40
DIST	740	300	1470	900	950	60	500

Table IV.3

C.I.P.W. norms and other petrochemical functions for the analyses listed in Table IV.2. The table is arranged in the same order as the previous table with norms of complete analyses followed by norms based on an X.R.F. analysis only. In the latter, a common  $\text{Fe}_2\text{O}_3/\text{FeO}$  ratio is read in for all the analyses in each unit, equal to the average ratio of the complete analyses in the same unit. In units for which no complete analyses are available (e.g. the Essexite) a suitable estimate has been made. Norms for which an  $\text{Fe}_2\text{O}_3/\text{FeO}$  ratio has been read in are identified by "EMPIRICAL FE RATIO" being included in the title.

The norms were calculated using the program "NORMCAL" developed by R. C. O. Gill. The norm and Differentiation Index (the latter being the sum of all components in the system  $\text{SiO}_2 - \text{NaAlSi}_3\text{O}_8 - \text{KAlSi}_3\text{O}_8$ , Thornton and Tuttle, 1960) are given in Wt.%; the other functions are calculated from cation Mol.%.

Symbols as for Table IV.2

S. QORDQ CENTRE - TINUGDLIARFIK SYFNITE

NORMCAL .. R.C.O.GILL

SUMMARY NORM TABLE

58215 127011

OPHOCLEASE	30.4	41.1
ALBITE	27.2	28.2
ANORTHITE	1.3	1.3
NEPHELINE	22.6	29.5
ACMITE	2.1	2.3
DIOPSIDE	4.3	4.4
OLIVINE	1.1	0.1
MAGNETITE	2.0	1.8
ILMENITE	1.4	0.4
APATITE	. .	0.2
WATER	. .	0.8
DIFF. INDEX	80.2	90.8
NA/(NA+K)	0.65	0.67
(NA+K)/AL	0.00	1.02
F3/(F2+F3)	0.37	0.52

## S. QORQQ CENTRE - OSTFJORDSDAL SYENITE

NORMCAL .. R.C.D.GILL

## SUMMARY NORM TABLE

52258

ORTHOCLASE	36.9
ALBITE	20.2
NEPHELINE	31.1
ACMITE	5.5
SOD METASIL	1.1
DIOPSIDE	4.3
OLIVINE	1.1
ILMENITE	.4
APATITE	1.3
WATER	0.7
DIFF. INDEX	88.2
NA/(NA+K)	1.71
(NA+K)/AL	1.06
F3/(F2+F3)	0.49



S. QORDQ CENTRE - NARSSARSSUAQ SYENITE EMPIRICAL FE RATIO

NORMCAL .. R.C.C.O.GILL

SUMMARY NORM TABLE

	[44298]	52263	[52264]	[52240]
QUARTZ	0.0	0.0	0.0	0.5
CORUNDUM	0.0	0.0	0.1	2.5
ORTHOCLASE	30.2	31.1	33.7	43.5
ALBITE	49.5	28.6	38.7	38.0
ANORTHITE	6.0	5.0	11.3	5.7
NEPHELINE	0.0	24.8	3.0	0.0
ACMITE	0.0	6.6	0.0	0.0
SOD MFTASIL	0.0	0.4	0.0	0.0
DIOPSIDE	3.5	5.6	0.0	0.0
HYPERSTHENE	1.8	1.0	0.0	5.7
OLIVINE	2.4	2.1	6.7	0.0
MAGNETITE	4.5	0.0	4.0	2.5
ILMENITE	2.2	0.6	1.6	1.2
APATITE	0.8	0.2	0.8	0.5
DIFF. INDEX	79.9	84.5	75.4	82.0
NA/(NA+K)	0.62	0.74	0.58	0.48
(NA+K)/AL	0.87	1.19	0.78	0.77
F3/(F2+F3)	0.41	0.41	0.41	0.41



## S. QOROO CENTRE - ESSEXITE      EMPIRICAL FE RATIO

NORMCAL .. R.C.O.GILL

## SUMMARY NORM TABLE

58136

	C	R
ORTHOCLASE	14.6	
ALBITE	33.9	
ANORTHITE	14.1	
NEPHELINE	5.	
DIPSIDE	3.5	
OLIVINE	11.3	
MAGNETITE	4.8	
ILMENITE	5.7	
APATITE	7.1	
DIFF. INDFX	53.5	
NA/(NA+K)	0.76	
(NA+K)/AL	0.68	
F3/(F2+F3)	0.26	

## S. QOROQ CENTRE - SYENITE SS.1

NORMCAL .. R.C.O.GILL

## SUMMARY NORM TABLE

	52254	52255	52259
ORTHOCLASE	37.5	39.2	29.8
ALBITE	21.8	38.6	41.2
ANORTHITE	1.6	4.0	12.4
NEPHELINE	21.2	8.3	1.7
DIOPSIDE	3.3	3.3	2.9
OLIVINE	2.2	2.5	5.6
MAGNETITE	2.4	2.1	1.9
ILMENITE	3.7	1.6	3.8
APATITE	1.3	0.4	1.7
WATER	0.5	0.5	0.8
DIFF. INDEX	89.5	86.1	75.7
NA/(NA+K)	0.66	0.59	0.68
(NA+K)/AL	0.97	0.92	0.75
F3/(F2+F3)	0.34	0.27	0.18

S. QOROQ CENTRE - SYENITE SS.2

NORMCAL .. R.C.C.O.GILL

SUMMARY NORM TABLE

	46250	46255	46273	46276	52296	[52299]	58202	58211	58231	58245	[58256]	58266
CORUNDUM	0.0	0.0	0.0	0.0	0.0	0.0	0.0	0.0	0.0	0.0	0.0	0.0
ORTHOCLASE	36.7	35.4	37.4	36.5	37.6	36.5	37.4	38.5	35.2	30.2	0.0	0.0
ALBITE	27.3	29.3	26.9	27.2	23.5	32.1	27.7	27.2	28.8	25.0	37.9	35.7
ANORTHITE	0.5	1.3	0.0	0.0	0.0	14.5	0.0	1.3	0.0	0.0	38.1	26.4
NEPHELINE	24.6	21.7	24.4	27.8	25.3	4.7	23.5	24.8	20.8	28.2	7.1	0.0
ACMITE	0.0	0.0	0.6	0.4	2.9	0.0	1.1	0.0	2.5	7.5	0.0	22.0
DIOPSIDE	5.1	5.4	5.6	4.5	5.6	3.5	5.4	3.2	6.6	4.4	0.0	2.9
WOLLASTONITE	0.0	0.0	0.0	0.0	0.0	0.0	0.0	0.0	0.0	1.5	0.0	7.0
OLIVINE	1.5	2.0	1.1	0.5	1.7	2.4	0.9	0.8	1.6	0.0	0.0	0.0
MAGNETITE	3.2	3.7	3.0	2.1	2.4	4.9	2.9	3.2	3.2	2.6	3.4	1.9
ILMENITE	0.9	0.0	0.8	0.8	0.7	0.9	0.9	0.8	1.0	0.5	5.2	2.7
APATITE	0.3	0.3	0.3	0.2	0.2	0.3	0.2	0.2	0.3	0.0	0.9	1.1
WATER	0.0	0.6	0.4	0.3	0.5	2.3	0.5	0.6	0.9	1.5	0.2	0.3
DIFF. INDEX	88.6	86.4	88.7	91.5	86.4	73.3	88.6	90.4	84.8	83.5	81.0	84.1
NA/(NA+K)	0.68	0.68	0.67	0.70	0.67	0.54	0.67	0.67	0.68	0.75	0.57	0.68
(NA+K)/AL	0.99	0.98	1.01	1.00	1.03	0.73	1.01	0.98	1.03	1.08	0.77	1.03
F3/(F2+F3)	0.37	0.37	0.40	0.40	0.42	0.44	0.42	0.44	0.43	0.70	0.49	0.40

S. QOROQ CENTRE - SYENITE SS.2

NORMAL .. R.C.O.GILL

SUMMARY NORM TABLE

	58267	[58268]	58269	[58271]	58273	[58274]	58275	12681	[12707]	[12709]	12720	12721
QUARTZ	0.0	0.0	0.0	0.0	0.0	0.0	0.0	1.4	0.0	0.0	0.0	0.0
CORUNDUM	0.0	1.0	0.0	0.0	0.0	3.9	0.0	0.0	2.2	0.0	0.0	0.0
ORTHOCLASE	36.7	38.0	36.3	37.4	39.2	41.2	38.1	34.5	38.1	34.4	36.5	36.5
ALBITE	28.5	35.5	30.5	30.0	25.8	36.2	28.8	48.9	38.4	34.6	32.2	31.9
ANORTHITE	0.0	7.7	0.8	20.7	1.8	7.6	2.5	7.4	8.1	14.0	3.9	3.9
NEPHELINE	22.9	8.7	20.1	4.9	26.3	3.6	23.1	0.0	4.7	5.7	16.5	15.6
ACMITE	0.2	0.0	0.0	0.0	0.0	0.0	0.0	0.0	0.0	0.0	0.0	0.0
DIOPSIDE	5.0	0.0	6.0	1.1	3.3	0.0	1.8	0.1	0.0	4.3	3.5	3.3
HYPERSTHENE	0.0	0.0	0.0	0.0	0.0	0.0	0.0	0.0	0.0	0.0	0.0	0.0
OLIVINE	0.7	2.9	1.0	0.5	1.4	2.8	1.4	3.7	0.0	1.4	1.5	3.2
MAGNETITE	4.0	4.5	3.8	3.5	2.3	3.6	3.2	3.0	4.4	4.5	4.6	3.0
ILMENITE	0.9	1.4	1.1	0.8	0.8	0.9	0.7	0.6	1.0	0.8	0.9	0.9
APATITE	0.3	0.3	0.3	0.3	0.2	0.3	0.3	0.3	0.3	0.4	0.4	0.4
WATER	0.6	1.8	0.9	2.3	0.5	1.8	0.9	2.0	2.4	2.6	1.3	1.9
DIFF. INDEX	88.0	82.2	87.0	73.2	90.3	81.0	90.0	84.0	81.2	74.6	85.2	84.4
NA/(NA+K)	0.67	0.59	0.66	0.53	0.67	0.53	0.67	0.61	0.57	0.58	0.65	0.64
(NA+K)/AL	1.00	0.81	0.90	0.66	0.97	0.70	0.96	0.85	0.76	0.75	0.93	0.93
F3/(F2+F3)	0.44	0.44	0.41	0.56	0.34	0.46	0.45	0.41	0.32	0.46	0.47	0.38

## S. QORQQ CENTRE - SYENITE SS.2

NORMAL .. R.C.O.GILL

## SUMMARY NORM TABLE

127022 127075 127096 [127097]

CORUNDUM	0.0	0.0	0.0	0.0	2.6
ORTHOCLASE	37.1	35.3	36.3	36.3	40.7
ALBITE	27.7	25.6	32.0	32.0	36.5
ANORTHITE	0.0	0.0	2.4	2.4	7.7
NEPHELINE	21.5	23.9	16.4	16.4	5.7
ACMITE	1.0	5.1	0.0	0.0	0.0
DIOPSIDE	6.2	5.9	3.6	3.6	0.0
OLIVINE	1.0	2.5	2.2	2.2	3.4
MAGNETITE	3.3	0.2	5.4	5.4	3.1
ILMENITE	0.8	0.7	1.2	1.2	0.7
APATITE	0.3	0.7	0.4	0.4	0.2
WATER	1.0	0.6	1.4	1.4	1.0
DIFF. INDEX	84.3	84.8	84.8	84.8	82.2
NA/(NA+K)	0.67	0.69	0.65	0.65	0.55
(NA+K)/AL	1.02	1.06	0.96	0.96	0.75
F3/(F2+F3)	0.46	0.35	0.47	0.47	0.38



S. QOROO CENTRE - SYENITE SS.3

NORMCAL .. R.C.D.GILL

SUMMARY NORM TABLE

	46269	46270	46271	52297	52300	[58234]	58236	58257	127015	[127016]	127017	[127018]
CORUNDUM	0.0	0.0	0.0	0.0	0.0	8.1	0.0	0.0	0.0	2.7	0.0	0.0
ORTHOCLASE	36.1	34.5	35.5	36.7	36.6	51.4	37.1	38.2	37.4	37.6	38.1	33.5
ALBITE	2.2	22.3	20.9	31.9	29.2	26.7	31.0	33.2	26.9	40.1	31.9	40.1
ANORTHITE	0.1	0.0	0.4	0.1	0.8	5.7	2.3	4.0	0.0	6.4	1.3	5.0
NEPHELINE	22.2	31.1	21.9	15.1	22.2	0.0	19.8	15.2	23.1	4.6	19.3	4.0
ACMITE	0.0	1.0	0.0	0.0	0.0	0.0	0.0	0.0	1.9	0.0	0.0	0.0
DIOPSIDE	5.1	5.5	5.7	7.0	4.8	0.0	3.7	1.8	5.4	0.0	1.5	2.1
WOLLASTONITE	0.0	0.0	0.0	0.0	0.0	0.0	0.0	0.0	0.0	0.0	1.8	3.7
HYPERSTHENE	0.0	0.0	0.0	0.0	0.0	2.2	0.0	0.0	0.0	0.0	0.0	0.0
OLIVINE	2.4	2.0	2.2	2.6	0.7	3.3	1.7	2.2	0.4	1.3	0.0	0.0
MAGNETITE	2.5	2.3	3.1	5.2	4.4	1.8	3.6	4.5	4.0	6.6	5.6	9.8
ILMENITE	1.1	1.0	1.0	1.1	1.0	0.6	0.7	0.8	0.6	0.6	0.4	0.8
APATITE	0.2	0.3	0.6	0.3	0.3	0.2	0.2	0.1	0.2	0.2	0.1	0.1
WATER	1.0	0.3	0.5	0.0	0.8	2.4	0.0	1.2	1.2	2.5	1.2	2.5
DIFF. INDEX	80.5	87.9	87.3	83.7	87.9	78.1	87.8	86.6	87.5	82.3	89.3	78.5
NA/(NA+K)	0.69	0.71	0.68	0.63	0.67	0.36	0.64	0.63	0.67	0.58	0.65	0.61
(NA+K)/AL	1.00	1.00	0.99	1.00	0.99	0.59	0.96	0.93	1.02	0.76	0.98	0.90
F2/(F2+F3)	0.29	0.32	0.32	0.30	0.48	0.24	0.42	0.48	0.54	0.61	0.65	0.67

S. QOROQ CENTRE - SYENITE SS.3

NORMCAL ... R.C.O.GILL

SUMMARY NORM TABLE

[127033] 127038

CORUNDUM	7.6	7.0
ORTHOCLASE	39.2	36.5
ALBITE	33.8	27.5
ANORTHITE	6.8	6.2
NEPHELINE	12.4	22.1
ACMITF	0.0	3.7
DIOPSIDE	0.0	6.0
OLIVINE	3.1	0.3
MAGNETITE	3.2	2.9
ILMENITE	0.6	0.8
APATITE	0.2	0.2
WATER	1.4	5.9
DIFF. INDEX	85.4	86.2
NA/(NA+K)	0.61	0.68
(NA+K)/AL	0.85	1.14
F3/(F2+F3)	0.41	0.52

S. QOROQ CENTRE - SYENITE SS.3 EMPIRICAL FE RATIO

NORMCAL .. R.C.D.GILL

SUMMARY NORM TABLE

	58328	59659	59664
	R		
ORTHOCLASE	39.0	36.2	27.5
ALBITE	35.9	25.9	2.3
ANORTHITE	1.9	0.0	0.0
NEPHELINE	15.3	25.8	62.1
ACMITE	0.0	2.9	4.1
SOD METASIL	0.0	0.0	0.7
DIOPSIDE	3.1	5.3	1.5
WOLLASTONITE	0.5	0.0	0.0
OLIVINE	0.0	0.7	1.4
MAGNETITE	2.7	2.2	0.0
ILMENITE	1.2	0.7	0.2
APATITE	0.3	0.3	0.1
DIFF. INDEX	9.2	88.7	92.7
NA/(NA+K)	0.64	0.69	0.82
(NA+K)/AL	0.97	1.03	1.05
F3/(F2+F3)	0.47	0.47	0.47

## S. QOROQ CENTRE - SYENITE SS.4A

NORMCAL ... R.C.D.GILL

## SUMMARY NORM TABLE

	[59149]	5815A	58228	58258A	58258B	[127024]	127025	127086	127093
CORUNDUM	3.5	0.0	0.0	0.0	0.0	2.9	0.0	0.0	0.0
ORTHOCLASE	38.2	38.6	35.3	36.4	33.0	33.8	34.5	31.3	34.1
ALBITE	35.8	32.6	35.8	36.2	21.9	44.2	34.4	42.5	23.6
ANORTHITE	4.5	2.3	4.2	4.4	0.0	5.5	2.7	7.3	0.9
NEPHELINE	11.7	17.1	15.5	13.6	27.1	3.1	18.2	11.3	17.1
ACMITE	0.0	0.0	0.0	0.0	7.0	0.0	0.0	0.0	2.0
SOD METASIL	0.0	0.0	0.0	0.0	1.3	0.0	0.0	0.0	0.0
DIOPSIDE	0.0	3.7	2.7	2.7	7.0	0.0	4.2	3.9	6.8
OLIVINE	2.2	2.4	2.5	2.6	2.5	6.3	2.7	1.5	1.9
MAGNETITE	3.7	1.7	2.4	2.6	0.0	2.5	1.6	1.5	2.8
ILMENITE	0.4	1.2	1.1	1.1	0.9	1.2	1.1	0.6	1.1
APATITE	0.1	0.5	0.5	0.5	0.3	0.5	0.6	0.2	0.6
WATER	2.2	0.5	0.6	0.6	0.6	2.7	0.5	0.8	0.7
DIFF. INDEX	85.7	88.3	86.7	86.2	82.0	81.1	87.1	85.0	84.8
NA/(NA+K)	0.61	0.64	0.66	0.64	0.72	0.61	0.68	0.68	0.68
(NA+K)/AL	0.78	0.96	0.92	0.92	1.09	0.76	0.95	0.87	1.02
F2/(F2+F3)	0.48	0.25	0.32	0.33	0.38	0.27	0.24	0.31	0.38

S. QORQO CENTRE - SYENITE SS.4A EMPIRICAL FE RATIO

NORMCAL .. R.C.D.GILL

SUMMARY NORM TABLE

58327 59676

	R	
ORTHOCLASE	42.4	32.8
ALBITE	29.0	40.6
ANORTHITE	2.4	4.1
NEPHELINE	18.9	10.6
DIOPSIDE	3.7	4.9
OLIVINE	0.9	1.7
MAGNETITE	1.7	2.6
ILMENITE	1.7	1.8
APATITE	.4	0.9
DIFF. INDEX	91.3	84.1
NA/(NA+K)	0.62	0.66
(NA+K)/AL	0.96	0.92
F3/(F2+F3)	0.34	0.34

S. QOROQ CENTRE - SYENITE SS.4B

NORMCAL .. R.C.O.GILL

SUMMARY NORM TABLE

	[58144]									
	58146	58147	58148	58164	58165	58220	58221	58259		
	C					R				
CORUNDUM	0.0	0.0	0.0	0.0	0.0	0.4	0.0	0.0	0.0	0.0
ORTHOCLASE	32.7	27.7	35.6	32.6	34.6	24.8	32.2	32.7		
ALBITE	37.2	41.1	29.8	39.1	27.7	45.4	39.4	35.8		
ANORTHITE	11.7	12.0	0.0	1.8	3.5	15.0	7.1	4.6		
NEPHELINE	2.7	4.7	20.7	10.7	24.7	1.0	10.1	14.1		
ACMITÉ	0.0	0.0	2.5	0.0	0.0	0.0	0.0	0.0		
DIOPSIDE	1.6	2.7	6.8	9.5	2.6	0.0	2.4	4.9		
OLIVINE	7.6	6.3	1.2	0.4	2.4	8.0	4.0	4.1		
MAGNETITE	4.4	1.4	1.8	2.8	2.3	0.6	2.1	1.2		
ILMENITE	2.2	3.3	1.1	2.1	1.5	2.9	1.9	1.9		
APATITE	0.8	1.8	0.5	0.9	0.7	1.8	0.8	0.8		
WATER	1.4	0.1	0.8	0.8	0.7	1.3	1.2	0.5		
DIFF. INDEX	72.6	72.5	86.1	82.4	87.0	71.3	81.7	82.5		
NA/(NA+K)	0.58	0.65	0.68	0.66	0.69	0.67	0.66	0.67		
(NA+K)/Al	0.77	0.77	1.03	0.96	0.94	0.70	0.87	0.91		
F3/(F2+F3)	0.32	0.14	0.39	0.35	0.34	0.07	0.24	0.15		

## S. QOROQ CENTRE - SYENITE SS.48 EMPIRICAL FE RATIO

NORMCAL .. R.C.O.GILL

## SUMMARY NORM TABLE

	59333	59671	59672	59673	59675
ORTHOCLASE	32.9	22.4	23.4	26.6	31.1
ALBITE	42.0	21.1	30.4	40.2	43.0
ANORTHITE	5.8	6.1	10.1	11.7	8.1
NEPHELINE	6.8	0.0	1.9	2.6	5.4
DIPSIDE	4.1	8.6	5.9	2.6	3.0
HYPERSTHENE	0.0	1.3	0.0	0.0	0.0
OLIVINE	2.7	11.8	7.3	6.5	3.7
MAGNETITE	2.1	5.8	3.9	3.3	2.3
ILMENITE	2.5	7.1	4.7	4.2	2.4
APATITE	1.1	5.8	3.4	2.3	1.0
DIFF. INDEX	81.7	53.5	64.7	69.4	79.5
NA/(NA+K)	0.64	0.60	0.66	0.64	0.64
(NA+K)/AL	0.89	0.82	0.77	0.76	0.84
F3/(F2+F3)	0.26	0.26	0.26	0.26	0.26

S. QOROO CENTRE - SYENITE SS.5

NORMCAL .. R.C.C.O.GILL

SUMMARY NORM TABLE

	[4623P]	[46241]	46242	46243	46244	46245	46246	58121	[58143]	58153	58154	58222
										R	R	
CORUNDUM	4.1	3.3	0.0	0.0	0.0	0.0	0.0	0.0	0.5	0.0	0.0	0.0
ORTHOCLASE	38.2	40.6	36.0	37.8	38.6	36.5	36.2	37.5	38.7	40.3	37.2	37.0
ALBITE	36.3	36.3	20.6	29.0	26.9	29.2	17.4	20.6	30.8	23.8	22.2	28.1
ANORTHITE	3.9	7.1	0.0	2.6	0.0	0.6	0.0	0.0	9.2	0.1	0.1	0.0
NEPHELINE	11.5	6.2	28.7	20.9	26.7	21.4	28.6	24.7	12.3	25.3	28.3	20.2
ACMITT	0.0	0.0	5.6	0.0	1.2	0.0	7.7	3.2	0.0	0.0	0.0	0.2
DIPSIDE	0.0	0.0	6.8	3.7	2.1	6.4	7.6	7.1	0.0	5.0	5.5	7.2
WOLLASTONITE	0.0	0.0	0.0	0.0	0.9	0.0	0.0	0.0	0.0	0.0	0.0	0.0
OLIVINE	0.2	2.1	0.7	2.1	0.0	1.6	1.5	1.4	3.0	3.9	2.1	1.7
MAGNETITE	4.7	3.3	0.5	2.6	2.5	3.1	0.0	1.3	3.9	0.6	2.4	4.5
ILMENITE	1.0	0.8	0.8	0.9	0.8	0.9	0.7	0.8	1.2	0.8	1.6	1.0
APATITE	0.1	0.2	0.3	0.3	0.2	0.5	0.4	0.4	0.3	0.2	0.6	0.1
WATER	1.9	2.1	0.7	0.4	0.5	0.7	0.8	0.2	0.3	0.7	0.7	1.4
DIFF. INDEX	86.0	83.2	85.2	87.7	92.3	87.0	82.2	85.8	81.8	89.4	87.7	85.3
NA/(NA+K)	0.61	0.56	0.70	0.66	0.68	0.67	0.70	0.67	0.59	0.65	0.68	0.65
(NA+K)/AL	0.77	0.74	1.06	0.95	1.01	0.99	1.08	1.04	0.82	1.00	1.00	1.00
F3/(F2+F3)	0.60	0.45	0.45	0.34	0.57	0.34	0.50	0.39	0.42	0.08	0.28	0.41

## S. 30R00 CENTRE - SYENITE SS.5

NORMAL .. R.C.O.GILL

## SUMMARY NORM TABLE

	58230	58348	[127026]	127091	127092
CORUNDUM	0.0	0.0	0.0	0.0	0.0
ORTHOCLASE	37.8	40.4	44.1	38.3	36.1
ALBITE	22.4	23.3	25.5	21.0	27.1
ANORTHITE	0.0	0.0	6.2	4.5	0.0
NEPHFLINE	28.7	21.8	8.6	18.2	27.0
ACMITE	3.4	3.7	0.0	0.0	2.4
DIOPSIDE	4.8	6.5	0.0	1.7	4.3
OLIVINE	1.0	0.7	2.6	2.0	1.7
MAGNETITE	1.1	2.2	2.4	3.6	0.7
ILMENITE	0.6	0.8	0.4	0.5	0.6
APATITE	0.2	0.3	0.2	0.2	0.2
WATER	0.6	0.8	2.3	1.3	0.6
DIFF. INDEX	88.9	85.6	88.1	87.5	90.2
NA/(NA+K)	0.60	0.64	0.55	0.64	0.70
(NA+K)/AL	1.02	1.04	0.80	0.92	1.02
F3/(F2+F3)	0.43	0.50	0.45	0.45	0.32



REFERENCES

REFERENCES

- Ahrens, L.H., Pinson, W.H. and Kearns, M. (1952) Association of rubidium and potassium and their abundance in common igneous rocks and meteorites. *Geochim. Cosmochim. Acta.* 2, 229-242.
- Albee, A.L. and Chodos, A.A. (1970) Semiquantitative electron microprobe determination of  $Fe^{2+}/Fe^{3+}$  and  $Mn^{3+}/Mn^{2+}$  in oxides and silicates and its application to petrologic problems. *Amer. Mineral.* 55, 491-501.
- Allaart, J.H., Bridgwater, D. and Henriksen, N. (1969) Pre-Quaternary geology of Southwest Greenland and its bearing on North Atlantic correlation problems. *Amer. Ass. Petrol. Geol.* 12, 859-882.
- Aoki, K. (1964) Clinopyroxenes from alkaline rocks of Japan. *Amer. Mineral.* 49, 1199-1223.
- Bailey, D.K. (1964) Crustal warping - a possible tectonic control of alkaline magmatism. *J. Geophys. Res.*, 69, 1103-1111.
- (1969) The stability of acmite in the presence of  $H_2O$ . *Amer. J. Sci.* 267A, 1-16.
- , and Schairer, J.F. (1964) Feldspar - liquid equilibria in peralkaline liquids - the orthoclase effect. *Amer. J. Sci.*, 262, 1198-1206.
- , and Schairer, J.F. (1966) The system  $Na_2O-Al_2O_3-Fe_2O_3-SiO_2$  at 1 Atmosphere, and the petrogenesis of alkaline rocks. *J. Petrol.*, 7, 114-170.
- Barth, T.F.W. (1944) Studies on the igneous rock complex of the Oslo region. Part II. Systematic petrography of the plutonic rocks. *Norske Vidensk. Akad. Oslo I. Mat.-Naturv. Kl.*, No.9, 1-104.
- Berthelsen, A. and Noe-Nygaard, A. (1965) The Precambrian of Greenland. In Rankama, K. (editor) *The Geologic Systems, The Precambrian*, Vol. 2, 113-262.
- Bondam, J. (1955) Petrography of a group of alkali-trachytic dyke rocks from the Julianehaab District, South Greenland. *Medd. om Grønland*, Bd. 135, No.2, also *Bull. Grønlands Geol. Unders.* No. 7

- Bowden, P. (1966) Zirconium in Younger Granites of Northern Nigeria.  
*Geochim. Cosmochim. Acta*, 30, 958-993.
- Bowen, N.L. (1937) Recent high temperature research on silicates and its significance in igneous geology. *Amer. J. Sci.*, 33, 1-21.
- , and Tuttle, O. F. (1950) The system  $\text{NaAlSi}_3\text{O}_8 - \text{KAlSi}_3\text{O}_8 - \text{H}_2\text{O}$ .  
*Journ. Geol.*, 58, 489-511.
- Boyd, F.R., Finger, L.W., and Chayes, F. (1969) Computer reduction of electron-probe data. *Yearbook Carnegie Inst.* 67, 210-215.
- Bridgwater, D. (1965) Isotopic age determinations from South Greenland and their geological setting. *Medd. om. Grønland* 179, No.4, also *Bull. Grønlands Geol. Unders.* No. 53.
- , and Harry, W. T. (1968) Anorthosite xenoliths and plagioclase megacrysts in Precambrian intrusions of South Greenland. *Medd. om. Grønland.* 185, No. 2, also *Bull. Grønlands Geol. Unders.* No.77.
- Brown, G.M., Emeleus, C. H., Holland, J.G. and Phillips, R. (1970) Petrographic, mineralogic, and X-Ray fluorescence analysis of lunar igneous-type rocks and spherules. *Science*, 167, 599-601.
- Buddington, A.F. and Lindsley, D.H. (1964) Iron-titanium oxide minerals and synthetic equivalents. *J. Petrol.* 5, 310-357.
- Carmichael, I.S.E. (1967) The iron-titanium oxides of salic volcanic rocks and their associated ferromagnesian silicates. *Contr. Mineral. and Petrol.* 14, 36-64.
- , and Nicholls, J. (1967) Iron-titanium oxides and oxygen fugacities in volcanic rocks. *J. Geophys. Res.* 72, 4665-4687.
- , Nicholls, J. and Smith, A.L. (1970) Silica activity in igneous rocks. *Amer. Mineral.* 55, 246.
- Duchesne, J.C. (1972) Iron-titanium oxide minerals in the Bjerkrem-Sogndal Massif, South-western Norway. *J. Petrol.* 13, 57-81.
- Emeleus, C.H. (1961, 62, 63, 66, 69) *G.G.U. Field Diary*.
- (1966, 69) *G.G.U. Field Reports*.

- Emeleus, C.H. and Harry W.T. (1961, 62, 63) G.G.U. Field Reports.
- , - (1970) The Igaliko Nepheline Syenite complex. General Description. Medd. om. Grønland 186, No. 3, also Bull. Grønlands Geol. Unders. No. 85.
- , and Smith, J.V. (1959) The alkali feldspars VI. Sanidine and orthoclase perthites from the Slieve Gullion area, Northern Ireland. Amer. Mineral., 44, 1187-1209.
- , and Stephenson, D. (1970) Field work between Tunugdliarfik and Tasiussaq. Rapp. Grønlands Geol. Unders. No. 28, 30-32.
- Engell, J. (in press) Lithos.
- Ernst, W.G. (1962) Synthesis, stability relations, and occurrence of riebeckite and riebeckite-arfvedsonite solid solutions. Journ. Geol., 70, 689-736.
- Eugster, H.P. and Wones, D.R. (1962) Stability relations of the ferruginous biotite, annite. J. Petrol. 3, 82-125.
- Ferguson, J. (1970) The significance of the kakortokite in the evolution of the Ilímaussaq intrusion South Greenland. Medd. om. Grønland, 190, No. 1, also Bull. Grønlands Geol. Unders. No. 89.
- Fitton, J.G. and Gill, R.C.O. (1970) The oxidation of ferrous iron in rocks during mechanical grinding. Geochim. Cosmochim. Acta 34, 518-523.
- Fleischer, M. (1969) United States Geological Survey Standards - I. Additional data on rocks G-1 and W-1, 1965-1967. Geochim. Cosmochim. Acta 33, 65-80.
- Flink, G. (1898) Berättelse om en Mineralogisk Resa i Syd-Grönland sommaren 1897. Medd. om. Grønland Bd. 14, No. 2.
- Gibson, I.L. (1970) A pantelleritic Welded Ash-Flow Tuff from the Ethiopian Rift Valley. Contr. Mineral. and Petrol., 28, 89-111.
- Giesecke, K.L. (1910) Karl Ludwig Gieseckes mineralogisches Reisejournal über Grönland. Medd. om. Grønland Bd. 35.
- Gill, R.C.O. (1972) The geochemistry of the Grønvedal-Íka alkaline complex, South Greenland. Unpublished Ph.D. thesis, University of Durham.

- Gomes, C. de B., Moro, S.L. and Dutra, C.V. (1970) Pyroxenes from the alkaline rocks of Itapirapuã, São Paulo, Brazil. *Amer. Mineral.* 55, 224-230.
- Hamilton, D.L. (1961) Nephelines as crystallisation temperature indicators. *Jour. Geol.* 69, 321-329.
- , and MacKenzie, W.S. (1965) Phase equilibrium studies in the system  $\text{NaAlSi}_3\text{O}_8$ - $\text{KAlSi}_3\text{O}_8$ - $\text{SiO}_2$ - $\text{H}_2\text{O}$ . *Mineral. Mag.*, 34, 214-231.
- Hamilton, E. , (1964) The geochemistry of the northern part of the Ilímaussaq intrusion, Southwest Greenland. *Medd. om Grønland.* 162, No.10 also *Bull. Grønlands Geol. Unders.* No. 42.
- Harris, P.G. (1969) Basalt types and African rift valley tectonism. *Tectonophysics* 8, 427-436.
- (1970) Convection and magmatism with reference to the African continent. In Clifford, T.N. and Gass, I.G. (editors) *African Magmatism and Tectonics.* 419-427. Oliver and Boyd, Edinburgh.
- Harry, W.T. (1961, 62, 63) *G.G.U. Field Diary.*
- , and Richey, J.E. (1963) Magmatic pulses in the emplacement of plutons. *L'pool. Manchr. geol. J.*, 3, 254-268.
- Heier, K.S. and Taylor, S.R. (1959) Distribution of Li, Na, K, Rb, Cs, Pb and Ti in southern Norwegian Precambrian alkali feldspars. *Geochim. Cosmochim. Acta*, 15, 284-304.
- Heier, K.S. (1966) Some crystallo-chemical relations of nephelines and feldspars from Stjernøy, North Norway. *J. Petrol.* 7, 95-113.
- Henriksen, N. (1960) Structural analysis of a fault in Southwest Greenland. *Medd. om. Grønland* 162, No. 9, also *Bull. Grønlands Geol. Unders.* No. 26.
- Holland, J.G. and Brindle, D.W. (1966) A self-consistent mass absorption correction for silicate analysis by X-Ray Fluorescence. *Spectrochim. Acta.* 22, 2083.
- Kempe, D.R.C. and Deer, W.A. (1970) The Mineralogy of the Kangerdlugssuaq alkaline intrusion, E. Greenland. *Medd. om Grønland.* 190, No. 3

- Kempe, D.R.C., Deer, W.A. and Wager, L.R. (1970) The petrology of the Kangerdlugssuaq Alkaline Intrusion, East Greenland. *Medd. om Grønland* 190, No.2
- Kennedy, G.C. (1955) Some aspects of the role of water in rock melts. In: Poldervaart, A. (editor) *The Crust of the Earth. Spec. Pap. geol. soc. Amer.*, 62, 489-503.
- Kushiro, I. (1960) Si-Al relations in clinopyroxenes from igneous rocks. *Amer. J. Sci.* 258, 548-554.
- Larsen, O. (1969) K-Ar age dates. *Rapp. Grønlands geol. Unders.* No. 19.
- Le Bas, M.J. (1962) The role of aluminium in igneous clinopyroxenes with relation to their parentage. *Amer. J. Sci.* 260, 267-288.
- Lipman, P.W. (1967) Mineral and chemical variations within an ash-flow sheet from Aso caldera, south western Japan. *Contr. Mineral. and Petrol.* 16, 300-327.
- (1971) Iron-titanium oxide phenocrysts in compositionally zoned ash-flow sheets from southern Nevada. *J. Geol.* 79, 438-456.
- , Christiansen, R.L. and O'Connor, J.T. (1966) A compositionally zoned ash-flow sheet in southern Nevada. *U.S. Geol. Survey Prof. Paper* 524-F, 1-47.
- MacDonald, R. (1969) The petrology of alkaline dykes from the Tugtutôq area, South Greenland. *Bull. Geol. Soc. Denmark*, 19, 257-282.
- , and Edge, R.A. (1970) Trace element distribution in alkaline dykes from the Tugtutôq region, South Greenland. *Bull. Geol. Soc. Denmark*, 20, 38-58.
- and Parker, Å. (1969) Zirconium in alkaline dykes from the Tugtutôq region, South Greenland. *Bull. Geol. Soc. Denmark*, 20, 59-63.
- MacKenzie, W.S. and Smith, J.V. (1961) Experimental and geological evidence for the stability of alkali feldspars. *Instituto Lucas Mallada C.S.I.C. Cursos y Conferencias. Madrid. VIII*, 53-64.

- MacKenzie, W.S. and Smith, J.V. (1962) Single crystal X-ray studies of crypto and micro-perthites. *Norsk Geol. Tidsskr.*, 42, 72-103.
- Miyashiro, A. (1957) The chemistry, optics and genesis of the Alkali Amphiboles. *Jour. Fac. Sci. Tokyo Univ.*, 11, 57-83
- Morse, S.A. (1969) Syenites. *Yearbook Carnegie Instn. Wash.* 67, 112-120.
- Muir, I.D. and Smith, J.V. (1956) Crystallisation of feldspars in larvikites. *Zeit. Krist.*, 107, 182-195.
- Nash, W.P., Carmichael, I.S.E. and Johnson, R.W. (1969) The Mineralogy and Petrology of Mount Suswa, Kenya. *J. Petrol.* 10, 409-439.
- and Wilkinson, J.F.G. (1970) Shonkin Sag Laccolith, Montana. I. Mafic Minerals and Estimates of Temperature, Pressure, Oxygen Fugacity and Silica Activity. *Contr. Mineral. and Petrol.* 25, 241-269.
- Nockolds, S.R. and Allen, R. (1954) The geochemistry of some igneous rock series: Pt. II. *Geochim. Cosmochim. Acta*, 5, 145-285.
- Nolan, J. (1966) Melting-relations in the system  $\text{NaAlSi}_3\text{O}_8$ - $\text{NaAlSiO}_4$ - $\text{NaFeSi}_2\text{O}_6$ - $\text{CaMgSi}_2\text{O}_6$ - $\text{H}_2\text{O}$ , and their bearing on the genesis of alkaline undersaturated rocks. *Quart. J. Geol. Soc. Lond.* 122, 119-157.
- Odé, H. (1957) Mechanical analysis of the dike pattern of the Spanish Peaks area, Colorado. *Bull. Geol. Soc. America*, 68, 567-575
- Parsons, I. (1965) The feldspathic syenites of the Lock Ailsh intrusion, Assynt, Scotland. *J. Petrol.* 6, 365-394.
- Phillips, R. (1963) The recalculation of amphibole analyses. *Mineral. Mag.* 33, 701-711.
- Piotrowski, J.M. and Edgar, A.D. (1970) Melting relations of undersaturated alkaline rocks from South Greenland. *Medd. om Grønland*, 181, No. 9.
- Poulsen, V. (1964) The sandstones of the Precambrian Eriksfjord Formation in South Greenland. *Rapp. Grønlands Geol. Unders.*, No. 2
- Pulvertaft, T.C.R. (1965) The Eqaloqarfia layered dyke, Nunarssuit, South Greenland. *Medd. om Grønland*, 169, No. 10, also *Bull. Grønlands Geol. Unders.* No. 55.

- Reeves, M.J. (1971) Geochemistry and mineralogy of British Carboniferous seatearths from northern coalfields. Unpublished Ph.D. thesis, University of Durham.
- Riley, J.P. (1958) Simultaneous determination of water and carbon dioxide in rocks and minerals. *Analyst* 83, 42-49.
- Rucklidge, J.C., Gasparrini, E., Smith, J.V. and Knowles, C.R. (1971) X-Ray Emission Microanalysis of Rock-forming Minerals. VIII. Amphiboles. *Canadian J. of Earth Sci.* 8, 1171-1183.
- Saether, E. (1957) The Alkaline rock province of the Fen area in southern Norway. *Det. Kgl. Norske Vidensk. Selskabs Skrifter*, 1, p.1.
- Schairer, J.F. (1950) The alkali feldspar join in the system  $\text{NaAlSi}_3\text{O}_8$ - $\text{KAlSi}_3\text{O}_8$ - $\text{SiO}_2$ . *Jour. Geol.* 58, 512-517.
- Simkin, T and Smith, J.V. (1970) Minor element distribution in olivine. *Jour. Geol.* 78, 304-325.
- Sine, N.M., Taylor, W.D., Weber, G.R. and Lewis, C.L. (1969) Third report of analytical data for C.A.A.S. sulphide ore and syenite rock standards. *Geochim. Cosmochim. Acta* 33, 121-131.
- Smith J.V. and MacKenzie, W.S. (1958) The alkali feldspars, IV. The cooling history of high temperature sodium-rich feldspars. *Amer. Mineral.* 43, 872-889.
- and Muir, I.D. (1958) The reaction sequence in larvikite feldspars. *Zeit. Krist.*, 110, 11-20.
- Sood, M.K. and Edgar, A.D. (1970) Melting relations of undersaturated alkaline rocks. *Medd om Grønland.* Bd. 181, No. 12
- Steenstrup, K.J.V. and Kornerup, A. (1881) Beretning om Expeditionen til Julianehaabs Distrikt; 1876. *Medd. om Grønland.* Bd. 2, No. 1.
- Stephenson, D. (1972) Alkali clinopyroxenes from nepheline syenites of the South Qôroq Centre, South Greenland. *Lithos* 5, 187-201.

- Stewart, J.W. (1964) The earlier Gardar igneous rocks of the Ilimaussaq area, South Greenland. Unpublished Ph.D. thesis, University of Durham.
- (1970) Precambrian alkaline - ultramafic/carbonatite volcanism at Qagssiarssuk, South Greenland. Medd. om Grønland 186, No. 4, also Bull. Grønlands Geol. Unders. No. 84.
- Sweatman, T.R. and Long, J.V.P. (1969) Quantitative electron probe microanalysis of rock-forming minerals. J. Petrol. 10, 332-379.
- Sørensen, H. (1960) On the Agpaitic Rocks. Rep. 21st Intern. Geol. Congr. Norden, 13, 319-327.
- (1962) On the occurrence of Steenstrupine in the Ilimaussaq Massif, South West Greenland. Medd. om Grønland 167, No.1, also Bull. Grønlands Geol. Unders. No. 32.
- (1966) On the magmatic evolution of the alkaline igneous province of South Greenland. Rapp. Grønlands Geol. Unders. No. 7.
- Taylor, S.R. (1965) The application of trace element data to problems in petrology. Phys. Chem. Earth 6, 133-213.
- , Ewart, A. and Capp, A.C. (1968) Leucogranites and rhyolites: Trace element evidence for fractional crystallisation and partial melting. Lithos, 1, 179-186.
- Thompson, R.N. and MacKenzie, W.S. (1967) Feldspar - liquid equilibria in peralkaline acid liquids: an experimental study. Amer. J. Sci., 265, 714-734.
- Thornton, C.P. and Tuttle, O.F. (1960) Chemistry of igneous rocks. I. Differentiation Index. Amer. J. Sci. 258, 664-684.
- Tyler, R.C. and King, B.C. (1967) The pyroxenes of the alkaline igneous complexes of eastern Uganda. Mineral Mag. 36, 5-21.

- Upton, B.G.J. (1960) The Alkaline igneous complex of Kûngnât Fjeld, South Greenland. Medd. om Grønland. 123, No. 4, also Bull. Grønlands Geol. Unders. No. 27.
- (1962) Geology of Tugtutôq and neighbouring islands, South Greenland. Part I. Medd om Grønland. 169, No. 8, also Bull. Grønlands. Geol. Unders. No. 34
- (1964a) The geology of Tugtutôq and neighbouring islands, South Greenland. Part II. Nordmarkitic syenites and related alkaline rocks. Medd. om Grønland. 169, No. 2, also Bull. Grønlands Geol. Unders. No. 44.
- (1964b) The geology of Tugtutôq and neighbouring islands, South Greenland. Part III. Olivine gabbros, syeno-gabbros and anorthosites. Medd. om Grønland. 169, No. 3, 6-49. also Bull. Grønlands Geol. Unders. No. 48.
- (1964c) The geology of Tugtutôq and neighbouring islands, South Greenland. Part IV. The nepheline syenites of the Hviddal composite dyke. Medd. om Grønland. 169, No. 3, 50-80, also Bull. Grønlands Geol. Unders. No. 48.
- (1970) Basic rocks of the Gardar igneous province. Rapp. Grønlands Geol. Unders. No. 28, 26-29.
- (in press) The Alkaline Province of Southwest Greenland. In: Sørensen, H. (editor): Alkaline Rocks. Interscience.
- , Thomas, J.E. and MacDonald, R. (1971) Chemical variation within three alkaline complexes in South Greenland. Lithos 4, 163-184.
- Ussing, N.J. (1894) Mineralogisk - petrografiske Undersøgelser af Grønlandske Nefelinsyeniter og beslægtede Bjærgarter. Anden del: De Kiselsyrefattige Hovedminerdlar. Medd om Grønland. Bd. 14, No. 1.
- Ussing, N.V. (1912) Geology of the country around Julianehaab, Greenland. Medd om Grønland, Bd. 38.

- van Breemen, O and Upton, B.G.J. (1972) Age of some Gardar intrusive complexes, South Greenland. *Geol. Soc. Amer. Bull.* 83, 3381-3390.
- Vlasov, K.A., Kuz'menko, M.V. and Es'kova, E.M. (1966) The Lovozero Alkali Massif. Oliver and Boyd. Edinburgh and London.
- Wager, L.R. and Brown, G.M. (1968) Layered Igneous Rocks. Oliver and Boyd. Edinburgh and London, 588 pp.
- Washington, H.S. and Merwin, H.E. (1927) The Acmitic Pyroxenes. *Amer. Mineral.* 12, 233-252.
- Watt, W.S. (1966) Chemical analyses from the Gardar Igneous Province, South Greenland. *Rapp. Grønlands Geol. Unders.* No. 6.
- Wegmann, C.E. (1938) Geological investigations in Southern Greenland, Part I. On the structural divisions of Southern Greenland. *Medd. om Grønland*, Bd. 113, No. 2.
- Widenfalk, L. (1972) Myrmekite-like intergrowths in larvikite feldspars. *Lithos* 5, 255-267.
- Wilkinson, J.F.G. (1957) The clinopyroxenes of a differentiated teschenite sill near Gunnedah, New South Wales. *Geol. Mag.* 94, 123-134.
- Wilson, A.D. (1955) A new method for the determination of ferrous iron in rocks and minerals. *Bull. Geol. Surv. Gt. Br.* No. 9, 56-58.
- Wones, D.R. and Gilbert, M.C. (1969) The fayalite-magnetite-quartz assemblage between 600 and 800°C. *Amer. J. Sci.* 267A, 480-488.
- Wright, J.B. (1971) The phonolite-trachyte spectrum. *Lithos*, 4, 1-5.
- Yagi, K. (1953) Petrochemical studies on the alkalic rocks of the Morotu district, Sakhalin. *Geol. Soc. Amer. Bull.* 64, 769-810.
- Yoder, H.S., Jr., Stewart, D.B. and Smith, J.R. (1957) Ternary Feldspars. *Carn. Inst. Washington. Ann. Rept. Geophys. Lab.*, 56, 206-214.
- Ødum, H. (1927) Geologiske Iagttagelser i Landet Øst for Igaliko Fjord. *Medd. om Grønland*, Bd. 74, No. 4.

Plate 1

Geological map of the Igaliko Nepheline Syenite Complex.

Scale 1:50,000. Taken from Emeleus and Harry (1970) with modifications based upon the present work.

N.B. The newly defined area of SS5 west of Qôroq Fjord; the approximate SS4a/SS4b boundary; the distinct south-eastern area of SS2; and the limit of recrystallisation around the Igdlerfigssalik Centre.

Plate 1A

Specimen locality map for the South Qôroq Centre. Scale 1:50,000.

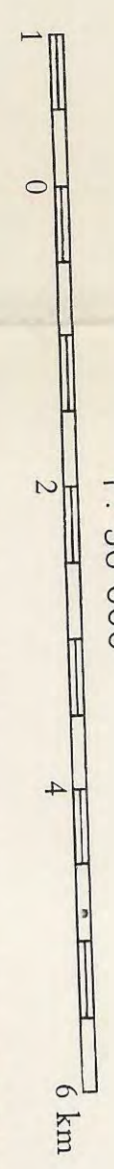
Specimen numbers are all in the Grønlands Geologiske Undersøgelse series.



GEOLOGICAL MAP OF THE IGALIKO NEPHELINE SYENITE COMPLEX SOUTH GREENLAND

by C. H. Emeleus and W. T. Harry

1 : 50 000



Geology of adjoining areas from maps by S. Andersen, V. Poulsen, J. W. Stewart and B. J. Walton



South-eastern area of South Qorooq Centre - possibly a separate, satellite intrusion. Not mapped in detail.

GARDAR NEPHELINE SYENITES

- Igalifigssalik Centre
- Other syenites
- North Moerfeldt syenites
- SI 1
- SI 2
- SI 3
- SI 4
- SI 5
- SI 6
- SI 7
- NM 1
- NM 2
- East Moerfeldt syenite
- Narsarsuaq stock
- Trangdliarfik syenite
- Økfyfordal syenite
- Microsyenite (of various ages)
- Syringobro, alkali gabbro (of various ages)

GEOLOGICAL SYMBOLS

- Geological boundaries (line broken where uncertain or arbitrary)
- Fault
- Dip of sediments
- Horizontal sediments
- Strike and dip of mineral layering
- Strike of vertical mineral layering
- Strike and dip of igneous lamination
- Strike of vertical igneous lamination
- DYKES (only Gardar and here shown):-
  - Trachyte, phonolite
  - Carbonate
  - Basalt, dolerite, etc.
  - Basalt, dolerite with large plagioclase crystals and/or anorthositic inclusions
  - Lampophyre
- Basaltic volcanic pipe
- Carbonatite
- Breccia
- Supraclastic deposits, where extensive

TOPOGRAPHICAL SYMBOLS

- Heights in metres:-
  - From existing maps
  - Based on altimeter readings
- Glacier
- Isolated building
- Road
- Track

MOERFELDT CENTRE

- SM 1
- SM 2
- SM 3
- SM 4
- SM 5
- SN 1
- SN 2
- SN 3
- SN 4
- SN 5
- SS 1
- SS 2
- SS 3
- SS 4
- SS 5
- SS 6
- SS 7
- SS 8
- SS 9
- SS 10
- SS 11
- SS 12
- SS 13
- SS 14
- SS 15
- SS 16
- SS 17
- SS 18
- SS 19
- SS 20
- SS 21
- SS 22
- SS 23
- SS 24
- SS 25
- SS 26
- SS 27
- SS 28
- SS 29
- SS 30
- SS 31
- SS 32
- SS 33
- SS 34
- SS 35
- SS 36
- SS 37
- SS 38
- SS 39
- SS 40
- SS 41
- SS 42
- SS 43
- SS 44
- SS 45
- SS 46
- SS 47
- SS 48
- SS 49
- SS 50
- SS 51
- SS 52
- SS 53
- SS 54
- SS 55
- SS 56
- SS 57
- SS 58
- SS 59
- SS 60
- SS 61
- SS 62
- SS 63
- SS 64
- SS 65
- SS 66
- SS 67
- SS 68
- SS 69
- SS 70
- SS 71
- SS 72
- SS 73
- SS 74
- SS 75
- SS 76
- SS 77
- SS 78
- SS 79
- SS 80
- SS 81
- SS 82
- SS 83
- SS 84
- SS 85
- SS 86
- SS 87
- SS 88
- SS 89
- SS 90
- SS 91
- SS 92
- SS 93
- SS 94
- SS 95
- SS 96
- SS 97
- SS 98
- SS 99
- SS 100

Reproduced with permission from the Geological Survey of Greenland

